Final Report

DEVELOPMENT OF A COUPLED BRIDGE SUPERSTRUCTURE-FOUNDATION FINITE ELEMENT CODE

State Project No.: 99700-7564-010

UF Project No.: 4910450445912

WPI No.: 0510627

Contract No.: B-8415

Principal Investigator:
Dr. Michael McVay

Co-Principal Investigators:
Dr. Cliff Hays
Dr. Marc Hoit

Graduate Assistants:
Thomas Molnit
Andrade Prashant
Mike Ahrens
Dan Fitzwilliam
Limin Zhang

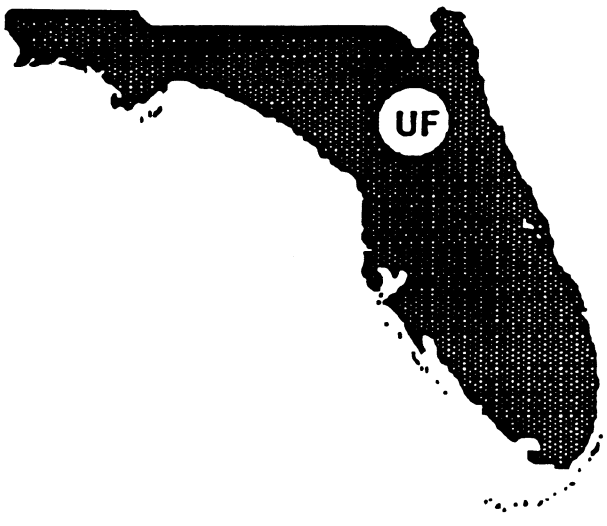

Department of Civil Engineering
College of Engineering
University of Florida

Submitted to
Florida Department of Transportation
June 1996

TABLE OF CONTENTS

LIST OF TABLES

LIST OF FIGURES

LIST OF FIGURES continued

LIST OF FIGURES continued

LIST OF FIGURES continued

LIST OF FIGURES continued

LIST OF FIGURES continued

LIST OF FIGURES continued

CHAPTER 1
INTRODUCTION

1.1 General

The University of Florida is developing a finite element code for the analysis and design of bridge piers as identified in AASHTO for the Florida Department of Transportation (FDOT). Called FLORIDA-PIER, the program models the piers, piles and shafts with linear beam elements, and the soil with axial and lateral nonlinear springs. After discussion with FDOT and FHWA personnel, it was readily recognized that the analysis portion of the code needed to be improved to accommodate the new LRFD strength design (i.e., nonlinear piles and piers), as well as a better representation of the soil-pile group interaction. In addition, to improve production, a pre-processor to graphically display the pier, piles, and material properties was needed.

FLORIDA-PIER originally modeled pile-soil-pile interaction (i.e., group effects) through the use of linear springs. However, this approach gives similar shear distribution within the row of the groups which doesn't agree with field data. Consequently, it was decided to modify FLORIDA-PIER to include p-y multipliers which could be applied to individual rows. However, a major draw back of the p-y multipliers is that no information exists for groups greater than three rows or with fixed heads.

1.2 Objectives

The objective of this research was to incorporate p-y multipliers into FLORIDA-PIER to handle group effects, as well as a nonlinear pile/drilled shaft model; in addition, a pre-processor was developed to handle data input. To determine the appropriate p-y multipliers,

and verify the code, extensive centrifuge testing of various group configurations (3 to 7 rows, and spacing) was performed.

In the case of the graphical pre-processor, pop up windows on the soil information, and the nonlinear pile information was developed. Also, the designer has the option of displaying the input for the various structural members. Soil information is inputted by layer, independent of pile length and is graphically displayed for the whole deposit.

1.3 Scope

The following is a breakdown of the five specific tasks:

1.3.1 Task I - Nonlinear Pile Response

The nonlinearity occurs primarily in three areas:

1. As a pile reaches the maximum bending capacity, a plastic hinge forms and the bending moment remains essentially constant while the pile continues to deform.
2. As significant cracking occurs in the pile due to flexure and axial forces, the flexural and axial stiffness of the pile decreases.
3. As lateral displacements increase the P-Δ moments (moment of the axial force times the lateral displacement of one end of a pile relative to the other end) becomes a significant portion of the piles bending capacity.

A model which represents all three of these effects was developed (see Chapter 2) and verified against existing codes (see Chapter 3).

1.3.2 Task II - P-Y Multipliers

Presently, FLORIDA-PIER uses linear springs between piles. The former results in a fully populated stiffness matrix, whereas the latter effects only the diagonal soil stiffness. The use of p-y multipliers will result in an individual row's shear distribution to vary, as well

as greatly reduce the size of the global stiffness matrix. The latter would result in a tremendous speedup (order of magnitude) in the program's execution, since the soil-stiffness would be known automatically (no need to invert the soil flexibility).

Since there is little if any published information on appropriate p-y multipliers, the third task of this research, centrifuge testing of large lateral groups (3 to 7 rows of piles), was required. Presently, it was not known if the p-y multipliers were constant, or are a function of the group's ultimate load/and deformation. After the completion of Task III, the multipliers for the various group sizes (3 to 7 rows) were back fitted through the use of FLORIDA-PIER (Chapter 6, Section 6.2).

1.3.3 Task III - Centrifuge Testing

Centrifuge testing of small groups (three by three group) has shown excellent correlation to the limited field testing (Houston Texas Pile Study). Consequently, this work concerned testing large vertical groups in the centrifuge, i.e., three, four, five, six, and seven rows and back computing their the p-y multipliers. For reproducibility, two tests were performed under each condition in the following test matrix:

Table 1-1. Centrifuge Testing Plan

# of Rows in Group	3	4	5	6	7
Loose Sand at 3D pile spacing	2	2	2	2	2
Dense Sand at 3D pile spacing	2	2	2	2	2

The results of these tests are reported in Chapter 6 along with their predictions from FLORIDA-PIER with the proposed multipliers.

In addition to the testing, a number of modifications to the present centrifuge equipment were undertaken. To model the large pile group (i.e., 7 rows), the centrifuge

container bucket was enlarged, as well as a new pile cap was designed and constructed. Instead of the present three rows of load cells, all of the piles within the group were instrumented with strain gauges to measure shear directly. Chapters 4 and 5 discuss the modifications to the centrifuge and the pile instrumentation.

1.3.4 Task IV - Graphic Pre-processor Development

As an enhancement to the post processor, a pre-processor to help with data entry was developed. It was designed and coded to be graphically based so that as information is supplied, the defined parts will be displayed. As an example, once the number of piles are specified, they are drawn. Menu options defining the pile configuration, super structure, pile material properties (linear and nonlinear) and soil properties were developed. Defaults were coded when possible so that input was simplified. Missing piles can be chosen by clicking on the pile to be removed. Once defined, the structure can be viewed, rotated, zoomed etc., just like the post processor. Loads may be applied by clicking on the nodes on which they act and their values specified. Once all required input is supplied, a file is written which is the input for FLORIDA-PIER. The pre-processor also has the ability to read an existing input file so that it can be viewed and/or modified. Called PIERGEN, the preprocessor's windows or screens with the appropriate input are given and discussed in FLORIDA-PIER's manual.

CHAPTER 2
DISCRETE ELEMENT MODEL OF NONLINEAR PILE BEHAVIOR

This chapter describes the discrete element used to model the nonlinear behavior of the piles in FLORIDA-PIER. The discrete element models the nonlinear material and geometric behavior of the piles. The nonlinear material behavior is modeled by using input or default stress strain curves which are integrated over the cross-section of the piles. The nonlinear geometric behavior is modeled using the P-Δ moments (moments of the axial force times the displacements of one end of element to another) on the discrete element. And since the user subdivides the pile into a number of sub-elements, the P-y moments (moments of axial force times internal displacements within members due to bending) are also modeled.

The discrete element model described herein is used in the analysis for the pile whenever the nonlinear pile option is chosen. The piles are automatically divided into 16 elements below the soil line and the user has the option of selecting the number of elements above the soil line. The number of elements above the soil line should generally be such that the length of the subelements are about the same as the length below the soil line. The more elements used, the more accurate the representation of the P-Δ and P-y moments and the nonlinear material behavior including cracking of the concrete and yielding of the steel.

2.1 Discrete Element Model

The discrete element model (Mitchell 1973 and Andrade 1995) can be represented as a mechanical model as shown in Figure 2-1. The center bar can both twist and extend but is otherwise rigid. The center bar is connected by two universal joints to two rigid end blocks. The universal joints permit bending at the quarter points about the y and z axes Discrete deformational angle changes Ψ_1, Ψ_2, Ψ_3, Ψ_4 occur corresponding to the bending moments

M_2, M_1, M_4, M_3 , respectively. A discrete axial shortening δ corresponds to the axial thrust T and the torsional angle Ψ_5 corresponds to the torsional moment in the center bar M_5.

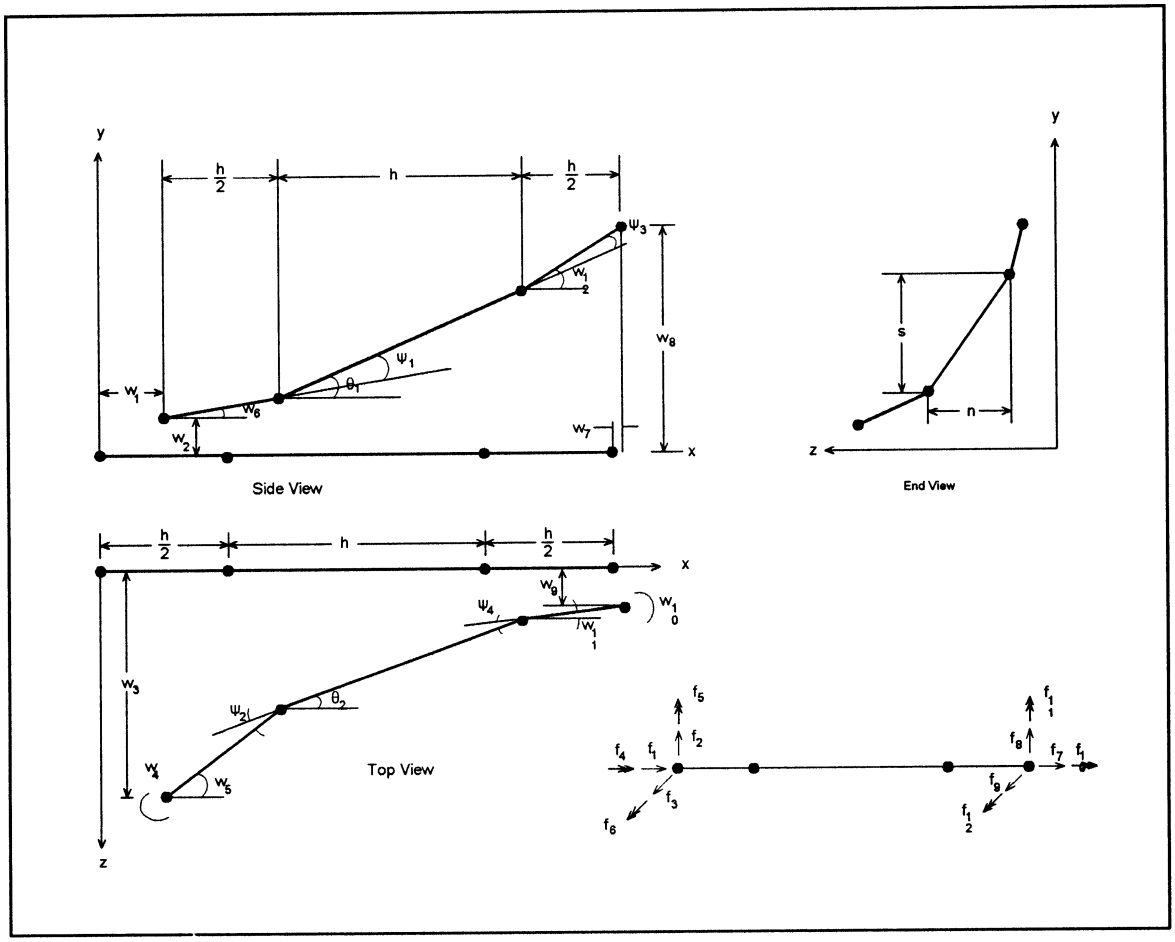

Figure 2-1. Discrete Element Model

2.1.1 Element Deformation Relations

In Figure 2-1, w_1 - w_3 and w_7 - w_9 represent displacements in the x, y and z directions at the left and right ends respectively, w_4 and w_{10} represent axial twists (twists about the x -axis) at the left and right ends, respectively, and w_5-w_6 and w_{11}- w_{12} represent the angles at the left and right end blocks about the x and z axes, respectively. Based on a small displacement geometric analysis.

$$n = w_3 - w_9 - \frac{h}{2}(w_5 + w_{11})$$
$$s = w_8 - w_2 - \frac{h}{2}(w_6 + w_{12}) \qquad (2\text{-}1)$$

The elongation of the center section of the element is calculated as follows:

$$\delta = w_7 - w_1 \qquad (2\text{-}2)$$

The angle changes for the center section about the z and y axes are then defined below:

$$\theta_1 = \frac{s}{h} = \frac{w_8 - w_2}{h} - \frac{w_6 + w_{12}}{2}$$
$$\theta_2 = \frac{n}{h} = \frac{w_3 - w_9}{h} - \frac{w_5 + w_{11}}{2} \qquad (2\text{-}3)$$

The discretized vertical and horizontal angle changes at the two universal joints are then :

$$\Psi_1 = \theta_1 - w_6$$
$$\Psi_2 = w_5 - \theta_2$$
$$\Psi_3 = w_{12} - \theta_1$$
$$\Psi_4 = \theta_2 - w_{11} \qquad (2\text{-}4)$$

and the twist in the center part of the element is defined as:

$$\Psi_5 = w_{10} - w_4 \qquad (2\text{-}5)$$

Thus, the internal deformations of the discrete element model are uniquely defined for any combination of element end displacements. The curvature for small displacements at the left and right universal joints about the y and the z axes are defined as follow :

At the left joint,

$$\phi_1 = \frac{\psi_1}{h}$$

$$\phi_2 = \frac{\psi_2}{h} \qquad (2\text{-}6)$$

At the right joint,

$$\phi_3 = \frac{\psi_3}{h}$$

$$\phi_4 = \frac{\psi_3}{h} \qquad (2\text{-}7)$$

The axial strain at the center of the section is given by

$$\epsilon_c = \frac{\delta}{2h} \qquad (2\text{-}8)$$

2.2 Integration of Stresses for Nonlinear Materials

For a beam subjected to both bending and axial loads, it is assumed that the strains vary linearly over the area of the cross-section. This assumption enables the strain components due to bending about the z and y axes, and the axial strain, to be combined using superposition. Examples of these three components are represented separately in Figure 2-2 (a through c) and combined in Fig. 2-2d. Also shown in Figure 2-2d is a differential force, dF_i, acting on a differential area, dA_i, relationship for the material.

$$dF_i = \sigma_i dA_i \qquad (2\text{-}9)$$

Finally, Figure 2-2 e represents the stress-strain l. Then For the left joint, the relationship for strain at any point in the cross-section is

$$\epsilon=\epsilon_c-\phi_1 Y-\phi_2 Z \tag{2-10}$$

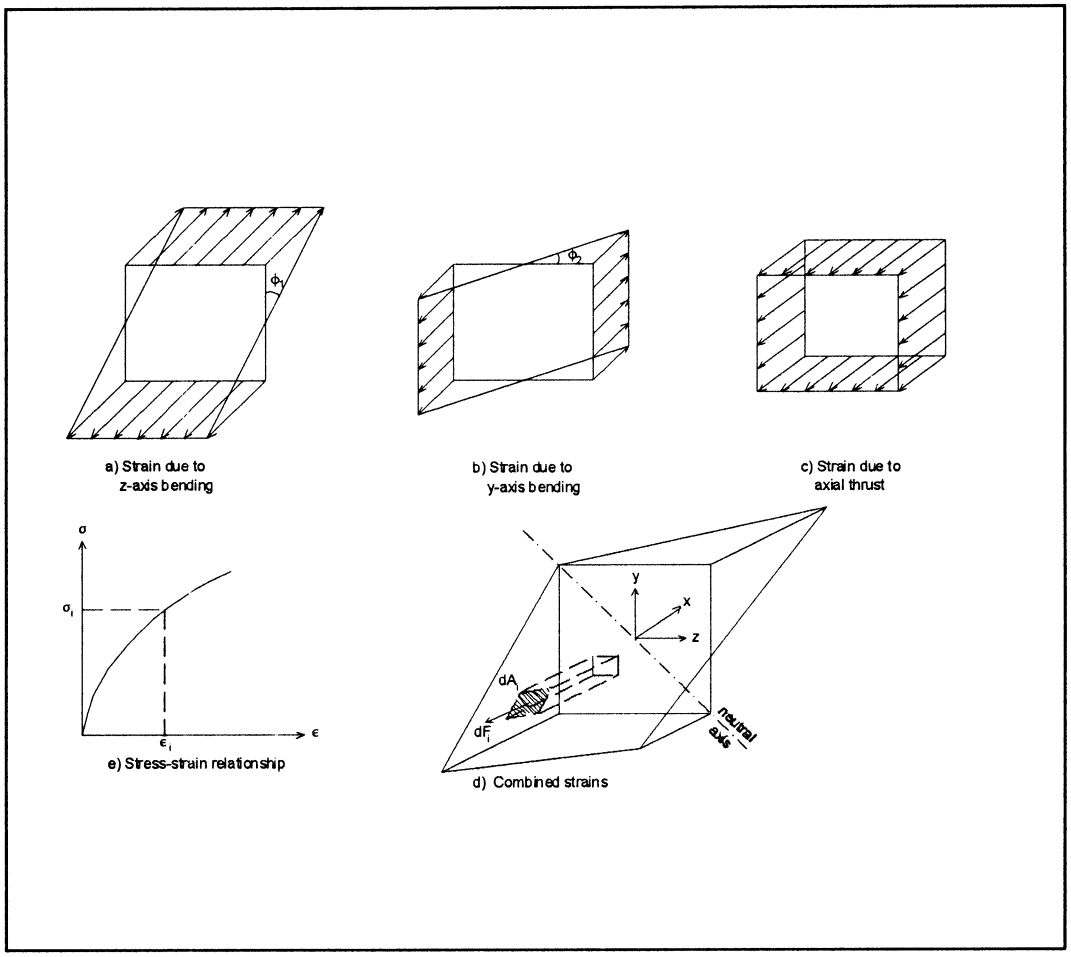

Figure 2-2. Linear Strain Distribution Over Square Cross-Section

Then to satisfy equilibrium

$$\begin{aligned} M_z &= \iint_A dF_i . Y_i = \iint_A \sigma_i Y_i dA \\ M_y &= \iint_A dF_i . Z_i = \iint_A \sigma_i Z_i dA \\ T &= \iint_A dF_i = \iint_A \sigma_i dA \end{aligned} \tag{2-11}$$

Numerical integration of equations 2-11 is done using Gaussian Quadrature. To use the method of Gaussian Quadrature, the function being integrated must be evaluated at those points specified by the position factors. These values are then multiplied by the appropriate weighting factors and the products accumulated. Figure 2-3a shows a square section with 25 integrations points (a 5 × 5 mesh). The number of defaults integration points for square pile is set at 49 (a 7 by 7 mesh). Users may change this to a NPTS x NPTS mesh by inserting a value for NPTS as the last input item in data line 6A.. For circular sections, the section is divided into circular sections (12 radial divisions and 5 circumferential divisions as shown in Figure 2-3b. The sections are integrated at the centroids of each sector using weighting factors of 1.0. The stress in all steel bars is evaluated at the centroid and a weighting factor of 1 is used for each bar.

When a circular void is encountered in a square section, the force is first computed on the unvoided section and then the force that would be acting on the voided circular area is computed and subtracted from the force computed for the unvoided section. Circular sections with voids are divided into sectors omitting the voided portion.

Even for nonlinear material analysis, the torsional moment M_5 is assumed to be a linear function of the angle of twist, Ψ_5, and the torsional stiffness GJ, where J is the torsional constant and G is the shear modulus as shown next

$$M_5 = GJ\frac{\Psi_5}{2h} \tag{2.12}$$

Since the curvatures are only evaluated at the two deformational joints inside the element, the effective position of any plastic hinge that might form in the structure is restricted to these two locations which are actually 1/4 of an element length from each element node (end point).

This should not cause any practical limitation. However, it should be considered if trying to match a theoretical solution with pure plastic hinges at theoretical ends of members

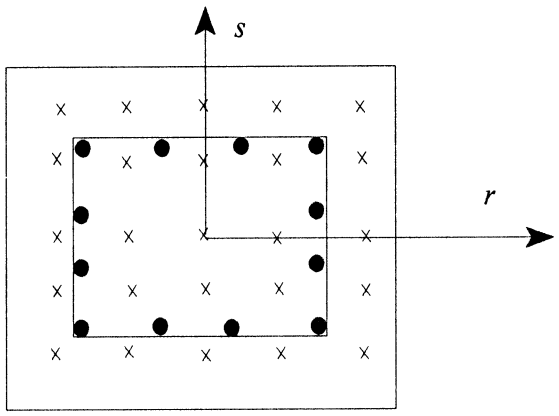

x - *Concrete Integration Points*

● - *Steel Rebar (1x1 Integration)*

a) Cross-Section of Square Pile Showing Integration Points

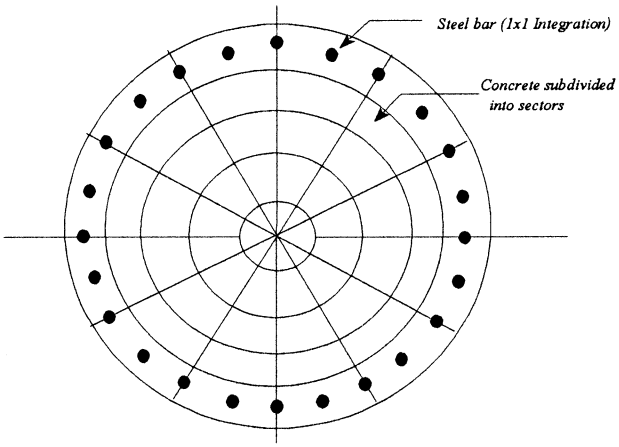

b) Circular Cross Section Pile with Steel Rebars

Figure 2-3 Rectangular and Circular Section Integration Divisions

2.3 Element End Forces

From equilibrium of the center bar

$$V_1=\frac{M_4-M_2}{h}-T\theta_1$$
$$V_2=\frac{M_1-M_3}{h}-T\theta_2 \qquad (2.13)$$

And from equilibrium of the end bars :

$$f_1=-T$$
$$f_2=V_1$$
$$f_3=-V_2$$
$$f_4=-M_5$$
$$f_5=M_1+V_2.\frac{h}{2}+T.\frac{h}{2}.w_5$$
$$f_6=-M_2+V_1.\frac{h}{2}+T.\frac{h}{2}.w_6 \qquad (2\text{-}14)$$
$$f_7=T$$
$$f_8=-V_1$$
$$f_9=V_2$$
$$f_{10}=M_5$$
$$f_{11}=-M_3+V_2.\frac{h}{2}+T.\frac{h}{2}.w_{11}$$
$$f_{12}=M_4+V_1.\frac{h}{2}+T.\frac{h}{2}.w_{12}$$

where f_1- f_3 and f_7 - f_9 are the acting end forces, and f_4 - f_6 and f_{10} - f_{12} are the end moments.

2.3.1 Element Stiffness

Using the standard definition, the stiffness of an element having n degrees of freedom (d.o.f.) is a square matrix [K] of order nxn in which K_{ij} is the force necessary in the I-th d.o.f. to produce a unit deflection of the j-th d.o.f. The secant stiffness computed is the stiffness

that the members would have if each of the integration points had the secant stiffness defined by dividing the present stress by the present strain as shown in Figure 2-4.

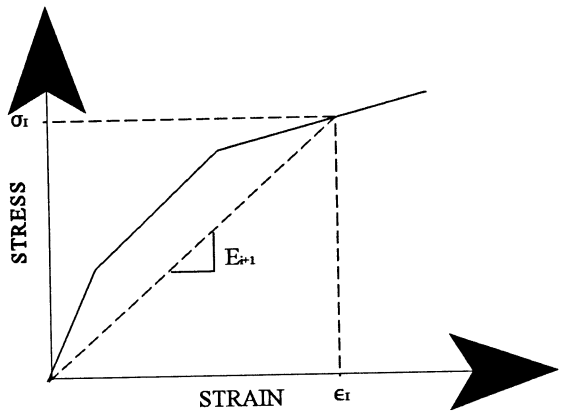

Figure 2-4. Secant Stiffness for Nonlinear Stress-Strain Curve

During the iteration process the element stiffness matrix is reevaluated in each new deformed position. For each iteration, initially the secant stiffnesses are stored at all integration points within an element. Then on 12 subsequent passes a unit displacement is applied to each element degree of freedom in turn keeping all other displacements as zero and the forces corresponding to that unit displacement are calculated by integrating the stresses over the cross-section of the element as described earlier. The previously stored secant moduli at each of the Gaussian integration points are used in this integration of stresses. The element end forces thus computed will be the nth column of the stiffness matrix corresponding to a case where the nth degree of freedom has a unit displacement imposed, all other displacements being held to zero.

2.4 Procedures for Defining Stress-Strain Curves

The user may define their own stress strain curves for concrete and steel or use the default values described next.

2.4.1 Concrete

Figure 2-5 shows the default value of stress-strain curve supplied by the program and is a function of f'_c and E_c input by the user. The compression portion of the concrete curve is highly non-linear and is defined by the Hogenstead parabola and straight line as shown in the figure. For the tension portion the curve is assumed linear up to a stress of f_r and then has a tension softening portion as shown. The tension softening portion attempts to account for the uncracked sections between cracks where the concrete still carries some stress. The value of f_r is based on the fixed value of ϵ_r shown in the figure and the modulus of elasticity E_c input by the user. For English units this will give a value of f_r of $7.5\sqrt{f'_c}$.

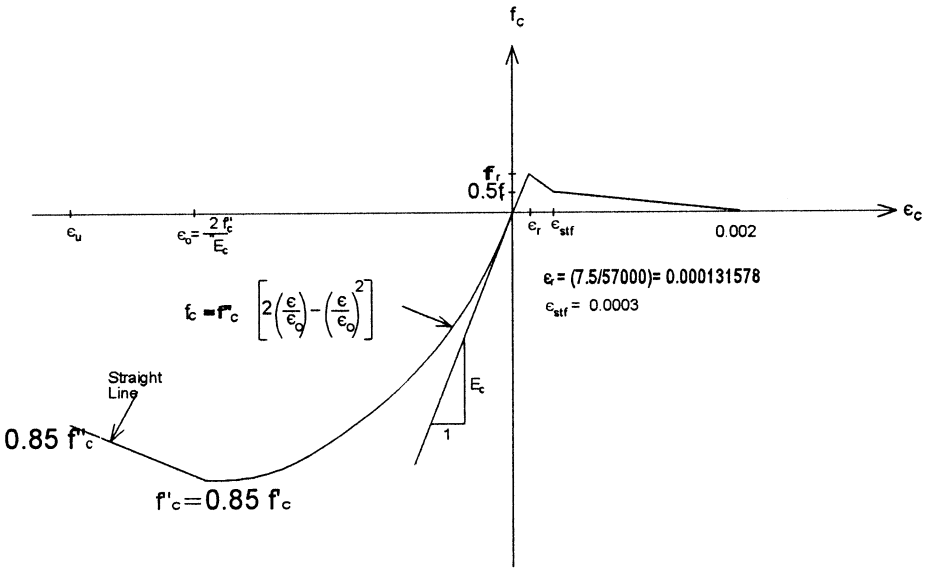

Figure 2-5. Default Stress-Strain Curve for Concrete

2.4.2 Mild Steel

For mild steel reinforcement the stress-strain relationship is assumed to be elastic-plastic and similar in both tension and compression. A yield strain ϵ_y is computed based on the yield stress, fy and the modulus of elasticity input E_s,

$$\epsilon_y = \frac{f_y}{E_s} \tag{2-15}$$

The default relations for the mild steel stress-strain curve are given by

$$\begin{aligned} f_s &= -f_y && \epsilon \le -\epsilon_y \\ f_s &= E_s\epsilon && -\epsilon_y < \epsilon < \epsilon_y \\ f_s &= f_y && \epsilon_y \le \epsilon \end{aligned} \tag{2-16}$$

The default stress-strain curve generated for steel with f'_y=60 ksi and E_c=29600 ksi is shown in Figure 2-6.

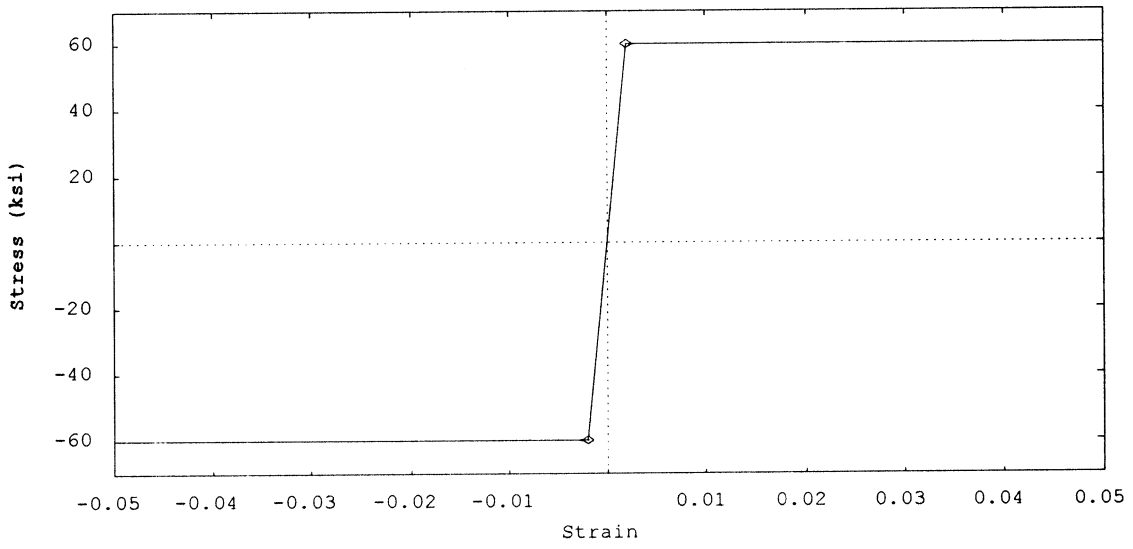

Figure 2-6. Mild Steel Stress-Strain Curve for F_y = 60 ksi

2.5 High Strength Prestressing Steels

The previous figures show reinforcing as rebars. However, the user may also select high strength reinforcing strands. The stress-strain curves for prestressing steels generally do not have a definite yield point as illustrated by the curve for f_{su} = 270 ksi in Figure 2-7. The most common values of f_{su} used in practice are f_{su} = 250 ksi and 270 ksi. For these two input values when using standard (English) units, the curves defined by the PCI design handbook (PCI 1992) will be used. For other strengths or when using nonstandard units, the default curves will be obtained by using nondimensional equations based on curve fitting the two cited curves. These curves are not recommended for use for values of f_{su} much different than the standard values.

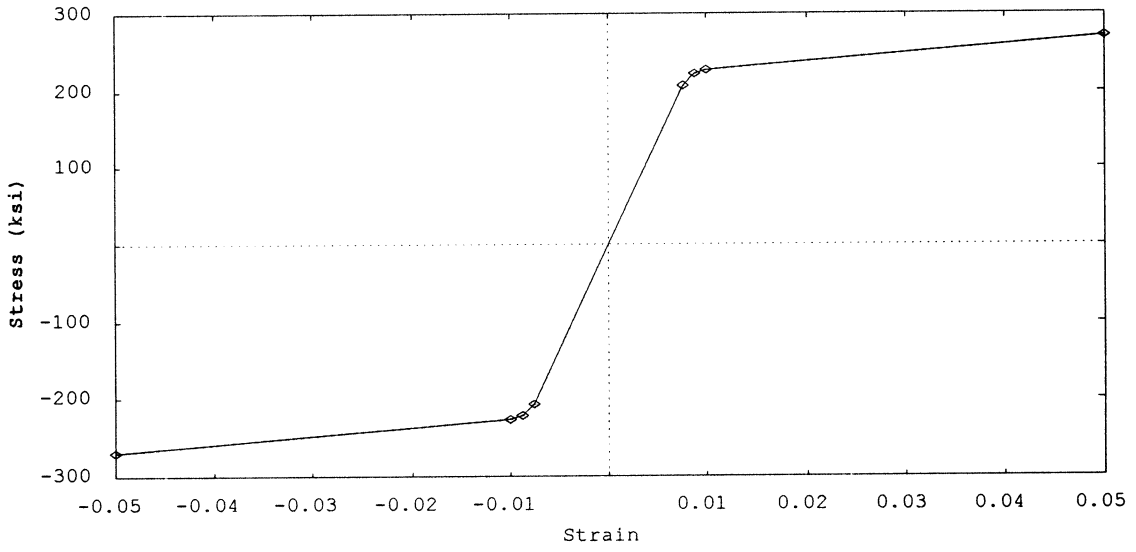

Figure 2-7. Prestressing Steel Stress-Strain Curve for f_{su} = 270 ksi

2.6 Adjusting Concrete and Steel Stress-Strain Curves for Prestressing

When piles are prestressed prior to installation, there are stresses and strains existing at the time of installation due to the prestressing. The program shifts the origin of the stress-

strain curve for the steel by the amount of the prestressing stress in the steel and the corresponding steel strain. Also, the program shifts the origin of the concrete stress-strain curve by the amount of compression introduced in the concrete by prestressing and the corresponding concrete strain. It is assumed that the prestressing is symmetrically placed and thus only a constant compressive stress is developed in the concrete due to the prestressing. Thus for a concrete area, A_c, and a total steel area, A_{st}, and a prestressing steel stress, f_{ps}, the resulting concrete stress, f_{pc}, is given by

$$f_{pc} = \frac{f_{ps} A_{st}}{A_c} \tag{2-17}$$

CHAPTER 3
EXAMPLES ILLUSTRATING NONLINEAR PILE BEHAVIOR

In this chapter, several examples considering the response of pile groups subjected to gravity and lateral loading are studied. Comparisons to different programs like FRM54 and COM624P are made.

3.1 Example One: Four Pile Structure With Pile Cap and No Soil

In this example the results obtained using FLORIDA-PIER are compared to those obtained by FRM54 [Hays 1974]. While the two dimensional discrete model used in FRM54 is similar to the one used in FLORIDA-PIER for bending in one plane, there are some differences in the program as noted

1) FLORIDA-PIER assumes small-displacements in the derivation of the stiffness matrices whereas FRM54 assumes large displacements.

2) FLORIDA-PIER has a three-dimensional capability while FRM54 implements a planar discrete element.

3) FLORIDA-PIER performs the stress integrations using a Gaussian integration procedure whereas FRM54 divides the section into as many rectangles as required to perform an exact integration for the piecewise linear stress-strain curve provided.

4) FLORIDA-PIER utilizes a secant-stiffness method whereas FRM54 uses a tangent stiffness approach.

5) FLORIDA-PIER connects the columns with shell elements to represent the pile cap while FRM54 uses the same two dimensional discrete element for the used for the pile cap as used for the piles. Because of this, the stiffness

properties of the discrete element used to model the pile cap in example 1 was chosen such that the FRM54 and FLORIDA-PIER solutions were essentially the same in the linear range, and then the results were compared as the loads were increased as the piles became highly nonlinear due to cracking of the concrete and yielding of the steel.

The structure and loading for example one is shown in Figure 3-1. Figure 3-2 shows a plot of the load applied at the top of pile 1 versus the lateral deflection of the top of pile 1 for both programs. Note that the same load was applied on piles 1 and 3 in all cases. There is very good agreement between the two curves in the figure with similar predictions of the cracking point and the point of steel yield. Figure 3-3 shows a plot of the moment along the length of the pile 1 for both programs for a load of P=420 kips on the tops of each of Piles 1 and 3 (the maximum load at which a solution was obtained for both programs). Figure 3-4 shows a similar plot for Pile 2.The results are seen to be in good agreement. Attempts to find a solution for a load level above 420 kips were unsuccessful for both FRM54 and FLORIDA-PIER, thus both programs predict the same ultimate loading of 420 kips.

To study the effect of significant axial force in the piles, vertical compressive axial loads of 4200 kips were applied to the top of each of the piles 1 through 4 and the analysis redone applying increasing lateral loads till failure. A plot of the lateral load applied on each of piles 1 and 3 versus the trailing row deflection is shown in Figure 3-5. The lateral failure was only 210 kips compared to lateral load of 420 kips without the lateral load. The reduction is due to two effects, the moment capacity of the sections are reduced due to the axial loading and the P-Δ moments increase the moments acting on the sections significantly.

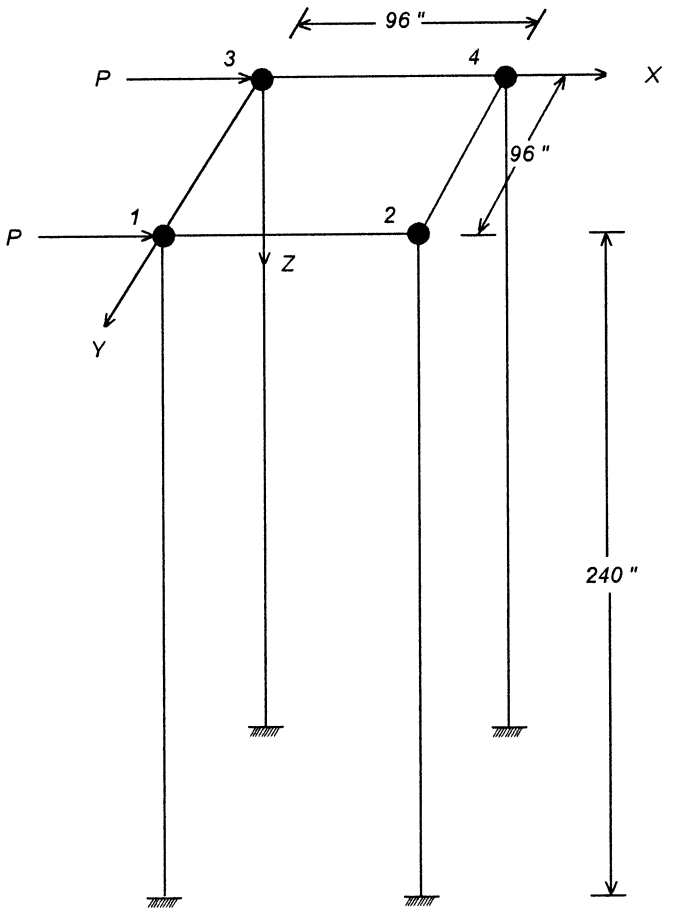

NOTES

Pile Cap Properties

Thickness = 84 in

E = 3300 ksi

Poisson's Ratio = 0.2

a) Pile Group Geometry and dimensions

f_c' = 5 ksi

f_y = 60 ksi

A_{steel} = 36 in^2

Cover for Rebar = 3 in

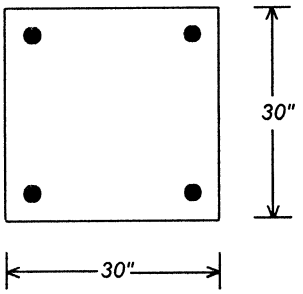

b) Cross section and material properties of each pile

Figure 3-1. Model for Comparison of LPGSTAN and FRM54

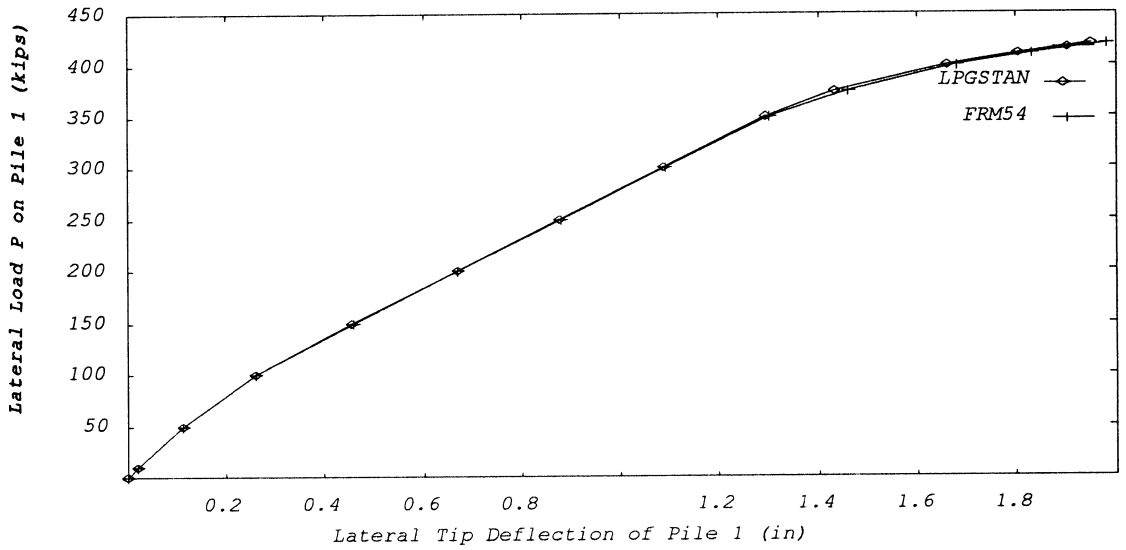

Figure 3-2. Trailing Row Load Deflection Comparison Between LPGSTAN and FRM54

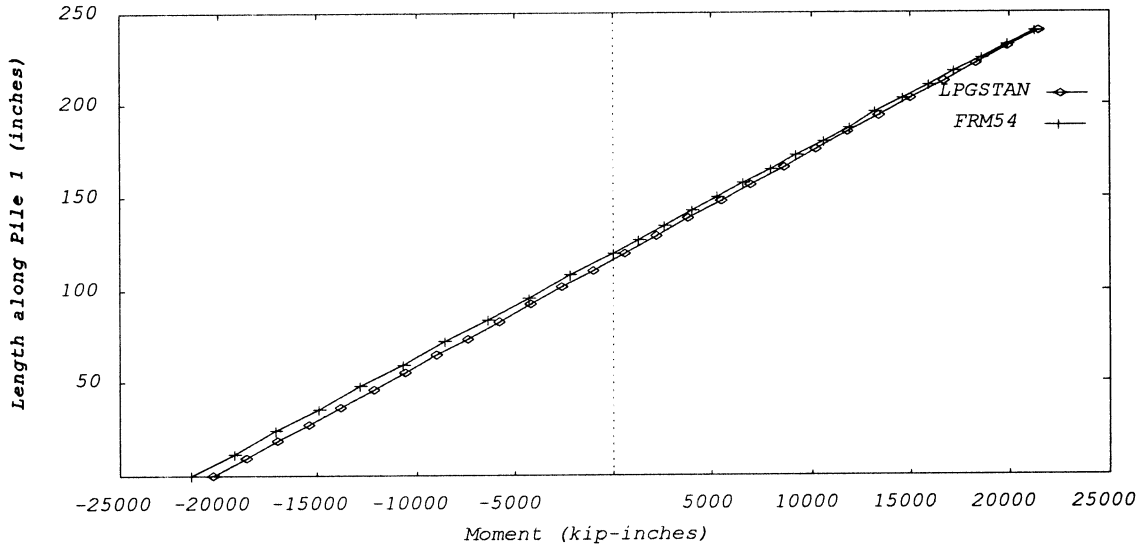

Figure 3-3. Comparison of Moments Along Length of Pile 1 at Ultimate Load

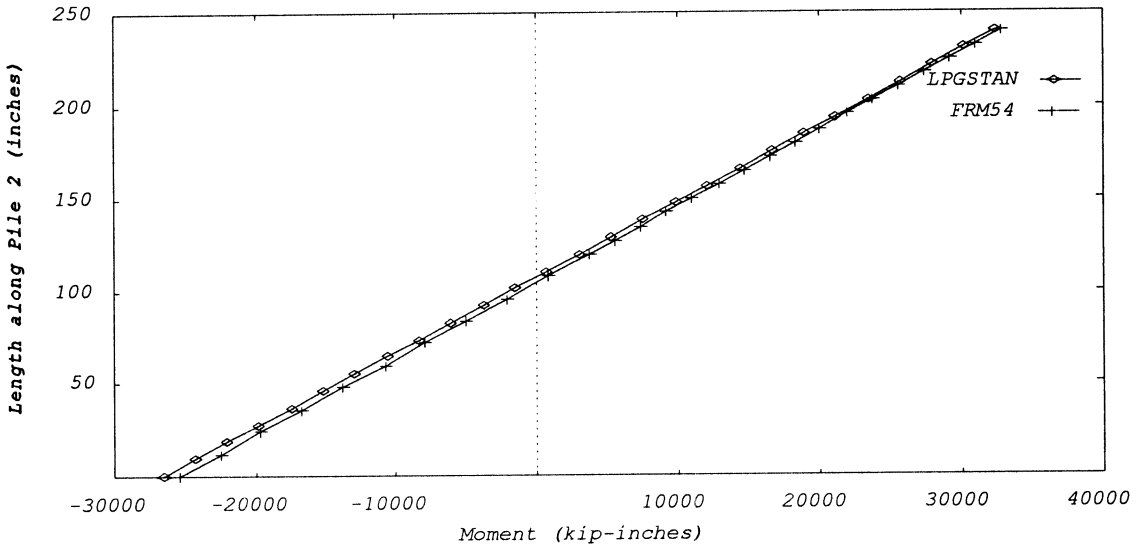

Figure 3-4. Comparison of Moments Along Length of Pile 2 at Ultimate Load

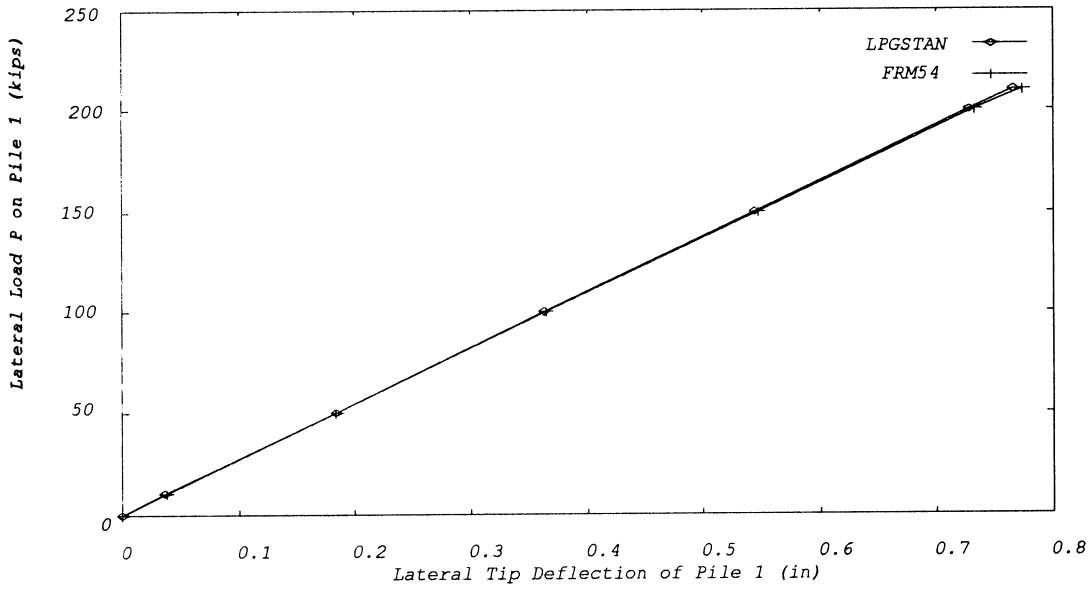

Figure 3-5. Trail Row Lateral Load vs. Defl. Plot for LPGSTAN & FRM54 With Axial Loads on Piles

In order to verify that the programs considers the P-Δ effect, a free body diagram of piles 1 and 2 is shown at the failure load for both programs (Figure 3-6). An equilibrium check for moments about point A is made below for the FLORIDA-PIER output for Pile 1.

Counterclockwise End Moments: 12570 + 17140 = 29710 kip-in

Clockwise Moment due to Shear : 111.2 x 240 = 26688 kip-in

Clockwise moment due to P-Δ effect = 3948 x 0.766 = 3024 kip-in

Equilibrium Error: $|29710 - 26688 - 3024| = 2$ kip-in

The equilibrium error is thus seen to be very small and would have been even smaller if higher accuracy was maintained in printing the output The input file for the FLORIDA-PIER model is shown in Figure 3-7.

3.2 Example Two: Single Pile

In this example the response of a single pile in sand is examined using FLORIDA-PIER. The model and the pile cross-section is shown in Figure 3-8. The section is circular and is a reinforced concrete section of diameter 20 inches. Twelve #8 bars are provided for the longitudinal reinforcement. The total length of the pile is 528 inches of which 33 inches are above the soil level. The results obtained from FLORIDA-PIER are compared with an analysis done using COM624P a software program developed by Ensoft for the Federal Highway Administration [11]. Before an interpretation of the results a few comments on the differences (and similarities) between COM624P and FLORIDA-PIER are in order. These comments will enhance an understanding of the interpretations.

1) Both FLORIDA-PIER and COM624P use a Hognestaad parabola to model the behavior of concrete in compression. FLORIDA-PIER uses a tension stiffening model to model the behavior of concrete in tension while COM624P ignores the concrete strength in tension.

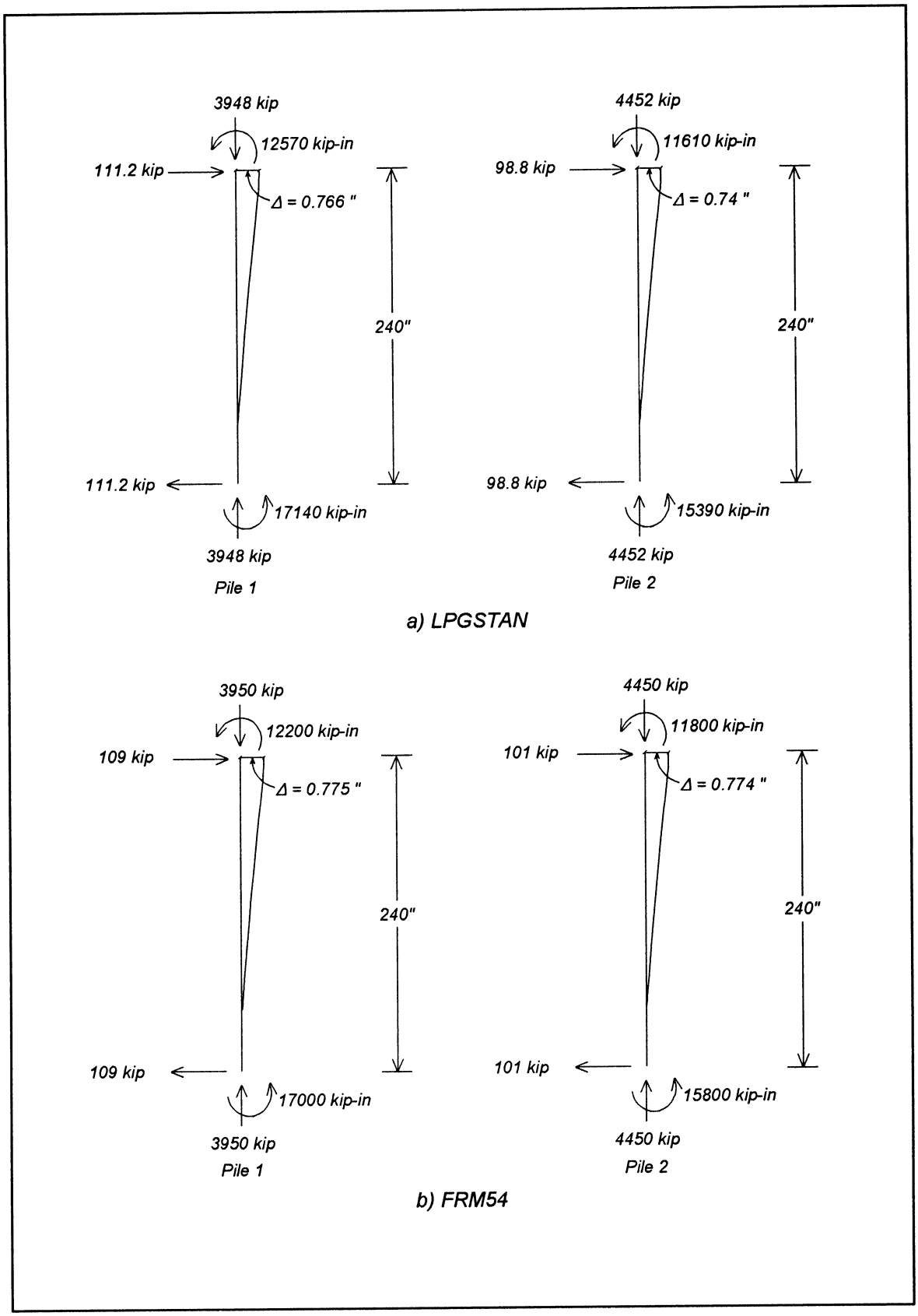

Figure 3-6. Free Body Diagrams for Piles 1 & 2 for Both Programs at Ultimate Load

```
Comparison of FRM54 and FLORIDA-PIER with the Soil Turned Off
INCHES KIPS
L=1 M=1 D=1 O=1 S=1 P=1 T=1 F=1 C=1 B=1 :OUTPUT FLAGS
1 U=0                    :NUMLC,U
2 2 1.5e30 2 2             :IFLEX,ITIP,TSTIFF,KTYPE,NLOPT
240.0 1 5 60 29600 4030 1    :TPL,MATOPT,FPC,FY,ES,EC,KSTEEL
30 0 2 0                 :WIDTH,DV,ISTNOPT,PREST
2                        :NGROUPS
9.0 12 12 N=2 D=X              :AREA,XS,YS,N,D
9.0 12 -12 N=2 D=X             :AREA,XS,YS,N,D
120.0 0 1 15             :Z,KCYC,KFIX,NSUB
2 2                      :NPX,NPY
96                       :DX1
96                       :DY1
1. 1.                    :PYMX1,PYMX2
1. 1.                    :PYMY1.PYMY2
0                        :NMPIL
200 0.05                 :MAXITER,TOLER
0                              :NLAYER
0                      :N1
STRUCTURE
N=0                            :N
: DUMMY PIER COL PROPERTIES
: DUMMY PIER BEAM PROPERTIES
: DUMMY EXTRA BEAM PROPERTIES
E=3.0E3 U=.20 T=84         :E,U.T
0                        :NS
1 L=1 F=420                :NF,L,F
3 L=1 F=420                    :NF,L,F
:
```

Figure 3-7. Input File for Comparison of FRM54 and FLORIDA-PIER

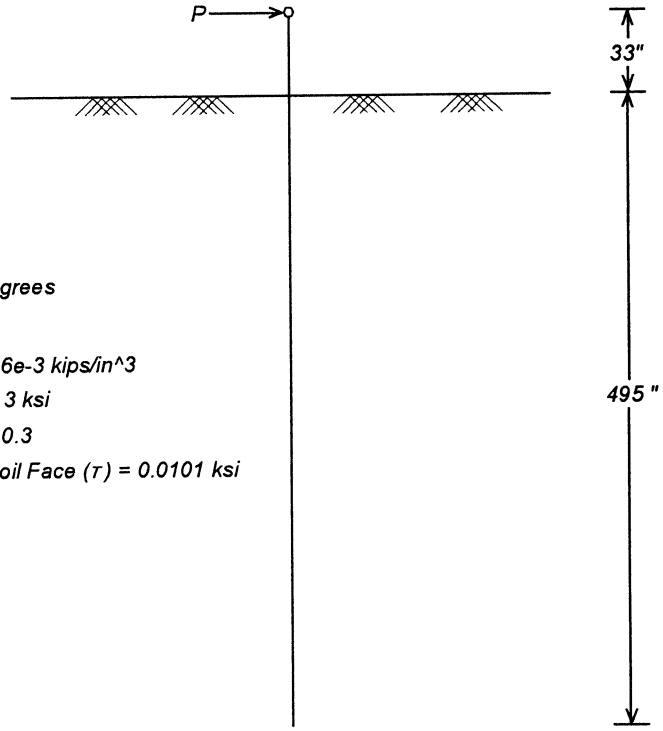

NOTES

Soil Properties One Layer

Angle of Internal Friction (ϕ) = 39 degrees

Soil Modulus (k) = 0.090 ksi

Effective Unit Wt. of Soil (γ) = 0.056e-3 kips/in^3

Shear Modulus of Vertical Soil (G) = 3 ksi

Poisson's Ratio of Vertical Soil (ν) = 0.3

Verti. Shear Failure Stress on Pile-Soil Face (τ) = 0.0101 ksi

a) Single Pile Model with Lateral Load (Free Head)

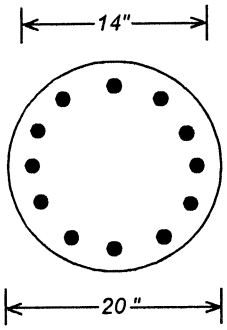

A_{steel} = 9.42 in^2

12 # 8 bars

f'_c = 5 ksi

f_y = 60 ksi

Cover of Rebar = 3 in

b)Cross-section and material properties of the pile

Figure 3-8. Model for Comparison of COM624P and LPGSTAN

2) FLORIDA-PIER can model prestressed concrete piles by effecting a shift in the concrete and steel stress strain curves equivalent to the amount of prestressing as described in Chapter 2. Also by allowing the user to input his or her stress -strain curves, piles of different materials can be modeled. COM624P cannot handle prestressed concrete piles

3) COM624P was written for analyzing a single pile subjected to a combination of lateral and axial loads with a capability of modeling the connection to a pile cap as fixed or pinned. FLORIDA-PIER can handle pile groups with a free or fixed pile head connection, subjected to a variety of loads..

4) FLORIDA-PIER uses a set of linear pile-soil-pile springs to model the influence of the piles on each other in a group. The user can also toggle these pile-soil-pile springs off and specify a set of p-y multipliers which account for the lateral force distribution in a pile.

5) COM624P calculates an equivalent EI for the section for various levels of distress for a given axial load. This EI value is used in the pile contribution to the stiffness and a finite difference technique is employed to find the unknowns. FLORIDA-PIER calculates the secant stiffness matrix of the pile elements depending on their current deformation states. The stiffnesses of the piles, soil and the superstructure are assembled and the resulting equations are solved for the unknowns and an iterative procedure as described in Chapter 2 is utilized until convergence is obtained.

A plot of the lateral deflection of the top of the pile against lateral load for both programs until the failure moment is reached is shown in Figure 3-9. A plot of the linear pile response for both programs is superimposed on this plot. The agreement between the two

programs is seen to be good for both the linear and non-linear pile cases. It can be noted that the FLORIDA-PIER non-linear analysis predicts a stiffer post cracking response due to the tension stiffening model used to simulate the behavior of concrete in tension. A plot of the moments along the length of the pile for the ultimate load of P = 47.5 kips is also presented in Figure 3-10 for a non-linear and linear analysis using both programs. The input file for the FLORIDA-PIER model is given in Figure 3-11.

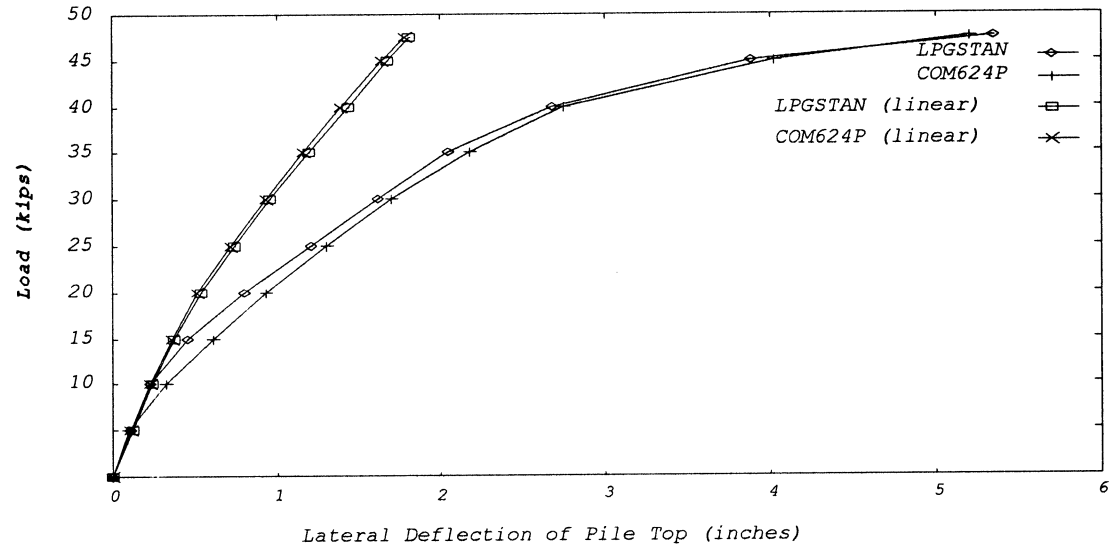

Figure 3-9. Lateral Pile Top Deflections, COM624P and LPGSTAN

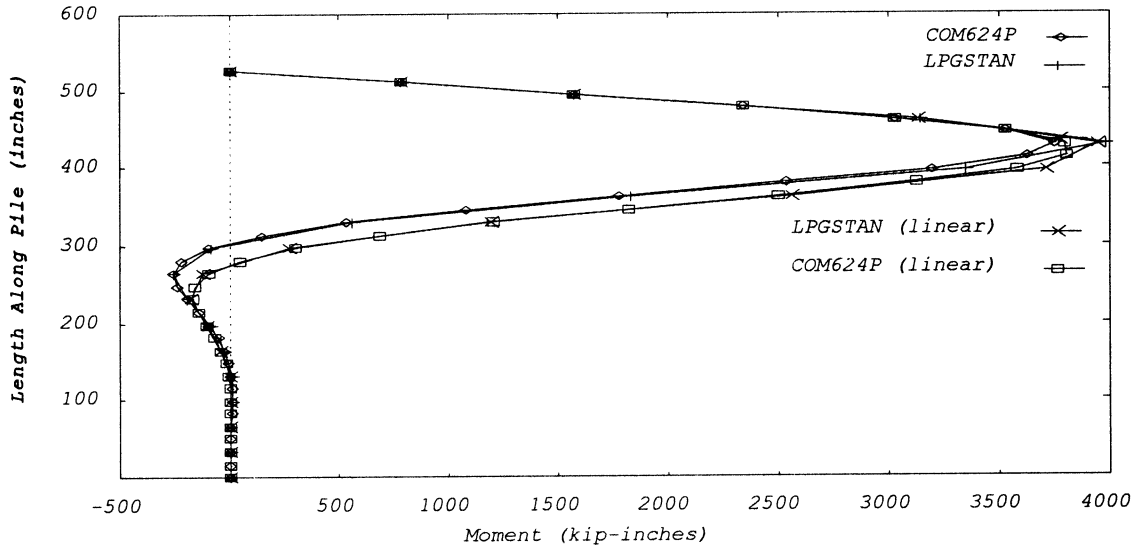

Figure 3-10. Comparison of Moments for COM624P and LPGSTAN

```
MODEL FOR THE COMPARISON OF FLORIDA-PIER WITH COM624P
INCHES KIPS
L=1 M=1 D=1 O=1 S=1 P=1 T=1 F=1 C=1 B=1 :OUTPUT FLAGS
2 U=0                          :NUMBER OF LOAD CONDITIONS
0 0 1.5e20 1 2                 :IFLEX,ITIP,TSTIFF,KTYPE,NLOPT
528. 1 5  60 29600 4030.51 1       :TPL,MATOPT,FPC,FY,ES,EC,KSTEEL
20 14 0 9.4 1 0                :DP,DS,DV,AS,NAS,PREST
33. 0 1 2                      :Z,KCYC,KFIX,NSUB
1 1                            :#PILES X Y
1                              :PYMX1
1                              :PYMX2
0                                    :NMPIL
200 .5                         :MAXITER,TOLER
1                              :NLAYER
39.  0.090  .056E-3  0. 0. 0. 3  0.3 .0101 600. 2 :SOIL PROPERTIES
39.  0.090  .056E-3  0. 0. 0. 3  0.3 .0101       :SOIL PROPERTIES
5.0 0.3  200                   :QZ(1),QZ(2),QZ(3)
0                                    :N1
STRUCTURE
N=0 : N
: DUMMY PIER COL PROPERTIES
: DUMMY PIER BEAM PROPERTIES
: DUMMY EXRA BEAM PROPERTIES
E=3.3E3 U=.20 T=84                   :E,U,T
0                              :NS
1 L=1 F=45                           :NF,L,F
1 L=2 F=47.5                         :NF,L,F
:
```

Figure 3-11. FLORIDA-PIER Input File for Comparison with COM624P

3.3 Example Three: Nine Pile Model

A nine-pile model in sand was run for both the fixed and a pinned head conditions. Details of the model are shown in Figure 3-12. A plot of the load applied to each pile of the trailing row versus the deflections of the leading row is shown in Figure 3-13 for both pile head conditions. A plot of the moments along the length of the pile for the pinned head condition for a load on each trailing row pile, of P=240 kips, is shown in Figure 3-14. A plot of the moments along the length of the pile for the fixed head condition for a load on each trailing row pile, of P=370 kips, is shown in Figure 3-15. These loads were the highest loads for which a solution was obtained.

The pile-soil-pile interaction was modeled using p-y multipliers. The values used were 0.35, 0.45, 0.75 for the trail, middle and lead row respectively. The percentage of the total lateral load carried by each pile row for the pinned head condition is plotted against an increase in lateral load for each pile in Figure 3-16. The maximum moment variation versus the lateral load for the three pile rows for the pinned head condition is shown in Figure 3-17. As the lead pile develops a plastic hinge, there is a more even distribution of shears and moments in the three piles than given by an elastic analysis. The input file for the FLORIDA-PIER model is shown in Figure 3-18.

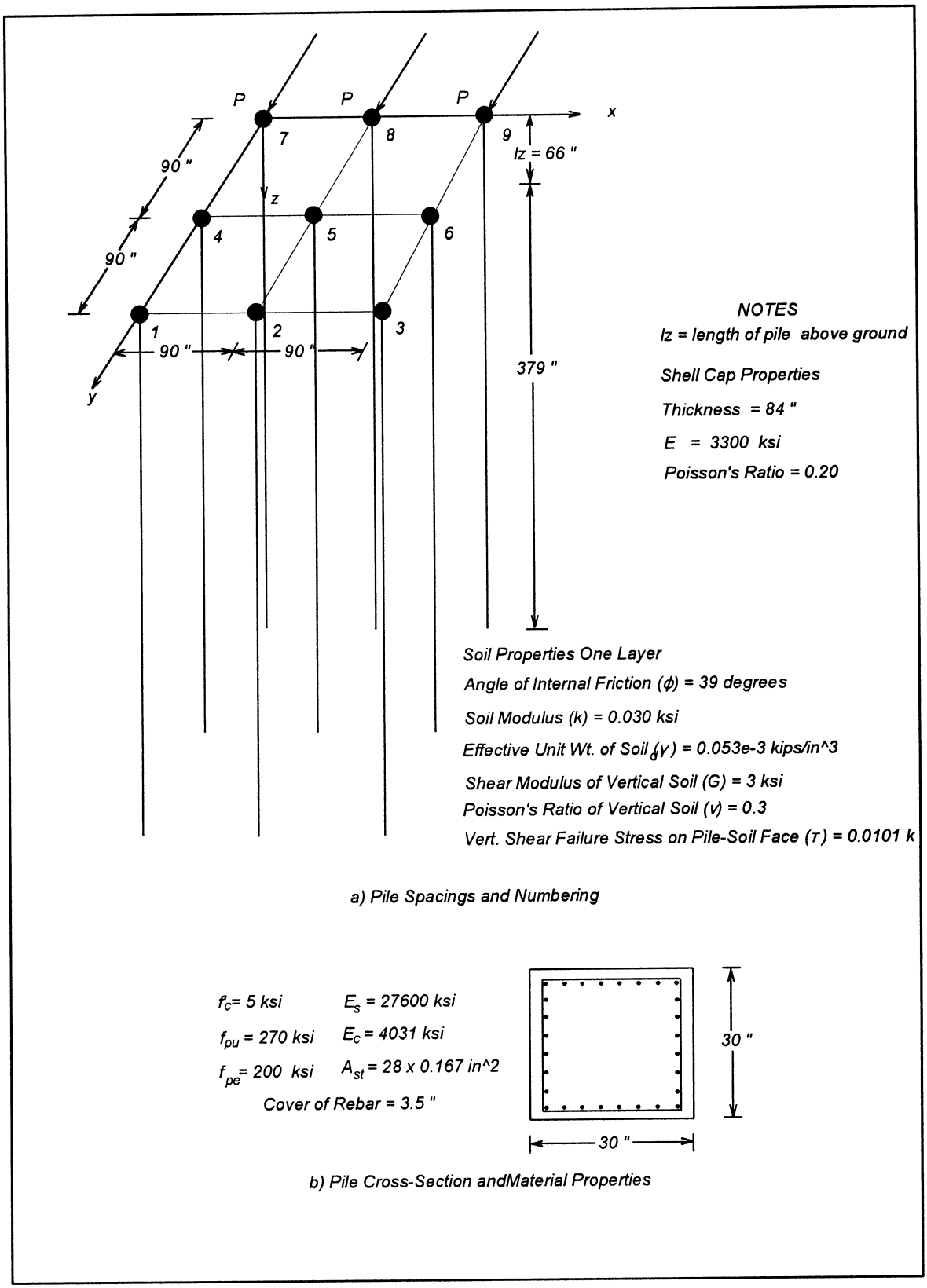

Figure 3-12. Nine Pile Laterally Loaded Group and Pile Cross-Section

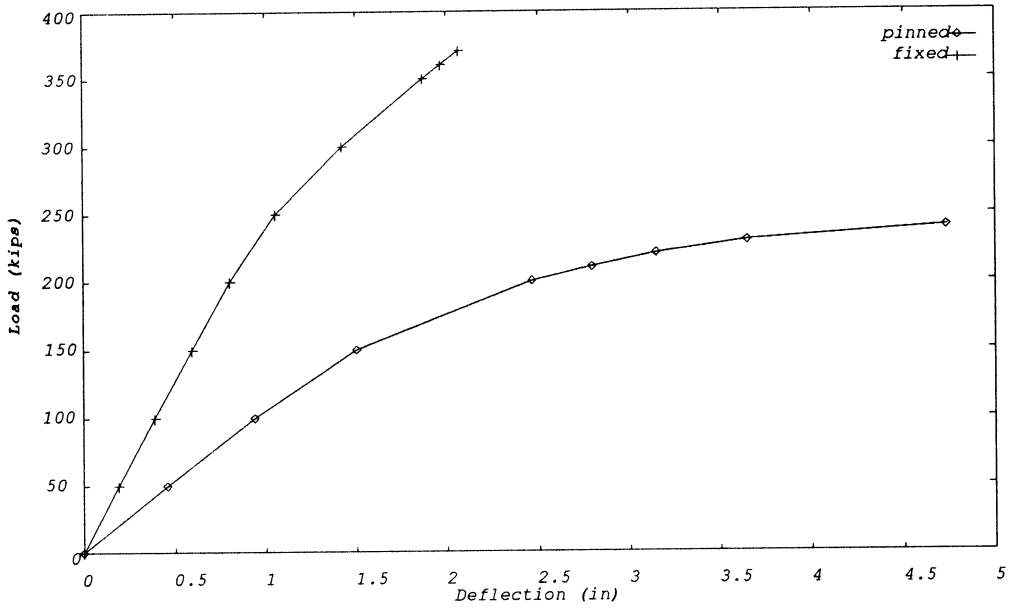

Figure 3-13. Plot of Lateral Load vs Leading Row Deflections

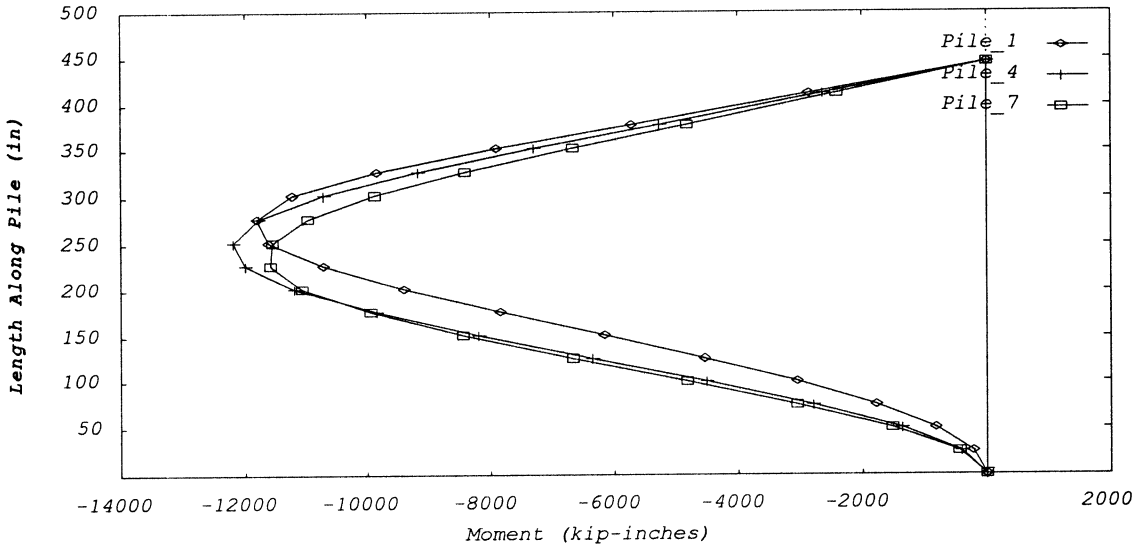

Figure 3-14. Plot of Moments Along Length of Pile (Free Head, P = 240 kips)

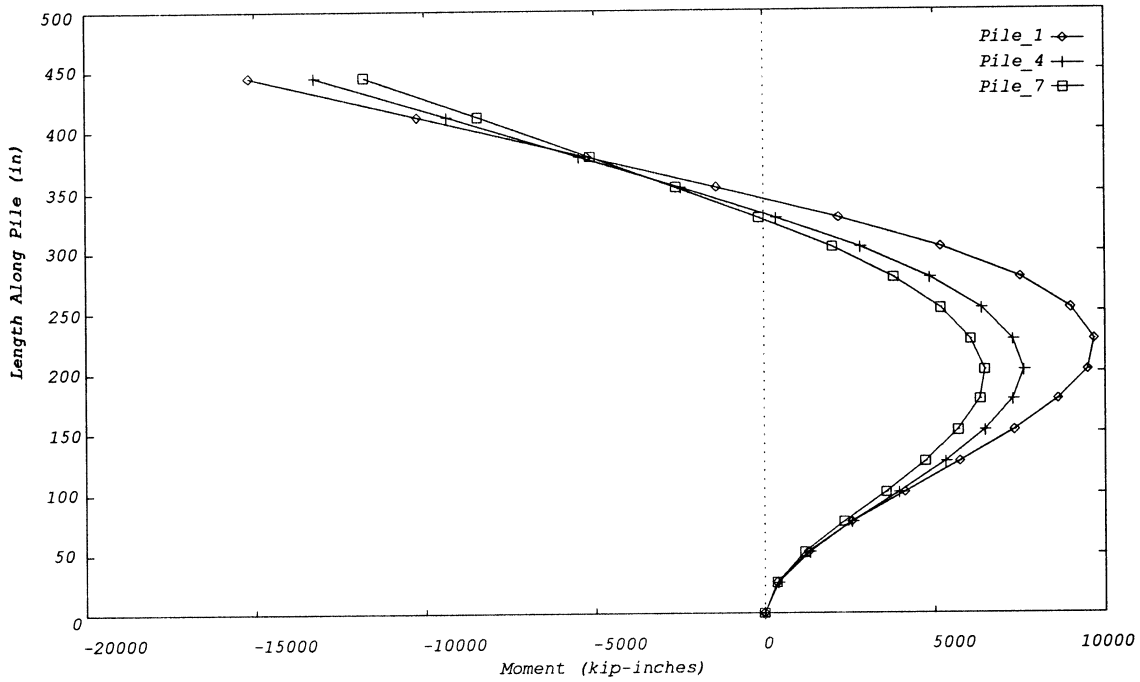

Figure 3-15. Plot of Moments Along Length of Pile (Fixed Head P=370 kips)

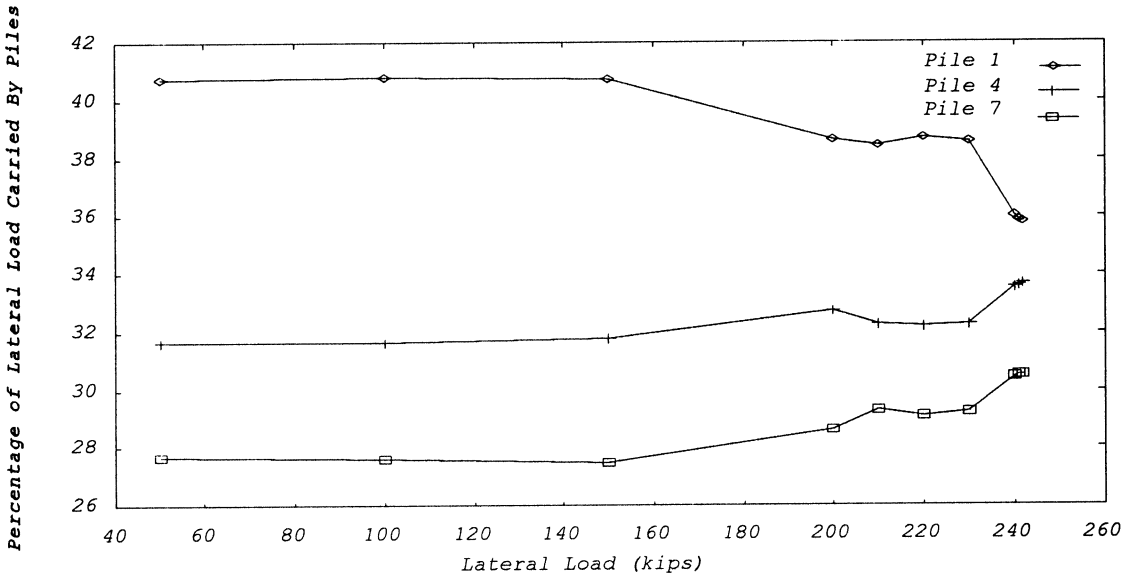

Figure 3-16. Lateral Load Distribution in a Nine-Pile Group

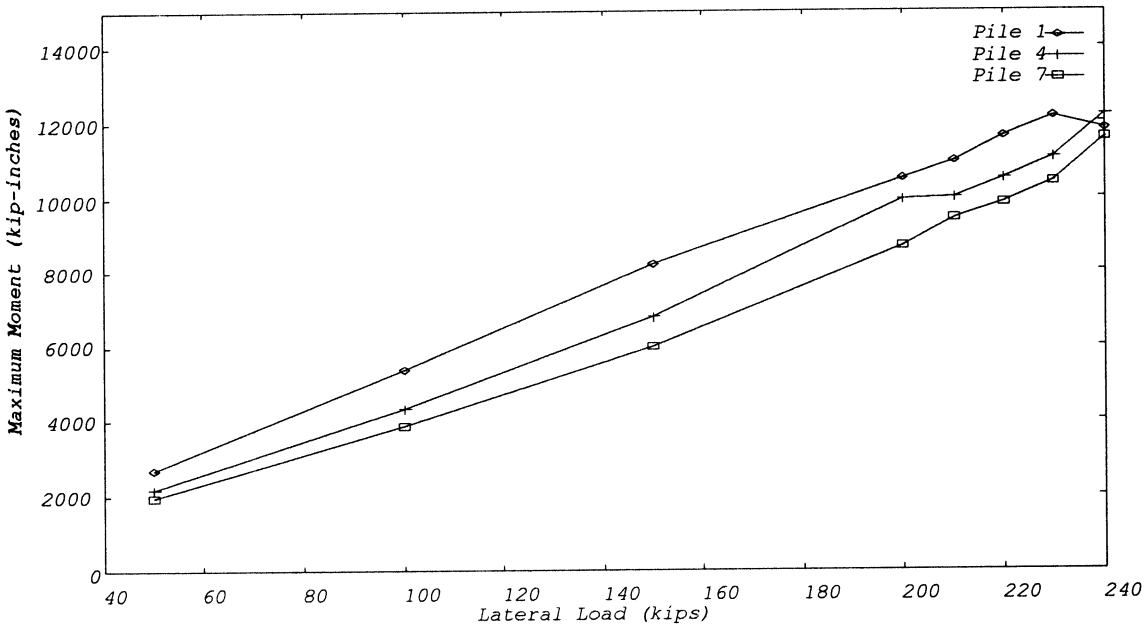

Figure 3-17. Variation of Maximum Moments vs. Load

```
9 PILE MODEL FOR REPORT
INCHES KIPS
L=1 M=1 D=1 O=1 S=1 P=1 T=1 F=1 C=1 B=1 : OUTPUT FLAGS
1 U=0                    :NUMLC,U
0 0 1.5e20 2 2             :IFLEX,IIP,TSTIFF,KTYPE,NLOPT
445.0 1 5 270 27600 4030 2  :TPL,MATOPT,FPC,FPU,ES,EC,KSTEEL
30 0 1 200                 :WIDTH,DV,ISTNOPT,PREST
66.0  0 1 2                ;Z,KCYC,KFIX,NSUB
3 3                        :NPX,NPY
90                         :DX1
90                         :DY1
.35 .45 .75                :PYMX1,PYMX2,PYMX3
.35 .45 .75                :PYMY1,PYMY2,PYmY3
0                          :NMPIL
150 0.25                   :MAXITER, TOLER
1                          :NLAYER
34.  0.030  .053E-3   0.  0.  0.  3 0.3 .0101 1425 2    :SOIL PROPERTIES
34.  0.030  .053E-3   0.  0.  0.  3 0.3 .0101           :SOIL PROPERTIES
5.0 0.3  200                  :QZ(1),QZ(2),QZ(3)
0                          :N1
STRUCTURE
N=0 :N
: DUMMY PIER COL PROPERTIES
: DUMMY PIER BEAM PROPERTIES
: DUMMY EXTRA BEAM PROPERTIES
E=3.3E3 U=.20 T=84         :E,U,T
0                          :NS
7 L=1 F=0,350              :NF,L,F
8 L=1 F=0,350                 :NF,L.F
9 L=1 F=0,350                 :NF,L,F
:
```

Figure 3-18. FLORIDA-PIER Input File for Nine Pile Model

CHAPTER 4
TEST EQUIPMENT

The existing centrifuge equipment for pile group modeling was not adequate for this research, and new equipment and centrifuge modifications had to be made before the testing program could be initiated. This chapter describes the modifications that have been made on the centrifuge and the new equipment that was constructed. This equipment will be used in future research, and a short description of the design criteria and factors of safety are mentioned when appropriate.

4.1 Geotechnical Centrifuge

The University of Florida has two centrifuges used for modeling and investigating geotechnical problems. The one used for this research is the larger of the two. The design capacity of the centrifuge was 6.5 g-tons when it was built in 1988 by John Gill. The radius from the center of rotation to the specimen platform was 1.613 meters (63.500 inches). The centrifuge has now been modified to allow a pay load of 12.5 g-tons, and the new distance from the center of rotation to the specimen platform is 1.610 meters (63.375 inches).

4.1.1 Centrifuge Changes and Capacities

The geotechnical centrifuge had to be modified in order to conduct this new experiment. The weight of the experiment including sample container, sand and pile driving equipment was considerably higher than the old experiments, and new changes had to be made. The old bearings for pivoting the swing up platform had to be changed. The new allowable capacity of the bearing plates and associated structure is 51,715 pounds, see Table 4-1 (the factor of safeties on the yield strengths are listed under F.S.). Using a factor of safety of 2.0 on the allowable capacity, the design capacity is 25,850 pounds.

Table 4-1. New Bearing Plates, Allowable Capacities

Item	Yield strength	F. S.	Allowable capacity
Steel bearing pins	36,000 psi	2.5	52,587 lbs
Bearing on steel plates	36,000 psi	1.11	71,360 lbs
Shear of bolts, grade 8	65,000 psi	1.54	51,715 lbs
Bearing on aluminum channels	35,000 psi	1.11	90,880 lbs
Aluminum channels, tension	35,000 psi	1.85	201,500 lbs

Allowable capacities (non factored) of new bearing plates and associated items. The factors of safety (F.S.) are on the yield strength of the materials.

The aluminum channels that carry the load, both counter weight and pay load, have not been changed because their capacity was found sufficient (90,880 pounds in bearing, and 201,500 pounds in tension). The counter weights are bolted onto two steel channels that transfer the load to the aluminum arms. The larger pay load of this experiment required that the old steel channels be replaced with larger and longer steel channels. The new steel channels have four stiffeners welded onto the c-channels between the webs. The stiffeners are used to prevent buckling of the channels.

4.1.2 New Model Platform

The old model platform on which the experiments were placed was designed by John Gill as part of his Ph.D. dissertation in 1988. The platform was designed to carry a point load of 29,750 pounds. The design of the platform was now found insufficient, and a new platform had to be constructed.

The old platform had a section modulus of 5.29 in^3, and the allowable stress for welded aluminum (alloy 6061) is 8,100 psi (1.85 factor of safety on the 15 ksi welded tensile yield strength). When assuming pinned connections and a point load acting at the center of the platform, the allowable stress was reached when the bending moment was 42,300 in-lbs.

The maximum allowable point load that the 24 inch long platform could carry was therefore 7,050 pounds (without a factor of safety on the applied load). This is 3 times less than the required capacity, and a new platform had to be constructed.

The new platform was constructed in regular A36 construction steel which can be welded without loss of strength. The platform was load tested in the centrifuge using a hydraulic jack . The platform was loaded against the center part of the centrifuge using a steel pipe device constructed for this purpose. On top of the platform the load was transferred in a fashion to simulate a uniform pressure like the one from the experiment during flight. Pinned connections at the vertical and horizontal interface between the platform and at the arms connecting it to the bearings was assumed. The platform was then constructed to withhold a design point load of 25,000 pounds. The factor of safety on the allowable capacity is 2.0. The platform carried 27,000 pounds of load for half an hour after which it was unloaded and reloaded to the same load. There was no visible permanent deformation to the construction and no deformation or buckling was visible during the load test. It can then be concluded that the design capacity of 25,000 pounds is safe against yielding the steel platform, and the overall capacity of the centrifuge has successfully been increased to a total pay load capacity of 12.5 tons.

4.1.3 Slip Rings and Rotary Union

The old slip rings were taken out because the new experiment had a need for 50 channels to transmit signals between the experiment and the data acquisition card in the computer. The old slip rings could transmit signals on a total of 40 channels. The four new slip rings have 24 channels each enabling transmission of a total of 96 channels. The channel wires from the slip rings have been permanently attached on two connection boards: one on the centrifuge and the other outside the centrifuge. The connection boards consists of four

screw terminals which are attached to a wooden board for electrical insulation. All the wires have been marked with numbers to enable identification of the individual channels.

The rotary union transfers the pneumatic and hydraulic pressure to the experiment. The rotary union has been used in past centrifuge experiments, but the seals were broken and it had to be rebuilt in order to function. The rebuilt rotary union has three ports which transfers air pressure on one port and inlet and outlet hydraulic fluids on the other two. The hydraulic system is closed and the supply/return fluid is supplied/recovered in two tanks outside the centrifuge. This operation requires two ports on the rotary union in order to function.

4.2 Model Equipment

The lateral loading of large pile groups requires a different approach when compared to the previous research on three row pile groups in the centrifuge. This experiment is testing groups with 4, 5, 6, and 7 rows of piles, and a larger sample container was needed. The pile driving has to be conducted in flight (at 45 g) otherwise the stress level and soil-pile interaction will differ from prototype behavior (McVay et al., 1994).

4.2.1 Sample Container

The old sample container is a cylindrical aluminum container 12 inches high and 11.9 inches in diameter. The largest pile group (8 pile rows with a 5 diameter pile spacing) measures 5 5/8 inches by 13 1/8 inches between the centers of the outer piles. It was therefore necessary to construct a new sample container. The new sample container is designed to contain the largest pile group mentioned above and fit on the centrifuge model platform. It was constructed with a rectangular shape having inside dimensions of 10 inches wide, 18 inches long and 12 inches high (see Figure 4-1). The container is constructed of aluminum

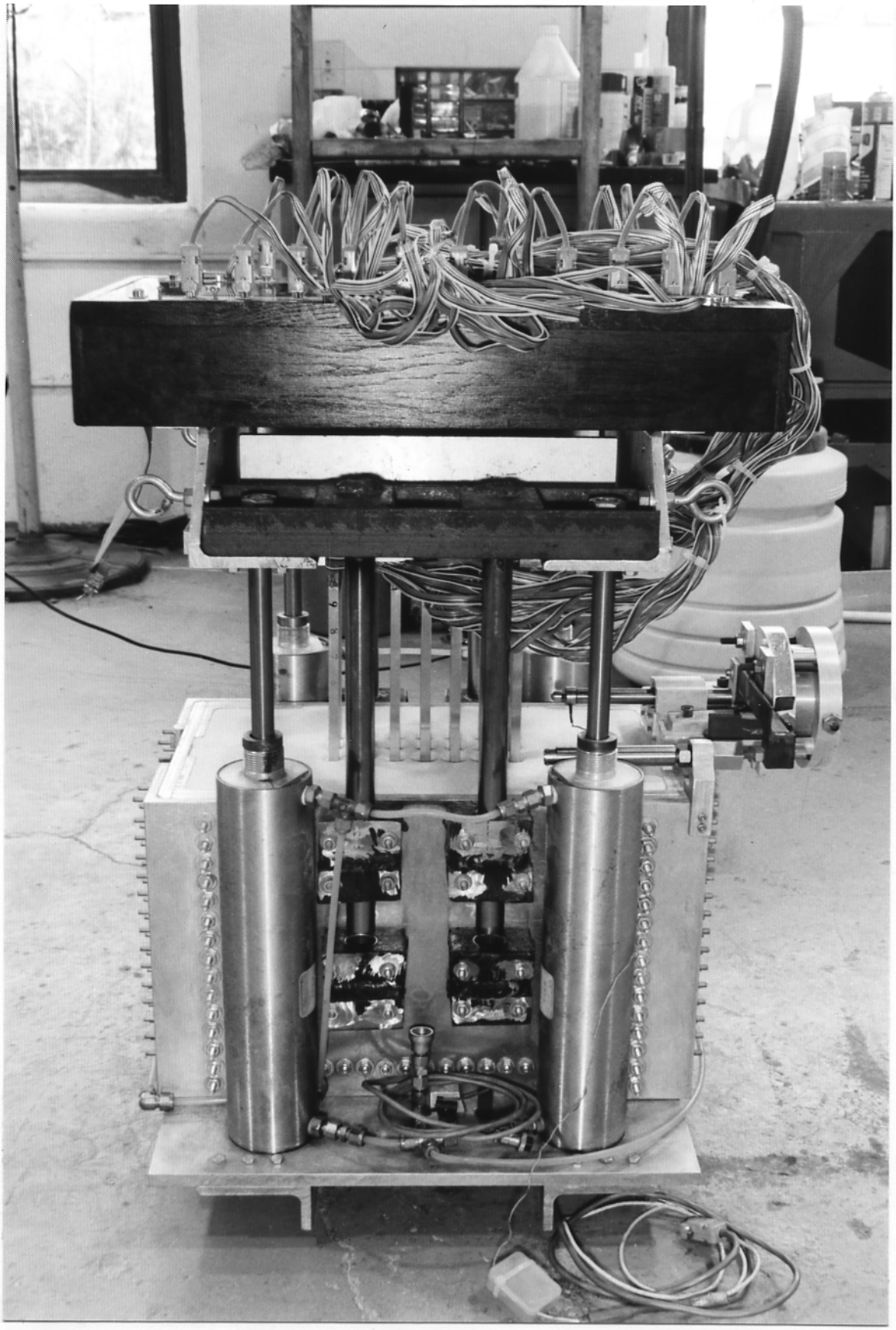

Figure 4-1. Sample Container, Driving Pistons and Data Acquisition

alloy 6061, and bolts are used for all connecting joints. The sample container is designed to withstand a triangular distributed soil pressure of 60 psi at the base of the container and 0 psi at the top (soil surface). A soil with a unit weight of 100 pcf and a 30 degree internal friction angle will at rest produce a horizontal triangular shaped pressure distribution on the wall with a maximum pressure of 17 psi (at 45 g's) at the base of the container. During the pile driving a maximum vertical pressure of 72 psi is transferred to the bottom plate through the soil.

The base plate of the sample container is made 5 inches wider on each side of the rectangular box in order to mount the hydraulic pistons on the base plate. The base plate is reinforced with two aluminum channels bolted to the under side of the plate. This prevents it from buckling during the pile driving.

A wind shield made of a 1/8 inch thick steel sheet covers the sand surface and is attached to the sample container with wing screws. A rectangular opening is cut in the wind shield to make a opening for the pile group. The shield keeps induced wind from blowing the sand during rotation in the centrifuge. A 1/4 inch vertical distance is kept between the sand surface and the shield so the surface is not disturbed.

4.2.2 Hydraulic Pile Group Driving

The pile groups are driven in flight at 45 times the normal gravitational field (45 g's), and the piles within the group are driven simultaneously. The pile driving requires a high driving force in order to drive the 12, 15, 18, 21, or 24 piles at the same time. The pile driver consists of four hydraulic pistons and a driving platform which inter connects the pistons. The pistons are heavy duty 3 inch diameter pistons with a 10 inch stroke. The pistons are rated at 500 psi hydraulic pressure and can withhold high eccentric loading because of their double seal construction and 3/4 inch solid steel shafts. Each piston can deliver a retraction force of 3,300 pounds at a hydraulic pressure of 500 psi which results in a total maximum

static driving force of 13,200 pounds. The solid square model piles have a width of 3/8 inches, and with a model factor of 45 (at 45 g's) the prototype piles are 16 7/8 inches wide. The maximum delivered driving force applies an equivalent prototype force of 1,110 tons on each pile in a 24 pile group. If the side friction is neglected and only tip resistance considered during driving, the pile driver is capable of delivering a pile tip pressure of 1,465 psi on a 24 pile group.

The four pistons are located close to the container wall (Figure 4-1) with one in each corner on the base plate of the sample container. The driving platform is mounted on top of the pistons (Figure 4-1) which as earlier mentioned interlocks the pistons and assures that they will move down simultaneously and drive the pile groups vertically downwards.

The hydraulic system that supplies the pile driving pistons with hydraulic fluid consists of two Freon recovery tanks containing hydraulic oil and a nitrogen tank delivering the driving pressure. The Freon tanks are 2/3 filled with hydraulic oil and are connected to the hydraulic pistons via the rotary union using 3/8" and 1/4" pressure tubings and Swagelock fittings. The four pistons are all inter connected on the experiment. One tank is for supply of hydraulic fluid and the other for recovery depending on if the pistons are expanding or retracting. A switch board in the control room has been made where valves are used to control the operation of the hydraulic system. The two saturated oil lines from the Freon tanks are routed to the control room and have on/off valves connected in order to stop the piston movement completely (Figure 4-2). Another valve controls which tank gets pressurized. Before the lines from this valve go to the tanks, a three way valve is inserted. The three way valve can be set to either closed, pressurizing, or vent. When a tank is pressurized the other tank is set for venting (atmospheric pressure). A schematic of the pressure system is shown of Figure 4-3 (the valves are set for expanding the pistons).

Figure 4-2. Hydraulic Control and Data Acquisition

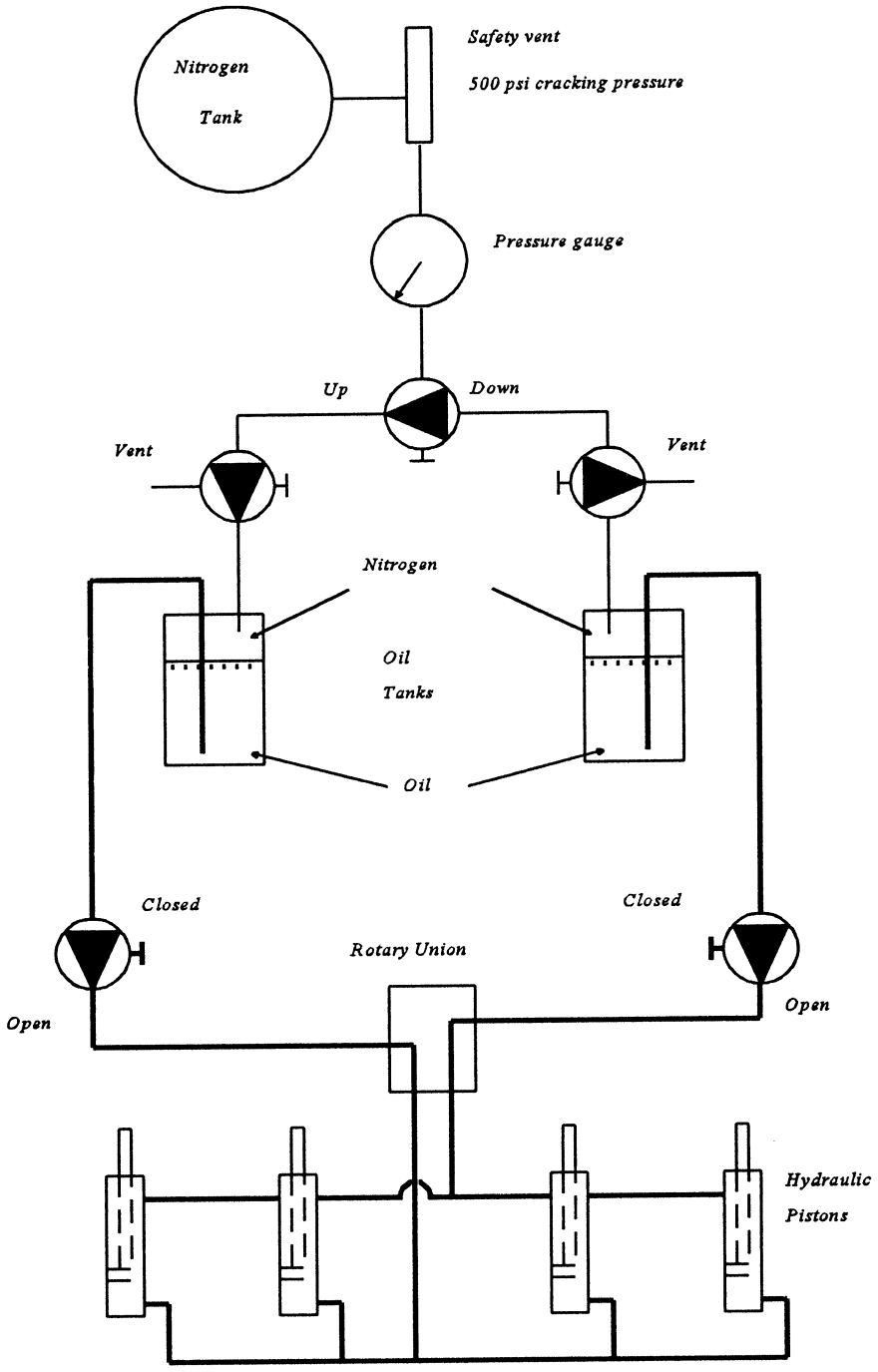

Figure 4-3. Hydraulic Schematic

The Freon recovery tanks have been tested at 750 psi by the manufacturer and they have been rated at 350 psi maximum pressure for safety reasons. The tanks have been tested at the University of Florida at 500 psi pressure, and no rupture or damage occurred. For safety reasons, the tanks are placed out of reach down a stairway next to the centrifuge. The nitrogen tank supplies a 2,000 psi pressure which is regulated to the necessary driving pressure. As an extra safety precaution a safety valve is connected to the nitrogen outlet and the cracking pressure is set for 500 psi which can never be exceeded.

4.2.3 Pneumatic Pile Group Loading

The pile groups are being subjected to a lateral load using an air piston (Figure 4-4). The air piston has a pressure rating of 125 psi. The inside diameter is 3.5 inches (maximum force -1200 lbs), and the maximum stroke length is one inch. The air piston is controlled in the control room using a regulator (Figure 4-2), and the pressure is read on a gauge with ½ psi divisions. The air pressure is supplied from the regulator through a 1/8 inch high pressure tubing and through the rotary union directly to the piston. The piston is connected for expansion of the piston rod only. The maximum load that the piston can supply is 5.35 kN (1,200 pounds) which in prototype dimensions (at 45 g) would be 10.84 MN (1,215 tons).

4.2.4 Piles and Pile Cap

The piles are made of solid square aluminum (alloy 6061) bars with a width of 9.525 mm (3/8 inches) and an overall length of 304.8 mm (12 inches). The pile cap is constructed of pieces where one pile cap piece holds one row of piles (3 piles). The pile cap pieces are then connected in the desired configuration (4, 5, 6, or 7rows) using threaded steel rods (Figure 4-5). The individual pile cap pieces hold the piles in position in a square slot (cut in the side of the cap piece). When all 3 piles are positioned in a pile cap piece, one side of the

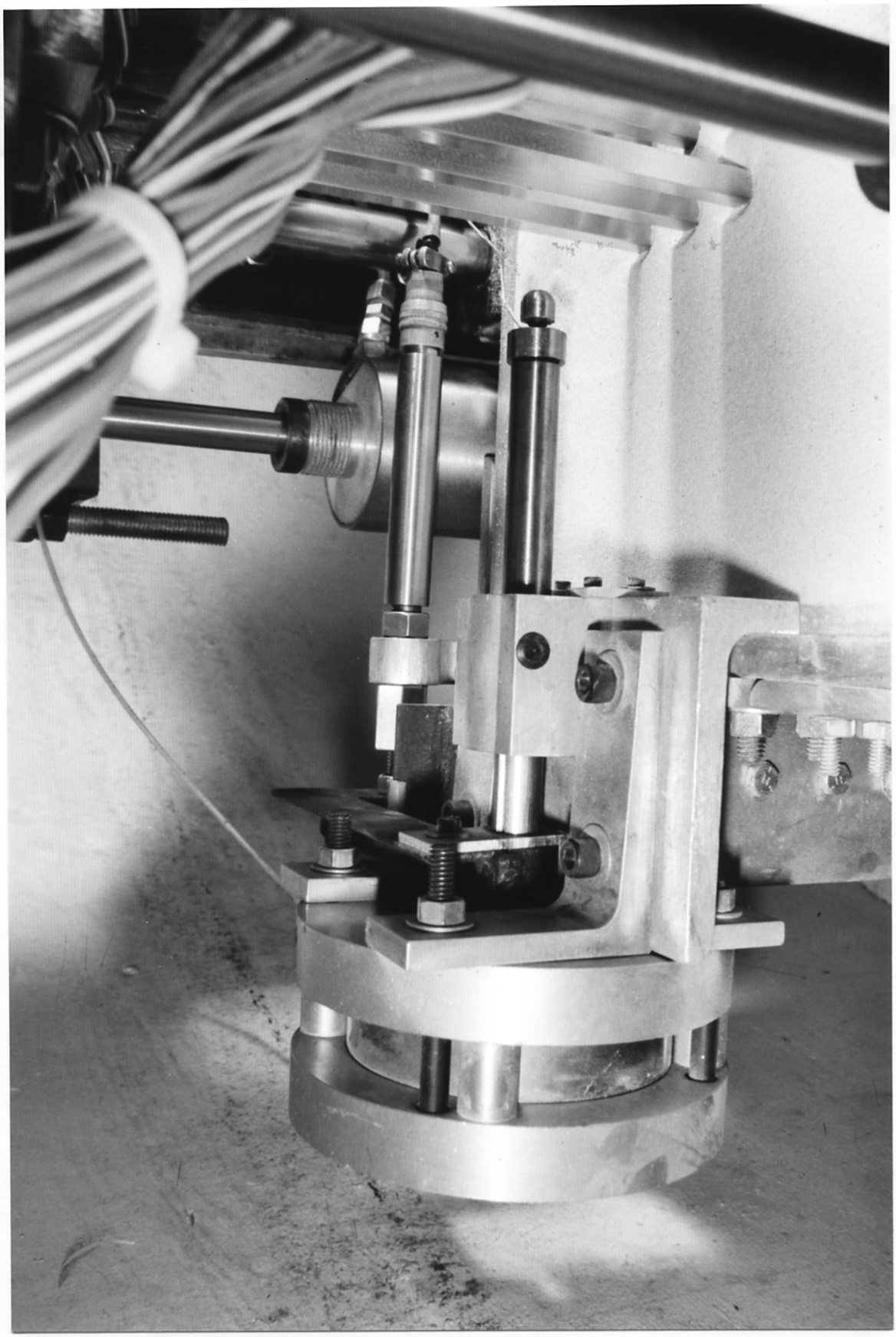

Figure 4-4. Lateral Loading Piston - Maximum Load of 1200 lbs

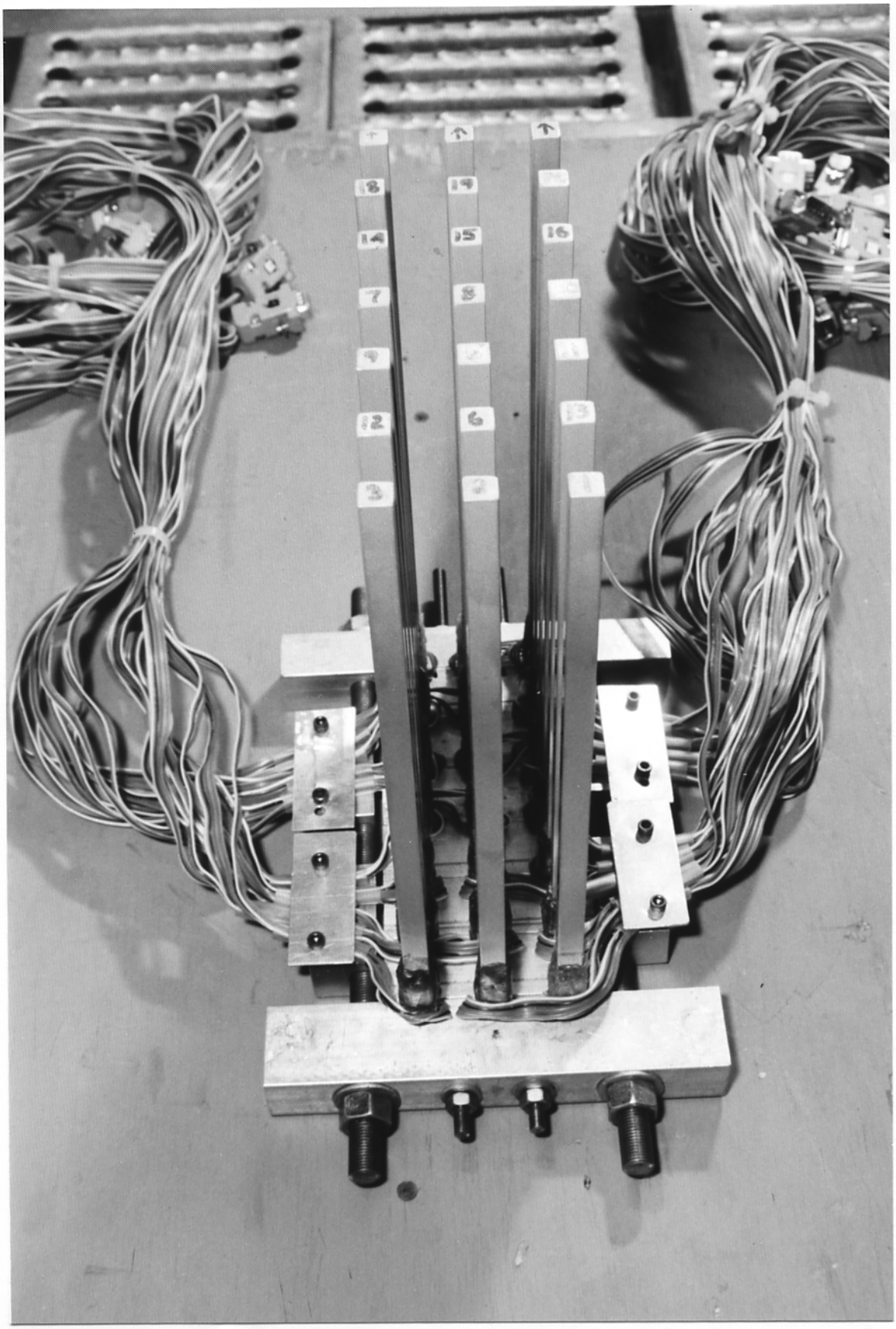

Figure 4-5. Model Square Piles and Pile Cap

piles are free. This side will be clamped to the next pile cap piece holding the piles in position in all directions.

For the 3D pile cap, two pile cap end pieces are made with their width larger than their center pieces. Two ½ inch holes are made in the end pieces, and they are located on the outside of the center pile cap pieces leaving a 1/16 inch space between them. Two threaded steel rods are inserted in the loading direction through the holes in the pile cap between the piles, and two larger rods are inserted through the end pieces going on the outside of the piles. When the pile cap pieces are put together in a desired pile cap configuration, and the steel rods are inserted, nuts are put on the end of the steel rods. The nuts are tightened, and the piles are then clamped effectively inside the pile cap. Figures 4-5 and 4-6 show how a 4 row pile cap with 3D spacing is assembled.

During the lateral loading, large bending moments will occur in the pile cap surrounding the piles. The pre compression of the pile cap (delivered by the steel rods) is dimensioned to exceed the tension forces in the outer fibers when the bending of the cap occurs during lateral loading. In this way, the piles will continue to have a fixed pile head condition throughout the test.

4.3 Electronic Measurement System

The experiment is designed to gather information about the load distribution within the pile group when the pile group is subjected to lateral loading. The applied lateral load is measured by a miniature 1,000 lb (455 kg) load cell, and the lateral displacement of the pile group is measured by a spring loaded linear variable differential transducer (LVDT). The load distribution within the pile group is measured by strain gages.

Pile Group 4 Rows, 3D Spacing.

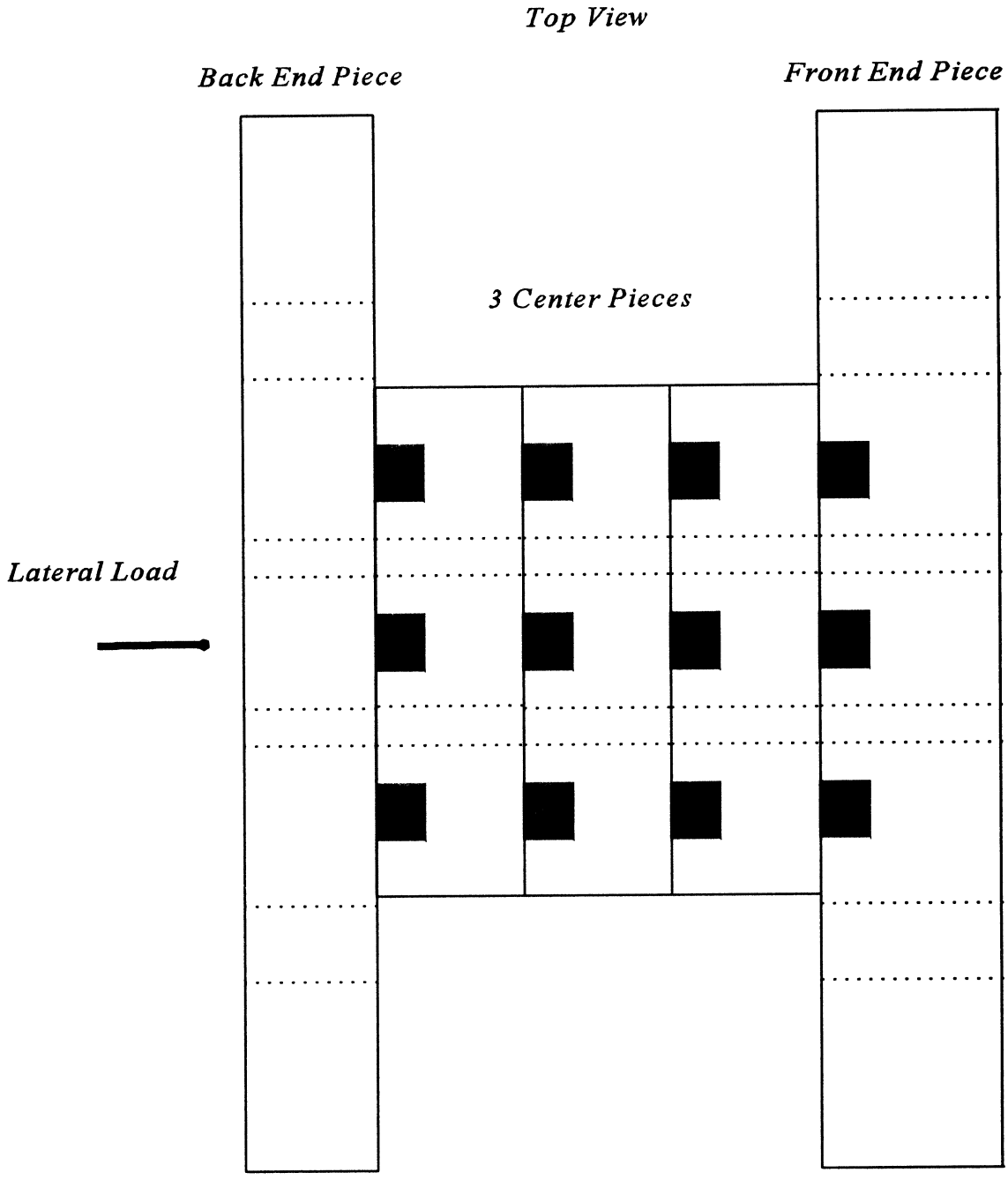

Figure 4-6. Pile Cap, 4 Rows, and 3D Spacing

4.3.1 Strain Gauges

The square aluminum piles have each been instrumented with two full circuit strain gage bridges (see Figures 4-7 and 4-8). The strain gages are of type SG-3/1000-DY43 from Omega. There are two parallel gages on each carrier which is encapsulated and has 4 solder pads for wire attachment. The gage carriers are attached to the piles, two on the front and two on the back, using a two component adhesive. The gage grids are each 3.0 mm wide and 3.0 mm high and the carriers measures 9.0 mm by 9.0 mm. The gages can tolerate a maximum strain of 3 percent meaning a maximum compression or stretching of 0.09 mm. The gages have an electrical resistance of 1000 ohms, a maximum permitted energizing voltage of 10 volts and a gage factor (GF) of 2.05.

The strain gages are connected in a full bridge configuration for measurements of the bending moments. Wires are soldered to the solder pads on the gages and are from there connected to terminal pads on the side of the piles. The gages are connected in the correct full bridge configuration on these solder terminals. Lead wires are also connected to the terminal pads, and they transmit the input and output signals to and from the strain gage bridges (4 wires from each bridge). The strain gage bridges are shown on Figures 4-9, 4-10, 4-11, and 4-12 where the locations and wiring schemes are indicated. The two carriers with two strain gages on each are located at the same horizontal level on the piles, and these gages are connected in the full bridge configuration. The two strain gage bridges are located between the under side of the pile cap and the sand surface with a center to center spacing of about 25.4 mm (1.0 inch). When the piles are subjected to a lateral load, the strain gages are in tension on the front side of the pile (side closest to the load) and in compression on the back.

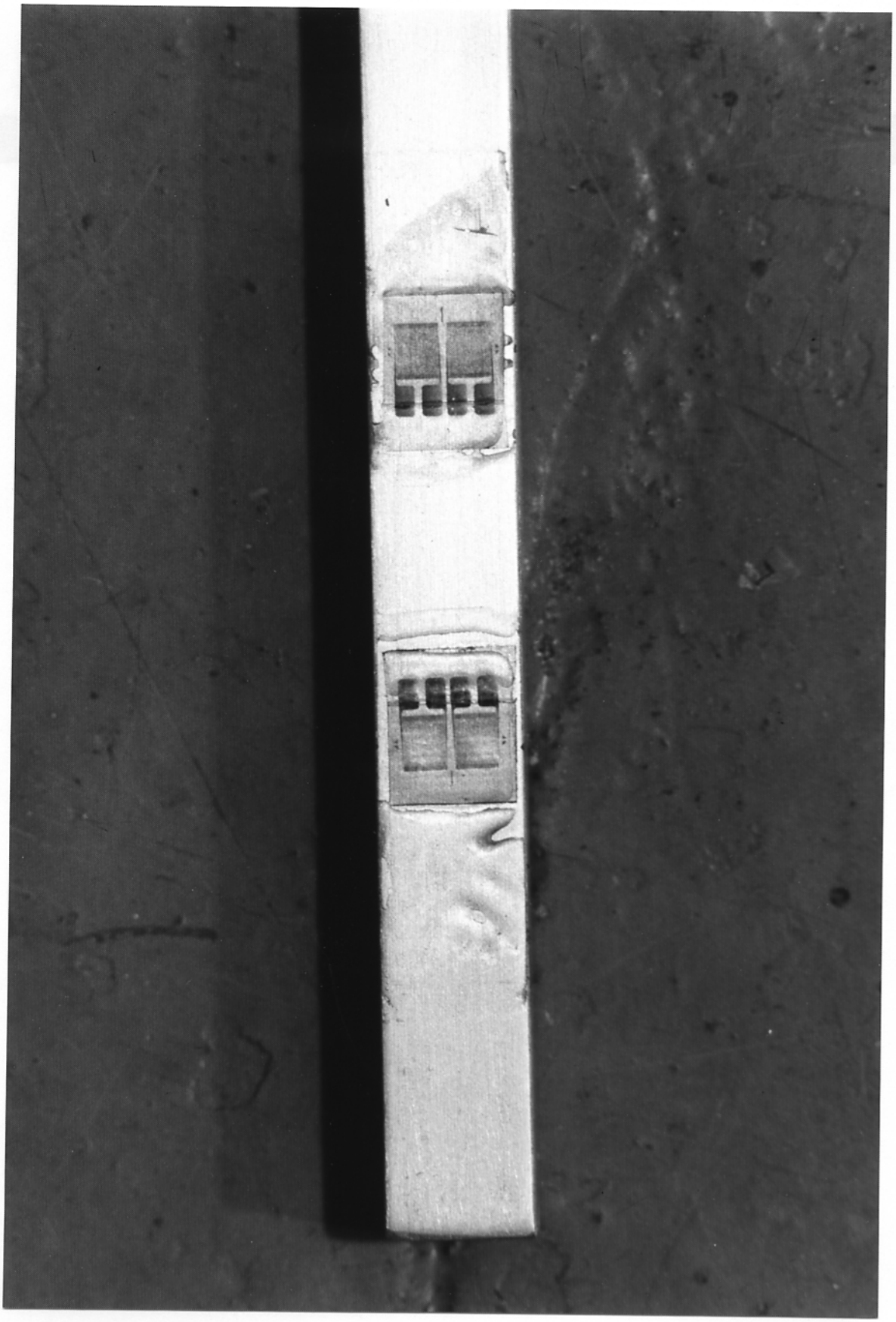

Figure 4-7. Strain Gauges

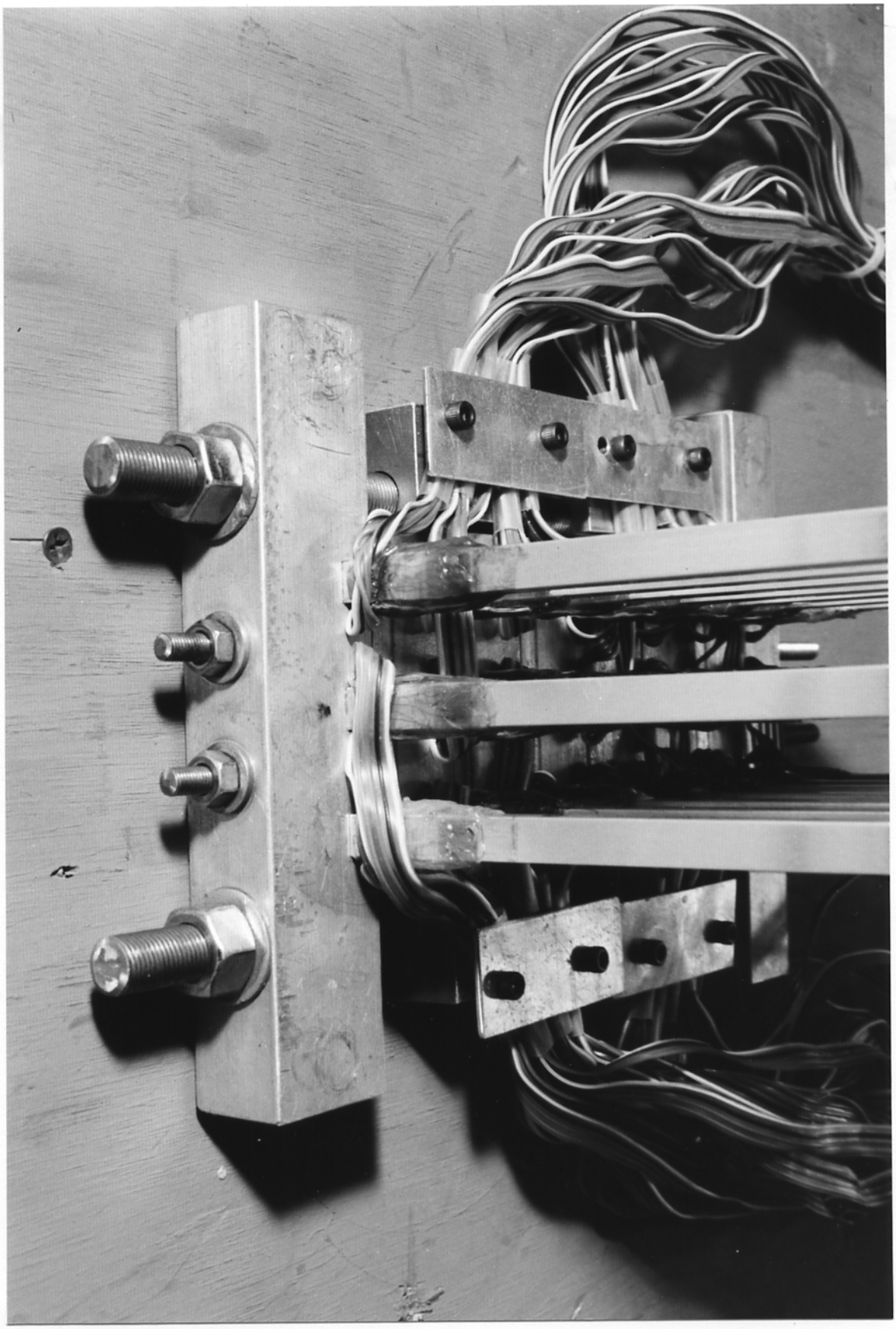

Figure 4-8. Instrumented Piles

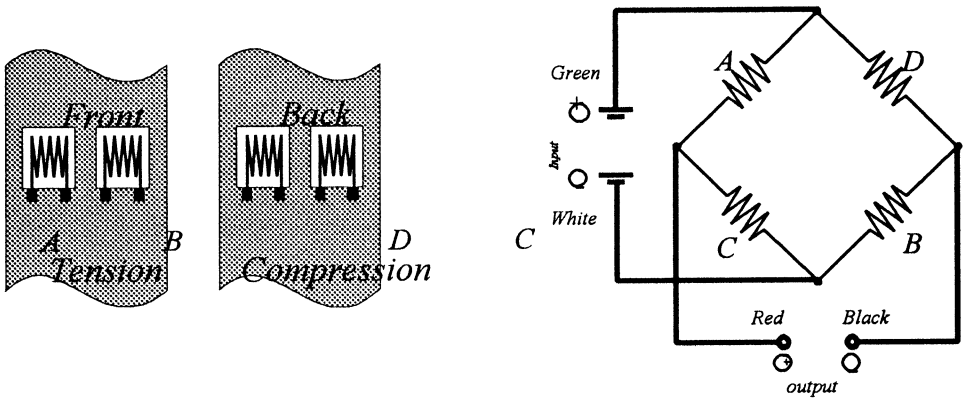

Figure 4-9. Strain Gauge Bridges

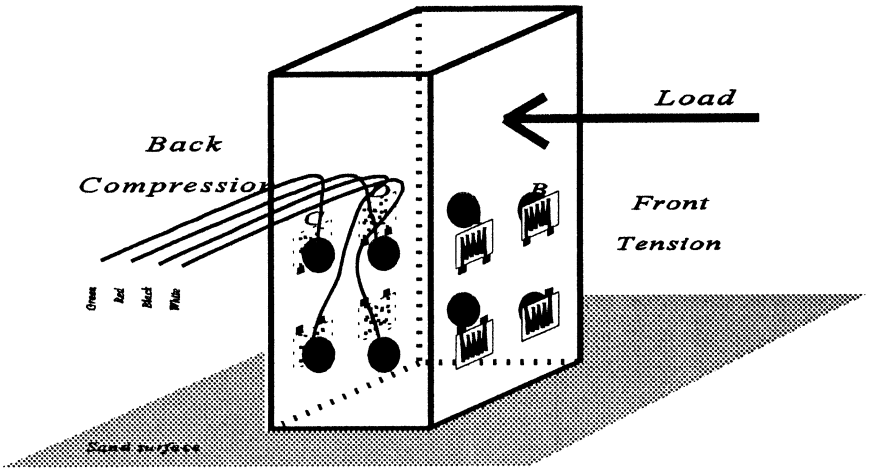

Figure 4-10. Strain Gauge Bridges on a Pile

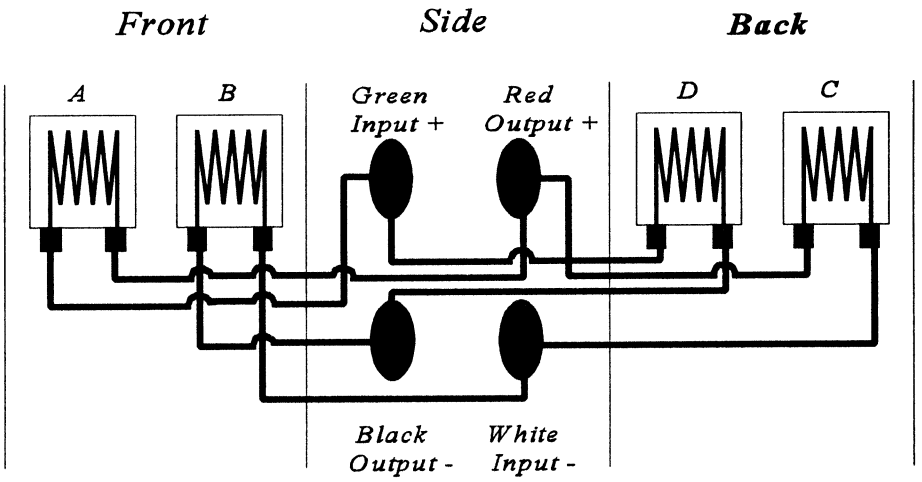

Figure 4-11. Top Strain Gauge Wiring

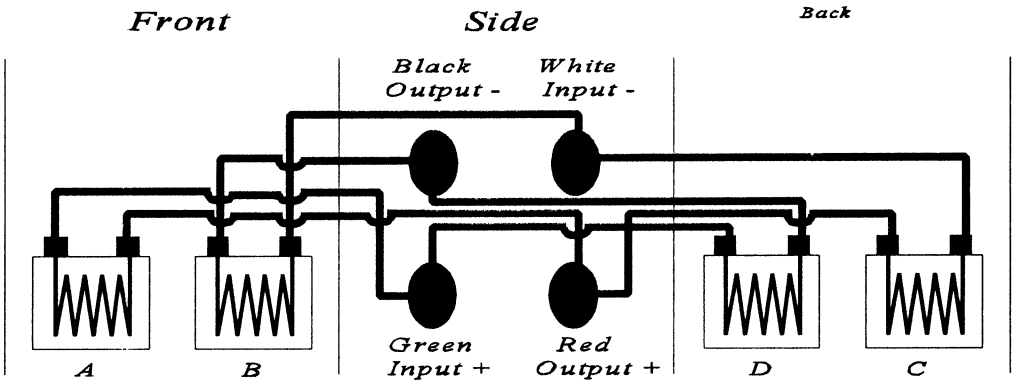

Figure 4-12. Bottom Strain Gauge Wiring

The strain and bending moment from a single strain gage bridge can be calculated from the following equations:

Strain $$\epsilon = \frac{\left(\frac{V_{out}}{V_{in}}\right)_{unstrained} - \left(\frac{V_{out}}{V_{in}}\right)_{straine}}{GF}$$

Bending Moment $M = E \bullet S \bullet \epsilon$

Section Modulus $S = b \bullet h^2 / 6$

GF Gage Factor (2.05)

V_{in} Input (energizing) voltage (10.0 Volt)

V_{out} Output voltage (range: 0 ± 0.001 Volt)

E Modulus of elasticity (73,100 MPa = $10.6\ 10^6$ psi

b Width of section (3/8 inch)

h Height of section (3/8 inch)

The bending moment and measured output voltage is linearly proportional, and the relationship can be established by calibrating the pile strain gage bridges with a known bending moment. The theoretical relationship is shown in the following example.

Example:

> The relationship between measured voltage output, strain and bending moment for a instrumented pile with a cross section area of 9.525 mm by 9.525 mm (3/8 inch by 3/8 inch) would be:

Section modulus $S = b \bullet h^2 / 6$

$$= \frac{1}{6}\cdot\left(\frac{3}{8}\ in\right)^3 = \frac{9}{1024}\ in^3 \approx 0.008789\ in$$

Bending Moment $M = E \bullet S \bullet \epsilon$

$$= 10.6 \cdot 10^6 \frac{lbs}{in^2} \cdot \frac{9}{1024} in^3 \cdot$$

$$M = 93{,}164\ in \cdot lbs \cdot \epsilon$$

Strain

$$\epsilon = \frac{\left(\frac{V_{out}}{V_{in}}\right)_{unstrained} - \left(\frac{V_{out}}{V_{in}}\right)_{straine}}{GF}$$

$$= \frac{\left(\frac{V_{out}}{10\ V}\right)_{unstrained} - \left(\frac{V_{out}}{10\ V}\right)_{straine}}{2.05}$$

Bending moment and measured voltage relationship

$$M = 4{,}545 \frac{in \cdot lbs}{Volt} \cdot \left[(V_{out})_{unstrained} - (V_{out})_{strained}\right]$$

The instrumented piles measure the bending moment at two locations above the sand surface. The relationship between bending moment and shear force can be expressed in the following equation:

$$V = -\frac{dM}{dx} + P\frac{dy}{dx}$$

Where

V Shear force

dM/dx Change in bending moment (M) with respect to vertical distance (x)

P Axial load

dy/dx Rotation

When the piles are subjected to an eccentric axial load it contributes to the shear force acting on the pile. This phenomena is called the P-delta effect and is represented in the above equation as P × dx/dy. The P-delta effect was ignored in this work since the dy/dx was identified as small. Since the strain gages are located between the pile cap and the sand surface, there are no external forces influence the moment between the two strain gage bridges. Therefore, the change in bending moment between them is a function of the total shear force acting on the pile below the sand surface. This is shown in the following example.

Example:

> The strain gages are placed with a center to center spacing of 1.01 inch and the output voltage on the top and bottom bridges are; -6.191 mV and 5.818 mV. The unstrained bridge outputs are -9.504 mV and 4.678 mV for the top and bottom bridges. The bending moments and shear force can be calculated as:

Bending moment at center of top strain gage bridge:

$$M_{top} = 4.545 \ \frac{in \cdot lbs}{mV} \cdot (-9.504-(-6.191)) \ mV = -15.06 \ in \cdot lbs$$

Bending moment at center of bottom strain gage bridge:

$$M_{bottom} = 4.545 \ \frac{in \cdot lbs}{mV} \cdot (4.678-5.818) \ mV = -5.18 \ in \cdot lbs$$

Total shear force acting on the pile (soil resistance):

$$V = -\frac{\Delta M}{\Delta x} = -\frac{(-15.06-(-5.18)) \ in \cdot lbs}{1.01 \ in} = 9.78 \ lbs$$

The relationship between output voltages, bending moments and shear force is determined by calibrating the piles. First the relationship between the output voltage and bending moments at the top and bottom strain gage bridges is established. Secondly, the

relationship between bending moments and shear force is determined. The strain gage bridges position on the piles are also determined using these calibration procedures. Each pile will have its own three calibration factors and bridge locations. The following formulas are used in calculating moments and shear force. The typical numbers for the moment factors are 48,000 kg-mm/volt, and the shear calibration factors are about 25.4 mm.

Bending moment (for both top and bottom bridges):

$$M_{bending}[kg \cdot mm] = (V_{out} - V_{out,zero})[volt] \cdot C_{moment}\left[\frac{kg \cdot mm}{volt}\right]$$

$$C_{moment} \approx -48{,}000 \frac{kgCDOTmm}{volt}$$

Shear force:

$$V_{shear}[kg] = \frac{(M_{bending,top} - M_{bending,bottom})[kg \cdot mm]}{C_{shear}[mm]}$$

$$C_{shear} \approx 25.4 \ mm$$

The calibration procedure is explained in Chapter 5.

4.3.2 Load Cell and LVDT

The load cell is mounted on the tip of the piston shaft which is used to transfer the pneumatic piston load to the pile group. The load cell has a small rounded steel piece mounted on it which is used to push against the pile group. The load cell has a 1,000 pound capacity, and the calibration factor for the load cell is 0.012871 mV/pound at 5 V excitation voltage. The voltage output is maximum at 2 mV, and it was therefore decided to connect the load cell to the multiplexers which are also used for transferring output signals from the strain gages to the computer. The multiplexers have an internal amplifier, and the low voltage

output from the load cell is amplified 300 times through the multiplexers. A low band pass filter on the multiplexers also helps to increase the accuracy on the load cell readings.

The Lateral deflection of the pile group is measured by a Linear Variable Transformer or LVDT which is mounted on the container wall parallel to the loading direction of the group. A solid steel cylinder is attached to the pneumatic piston shaft, and a steel angel is welded onto the cylinder. The steel angle is extended to reach the spring loaded LVDT shaft. This enables measurements of the piston displacement by the LVDT. The steel angle applies a torsional moment to the piston rod. Rotation of the angle is prevented by resting it on the corner of an aluminum plate. The friction between the steel angle and the plate (1/1000 square inch) is negligible. The mounting fixture for the LVDT is rigid and placed on the upper corner of the container where practically no deflections will occur. The LVDT is supplied through the slip rings with -15 V and +15 V for the low and high DC voltage supply. The output voltage is grounded to the voltage supply on the low output end. The LVDT has a travel of ± 1/4 inch in the linear range and the output voltage ranges from -13 V through 10 V. During the load test about 0.07 inch of displacement occurs. The output voltage from the LVDT is measured by the data acquisition card without being amplified or filtered.

4.3.3 HRES Data Acquisition Card

The data acquisition system used for this centrifuge research is new and differs from the one used earlier. The existing Hewlett Packard data acquisition system used in previous centrifuge research has been abandoned. The new system consists of a 486-33MHz Personal Computer with a 16 bit HRES card for voltage readings and three EXP-20 multiplexers with 16 channels each (48 channels total).

The data acquisition card can be programmed to handle polar or bipolar voltage readings and to amplify the input voltage with a gain of 1, 2, 4 or 8. The HRES card can

sample readings on 8 analog channels. The analog signals are measured and translated into a digital signal by the data acquisition (HRES) card. The precision on the 16-bit card is 2^{16} bytes (65,536 bytes) per 10 volt (uni polar) when the gain is set at one. Because negative voltage readings can occur the card is set for bipolar measurements. This enables voltage measurements between -10 V and +10 V with a translation factor of 0.305 mV/byte using a HRES programmable gain setting of one. The HRES card can transmit a 4 bit digital output signal which is used to control the relay boxes (EXP-20 multiplexers). The signals are transmitted through a 50 pin ribbon cable from the HRES to a connector box (placed out of the centrifuge) where all 8 input channels can be connected. The connector box (see Figure 4-13) is used for sampling the load cell (on channel 5) used in weighing the sample container (soil density determination) and for sampling the LVDT (on channel 4).

4.3.4 EXP - 20 Multiplexers

The three EXP-20 multiplexers are placed on top of the sample container and are used to sample the strain gage bridges and the load cell (see Figure 4-13). The multiplexer boxes have a low band pass filter which is connected using pin settings for each individual channel. The low band pass filters reduce the standard deviation when the centrifuge is operating with 50 percent on the strain gage readings and 80 percent on the load cell readings. The multiplexers are set to amplify the output signals 300 times. The amplification can also be set for gains of 1, 10, 100, 200, 300, 500, 600, 700 and 800. When using a HRES gain setting of one, and taking bipolar voltage readings, and a EXP-20 gain of 300, the voltage output from the signal source is translated to a digital signal by the HRES card with a factor of 1.017 microvolt per byte (calibrated using the strain gage bridges on the piles). When using this setting the maximum and minimum source outputs that can be read through the EXP-20's are ± 33,333 microvolt (equal to ± 32,768 bytes).

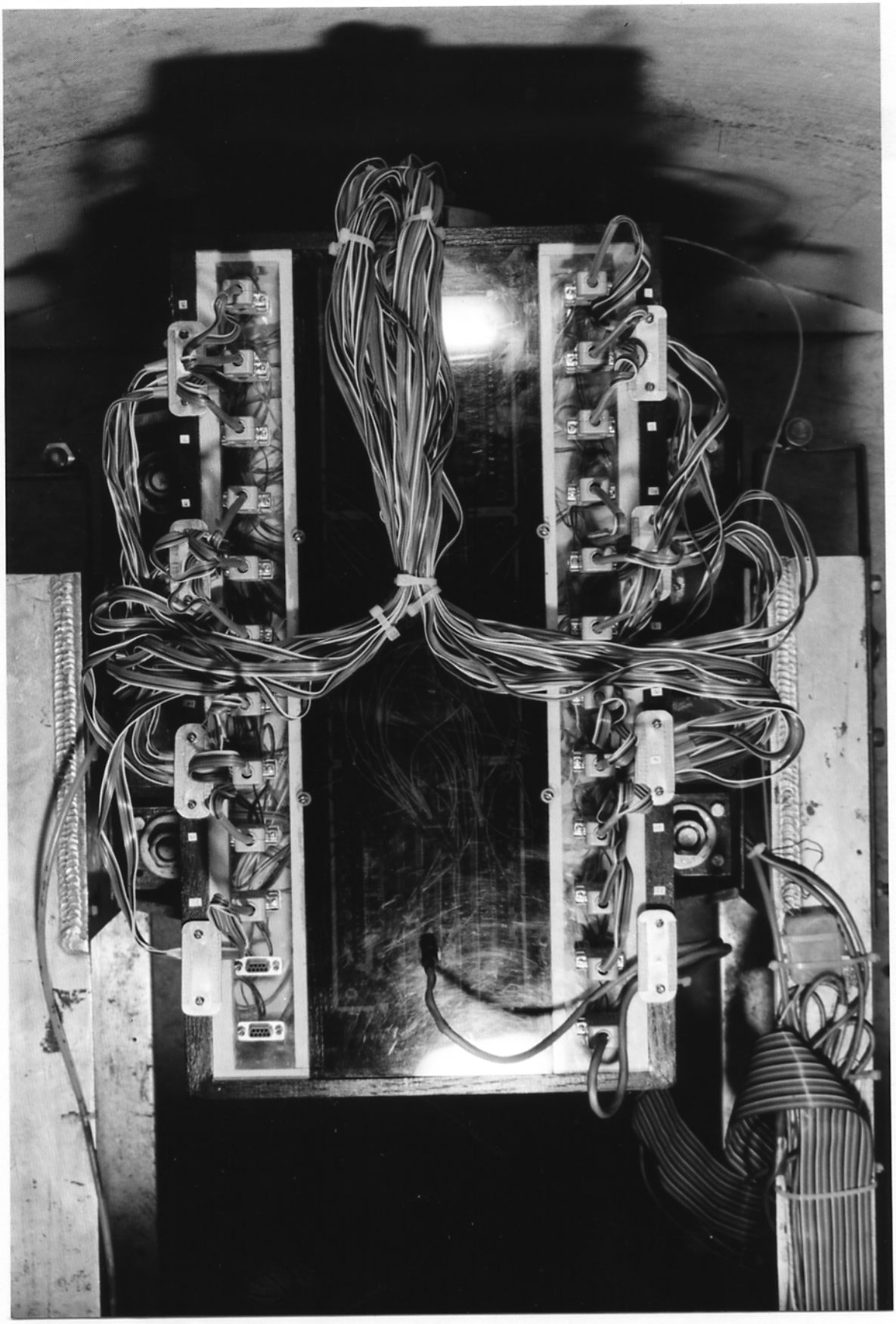

Figure 4-13. Data Acquisition Box (Multiplexers)

The three multiplexers are cascaded in a series connection using a 50 pin ribbon cable. Another ribbon cable carries the signals to the connection board where the signal is transmitted through the slip rings to the connection board outside the centrifuge. On this side of the slip rings the 50 channels are connected to the connector box (through a 50 pin ribbon cable, see Figure 4-13) which again is connected to the HRES card in the PC. Each individual multiplexer has 16 input channels and one output channel. A 4 bit digital control signal sent from the HRES card tells the EXP-20's which input channel to transmit on the output channel. All the multiplexers are transmitting the same input channel number (1-16) on their output. The EXP-20's are individually pin jumped to transmit their analog output signals to the HRES card on channels 0, 1, and 2. The multiplexers are therefore called Mux0, Mux1, and Mux2. When a specific signal source is sampled the multiplexers are sent a signal to open the channel where the source is connected. Then the HRES card is sampled on the multiplexer channel which the source is transmitting through. The following example illustrates the process.

Example:

A strain gage bridge is going to be sampled and it is connected to channel 9 on Mux2 (multiplexer connected to channel 2 on the HRES card). First a digital code (ASCII number: 0110) is transmitted telling all multiplexers to transmit on channel 9 on their output lines. On the HRES card channel 9 from the multiplexers can now be read on HRES channel 0, 1 and 2. The strain gage bridge of interest is connected to multiplexer 2 (Mux2), and it can be sampled on the HRES card channel 2.

4.4 Test Sand

Reid-Bedford sand had previously been used as the test sand for the centrifuge work at the University of Florida (e.g. McVay et al., 1994). Presently, there remains less than 3/4 of a cubic foot of this material at the University of Florida and more Reid-Bedford sand is not

available. The new experiment uses a sample container with a larger volume, and it was therefore necessary to find a substitution for the Reid-Bedford test sand.

4.4.1 Test Sand Properties

The new centrifuge test sand is called "Mixed Sand". The test sand is composed of a mix between two sand types from a nearby sand mine. Several sand mixes were analyzed, and it was concluded that portions of the sand had to be removed in order to get a mix close to the Reid-Bedford sand. The final Mixed Sand was obtained by removing percentages of what was retained on sieves number 30, 70, 100, and the pan. A total of 100 kg (220 lbs) of the new test sand "Mixed Sand" was produced this way.

The Mixed Sand was subjected to three sieve analyses after the sand was produced. The analysis was conducted following ASTM D-422 standards, and the average result of three sieve analyses is shown in Table 4-2.

Table 4-2. Sieve Analysis on Mixed Sand

Sieve number	20	30	40	50	60	100	200
Opening size [mm]	0.85	0.60	0.43	0.30	0.25	0.15	0.08
Percent passing	99.97	99.30	94.84	77.46	59.35	8.31	0.10

The sieve analyses data on the Mixed Sand are used in plotting a grain size distribution curve together with the Reid-Bedford sands grain size distribution; see Figure 4-14.

The laboratory testing of the Mixed Sand included a specific gravity test and determination of the minimum and maximum void ratio. These test were performed according to ASTM D-422 specifications and the results are shown in Table 4-3 along with the coefficient of uniformity and 50 percent passing size from the sieve analyses.

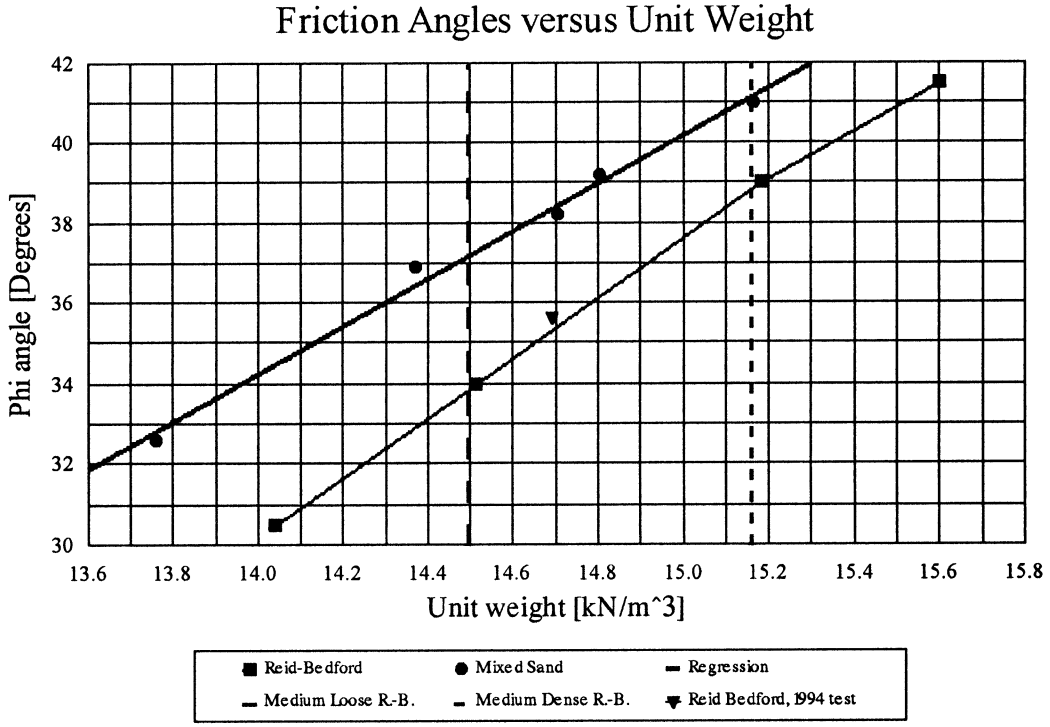

Figure 4-14. Friction Angles versus Unit Weights

Table 4-3. Mixed Sand Data from Laboratory Testing

Specific gravity	2.645
Maximum void ratio	0.957
Minimum void ratio	0.671
Minimum unit weight [kN/m^3]	13.28
Maximum unit weight [kN/m^3]	15.56
Uniformity coefficient	1.7
50 percent passing size [mm]	0.23

Several drained triaxial compression tests (CD tests) were conducted on the Mixed Sand at different densities to determine the angle of internal friction as reported in Table 4-4. The drained triaxial compression tests were conducted following the procedure outlined in the ASTM standards. The confining pressure was held constant at 103.5 kPa (103.5 kN/m^2 or 15.0 psi) in all the tests. The depth in the prototype with an equivalent effective

overburden stress depends on the unit weight of the soil. For a unit weight of 14.37 kN/m^3 the confining pressure is equivalent to the effective overburden pressure found in the prototype at a depth of 7.2 meters (23.6 feet), and for a unit weight of 15.16 kN/m^3 the equivalent depth is 6.8 meters (22.4 feet).

Table 4-4. Mixed Sand, Triaxial Test Results

Unit weight [kN/m^3]	13.76	14.37	14.71	14.81	15.16
Relative density	23.8 %	51.7 %	66.2 %	70.4 %	84.8 %
Phi angle [degrees]	32.6	36.9	38.2	39.2	41.0

The triaxial test results are presented in Figure 4-14 for both the Mixed Sand and the Reid-Bedford sand where the angles of internal friction are plotted against the unit weights. The Reid-Bedford sand data used in Figure 4-14 are reported by McVay et al. (1994). The previous centrifuge research on pile groups (i.e. McVay et al., 1994 and 1995a) have used the Reid-Bedford sand with densities of 14.51 kN/m^3 and 15.18 kN/m^3 corresponding to medium loose and medium dense sands with relative densities of 33% and 55%. These test densities are shown on Figure 4-14 marked "medium loose R.-B." and "medium dense R.-B.". For verification, a single triaxial test was performed on the Reid-Bedford sand using a confining pressure of 103.5 kPa and unit weight of 14.69 kN/m^3. The angle of internal friction was determined to be 35.6° which agrees very well with the data reported by McVay et al. (1994).

The two sand types, Reid-Bedford and Mixed Sand, have a similar grain size distribution but there is a difference between the angle of internal friction at same soil densities. The Reid-Bedford test density of 14.51 kN/m^3 (medium loose) has an angle of internal friction of 34°, and the test density of 15.18 kN/m^3 (medium dense) has a 39° angle of internal friction. The Mixed Sand has at the same dry densities angles of internal friction of 37°

(medium loose) and 41° (medium dense). These differences are a result of the particle angularity. The R.-B. sand is a marine sand, and the particles are well rounded. The Mixed Sand is from an inland sand mine and has more angular particles which results in a higher angle of internal friction.

CHAPTER 5
CENTRIFUGE CALIBRATION, SOFTWARE AND PROCEDURES

5.1 Strain Gauge Calibration

The strain gauge calibration was performed as follows. The piles were clamped to a horizontal board keeping the piles fixed at the pile heads (same location that was fixed in the pile cap). The two strain gage bridges were connected to the data acquisition system and supplied with 10 volts. The piles were marked, starting at 5 inches from the free end (opposite the clamped end) at every ½ inch, and the last mark was at 9.25 inches from the free end (total of 9 marks). A known weight of 9.2 kg (20.2 pounds) was hung from a string positioned at the marks on the pile; supplying the pile with a known weight (shear force) and position. At each position on the pile, the strain gage output was measured several times in order to establish a high confidence in the average readings. The output values were measured in 10 cycles of 5,000 samples each (50,000 readings total). By reading each cycle 5,000 times the error was minimized and the average value was established with a precision of ± 3 microvolts with a 99.9 % confidence level (this means there is a 99.9 % possibility the real mean is within the range of ± 3 microvolts of the calculated average). When the average value was determined using 10 cycles (of 5,000 readings) the possible error decreases even further, and the precision was ± 0.6 microvolts (down from ± 3 microvolts). The initial bridge readings (zero readings) were then subtracted from all of the following strained bridge readings. The exact bridge position on the piles was calculated by using linear regression on the load position versus bridge readings (bending moment readings with constant shear force). When the bridge positions were established, the known constant shear force and distance to the bridges were used in calculating the applied bending moments. The bending moments

versus bridge readings were then used in a linear regression, and the calibration constant for each bridge, from bits (or microvolts) to bending moment (kg-mm), was established. The data reduction of the moment calibration results were done on a Lotus spreadsheet program named: "p0bendm.wk4". The data gets imported and programmed macros do the calculations. An example of the moment calibration output results is shown in Figures 5-1, and 5-2 (moment calibration results for pile number 1). Each strain gage bridge on the piles has now been calibrated, and the bending moments at the two bridge positions can be calculated.

After the moment calibration procedure is completed the piles are subject to a shear force calibration procedure. Shear forces ranging from 300 grams to 28 kg are used in shearing the piles at the mark 9.25 inches from the bottom of the pile. At each load step the output from the strain gage bridges are read 50,000 times in 10 cycles (as for the moment calibration). The output readings are then calculated into bending moments (kg-mm) using the previous calculated calibration constants for bending moments. The difference of the top and bottom bending moments is compared to the known applied shear force. A linear regression is performed on the data, and the shear force calibration constant is calculated. The shear force calibration constants (units are in mm) are a measure of the distance between the two bridge positions. An example of the output results from the shear calibration is shown in Figures 5-3, and 5-4. The spreadsheet program used for the shear calculations is called "p0shear.wk4".

Moment Calibration: Pile # 1, March 29, 1995.

HRES Gain	1
EXP-20 Gain	300

	Top Gage		Bottom Gage	
	Zero Value [μ volts]	Confidence [μ volts]	Zero Value [μ volts]	Confidence [μ volts]
Before Test	-6197.8	± 1.19	4695.5	± 0.86
After Test	-6192.8	± 0.53	4683.9	± 0.46

	Top Gage		Bottom Gage	
Distance [inch]	Average Output [μ volts]	Confidence [μ volts]	Average Output [μ volts]	Confidence [μ volts]
9.25	-13635.82	± 0.54	7193.05	± 0.54
9.00	-14815.28	± 0.40	8368.33	± 0.45
8.50	-17312.35	± 0.65	10862.52	± 0.61
8.00	-19765.41	± 0.60	13313.77	± 0.45
7.50	-22182.82	± 0.61	15723.10	± 0.37
7.00	-24661.41	± 0.60	18204.81	± 0.48
6.50	-27079.54	± 0.70	20626.06	± 0.54
6.00	-29476.44	± 0.55	23021.01	± 0.51
5.50	-31906.38	± 1.09	25442.77	± 0.75

	Gage Position	
Top Gage	10.7756	inches
Bottom Gage	9.7627	inches

99.9 % confidence interval on the sample values of which each consists of the average off 5000 samples.				
	Top Gage		Bottom Gage	
Maximum	± 3.40	μ volts	± 3.10	μ volts
Minimum	± 3.05	μ volts	± 2.80	μ volts
Average	± 3.21	μ volts	± 2.95	μ volts

Figure 5-1. Example of Moment Calibration Results (Pile#1, page 1)

Moment Calibration: Pile # 1, March 29, 1995.

Top Gage: Bending Moment versus Zero Adjusted Output

Regression Output:

Constant	0
Std Err of Y Est	1.303368
R Squared	0.999980
No. of Observations	180
Degrees of Freedom	179
X Coefficient(s)	-0.0479851
Std Err of Coef.	0.0000056

M (kg-mm) = Output (Volt) * -47985.11 [kg-mm/V]

Bottom Gage: Bending Moment v. Zero Adjusted Output

Regression Output:

Constant	0
Std Err of Y Est	1.301630
R Squared	0.999980
No. of Observations	180
Degrees of Freedom	179
X Coefficient(s)	0.0480256
Std Err of Coef.	0.0000076

M (kg-mm) = Output (Volt) * 48025.56 [kg-mm/V]

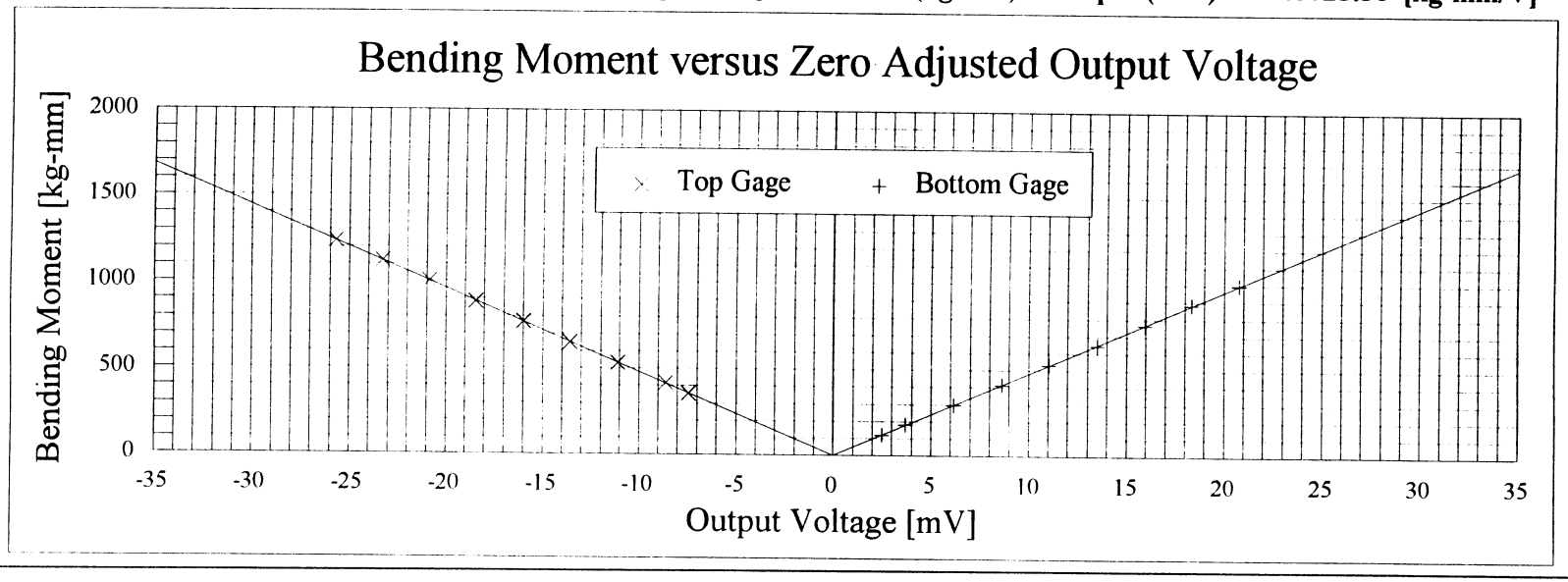

Figure 5-2. Example of Moment Calibration Results (Pile #1,page 2)

Shear Force Calibration: Pile # 1, March 29, 1995.

HRES Gain	1
EXP-20 Gain	300

	Top Gage		Bottom Gage	
	Zero Value [μ volts]	Confidence [μ volts]	Zero Value [μ volts]	Confidence [μ volts]
Before Test	-6190.6	± 0.41	4678.3	± 0.49
After Test	-6190.7	± 0.46	4677.2	± 0.49

	Top Gage		Bottom Gage	
Shear Force [grams]	Average Output [μ volts]	Confidence [μ volts]	Average Output [μ volts]	Confidence [μ volts]
299.69	-6431.11	± 1.22	4758.88	± 0.96
998.55	-6997.84	± 0.74	4952.55	± 0.71
1997.03	-7792.69	± 0.61	5214.25	± 0.62
2995.58	-8595.12	± 0.45	5484.10	± 0.55
4069.49	-9504.17	± 0.56	5818.38	± 0.55
7220.11	-12076.87	± 0.40	6708.04	± 0.45
9217.48	-13705.87	± 0.91	7274.01	± 0.78
11216.28	-15340.39	± 0.63	7837.53	± 0.64
13214.73	-16972.35	± 0.58	8403.04	± 0.59
15212.22	-18602.89	± 0.39	8964.29	± 0.45
17209.76	-20237.15	± 0.53	9529.44	± 0.53
19208.73	-21870.55	± 0.55	10092.07	± 0.28
21205.76	-23506.11	± 0.82	10659.51	± 0.64
23202.67	-25140.34	± 0.81	11229.81	± 0.76
25202.31	-26773.79	± 0.87	11793.13	± 0.62
26200.81	-27591.16	± 0.44	12075.08	± 0.42
27199.96	-28409.15	± 0.62	12355.99	± 0.64
28198.51	-29226.91	± 0.88	12638.97	± 0.95

99.9 % Confidence interval on the sample values of which each consists of the average off 5000 samples.							
	Top Gage				Bottom Gage		
Maximum	±	3.43	μ volts	±	3.18	μ volts
Minimum	±	2.98	μ volts	±	2.80	μ volts
Average	±	3.20	μ volts	±	2.98	μ volts

Figure 5-3. Example of Shear Calibration Results (Pile #1, page1)

Shear Force Calibration: Pile # 1, March 29, 1995.

Regression Output:		
Consta Constant		0
Std Err of Y Est		0.1758584
R Squared		0.9999995
No. of Observations		360
Degrees of Freedom		359
X Coefficient(s)	25.63313898	
Std Er Std Err of Coef.	0.00054482	

Load (kg) = Differential Bending Moment (kg-mm) / 25.6331 [mm]

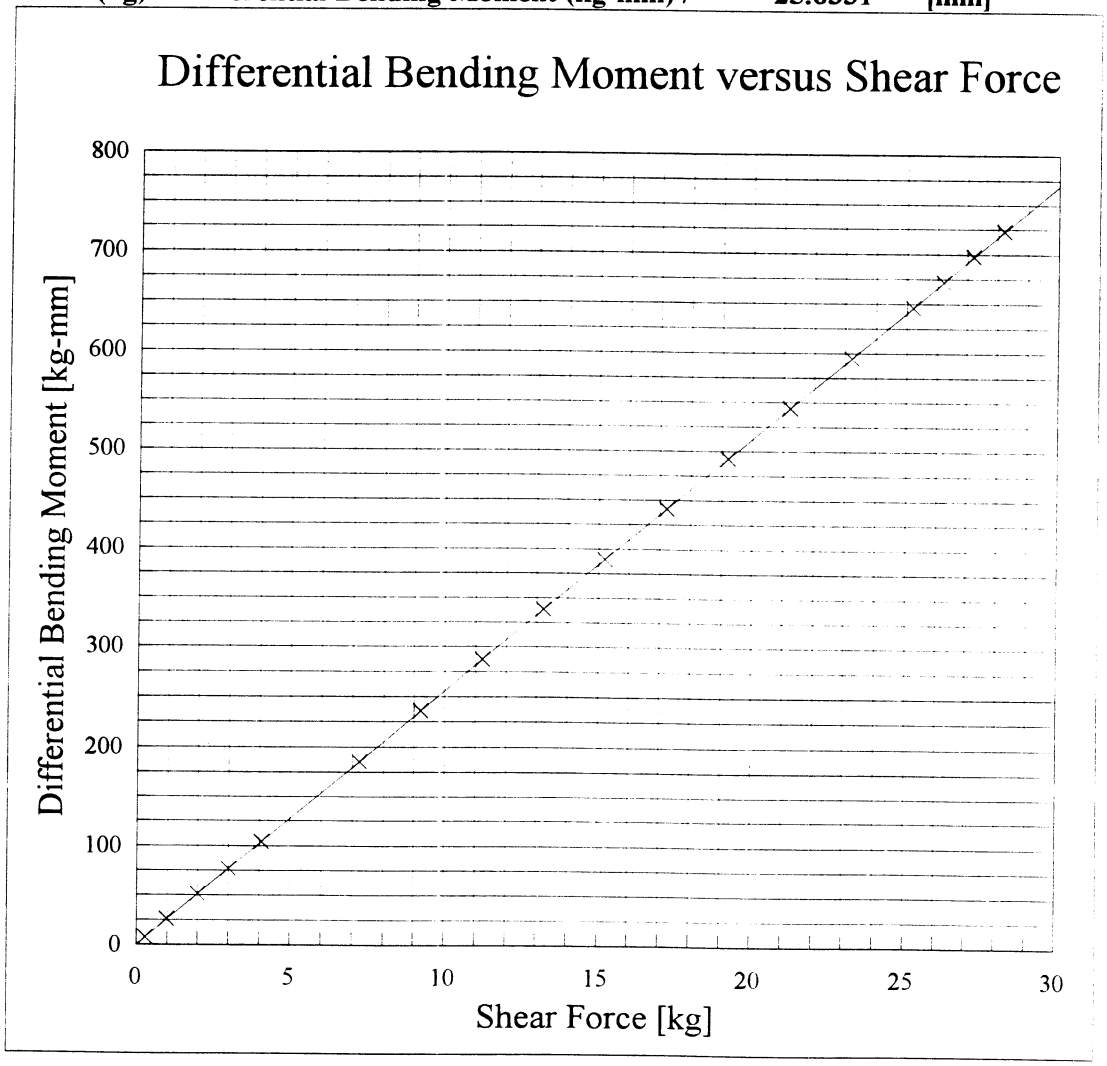

Figure 5-4. Example of Shear Calibration Results (Pile #1, page2)

5.2 Software Program

There are three software programs which are used to enable measurements and storage of data in this research. First there is an old BASIC program "WEIGH" which is used to weigh the experiment with and without soil in the sample container. The program calculates the weight difference between the initial reading and the following reading, and the sand weight is thereby determined. When the volume of the container is known the density of the soil can be determined. The weighing cell is set to be read on HRES channel 3 in the program.

The second program called "CALIBRAT" is also a BASIC program and is used in calibrating the instrumented piles. The program is very simple, and the user has to make notes on which step in the calibration procedure is being conducted. The output data can then be related to the correct loads and locations on the piles when the data reduction is conducted.

The third program is "LPGTOM" which is used in the centrifuge test to sample the data from strain gages, load cell, and LVDT. The program is a sophisticated BASIC program consisting of several sub programs and configuration files. The description here will only explain the procedures and necessary configuration setups in order to use the program properly.

There are four configuration files controlling setup parameters in the program. An example of each of the configuration file is shown in the following examples.

Examples of Configuration Files:

LPGTOM.CFG:

[default data directory]
c:\lpgtom\data\
[Inner and Outer Sampling Loops]
2000
10
[Tracking Default: 0=off, 1=on]
1
[Sample interval (sec), Number of automatic samples]
120 3
[Test RPM, Radius to Soil Surface]
176.5 50.875
[Load cell calibration (mv/lb), Load cell excitation (v)]
0.012871 5.0
[LVDT calibration (v/in), LVDT excitation (v)]
-39.6756 30.0
[Instantaneous LVDT and Load Cell settings: # samples, Units: 0=bits,1=dbits,2=volts,3=dV,4=model,5=prototype]
2000 5
[Delay: Cycles for calibration, Delay time before sampling]
100000 0.001

HRES.CFG:

[Base Address, Interrupt, DMA]
768
7
1
[CHANNEL GAIN]
1 1
2 1
3 1
4 1
5 1
6 1
7 1
8 1
[Multiplexer gain]
300

PLUG.CFG:

[Plug Configuration: Plug No , Mux, Top Channel, Bottom Channel]

1	0	0	1
2	0	2	3
3	0	4	5
4	0	6	7
5	1	0	1
6	1	2	3
7	1	4	5
8	1	6	7
9	2	0	1
10	2	2	3
11	2	4	5
12	2	6	7
13	0	8	9
14	0	10	11
15	0	12	13
16	0	14	15
17	1	8	9
18	1	10	11
19	1	12	13
20	1	14	15
21	2	8	9
22	2	10	11
23	2	12	13
24	2	14	15

CAP.CFG:

[Number of Piles]

12

[Position, Pile ID, Plug Number]

1	11	1
2	12	2
3	13	13
4	8	4
5	9	14
6	10	15
7	5	4
8	6	5
9	7	16
10	1	6
11	2	17
12	3	18

[Shaft Load Cell Plug No]

24

[LVDT Channel - HRES channel - not a plug number]

5

The configuration file "LPGTOM.CFG" contains information on where to store the output files, length of the inner and outer loops, time between the load step samples and number of load steps, calibration factors for the g-level (RPM and distance to the soil surface), LVDT and load cell calibration factors, number of samples used in displaying the instantaneous LVDT and load cell readings, and number of calibration samples and time delay. This configuration file should not be changed unless a different approach in sampling the pile groups is found necessary. As it is set up in the configuration file the program will automatically take 100,000 samples values for the zero readings. When a lateral load is applied the sampling sequence is started by pressing the F5 key. Three readings will be taken, and each reading consists of the average of 20,000 readings measured in 10 cycles with a average time since initiating the sequence of 2, 4, and 6 minutes.

The "HRES.CFG" configuration file is used in setting the gains on the HRES card and the multiplexers. The HRES card has a programmable gain setting option of 1, 2, 4, and 8. The multiplexer gain is set by switching pin settings on the multiplexers. The gain options are 1, 10, 100, 200, 300, 500, 600, 700 and 800. The HRES gain is set permanently for 1 and the multiplexer gain for 300. The configuration file should not be changed unless the strain gage readings and load cell readings exceed the maximum readable voltage of ±33,333 microvolts when the gain setting is 300 (and 1 on the HRES card).

The "PLUG.CFG" configuration file is used in describing which multiplexer and multiplexer channels the plugs are wired to. This file should not be changed unless the wiring between plugs and multiplexers is changed (very unlikely). Figure 5-5 shows the plugs (plug numbers in upper left corner), the multiplexer numbers (MUX 0, 1, or 2) and channel on the multiplexers (CHN 0, 1, 2, ..., 14, or 15) where the top gage (T) and bottom gage (B) are wired to.

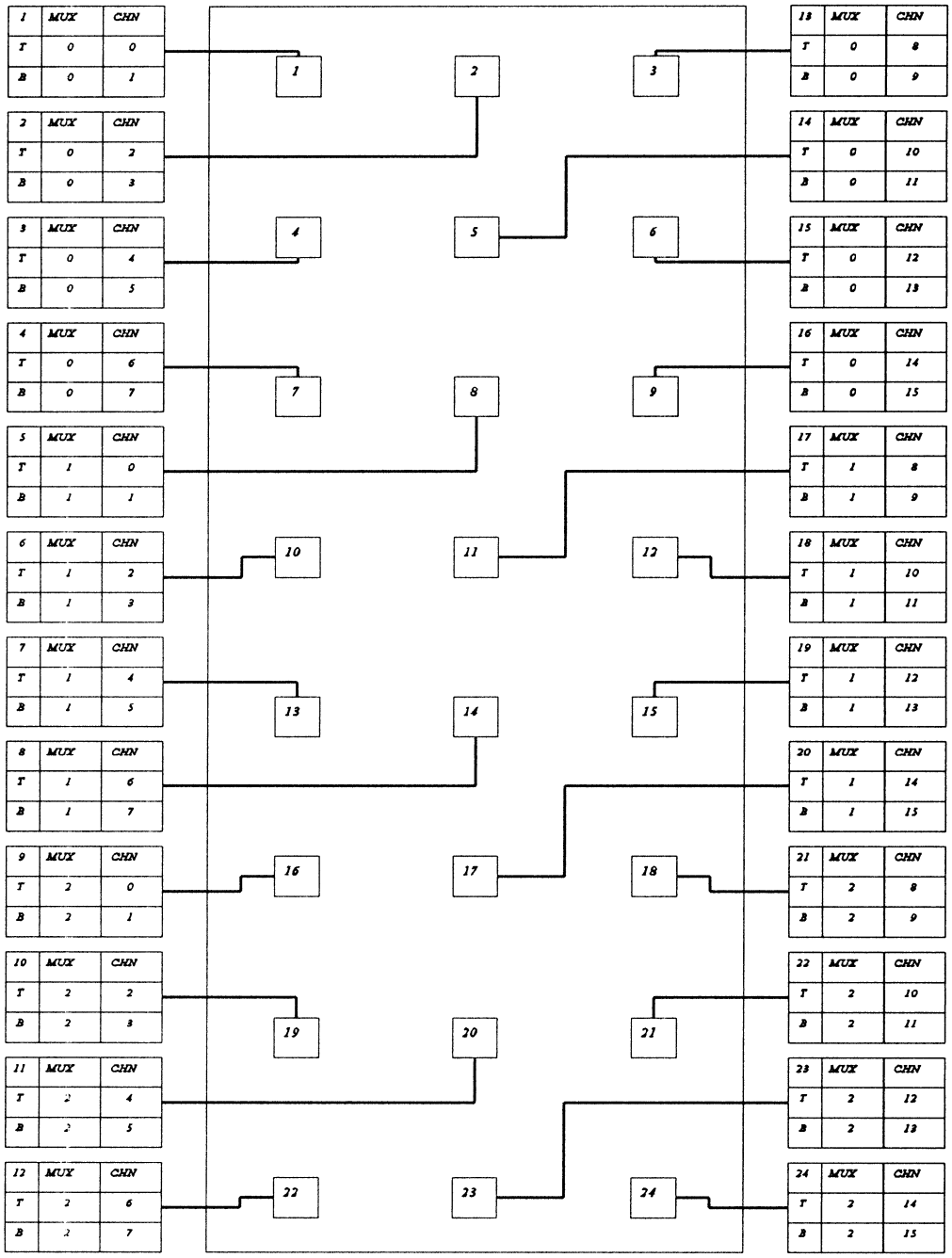

Figure 5-5. Pile Position Numbers and Plug Assignments

The "CAP.CFG" configuration file locates the piles, LVDT and load cell for each pile cap configuration setup and centrifuge test. The file is changed for each different centrifuge test (i.e. number of instrumented piles and their plug numbers). The configuration file con-

tains the total number of instrumented piles and their pile positions (see Figure 5-5), instrumented pile ID number and the plug number the piles are connected to. The pile positions are numbered as shown on Figure 5-5, where the lead row piles have number 1, 2, and 3 (from left to right). When a smaller pile group is tested the lead row and following rows are numbered the same, starting with pile position number one. For example the last pile position number of a 4 row pile group is 12. Also the load cell is connected to the plugs which number is identified in the configuration file. The LVDT is set for readings on channel 5 on the HRES, but this can be changed if necessary.

5.3 Test Procedures

The following test procedures have not been verified as ideal methods of conducting the centrifuge tests. Small changes to the procedures might be useful in establishing a repeatable test method and in the preparations of homogeneous soil samples.

5.3.1 Sample Preparation

Two soil densities will be used in the tests (medium dense and medium loose samples). The sand samples are prepared using two different methods in achieving the densities. The samples are constructed by letting the sand rain through 3 rectangular sieves mounted on a wooden box which keep the sand from falling outside the sample container. The wooden sand rainer is constructed of two pieces that allows a higher or lower falling height. The medium loose sample is constructed by using the sand rainer without the lower part, and keeping the falling height low (22 inches). The sand is poured through the sieves in large amounts at a time and a medium loose sample with a density of 87 pcf can be obtained. The medium dense sample is obtained by using the sand rainer with both pieces on, keeping the falling height high (31 inches) and letting the sand rain through the sieves in small quantities

at a time. The medium dense sample can then be obtained with a density of 92 pcf. When the sand has filled the container the surface may not be perfectly horizontal and flush with the top of the container. Therefor the top surface is leveled by scraping the uneven sand surface with a metal bar, having same width as the sample container (13 inches).

The weight of the sample container with and without the soil is determined using the weighing cell and the computer program "weigh" in the directory; "c:\weigh\weigh.exe". The volume of the container is 1.116 cubic feet (to the top edge). The sample density is then calculated by dividing the soil weight by the container volume.

5.3.2 Pile Group Setup

The pile group configuration depends on the pile spacing and the number of pile rows (4, 5, 6, 7, or 8 rows of piles). The desirable pile group configuration is assembled by adding more or less pile cap pieces to the pile cap (with the pile spacing chosen). Steel rods hold the pile cap pieces together, and they are provided in the correct length (depending on the number of rows). The two end pieces are wider than the center pile cap pieces and the end pieces are used for all pile cap configurations. The piles, either instrumented or dummy piles (not instrumented) are then pushed into the slots provided in the pile cap pieces. It is important to embed the piles into the pile cap keeping the pile top flush with the top of the pile cap piece. The instrumented piles have to be oriented with the strain gages perpendicular to the loading direction. An arrow is drawn on the piles pointing in the loading direction. When all the piles are placed in the pile cap pieces, the cap pieces are put together and the steel rods are inserted through them to hold them together. Steel nuts and washers are put on the ends and they are finger tightened. Using a large wrench the nuts are turned (in turns) as many rotations as possible (½-1 rotation). The compression force provided by the tightened steel nuts holds the piles in place in the pile cap and provides a fixed head condition.

The piles and pile cap are placed underneath the driving platform in a 1/4 inch deep slot provided for the pile cap. The slot keeps the pile cap aligned parallel to the loading direction. All the pile cap configurations have to be placed in the center of the four driving pistons. Two 1/4 inch thick aluminum plates are screwed onto the driving platform. They provide the space between the pile cap and the edge of the driving platform, in order to align the chosen pile cap configuration in the center between the driving pistons.

5.3.3 Electronic Setup

The instrumented piles are connected (through a plug) to the connectors on the data acquisition box (sitting on top of the driving platform). The pile positions, plug numbers, and pile ID's is noted and incorporated in the configuration files for the data acquisition software (see section 3.2). The wires from the piles are fastened to a aluminum block on the ½ inch threaded steel rods. This way the wire connections (at the strain gages) are protected from damage if the wires get pulled. The wires are attached to the driving platform with duct tape and it is important to leave free hanging wire (about 4 inches) between the pile driver and the pile cap. When the piles and driving platform are separating (after the pile driving) the free hanging wire provides slack as long as the extended length between the piles and the data acquisition box. The ribbon cable from the data acquisition box is connected to a plug from the connection board. The power supply for the strain gages (10 volt) is connected to the data acquisition box (via a 2 pin plug connected to the slip ring channels 58 and 59). The strain gage input voltage is supplied by a Hewlett Packard adjustable power supply (maximum 500 mA) and the supply voltage of 10.0 volt is adjusted using a multimeter (with 1/1000 volt precision).

The LVDT is connected to the mounting fixture on the experiment container and a 6 pin connector is plugged into the LVDT. The connector is permanently attached to the

connection board. The power supply for the LVDT (± 15 volt) is connected via the slip rings (on channels 50 and 51) to the LVDT connector. The output signal from the LVDT (± 10 volt) is connected (via slip ring channels 71 and 72) to the HRES card (via the connector box) on channel 3.

The load cell is mounted on the tip of the loading piston shaft and the wires for the power supply (5 volt) are connected to the screw terminals on the connector board on slip ring channel 52 and 53. The load cell has a plug attached to the output signal wires which is connected to the data acquisition box on a free connector (not used for strain gage measurements). The plug number for the load cell is incorporated in the configuration files for the data acquisition software.

5.3.4 Running Centrifuge Test

The sample container (filled with sand and the pile cap attached) is lowered down to the centrifuge (using a crane) and placed on the swing up platform. The sample container is secured with four steel bolts (3/8 inch, grade 8) to the swing up platform. The electronic equipment is connected and the centrifuge balance calculations checked. The floor in the centrifuge is cleaned (all loose material removed) and the electronic wires are checked and the loose wires are attached to the centrifuge with duct tape. The hydraulic lines are connected to the experiment with two quick connects and the air line for the loading piston is attached.

The centrifuge is started and accelerated to 176.5 RPM (producing 45g at the sand surface). The pile driving procedure is started by setting the valves on the control board (see Chapter 2) for pressurizing the hydraulic supply tank (retraction of the pistons) and setting the valve on the recovery tank for atmospheric pressure (vent). The pile driving is initiated by increasing the nitrogen pressure (maximum of 500 psi) which is pressurizing the hydraulic

oil (retracting the pistons). When the pistons are fully retracted (10 inch travel) the pile group has been driven to the testing position (keeping 1.5 inches of free pile length between the pile cap and the sand surface). The driving platform is retracted 3 inches by switching the valves and pressurizing the other tank (hydraulic fluid is flowing the opposite way expanding the pistons). The driving platform is stopped by turning the valves (to the off positions) connected to the hydraulic lines (3/8 inch valves between the tanks and the rotary union). The hydraulic lines are then closed and the piston movements are stopped completely.

The software program "LPGTOM" is then executed and the strain gage, LVDT, and load cell zero values are measured. The first lateral load step can begin and the air pressure valve (on the control board) is increased to 5 psi (25 tons prototype). The amount of additional load increases and pressures depends on the expected failure load (at about 3 inches of prototype translation). The load steps and pressures are chosen as a reasonable amount of steps (about 20 load steps) within the expected pressure range. After each load increase the automatic computer sampling is initiated (by pressing the F5 key). The program will sample all strain gages, LVDT, and load cell 20,000 times with an average reading at 2, 4, and 6 minutes after the program was initiated (can be changed in the LPGTOM configuration file). The sample values are stored on the PC hard drive immediately after they are taken. The program displays the last sample readings on the computer screen. Between readings the LVDT and load cell are measured continuously and displayed at the bottom of the screen. A choice between units (bits, model properties, prototype properties, or voltage reading) are made by pressing the F7 key. After the pile group is loaded to failure (the test is finished) the lateral load on the group is removed (the air pressure is turned down to zero). The centrifuge is then brought to a complete stop and the test equipment can be removed and a new test prepared.

CHAPTER 6
CENTRIFUGE RESULTS AND FLORIDA-PIER PREDICTIONS

6.1 Centrifuge Test Results

In order validate the soil properties, two sets of single piles tests were performed at soil relative densities of 36% and 55%. A schematic of the prototype single and 3 × 5 group tests are shown in Figure 6-1. After the single pile tests, more than 20 centrifuge tests were completed on the fixed headed groups in sand. The group layouts consisted of 3 × 3, 3 × 4, 3 × 5, 3 × 6, and 3 × 7 patterns for both loose (Dr=36%) and medium dense sands (Dr=55%). The pile spacings were at three diameters, and at least two tests were performed for each group layout for repeatability (accuracy) purposes. For the group test, the lead, 2nd, 3rd, etc pile rows are as identified (Figure 6-1). All of the group tests had similar geometries (i.e. embedment depths, and clear distance between cap and soil). All of the test results will be presented first, and then Florida-Piers prediction of the group, as well as the individual row values will be given.

Presented in Figure 6-2 (a) and (b) are the single pile response founded in the loose (Dr=36%) and medium dense (Dr=55%) sands. Note there are two sets of data in each plot, showing the centrifuge's repeatability.

Presented in Figure 6-3 (a) is the total lateral load versus lateral deflection of the 3 × 3 group founded in a medium dense sand (Dr=55%) for 2 tests (Mar 8 and Mar 11). Figure 6-3(b) is measured shear for each pile in the lead row (see Figure 6-1) for the 2 tests (Mar 8 and Mar 11). Figure 6-3(c) is the measured shear in each pile for the second row and Figure 6-3 (d) is the shear in the trail row piles. Given in Figure 6-4 (a) - (e) are the results of the 4 × 3 group in medium dense sand (Dr =55%). Figure 6-4 (a) is again the total lateral load

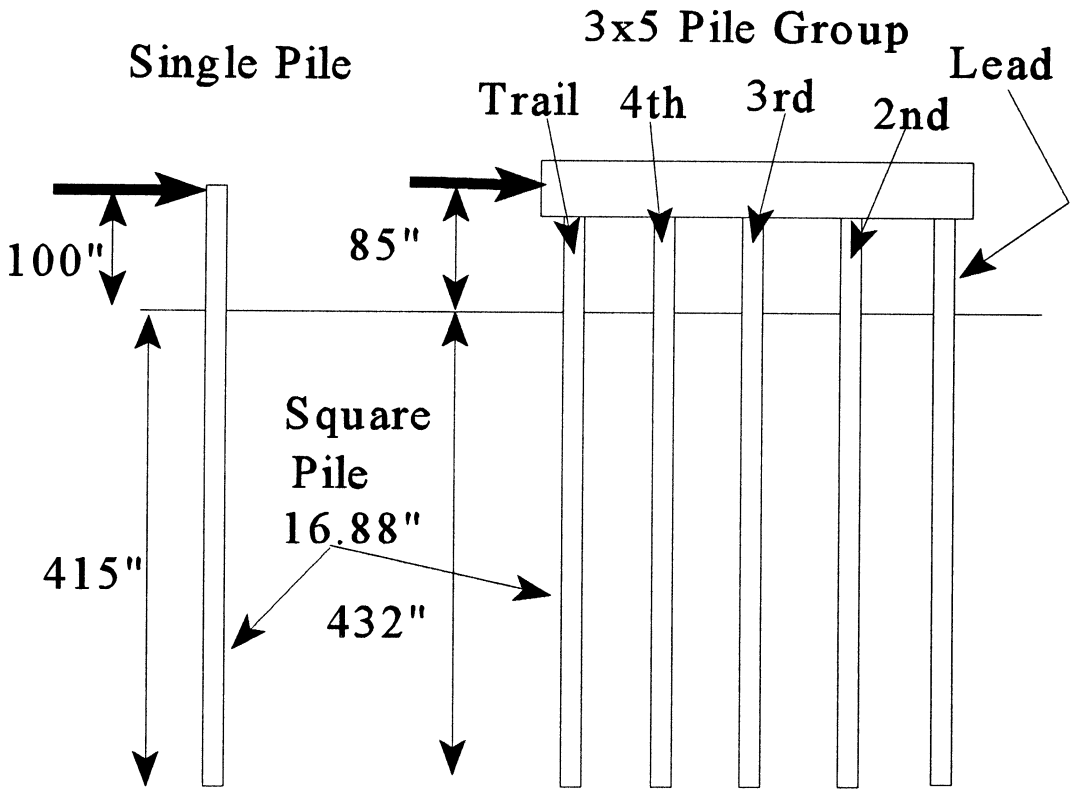

Figure 6-1. Single and Group Layout Geometry

versus lateral deflection, and Figures 6-4 (b)-(e) give the contributions of each row. Presented in Figure 6-5 (a) - (f) are the results of the 5 × 3 group tests, Figure 6-6 (a)-(g) for the 6 × 3 and Figure 6-7 (a)-(h) for the 7 × 3 group, all in the medium dense sand (Dr =55%).

In the case of the medium loose sand (Dr=36%), Figure 6-8 (a)-(d) presents the results for a 3 × 3 group, Figure 6-9 (a)-(e) a 4 × 3 group, Figure 6-10 (a)-(f) a 5 × 3 group, Figure 6-11 (a)-(g) a 6 × 3 group, and Figure 6-12 (a)-(h) a 7 × 3 group.

For all of the group tests, the summation of the individual shears in the piles was within 5% of the lateral load applied to the groups. Also, as evident from the figures, the repeatability among the tests was quite good. However, it was noted that a few of the instrumented piles (see Figure 6-7(b)) began to give erratic data due to the "wear and tear".

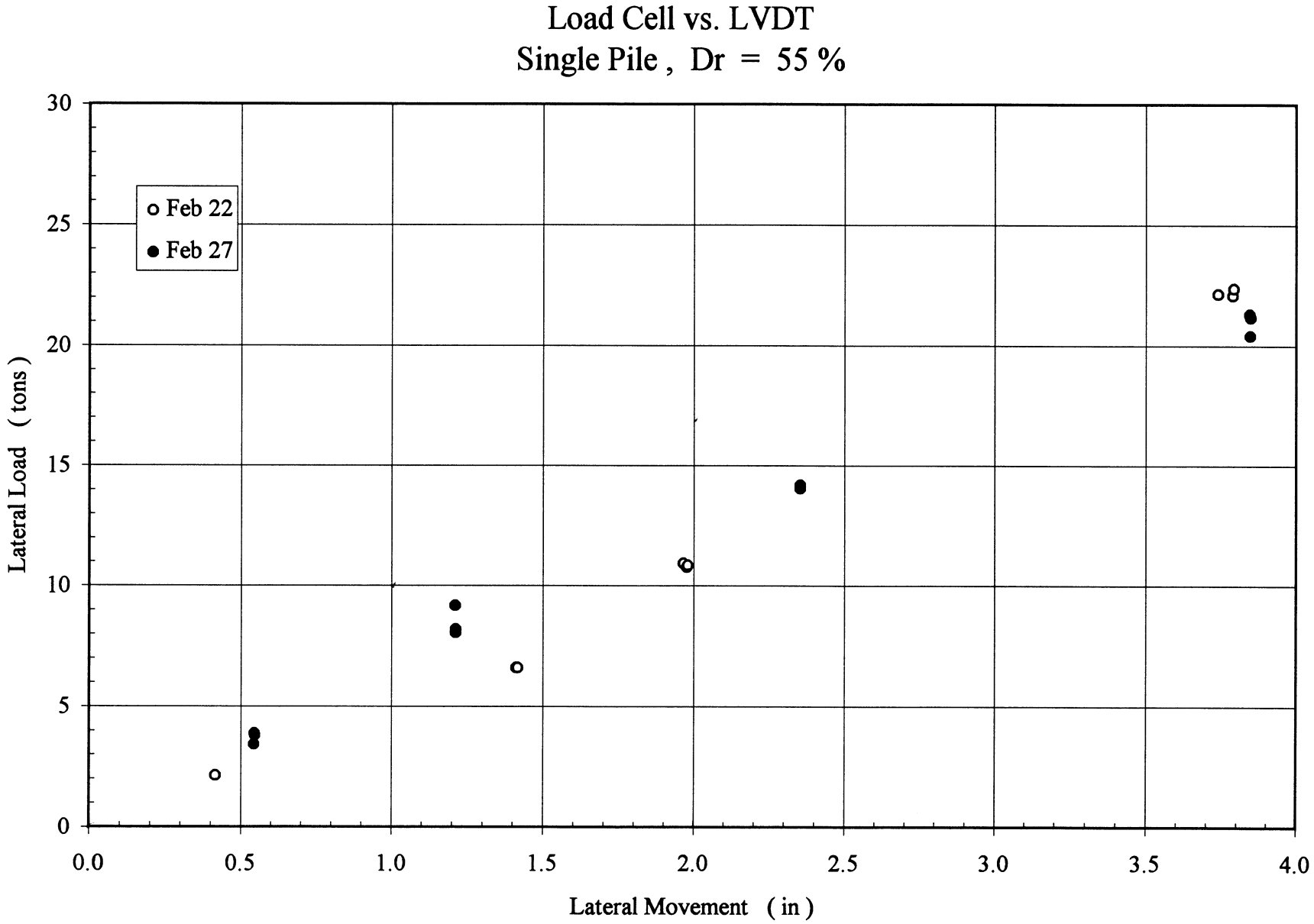

Figure 6-2(a). Single Pile Response in Medium Dense Sand, Load Cell vs. LVDT

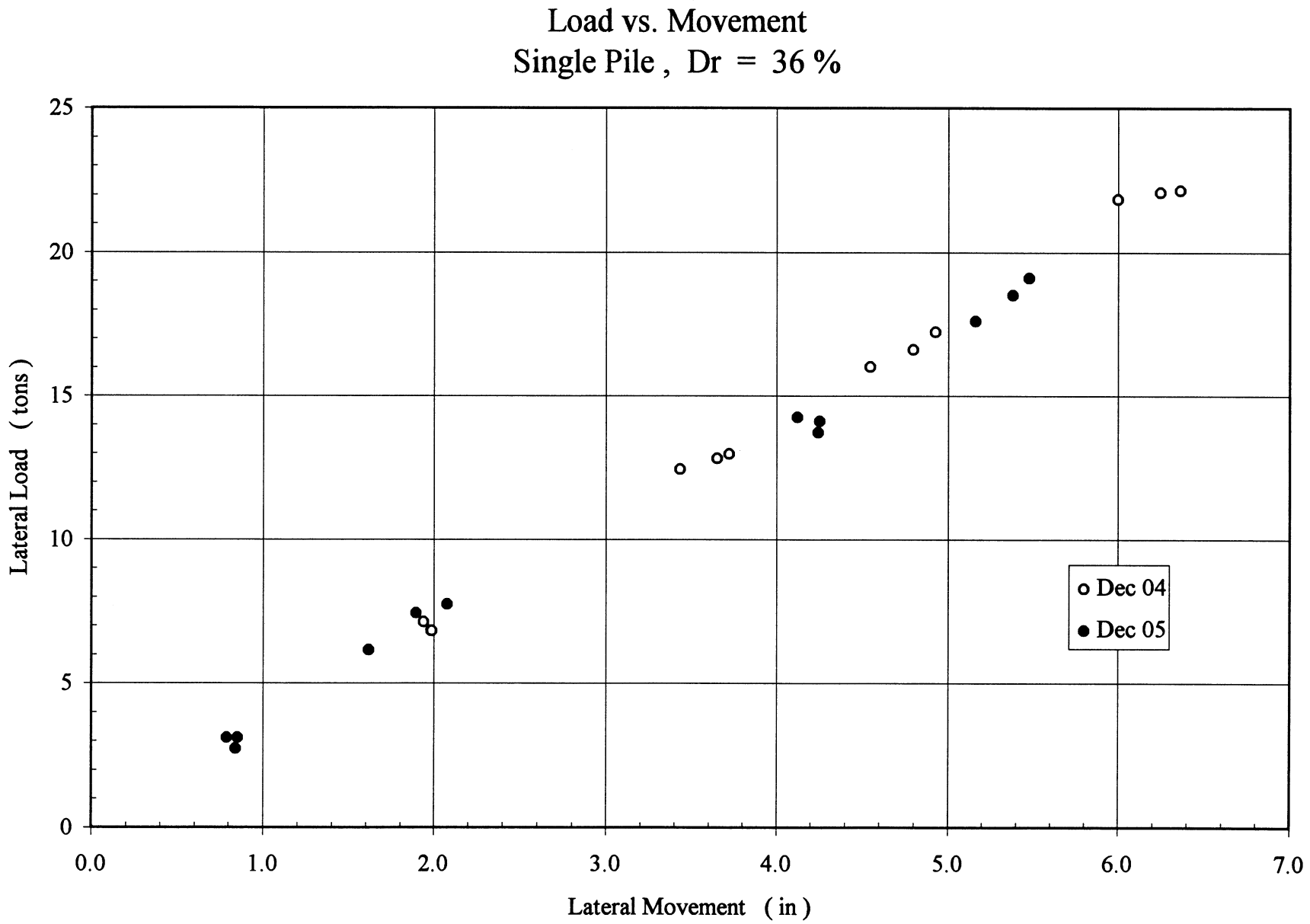

Figure 6-2(b). Single Pile Response in Loose Sand, Load vs. Movement

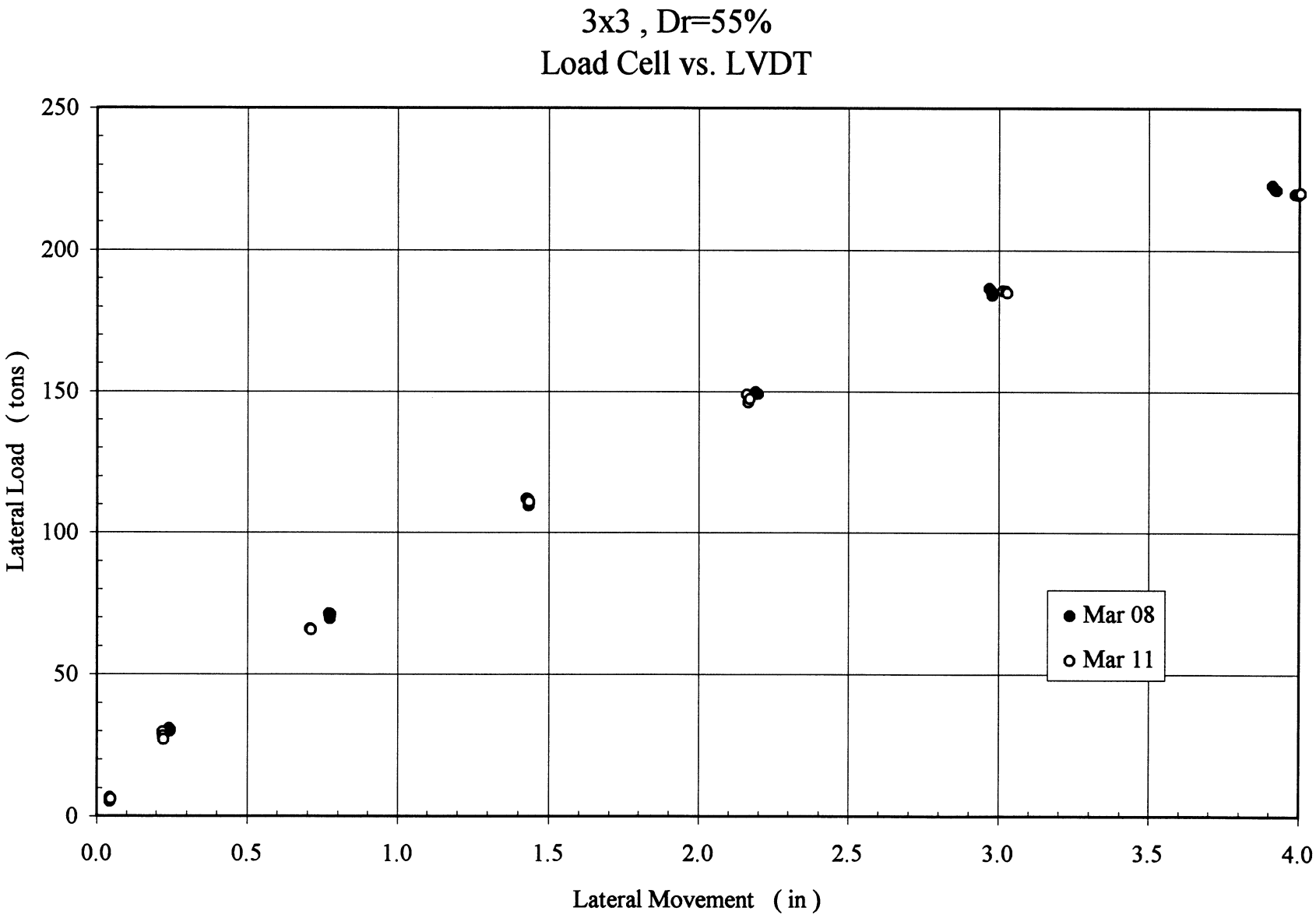

Figure 6-3(a). Results of 3 × 3 Group in Medium Dense Sand, Total Lateral Load vs. Lateral Deflection

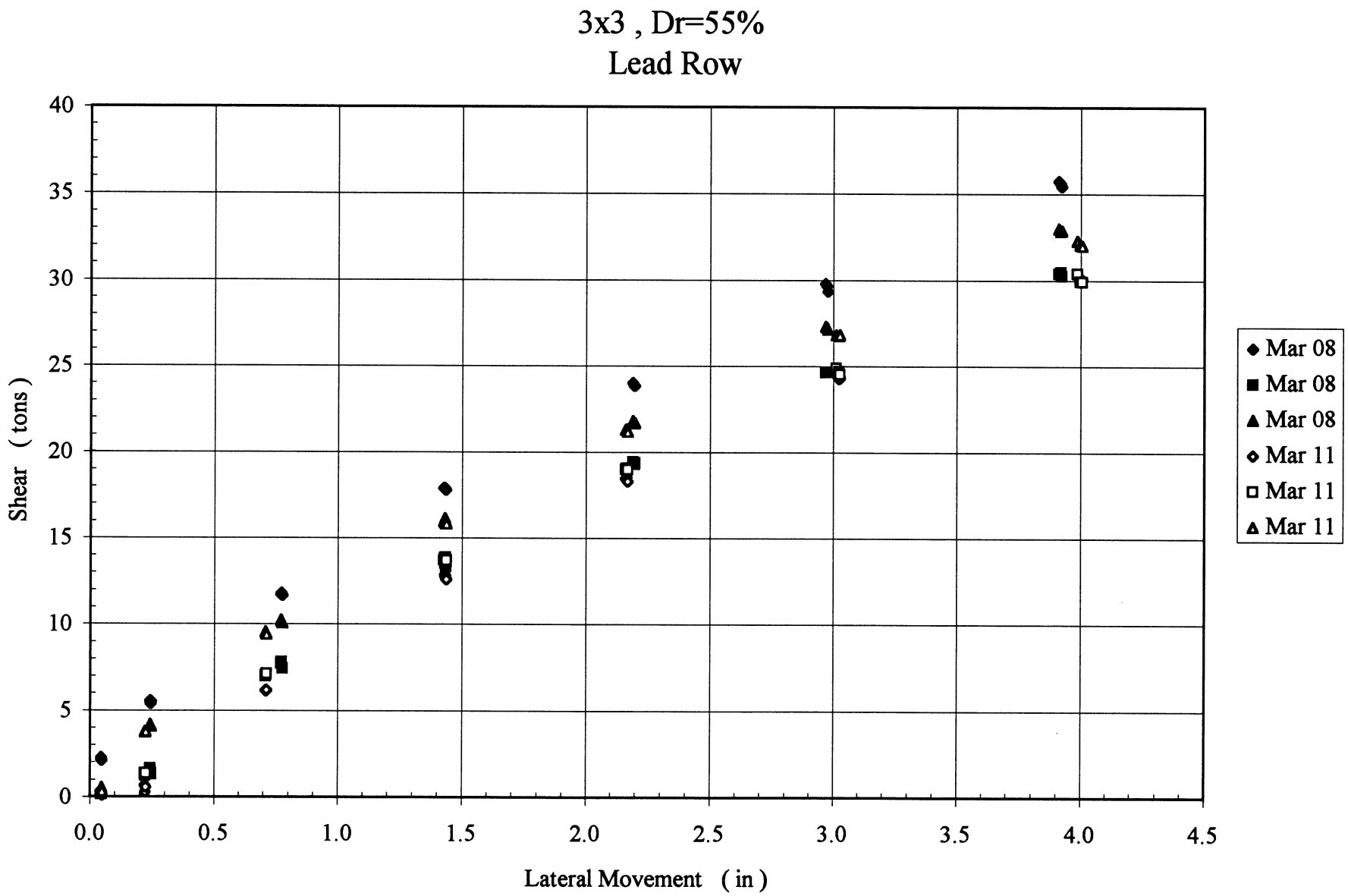

Figure 6-3(b). Results of 3 × 3 Group in Medium Dense Sand, Measured Shear for Each Pile in Lead Row

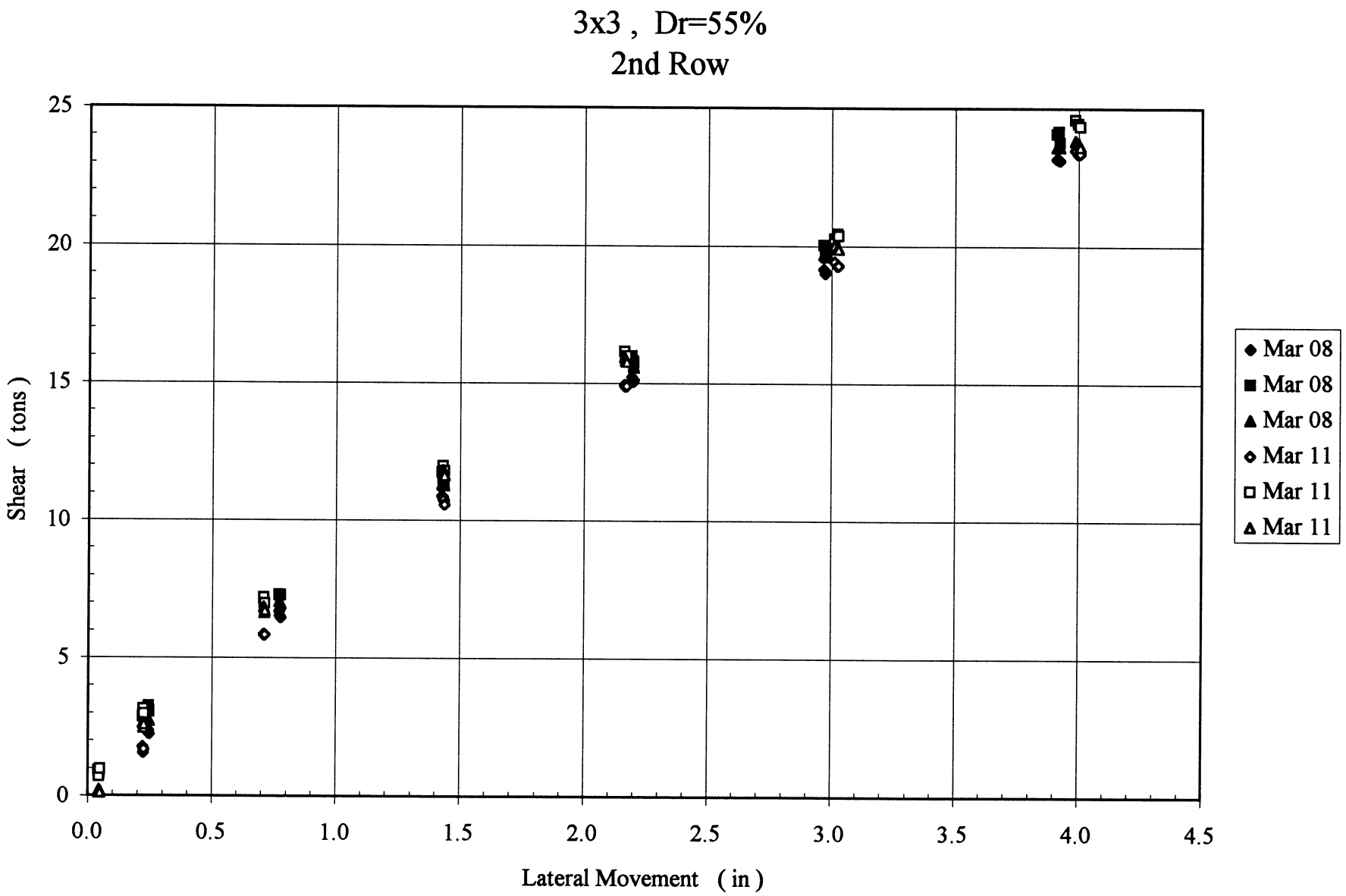

Figure 6-3(c). Results of 3 × 3 Group in Medium Dense Sand, Measured Shear for Each Pile in 2nd Row

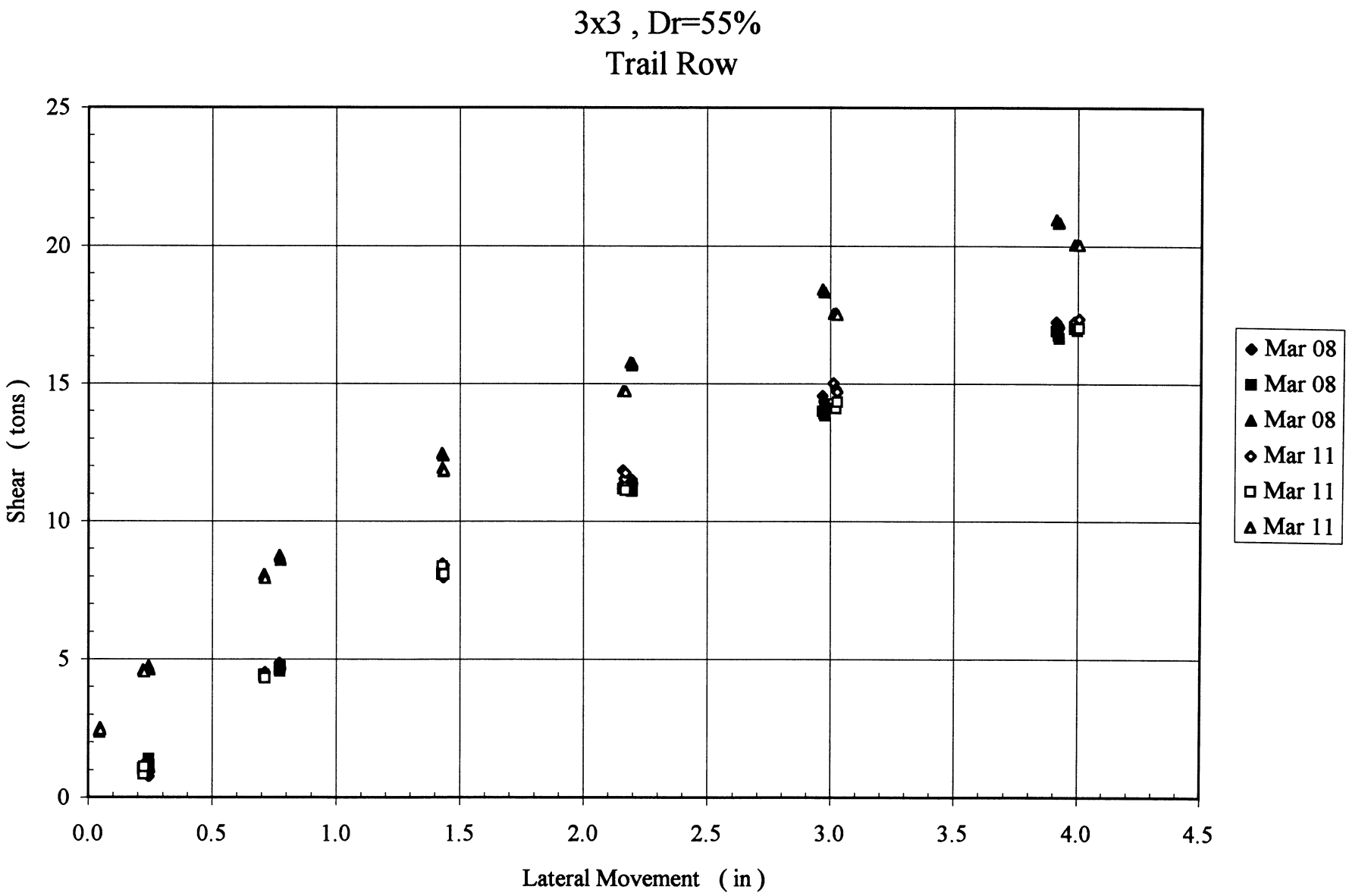

Figure 6-3(d). Results of 3 × 3 Group in Medium Dense Sand, Measured Shear for Each Pile in Trail Row

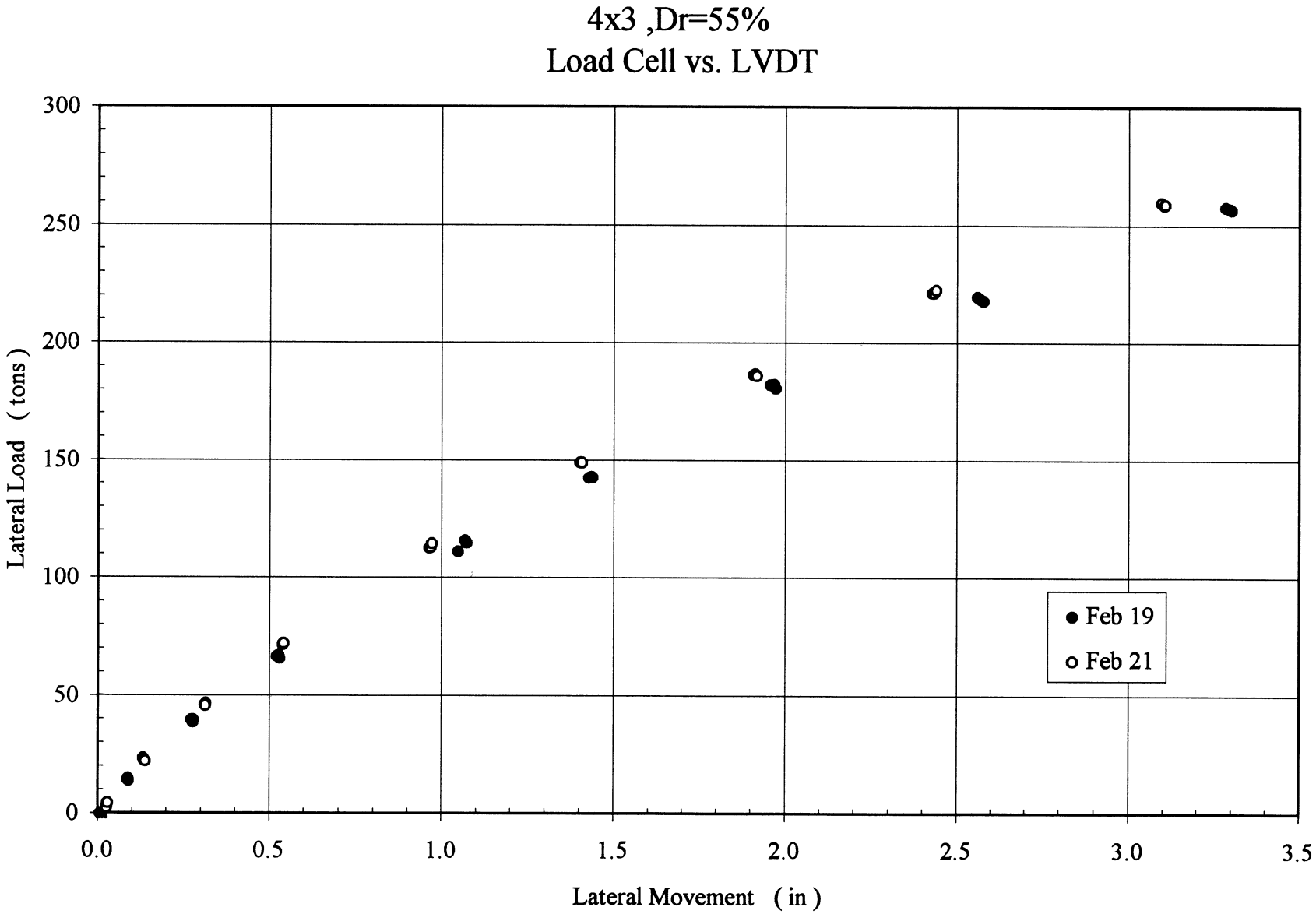

Figure 6-4(a). Results of 4 × 3 Group in Medium Dense Sand, Total Lateral Load vs. Lateral Deflection

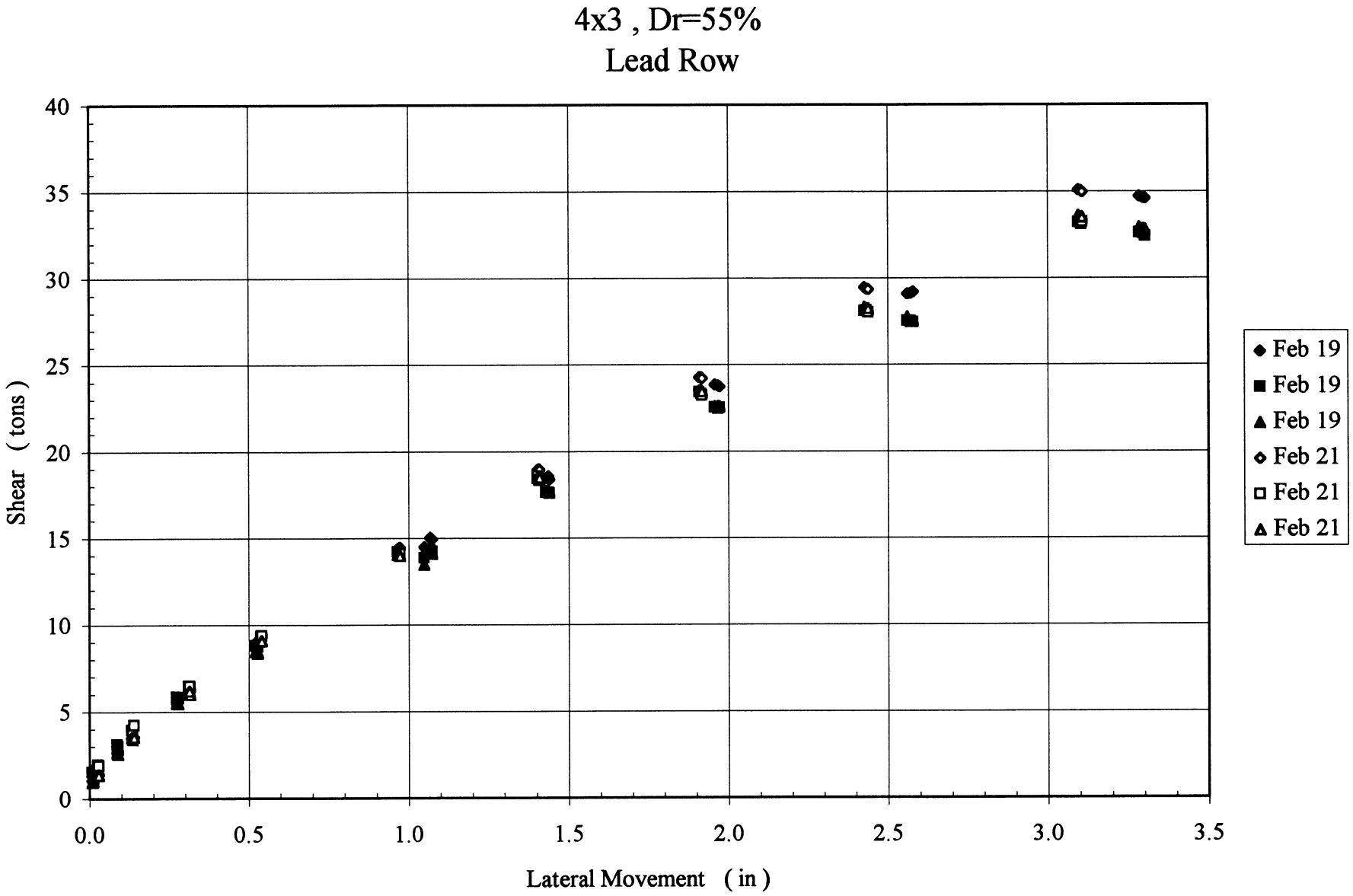

Figure 6-4(b). Results of 4 × 3 Group in Medium Dense Sand, Measured Shear for Each Pile in Lead Row

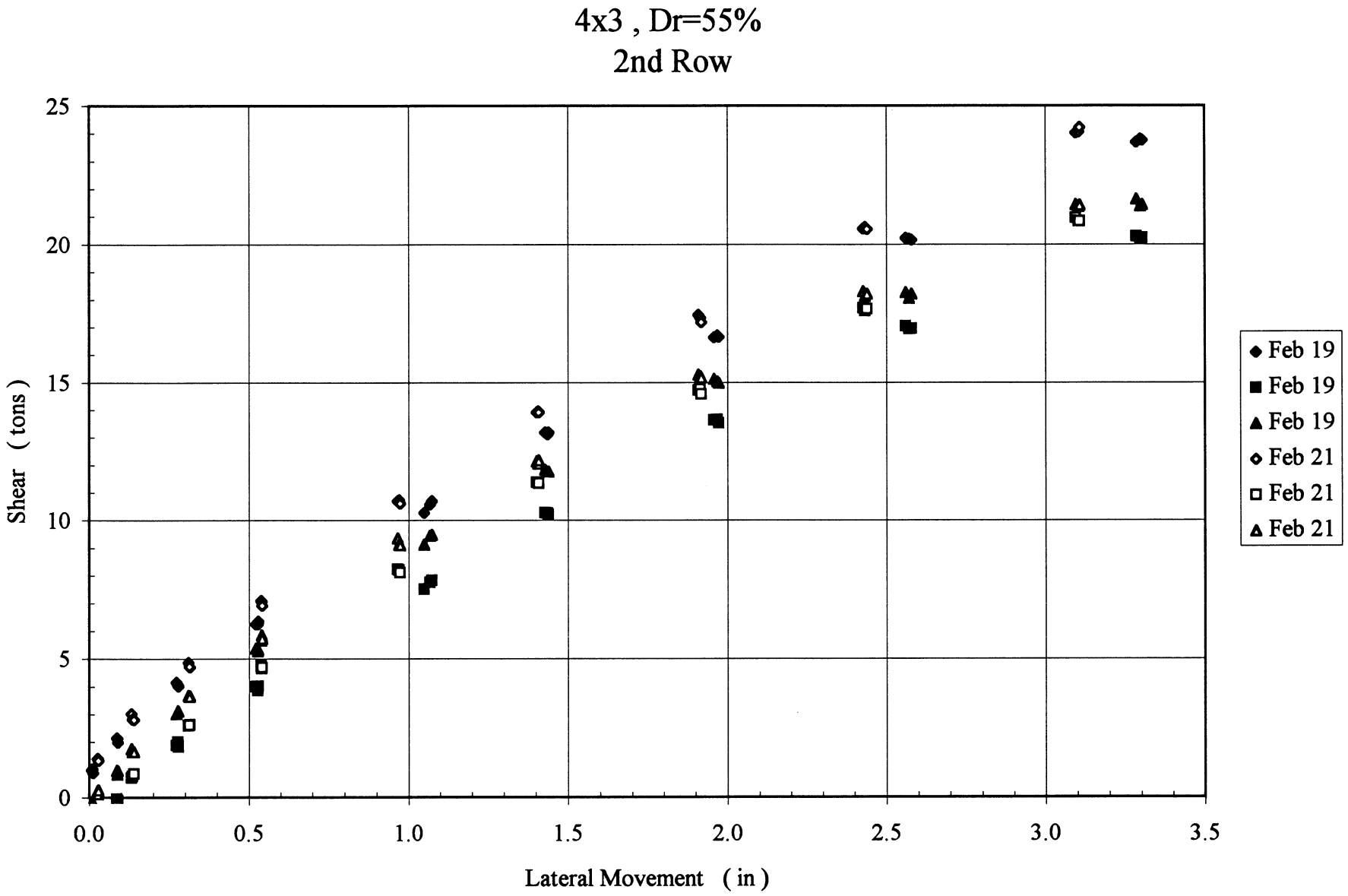

Figure 6-4(c). Results of 4 × 3 Group in Medium Dense Sand, Measured Shear for Each Pile in 2nd Row

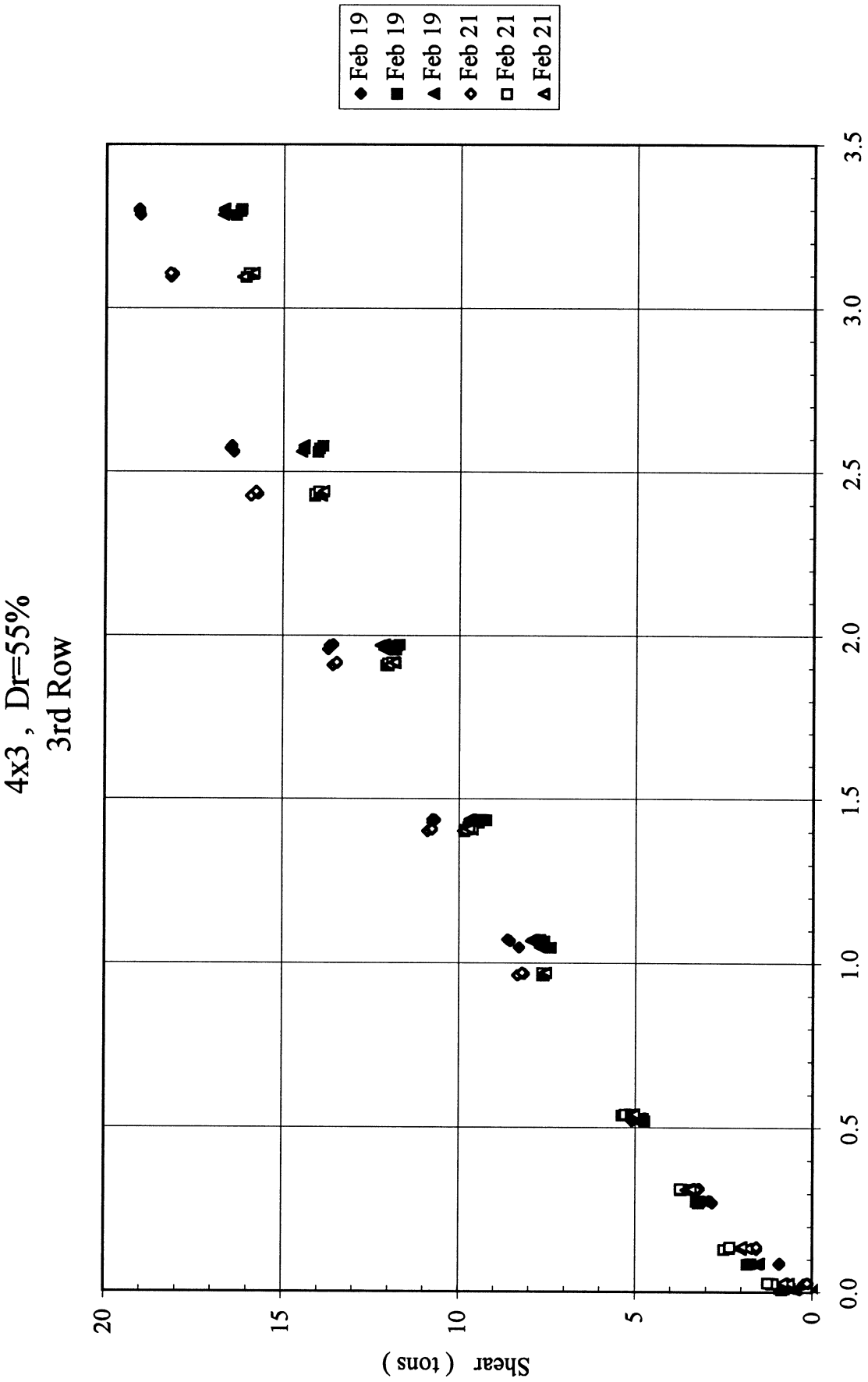

Figure 6-4(d). Results of 4 × 3 Group in Medium Dense Sand, Measured Shear for Each Pile in 3rd Row

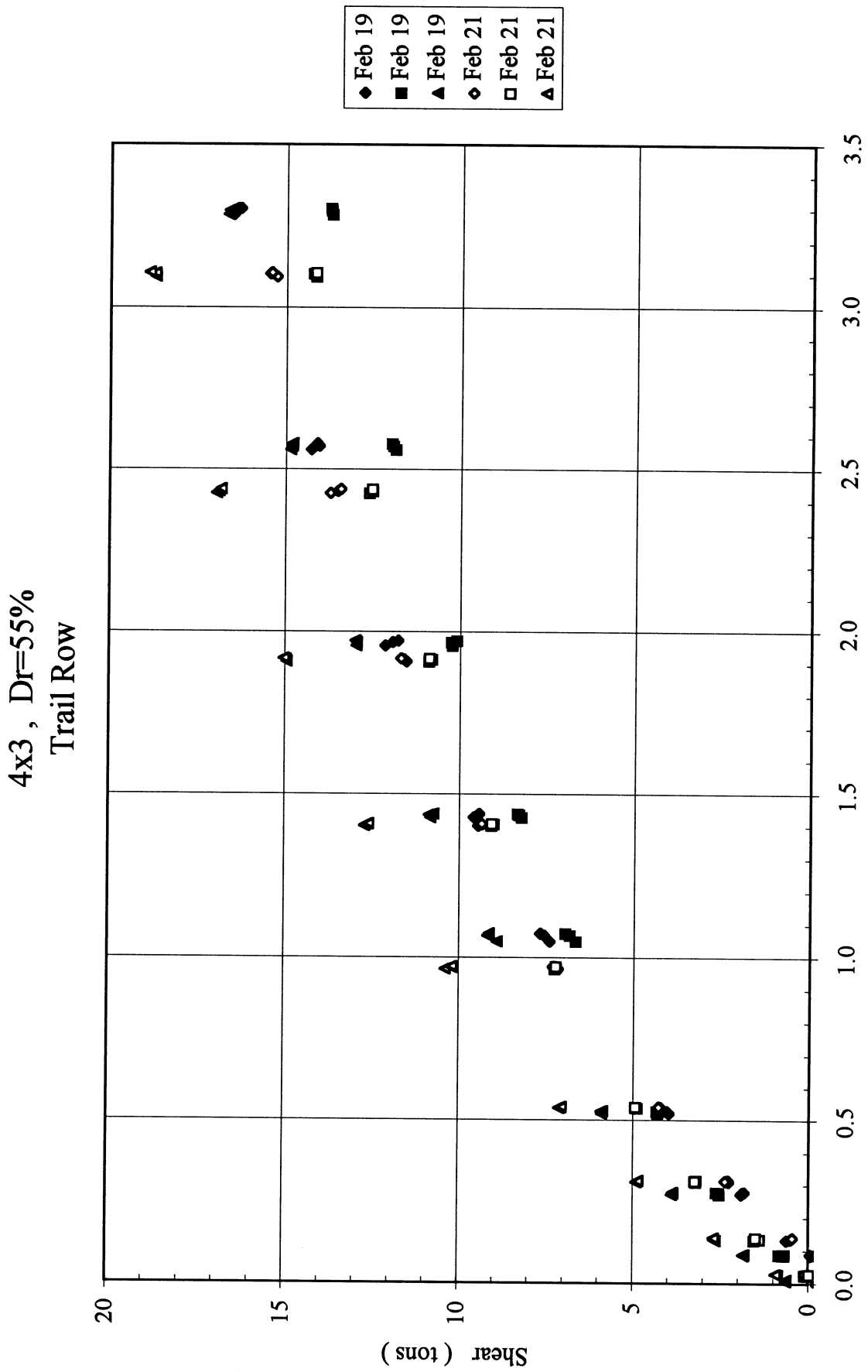

Figure 6-4(e). Results of 4 × 3 Group in Medium Dense Sand, Measured Shear for Each Pile in Trail Row

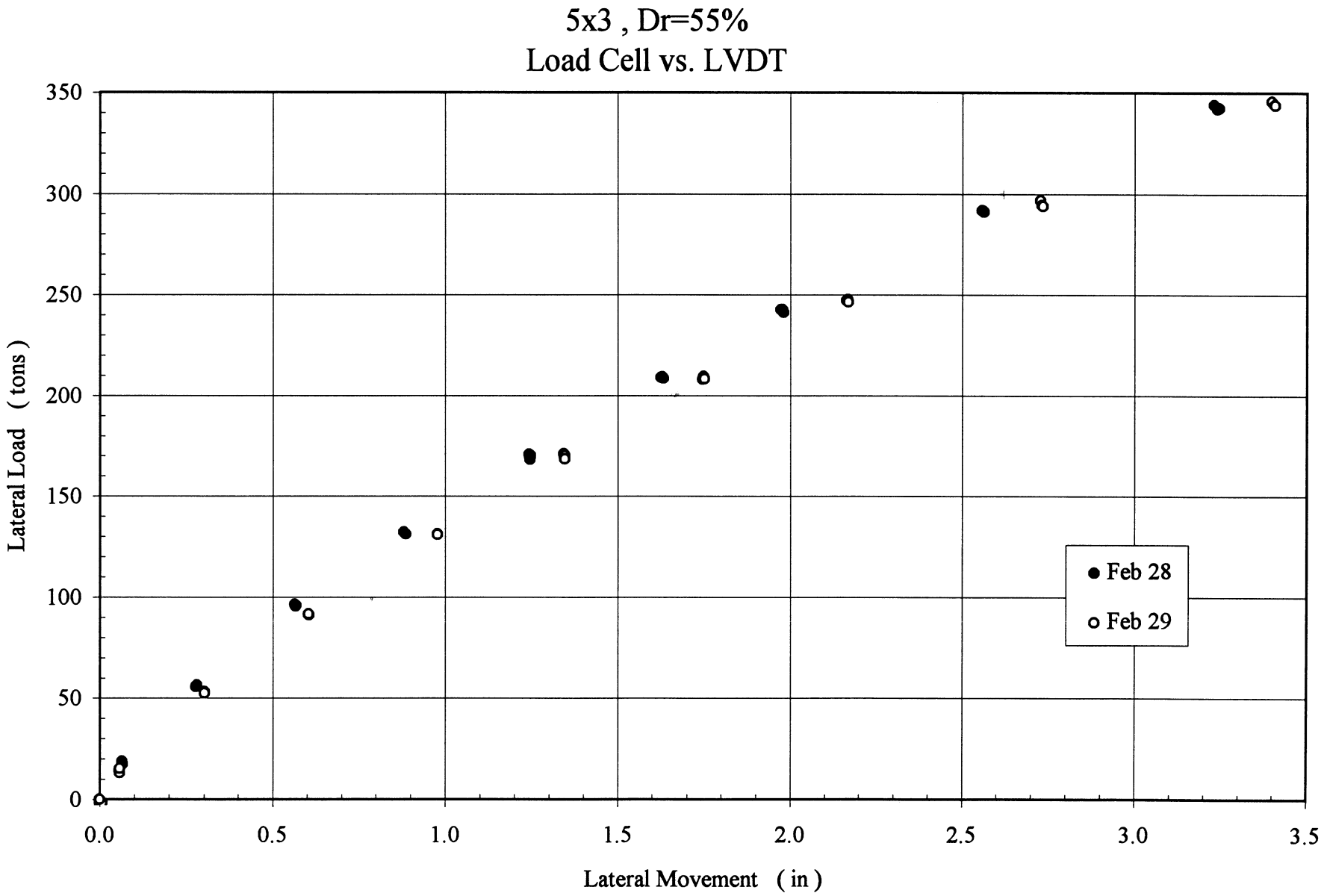

Figure 6-5(a). Results of 5 × 3 Group in Medium Dense Sand, Total Lateral Load vs. Lateral Deflection

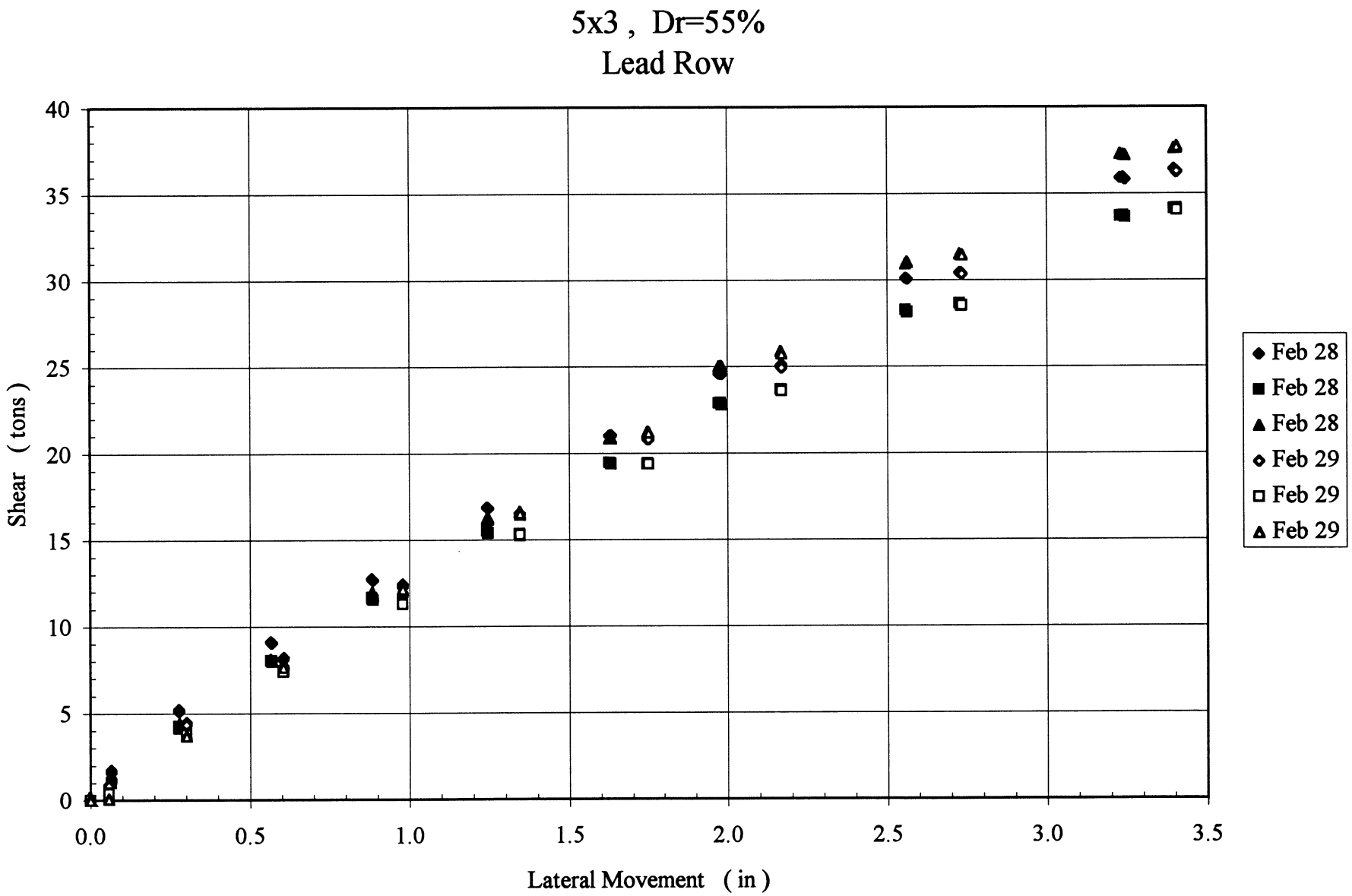

Figure 6-5(b). Results of 5 × 3 Group in Medium Dense Sand, Measured Shear for Each Pile in Lead Row

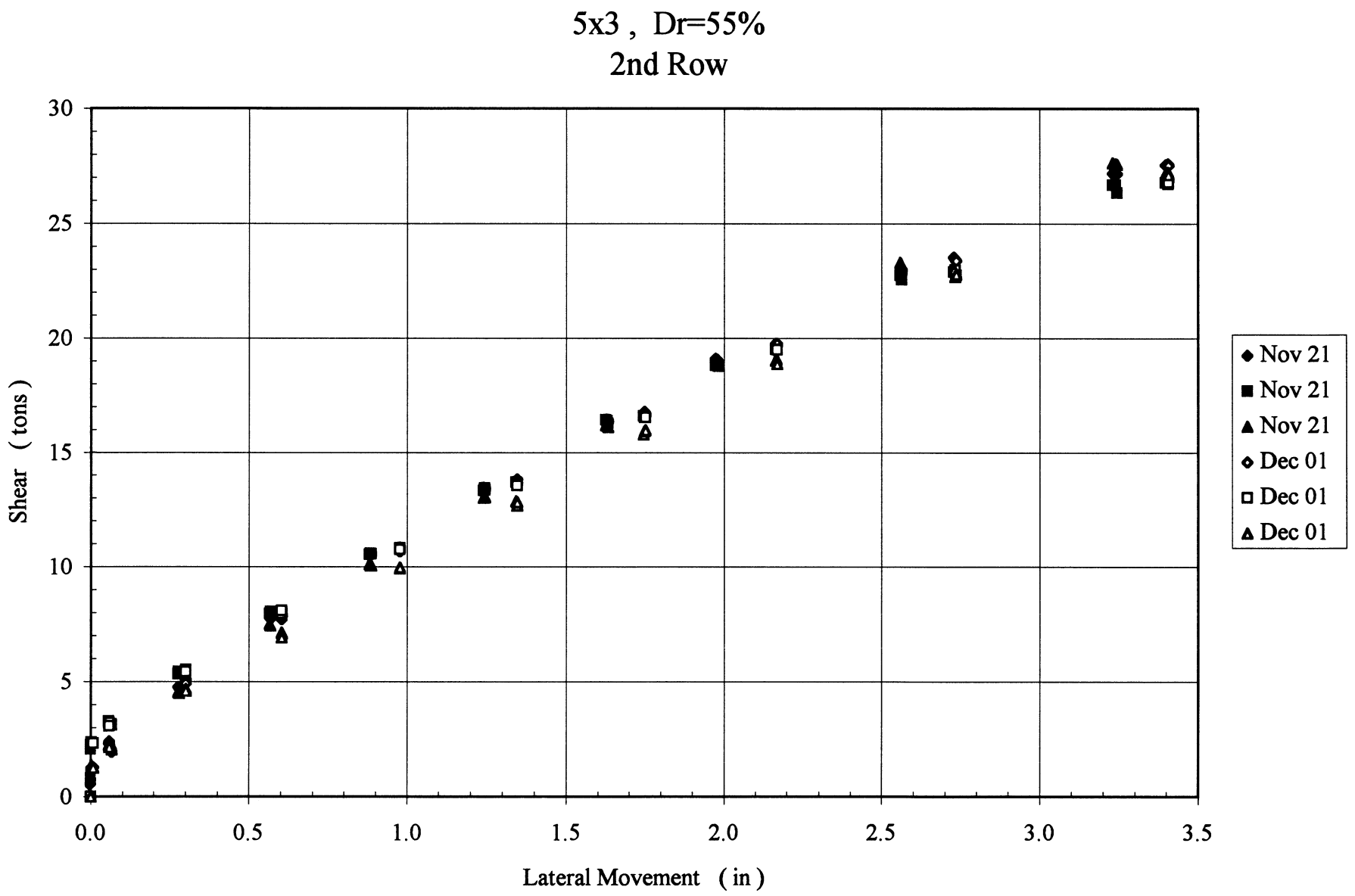

Figure 6-5(c). Results of 5 × 3 Group in Medium Dense Sand, Measured Shear for Each Pile in 2nd Row

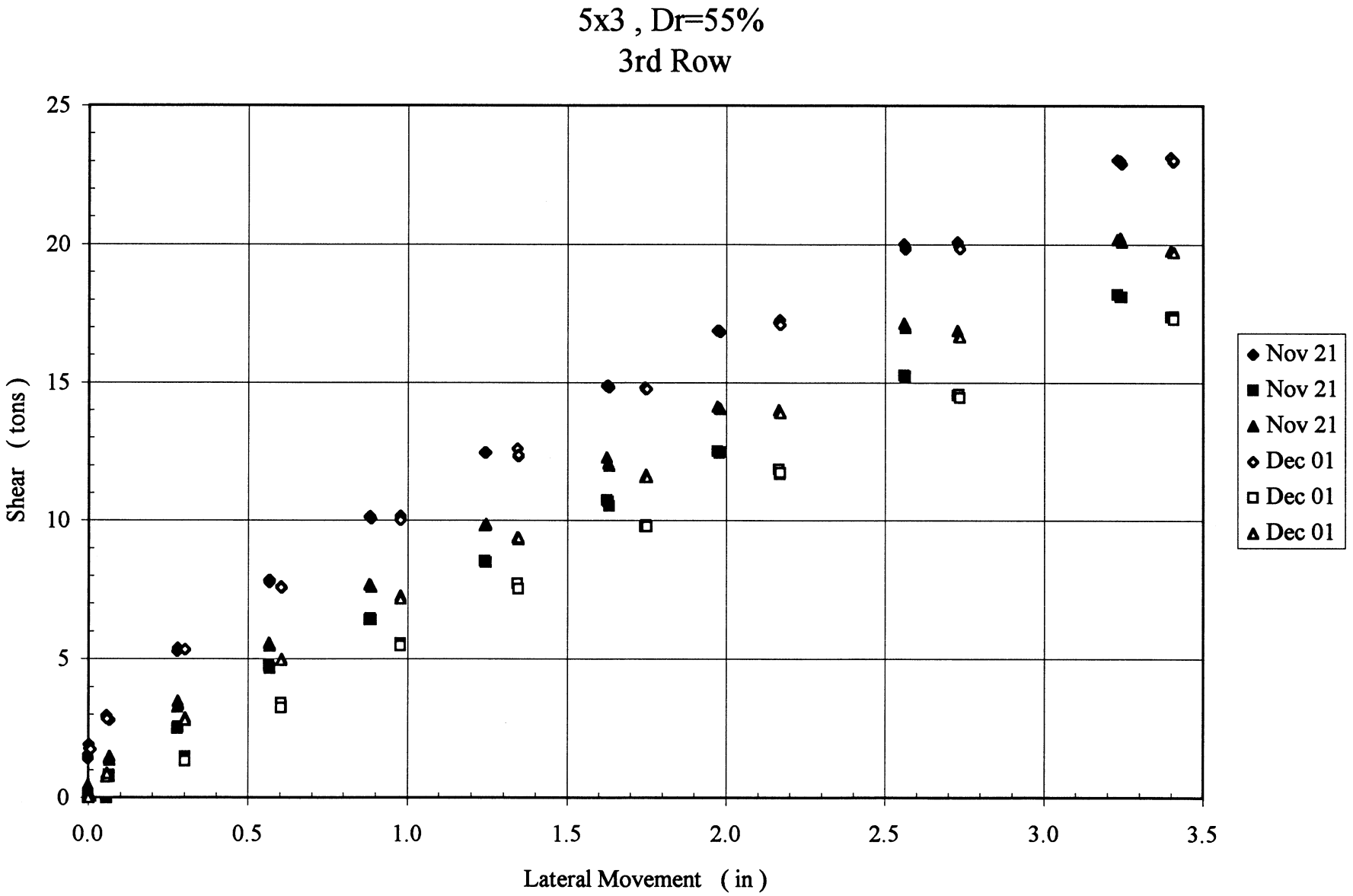

Figure 6-5(d). Results of 5 × 3 Group in Medium Dense Sand, Measured Shear for Each Pile in 3rd Row

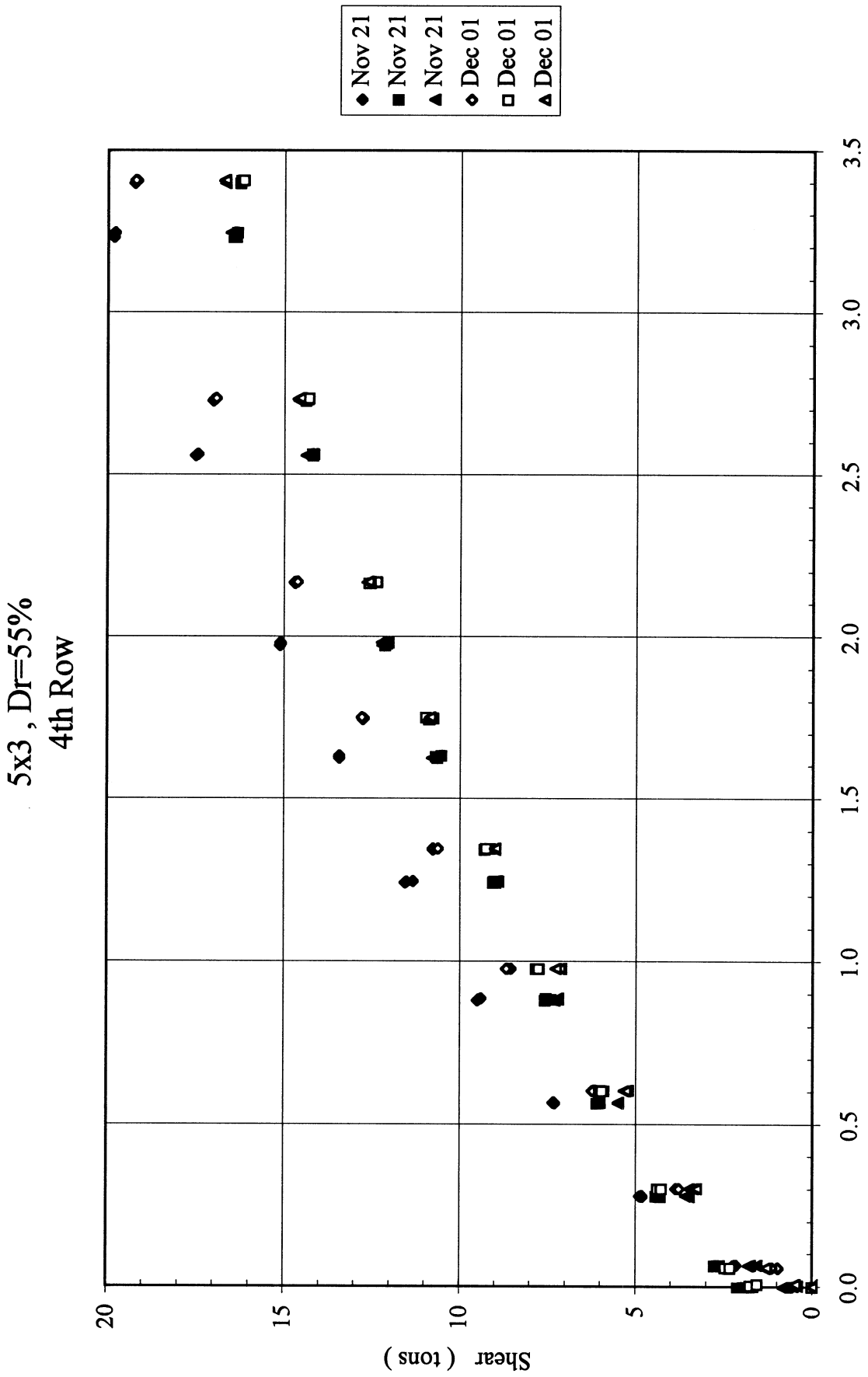

Figure 6-5(e). Results of 5 × 3 Group in Medium Dense Sand, Measured Shear for Each Pile in 4th Row

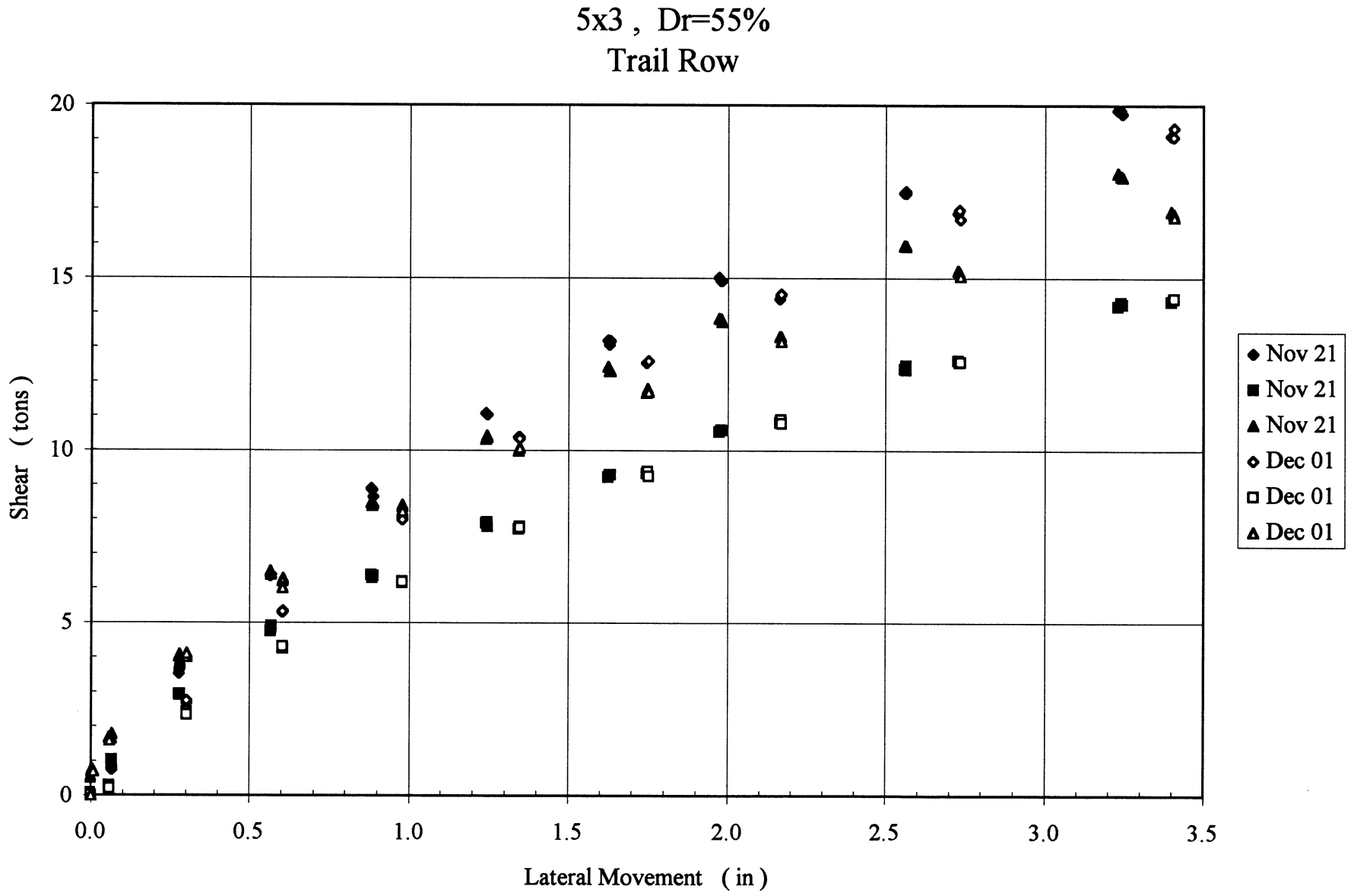

Figure 6-5(f). Results of 5 × 3 Group in Medium Dense Sand, Measured Shear for Each Pile in Trail Row

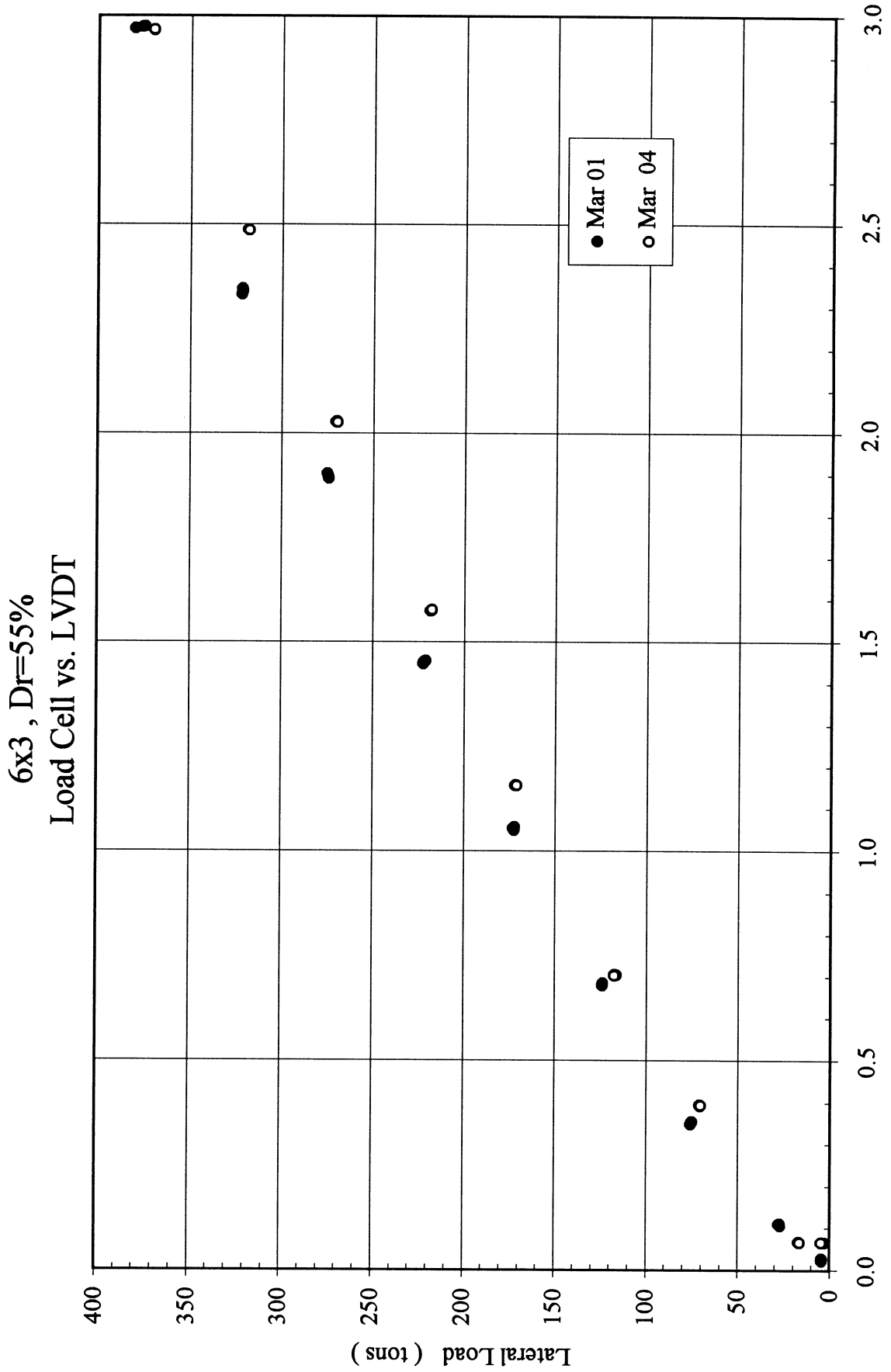

Figure 6-6(a). Results of 6 × 3 Group in Medium Dense Sand, Total Lateral Load vs. Lateral Deflection

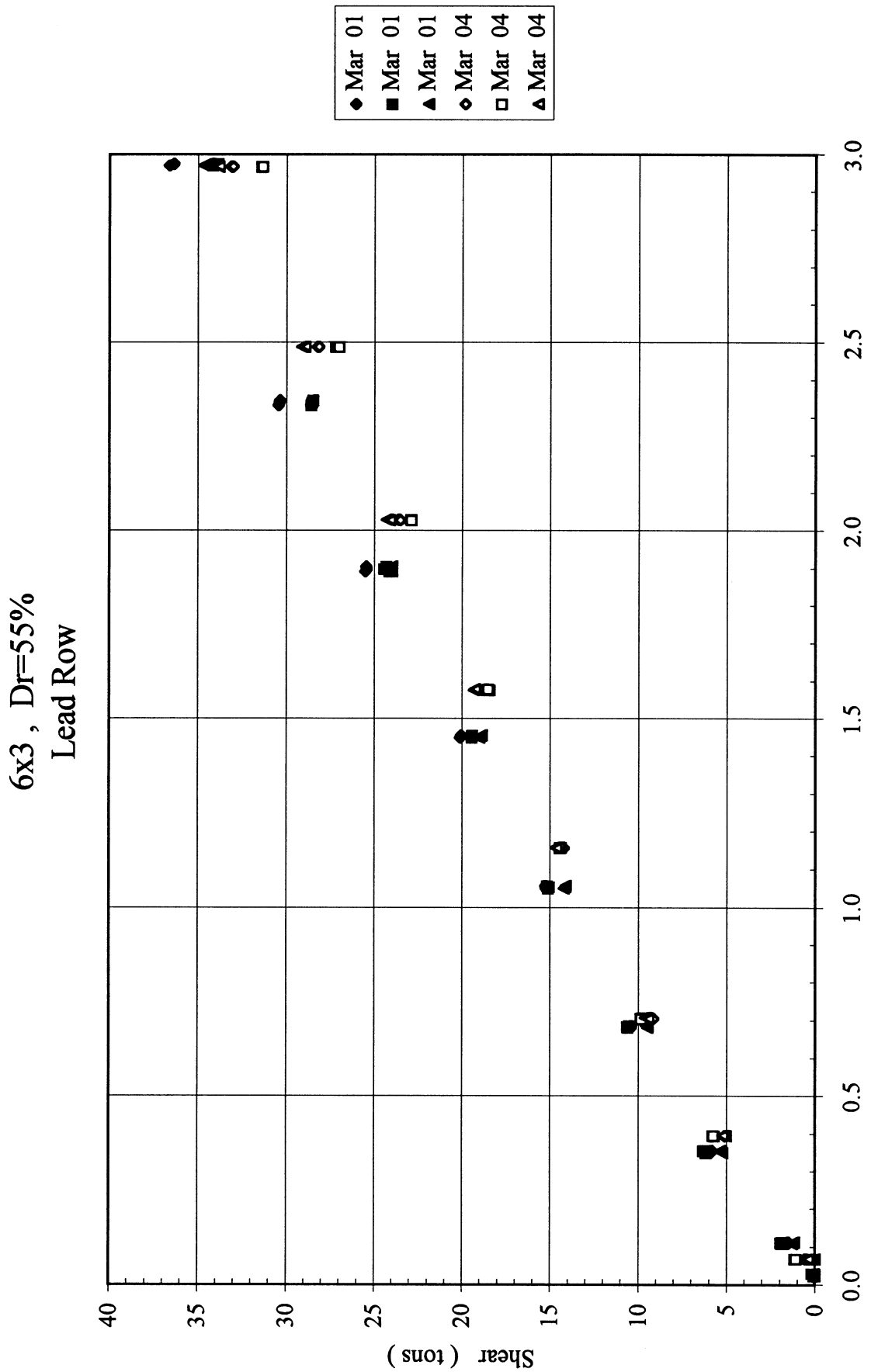

Figure 6-6(b). Results of 6 × 3 Group in Medium Dense Sand, Measured Shear for Each Pile in Lead Row

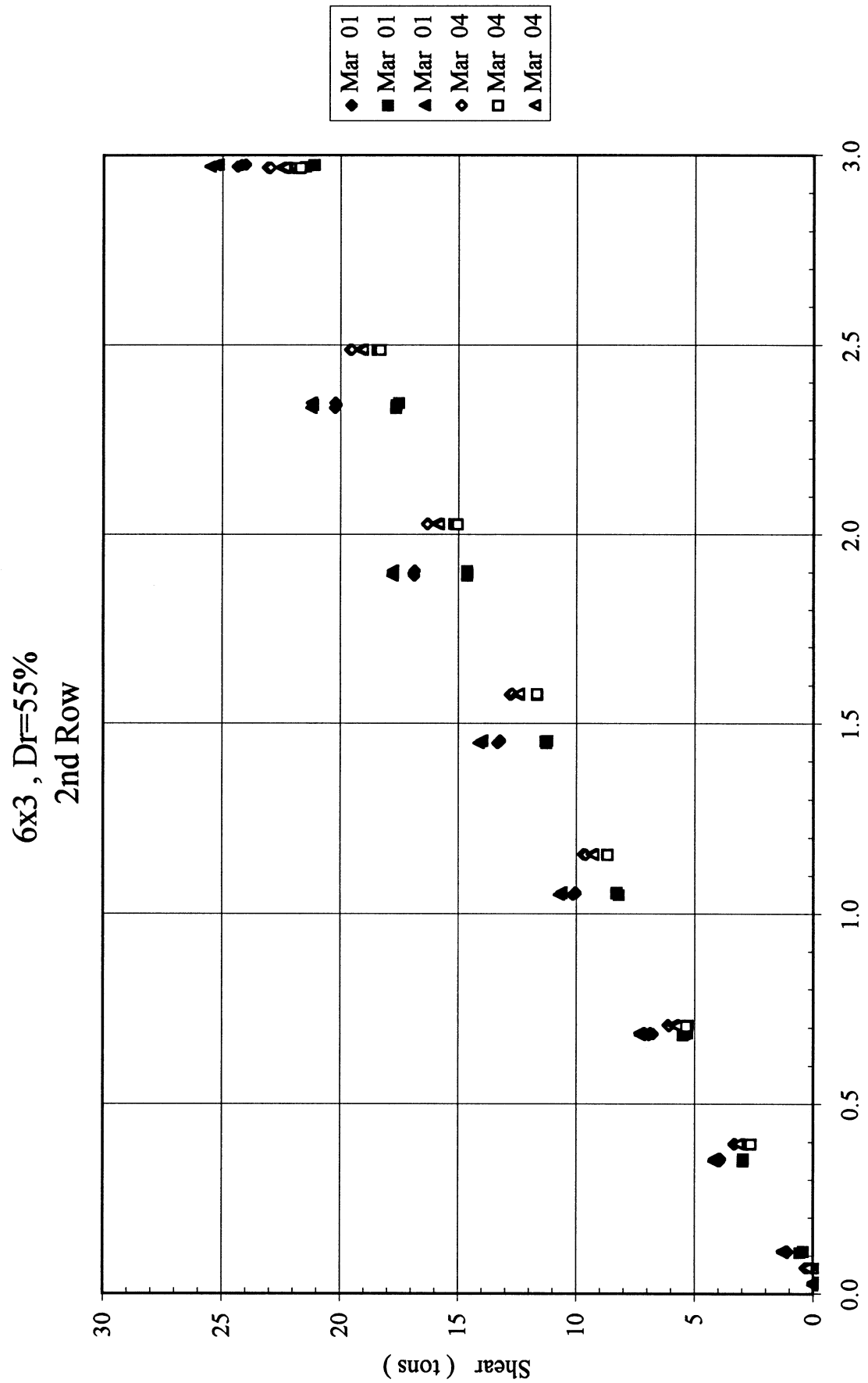

Figure 6-6(c). Results of 6 × 3 Group in Medium Dense Sand, Measured Shear for Each Pile in 2nd Row

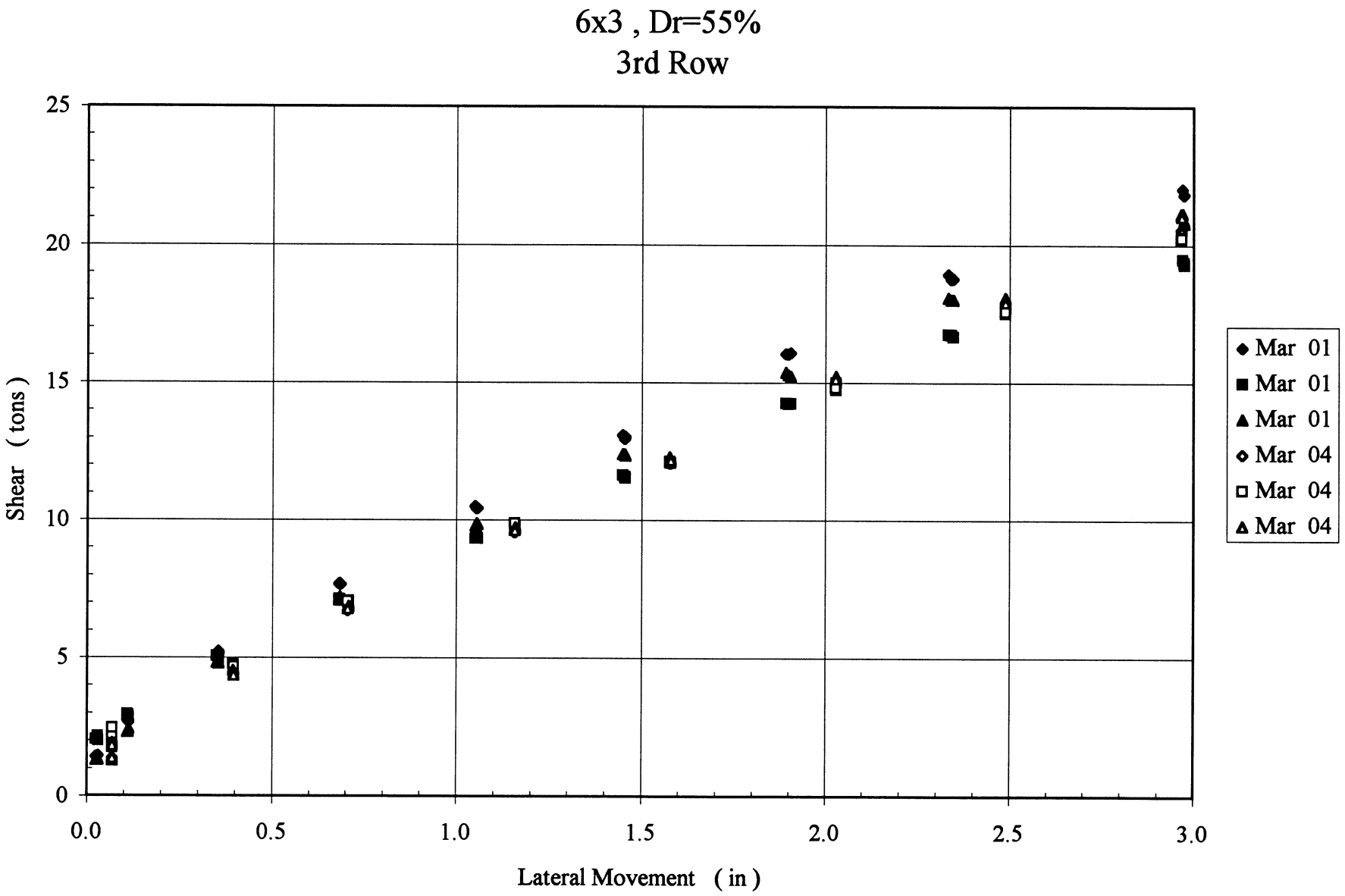

Figure 6-6(d). Results of 6 × 3 Group in Medium Dense Sand, Measured Shear for Each Pile in 3rd Row

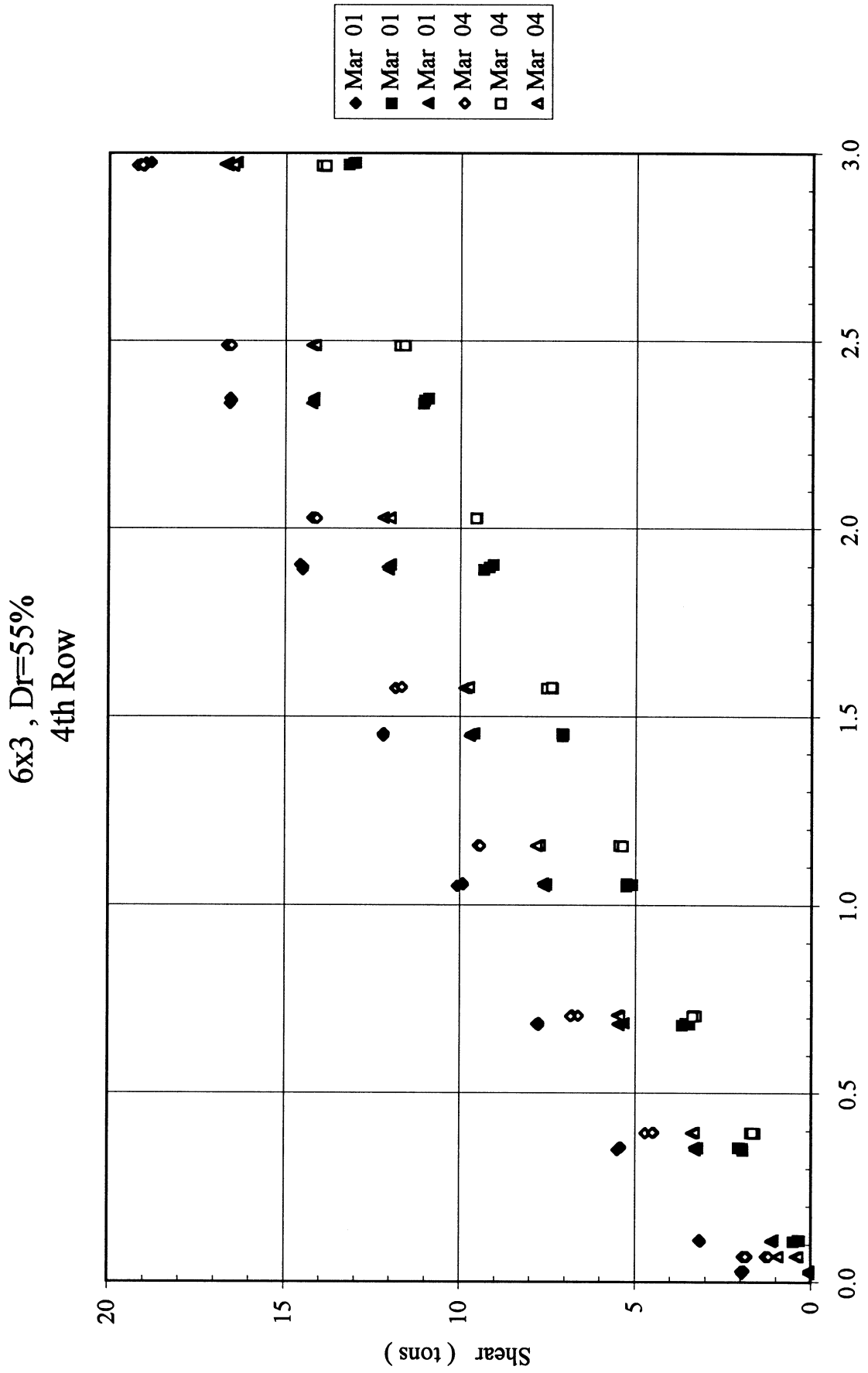

Figure 6-6(e). Results of 6 × 3 Group in Medium Dense Sand, Measured Shear for Each Pile in 4th Row

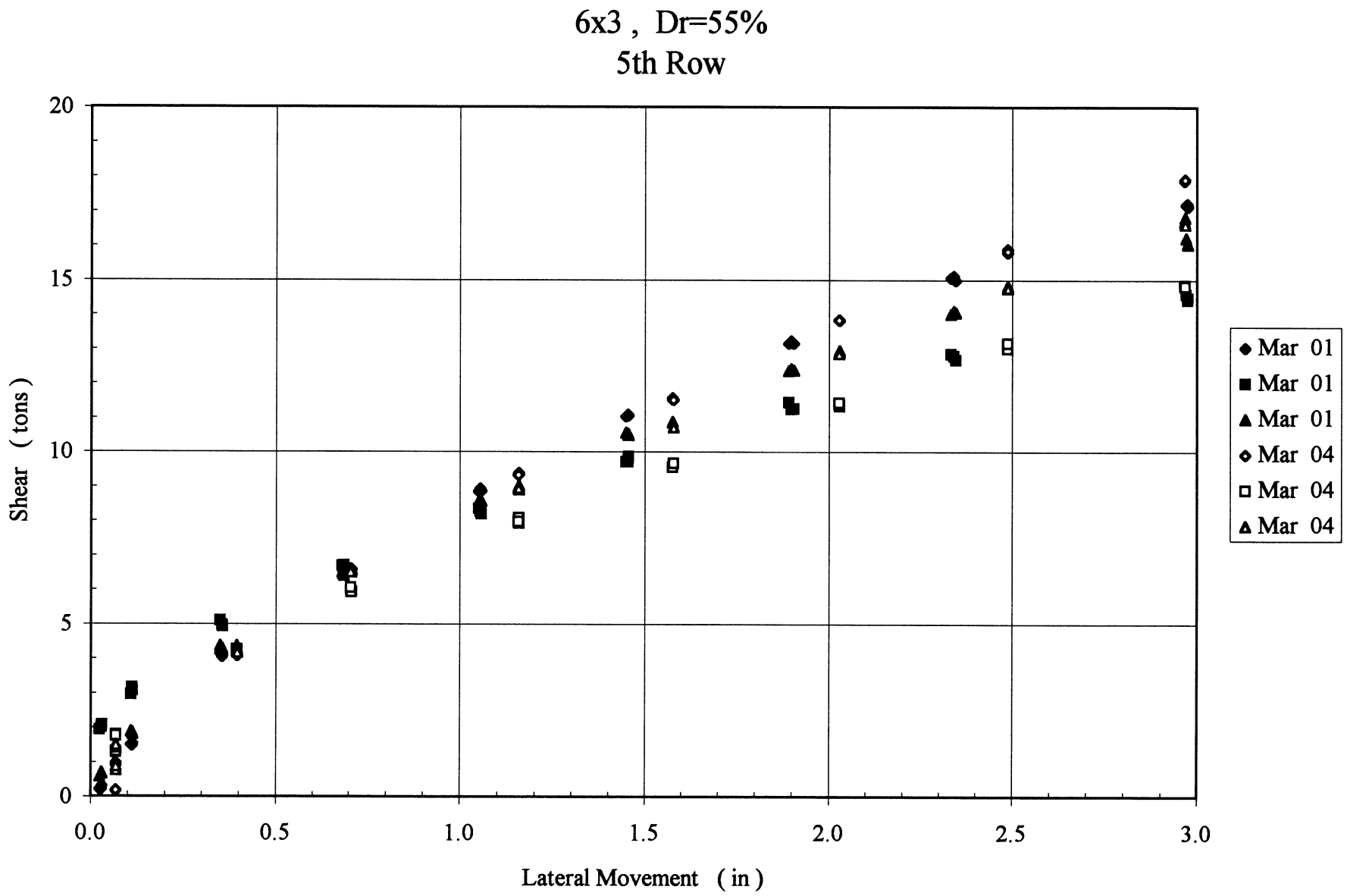

Figure 6-6(f). Results of 6 × 3 Group in Medium Dense Sand, Measured Shear for Each Pile in 5th Row

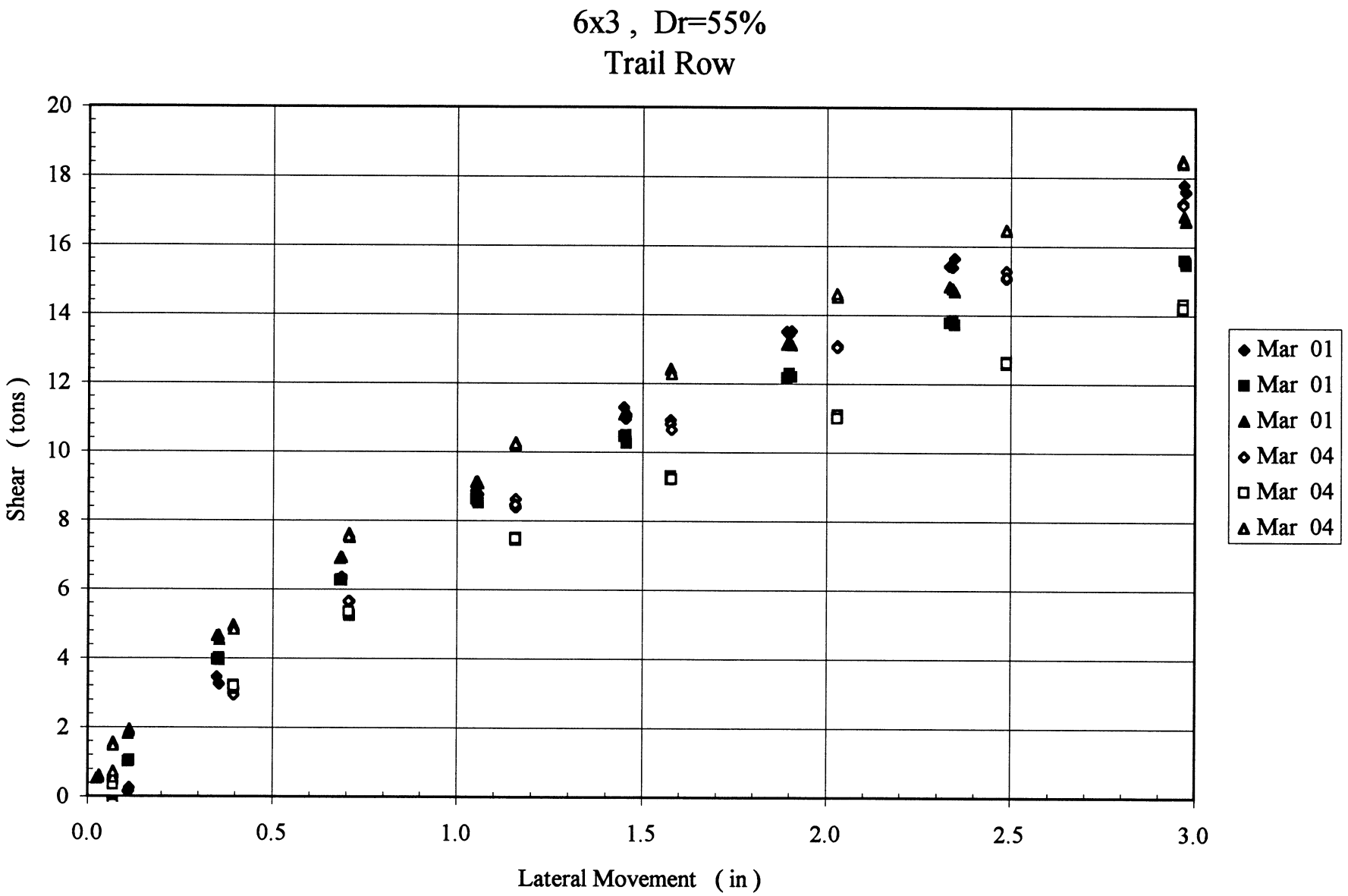

Figure 6-6(g). Results of 6 × 3 Group in Medium Dense Sand, Measured Shear for Each Pile in Trail Row

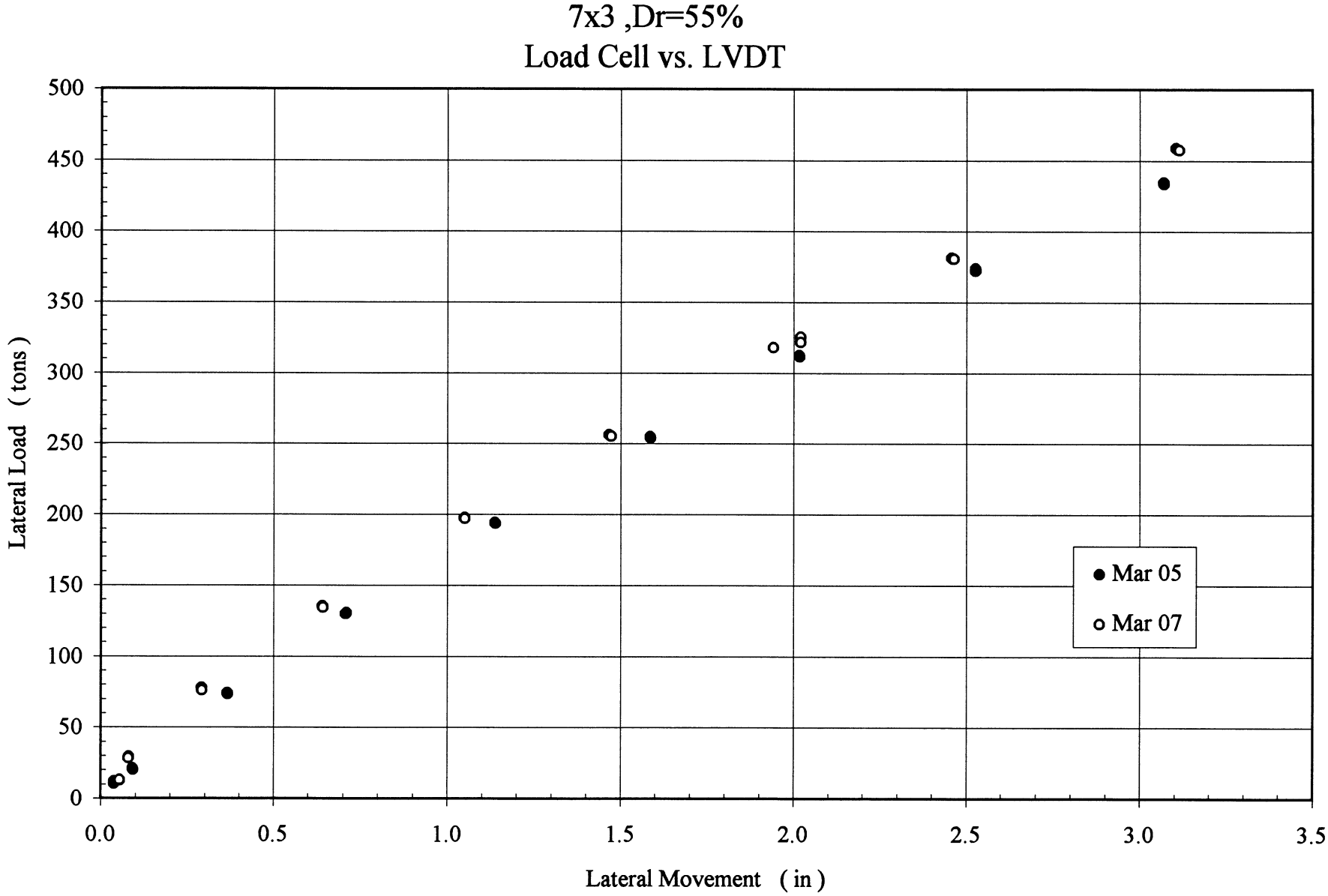

Figure 6-7(a). Results of 7 × 3 Group in Medium Dense Sand, Total Lateral Load vs. Lateral Deflection

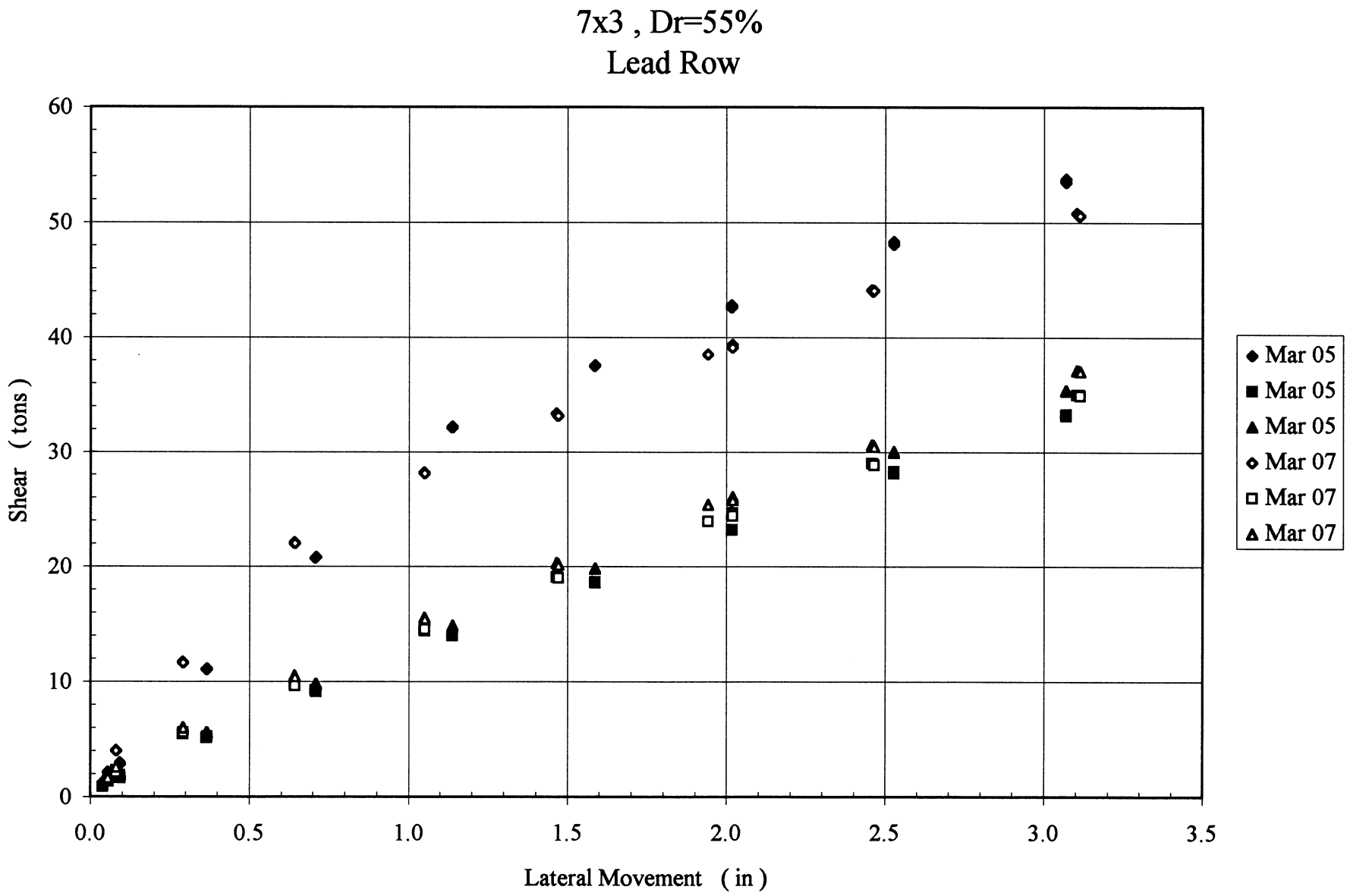

Figure 6-7(b). Results of 7 × 3 Group in Medium Dense Sand, Measured Shear for Each Pile in Lead Row

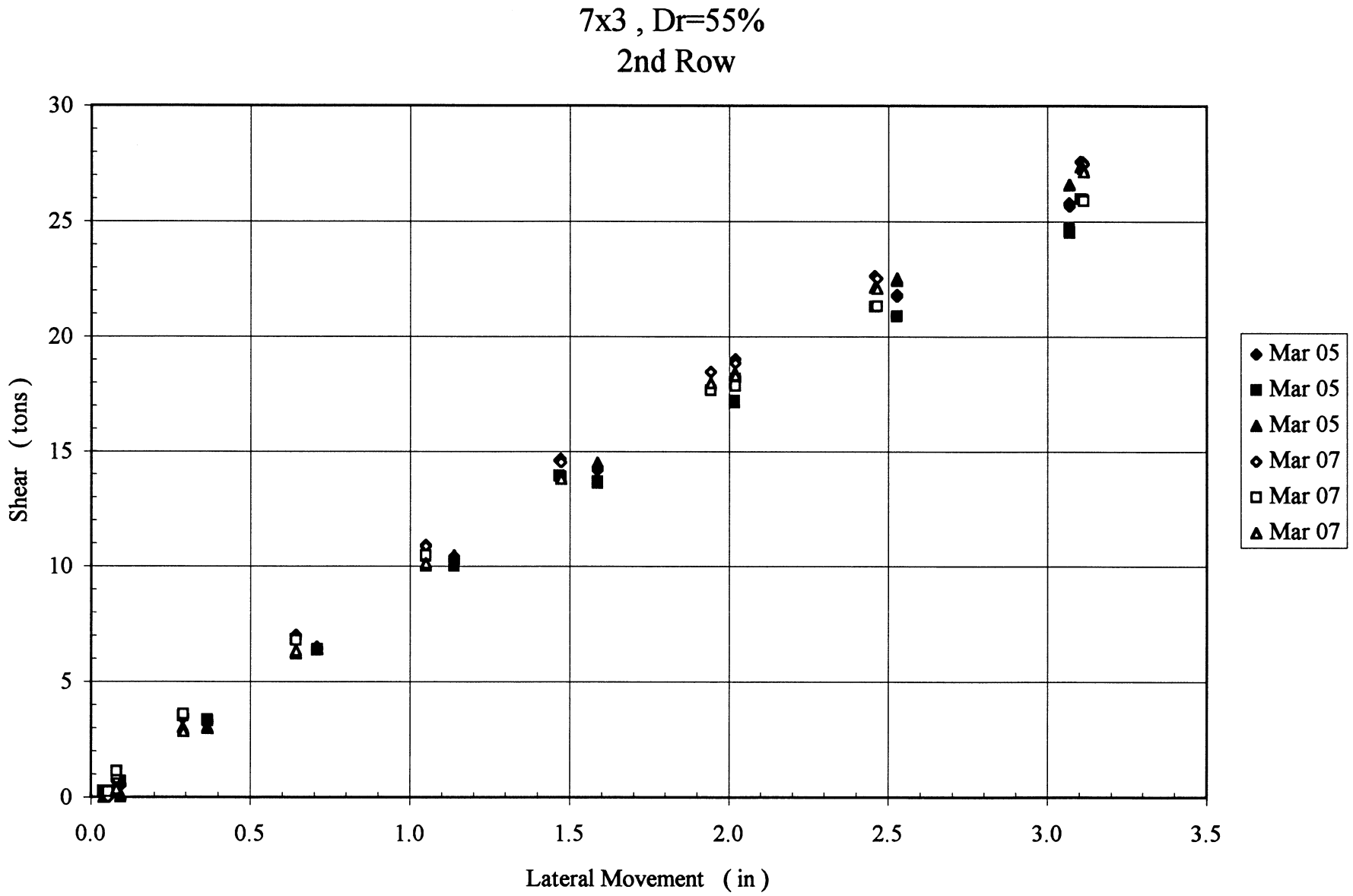

Figure 6-7(c). Results of 7 × 3 Group in Medium Dense Sand, Measured Shear for Each Pile in 2nd Row

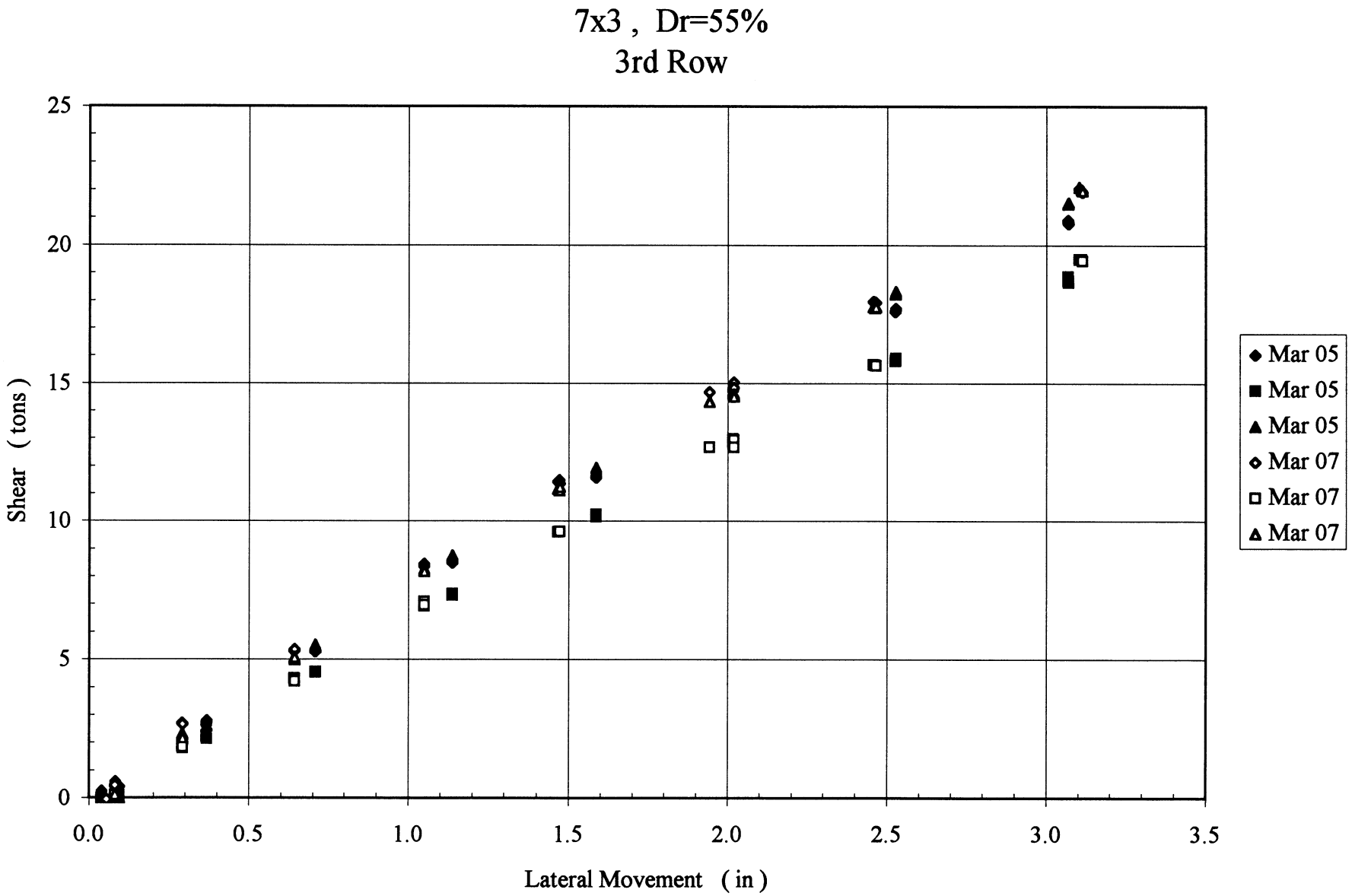

Figure 6-7(d). Results of 7 × 3 Group in Medium Dense Sand, Measured Shear for Each Pile in 3rd Row

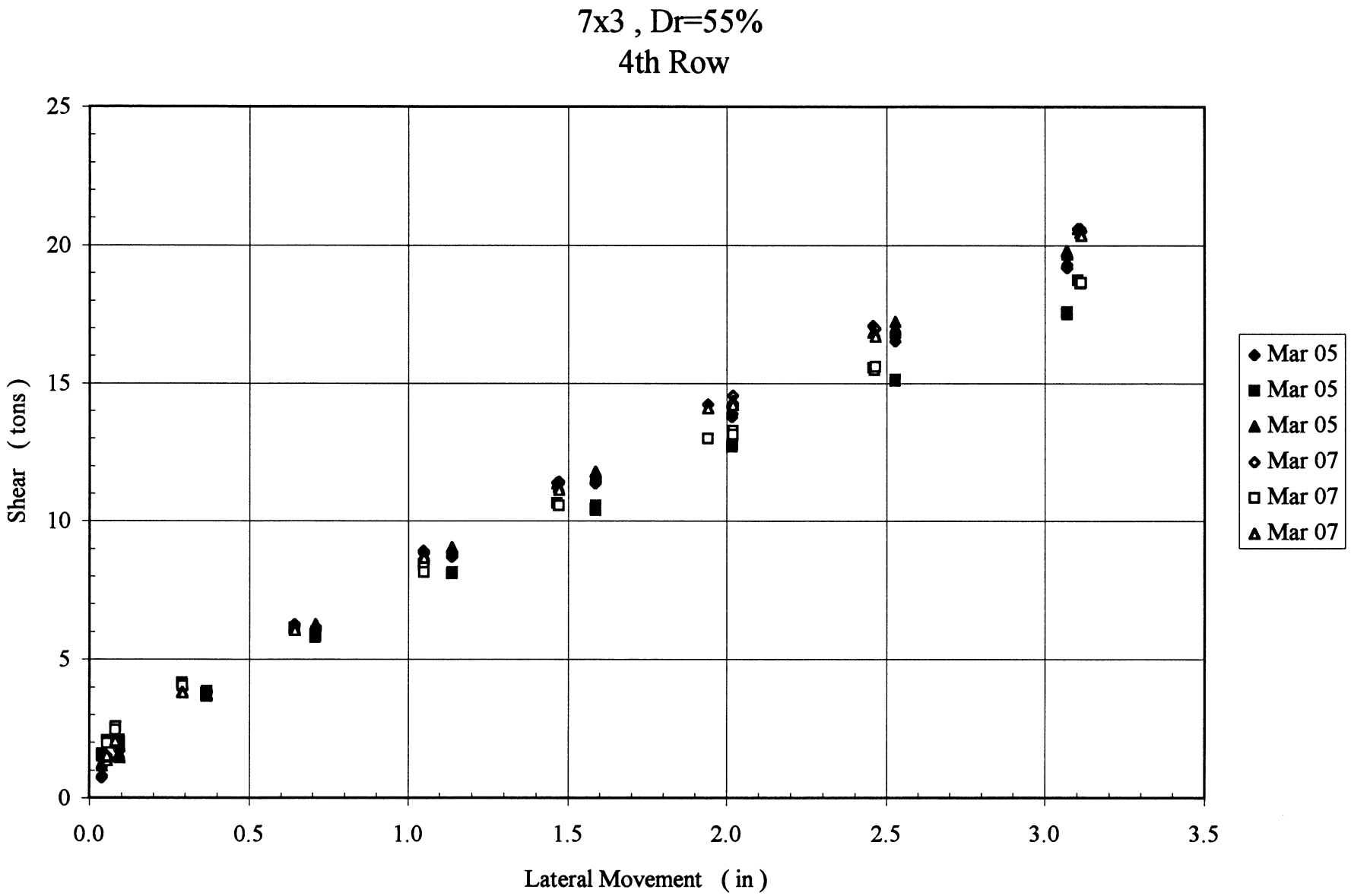

Figure 6-7(e). Results of 7 × 3 Group in Medium Dense Sand, Measured Shear for Each Pile in 4th Row

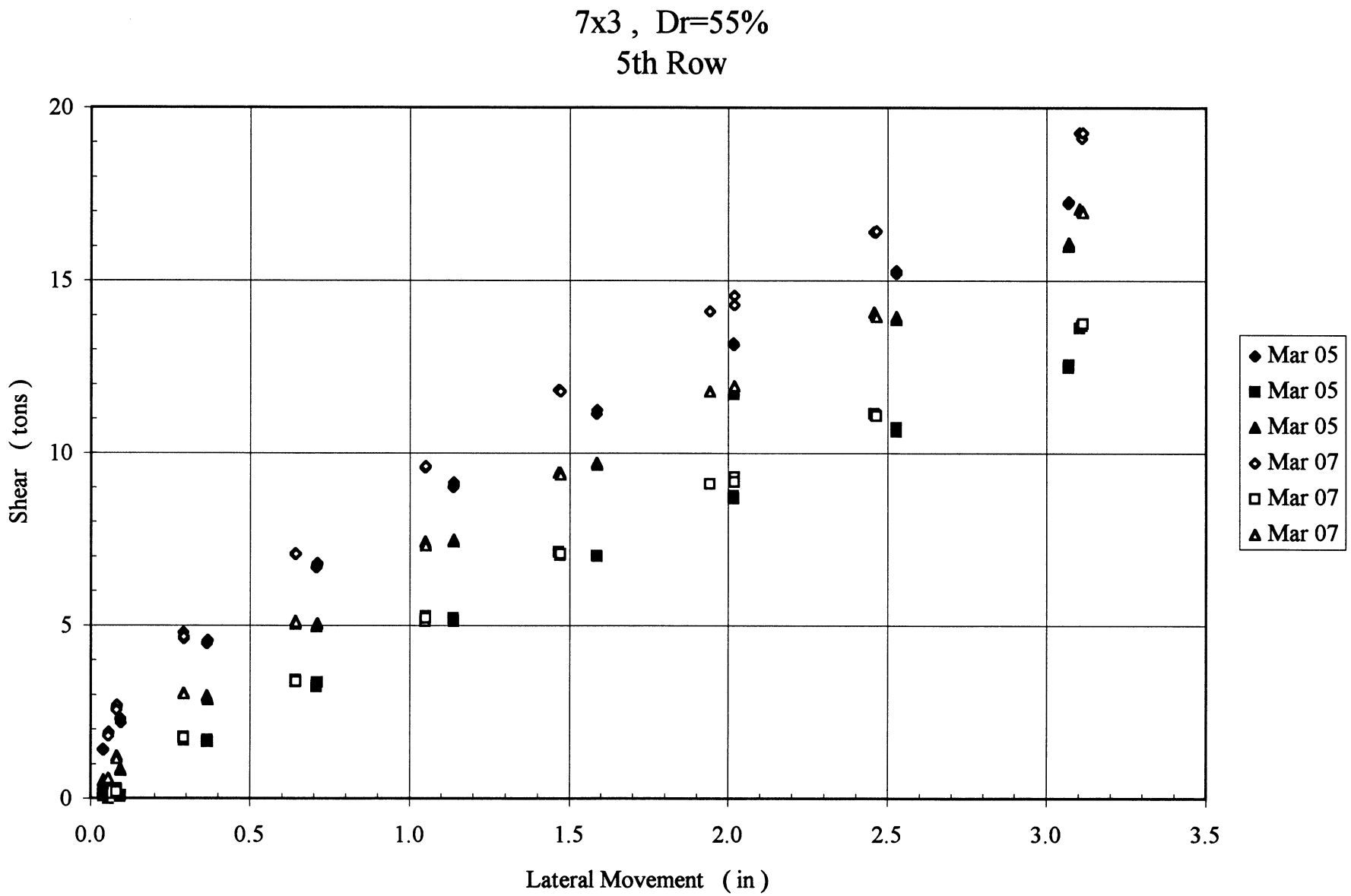

Figure 6-7(f). Results of 7 × 3 Group in Medium Dense Sand, Measured Shear for Each Pile in 5th Row

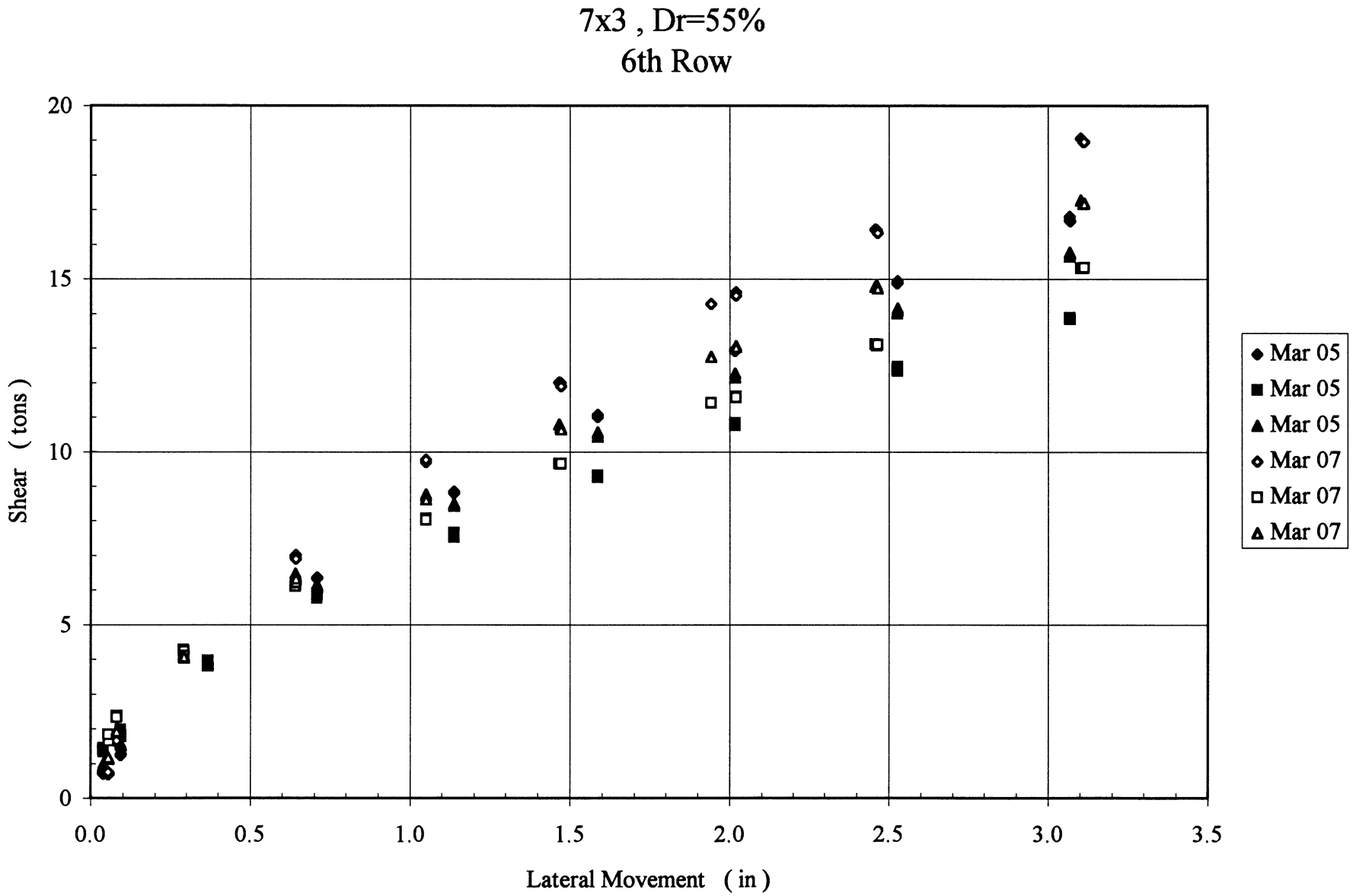

Figure 6-7(g). Results of 7 × 3 Group in Medium Dense Sand, Measured Shear for Each Pile in 6th Row

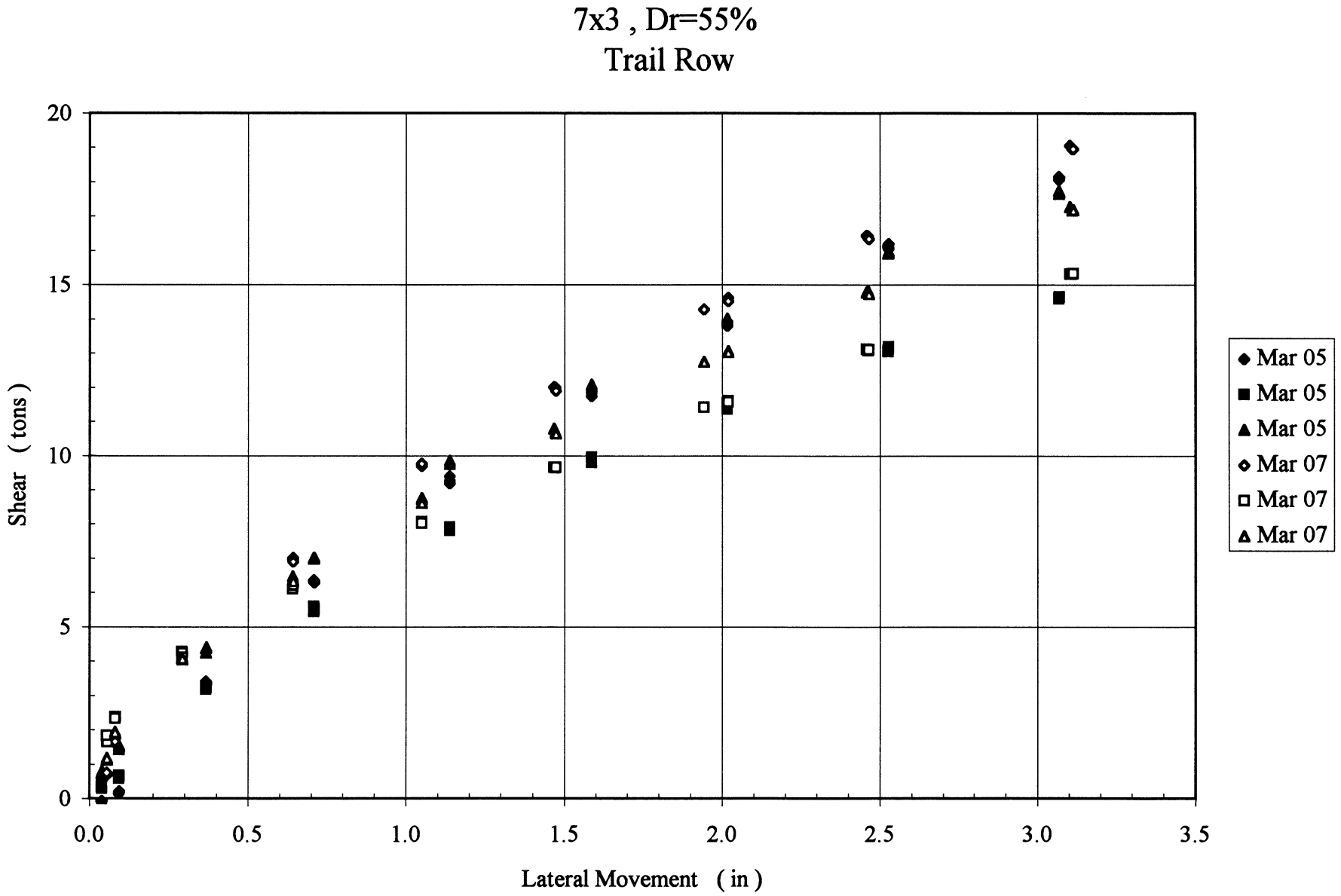

Figure 6-7(h). Results of 7 × 3 Group in Medium Dense Sand, Measured Shear for Each Pile in Trail Row

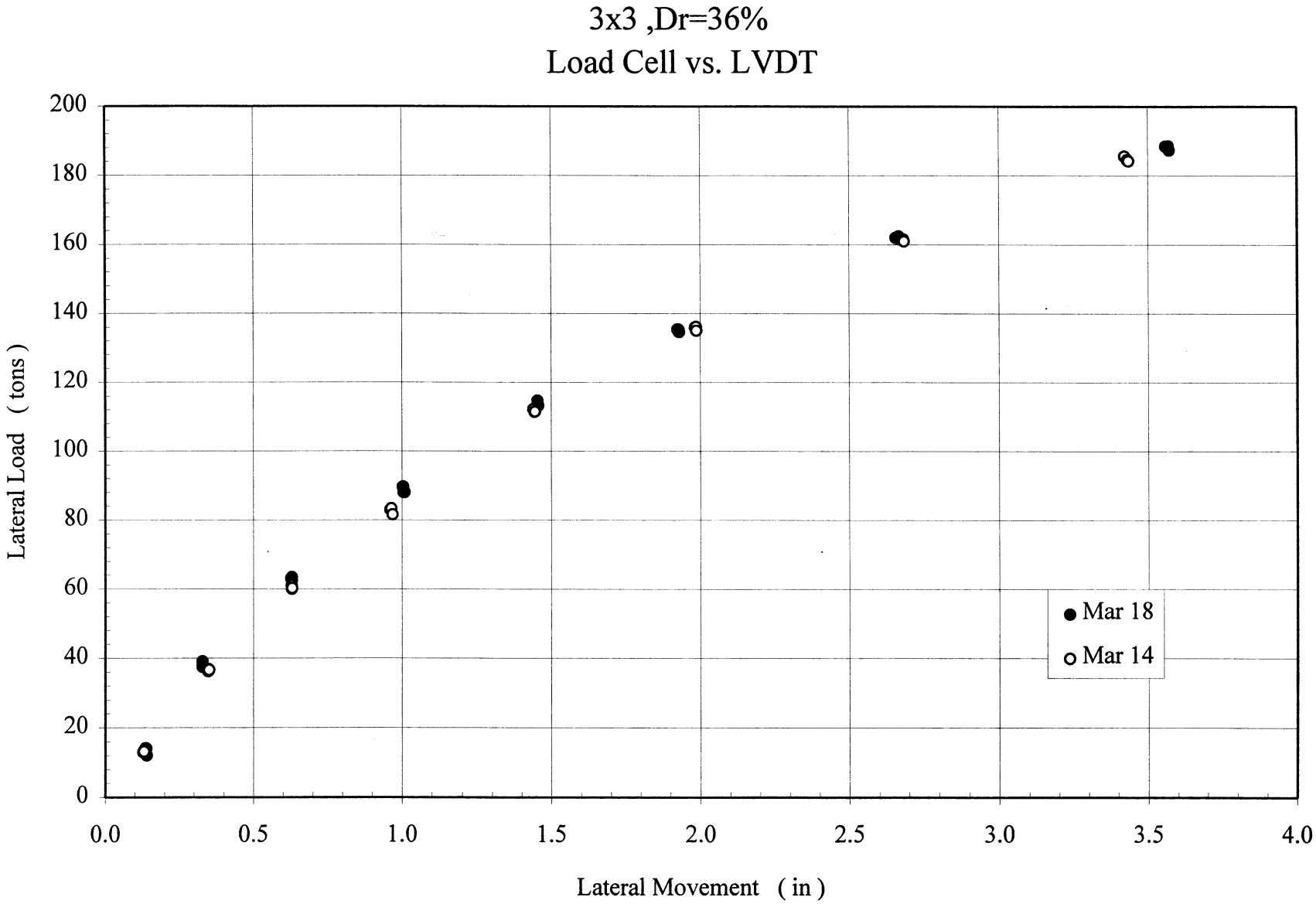

Figure 6-8(a). Results of 3 × 3 Group in Loose Sand, Total Lateral Load vs. Lateral Deflection

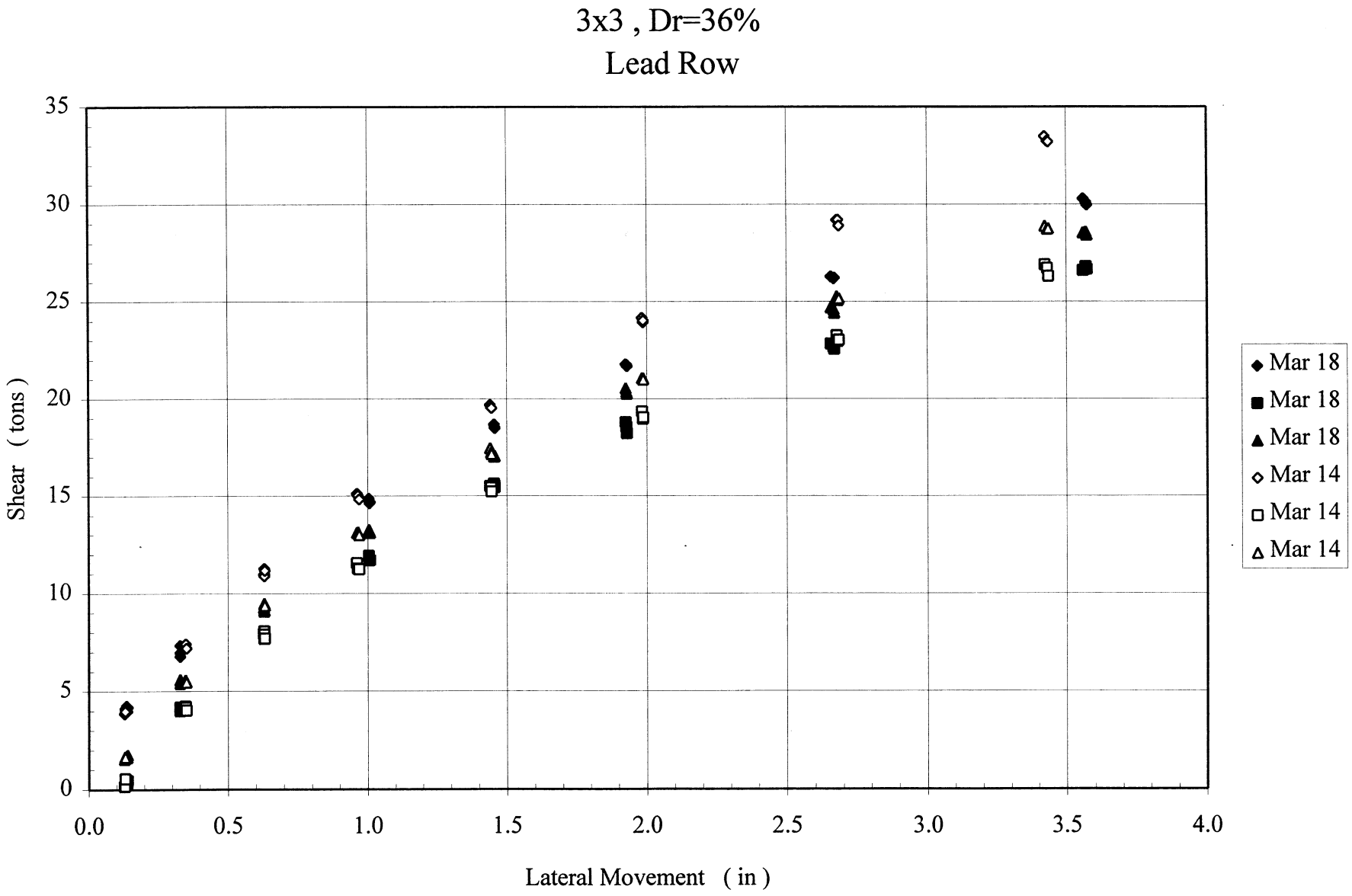

Figure 6-8(b). Results of 3 × 3 Group in Loose Sand, Measured Shear for Each Pile in Lead Row

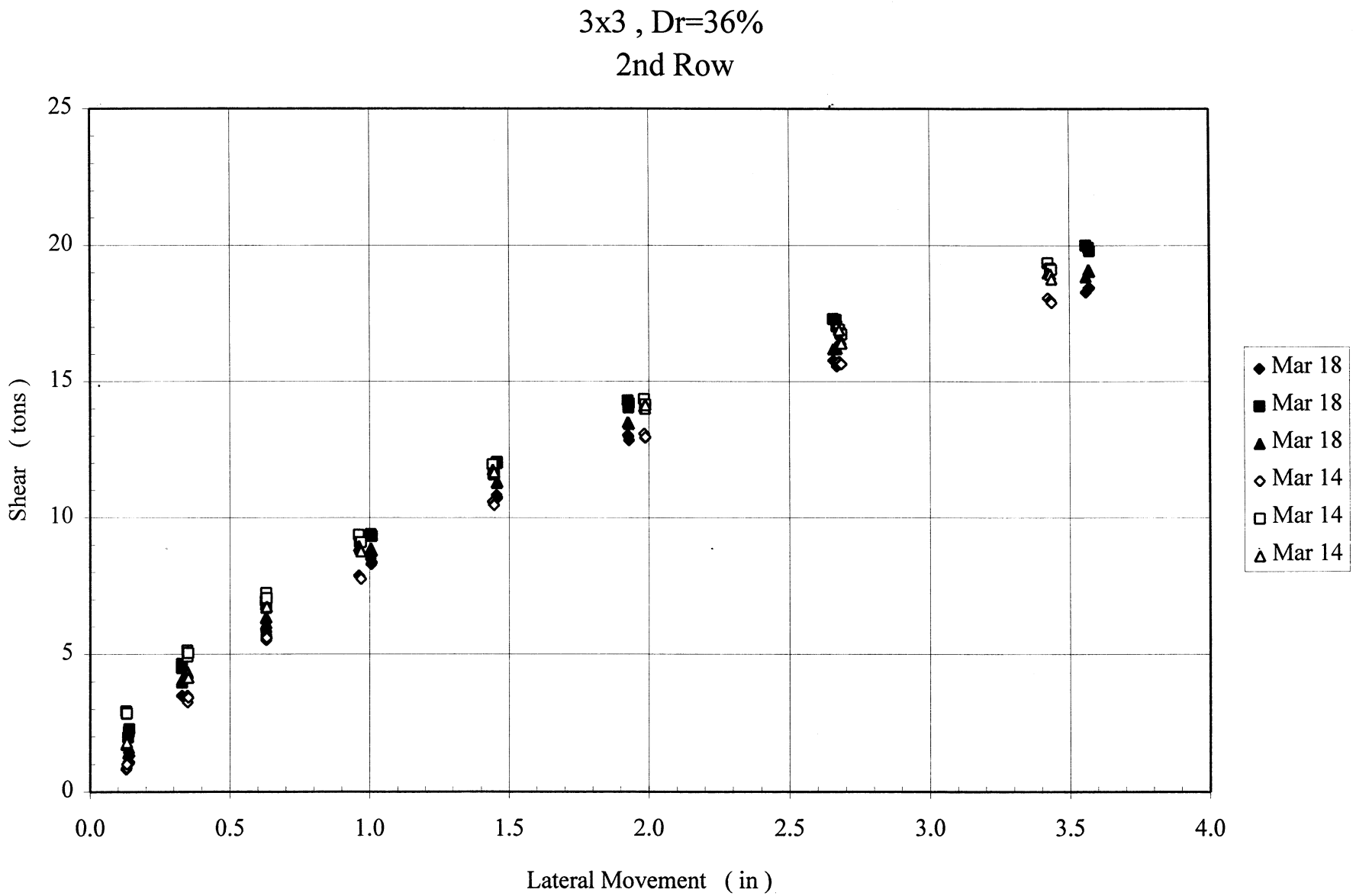

Figure 6-8(c). Results of 3 × 3 Group in Loose Sand, Measured Shear for Each Pile in 2nd Row

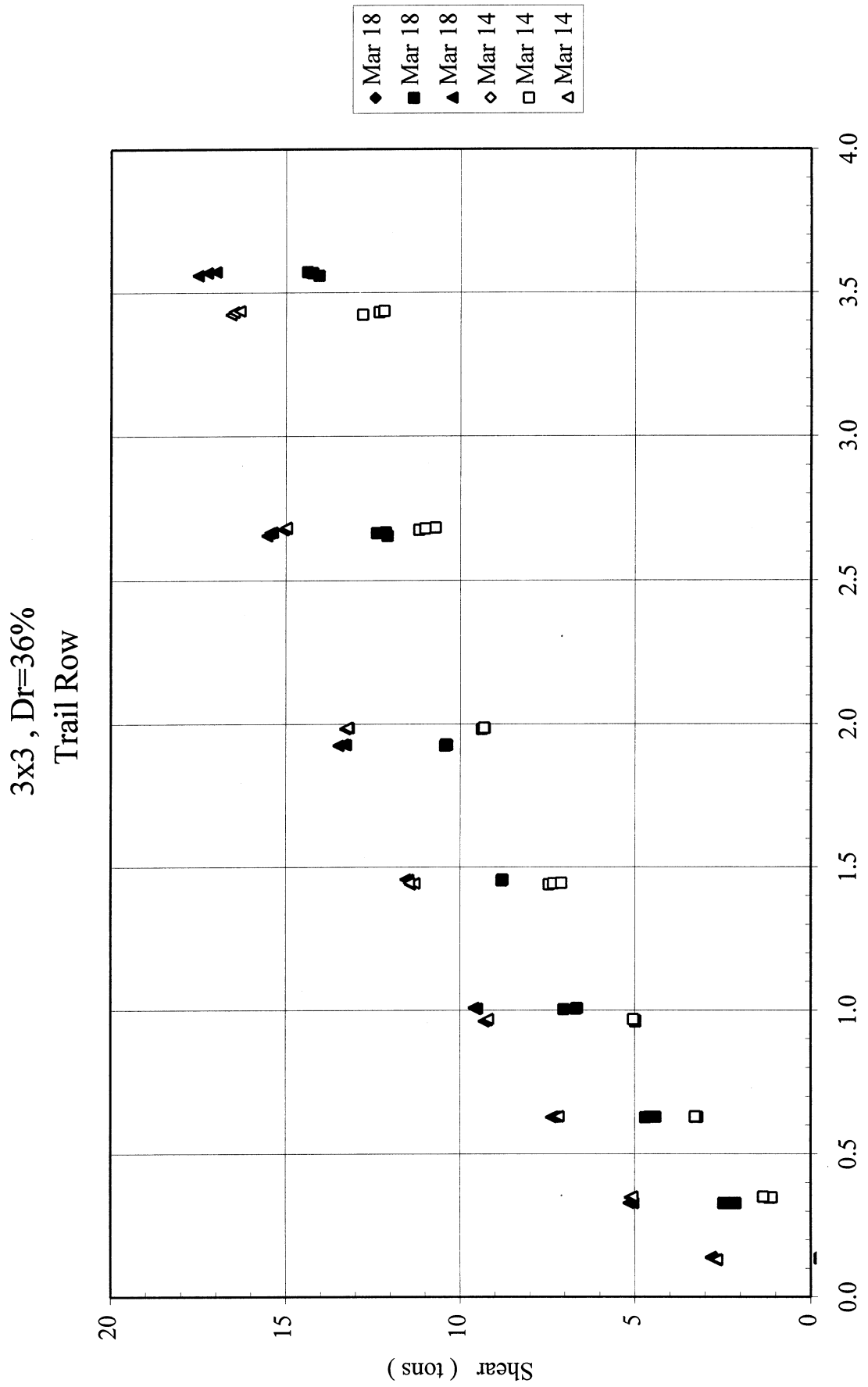

Figure 6-8(d). Results of 3 × 3 Group in Loose Sand, Measured Shear for Each Pile in Trail Row

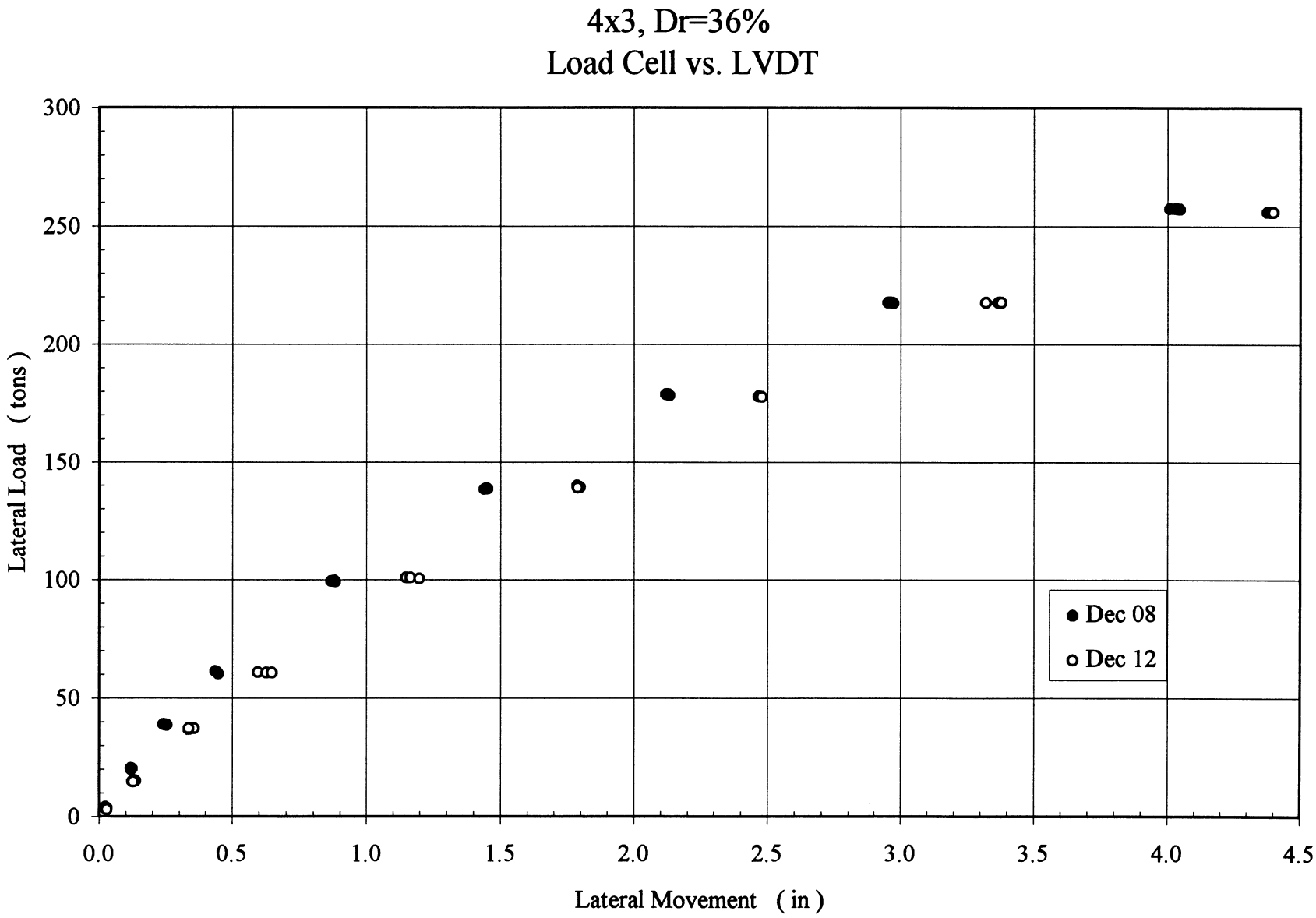

Figure 6-9(a). Results of 4 × 3 Group in Loose Sand, Total Lateral Load vs. Lateral Deflection

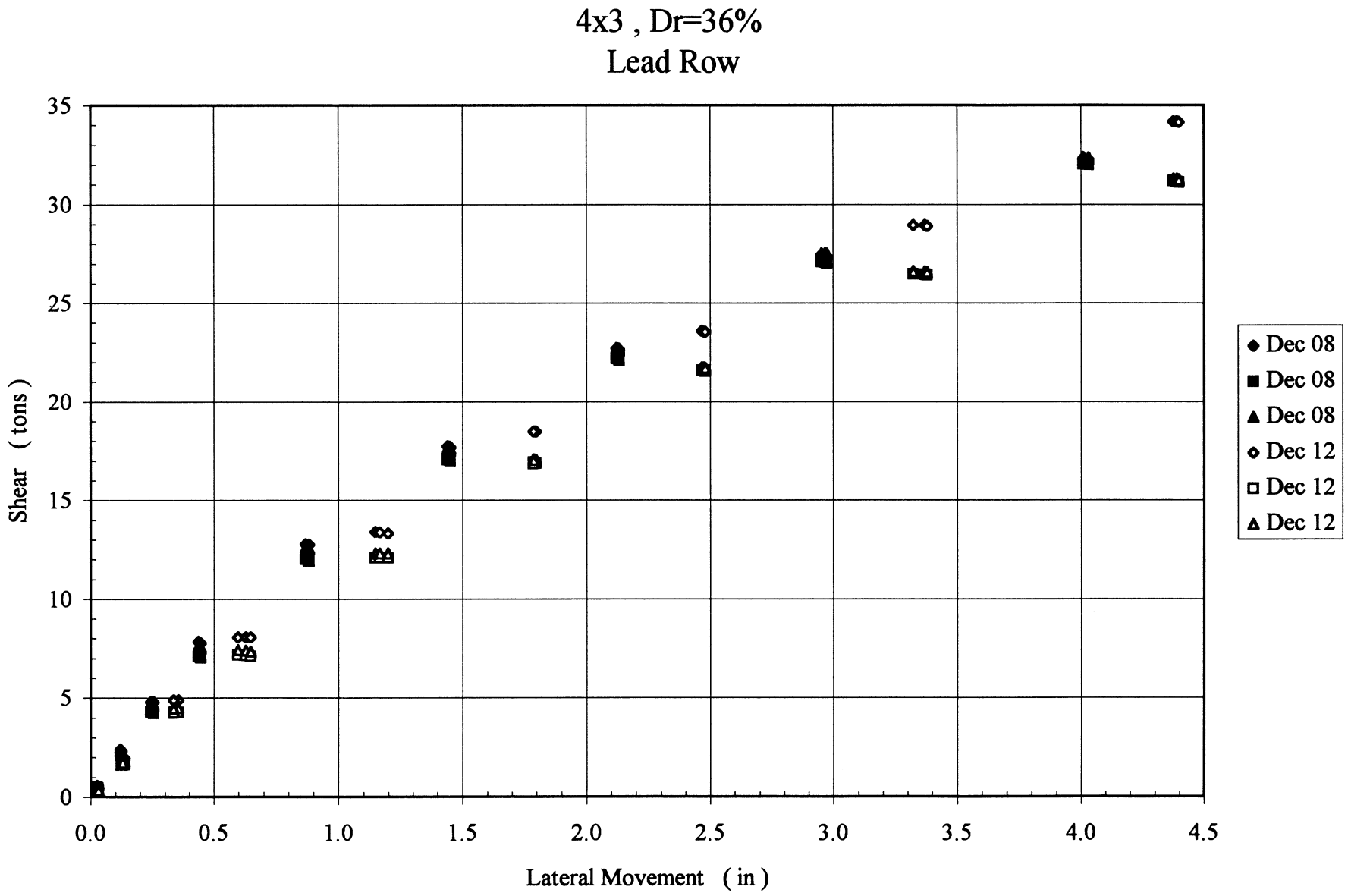

Figure 6-9(b). Results of 4 × 3 Group in Loose Sand, Measured Shear for Each Pile in Lead Row

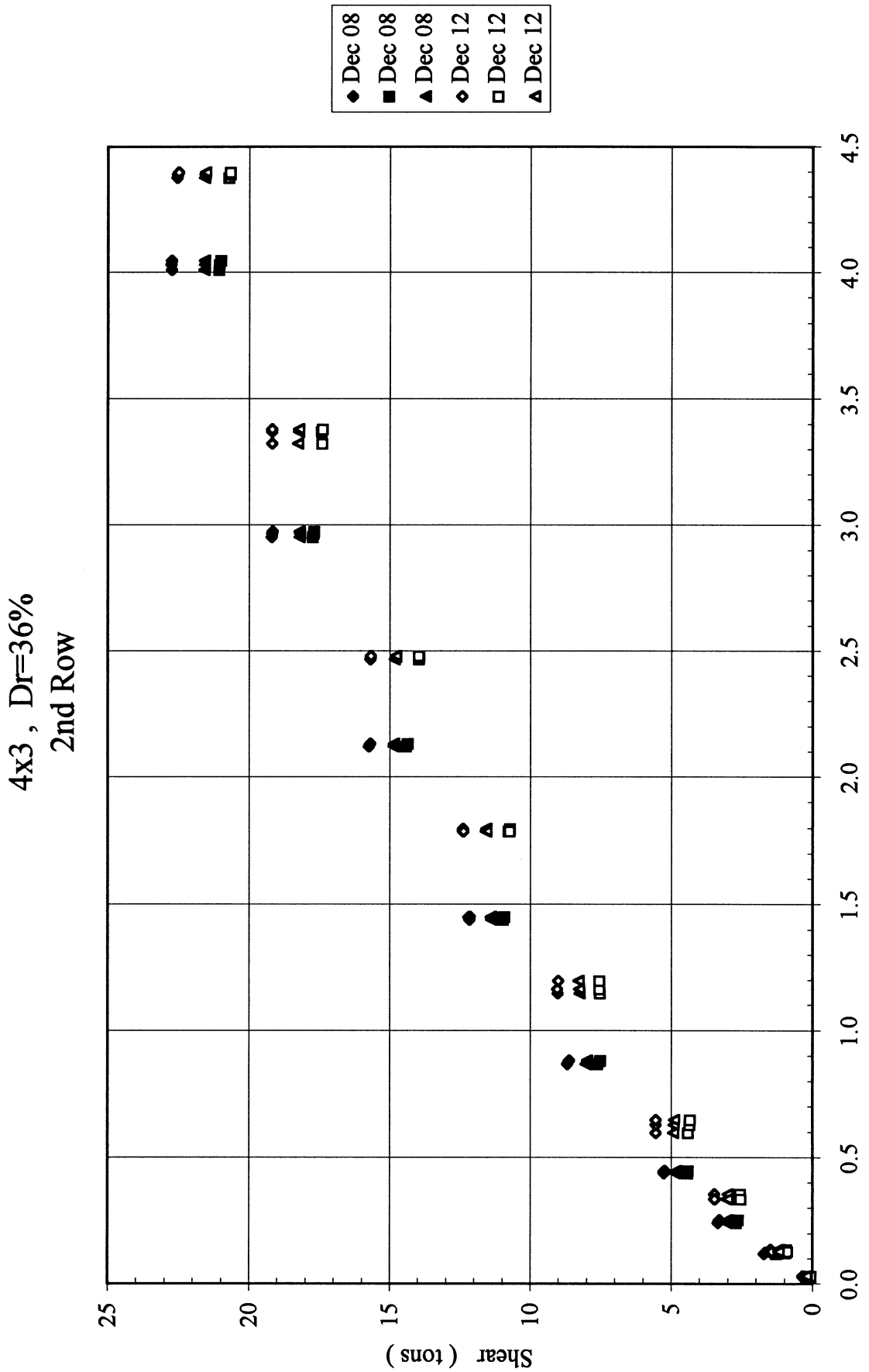

Figure 6-9(c). Results of 4 × 3 Group in Loose Sand, Measured Shear for Each Pile in 2nd Row

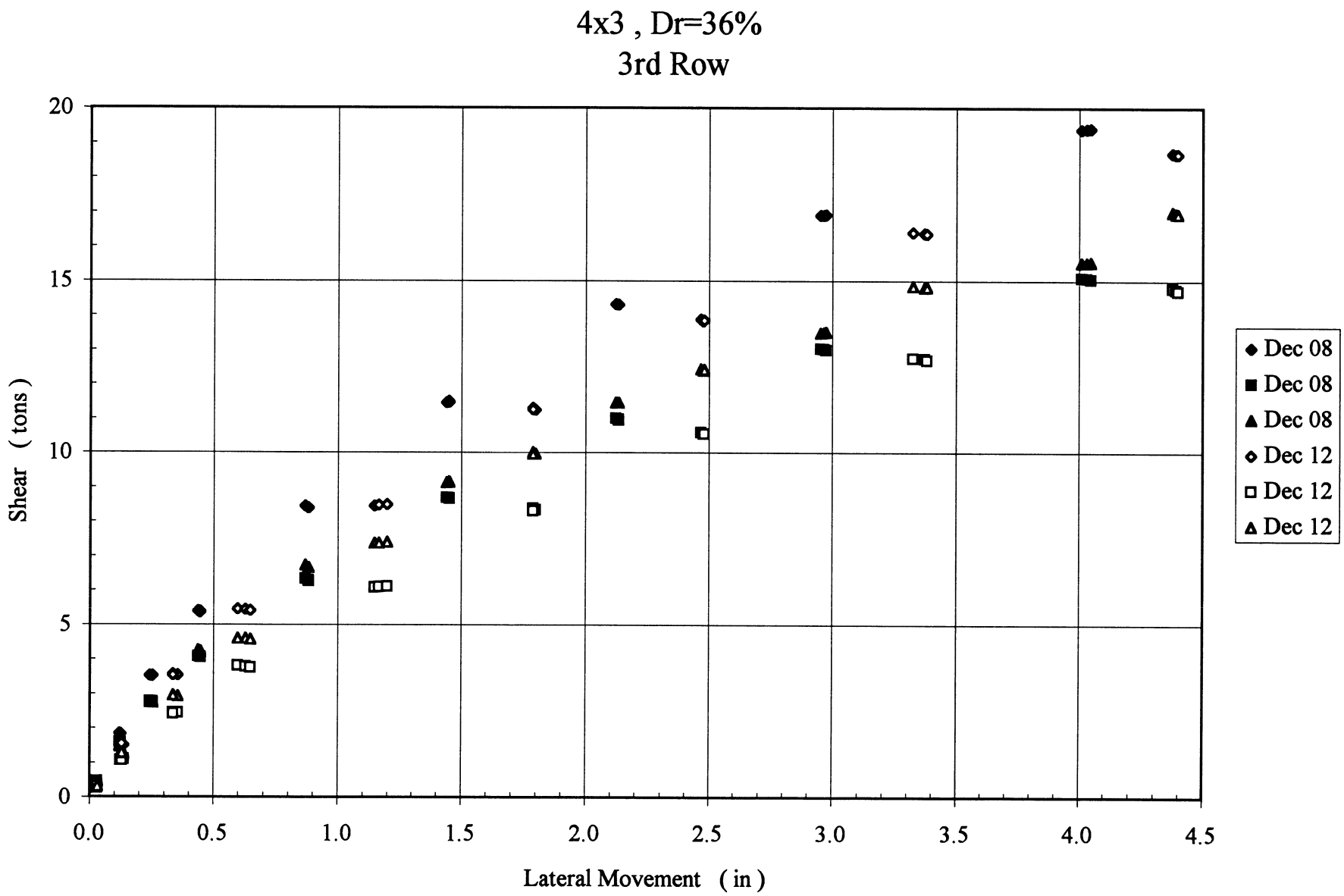

Figure 6-9(d). Results of 4 × 3 Group in Loose Sand, Measured Shear for Each Pile in 3rd Row

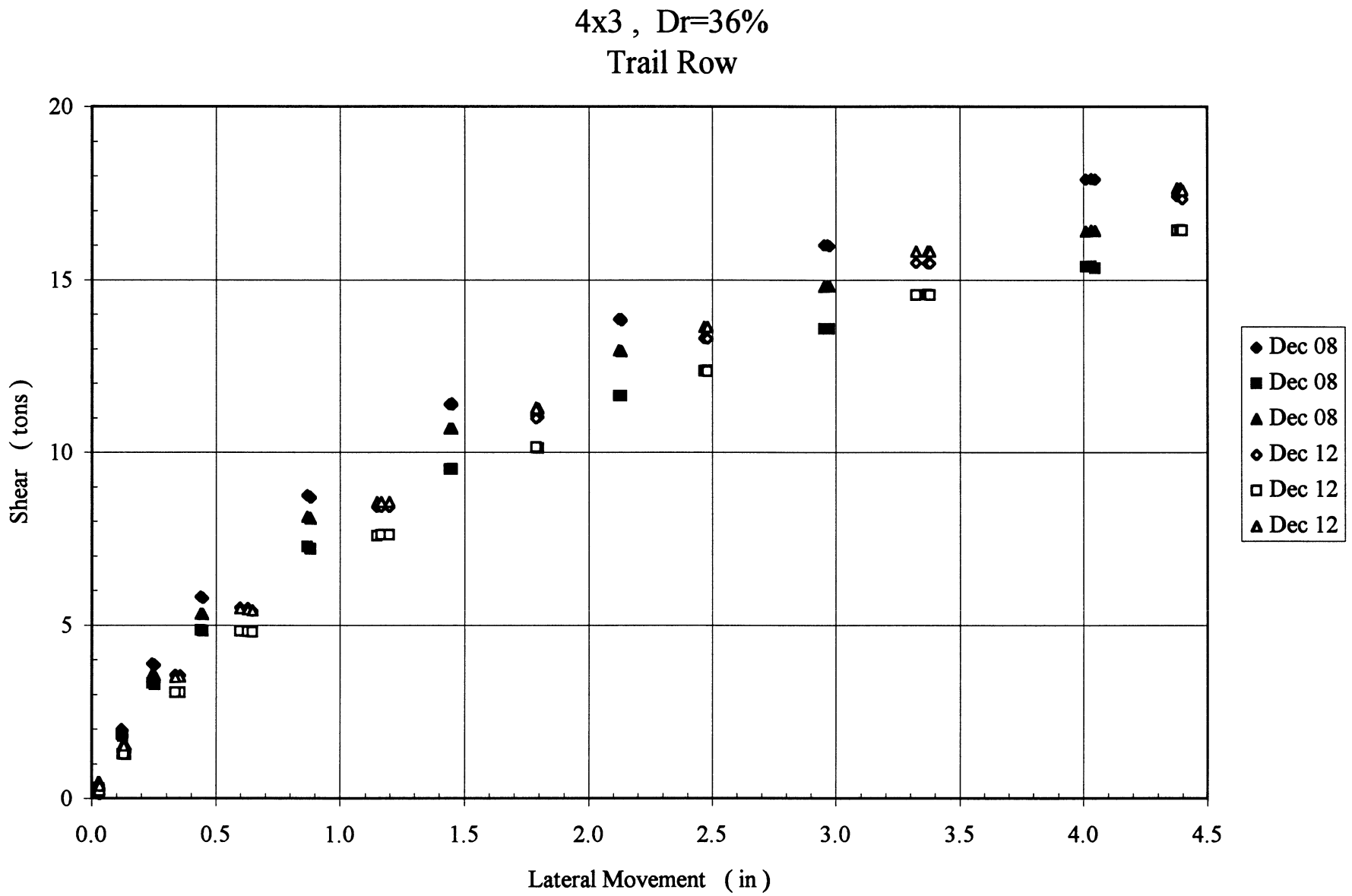

Figure 6-9(e). Results of 4 × 3 Group in Loose Sand, Measured Shear for Each Pile in Trail Row

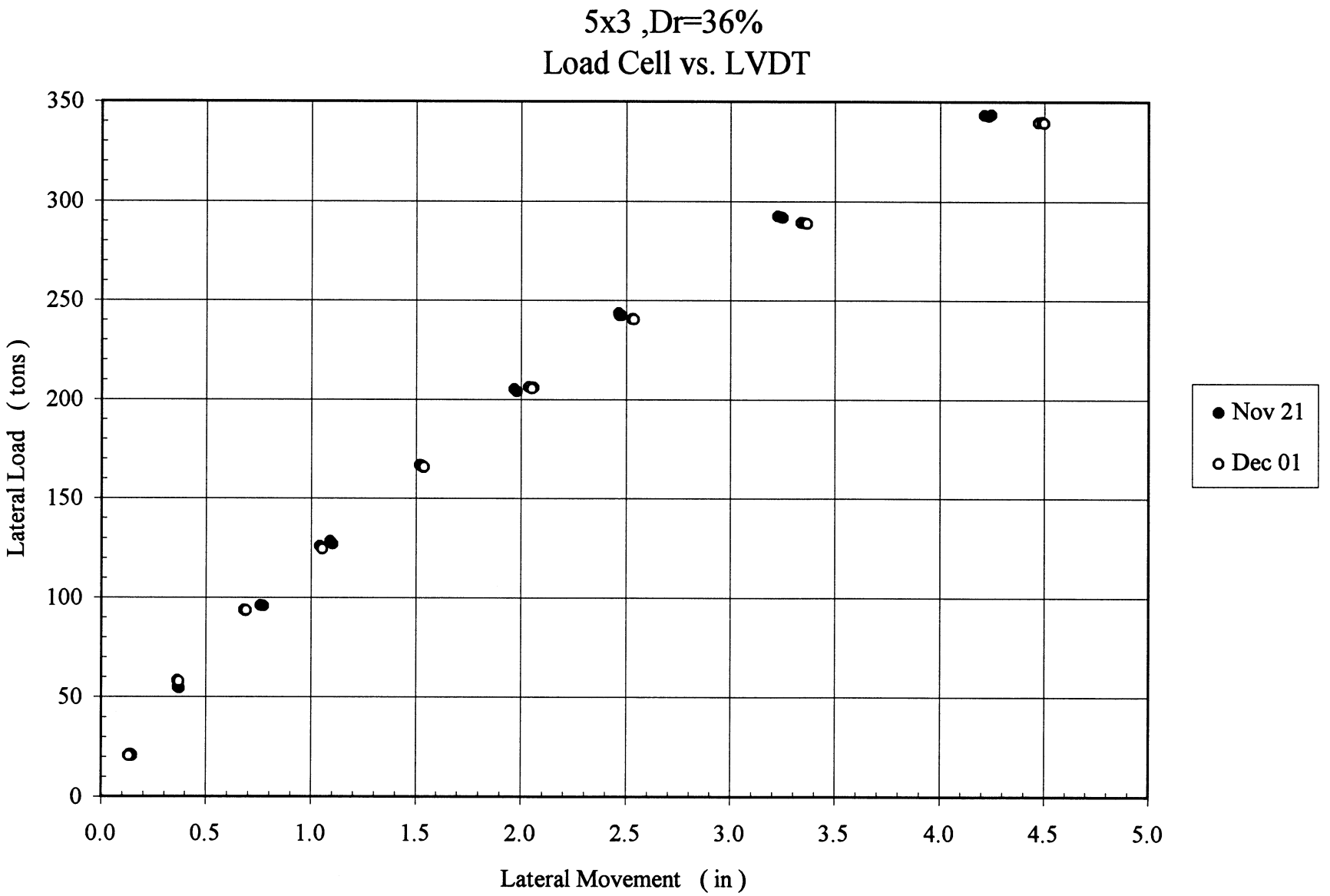

Figure 6-10(a). Results of 5 × 3 Group in Loose Sand, Total Lateral Load vs. Lateral Deflection

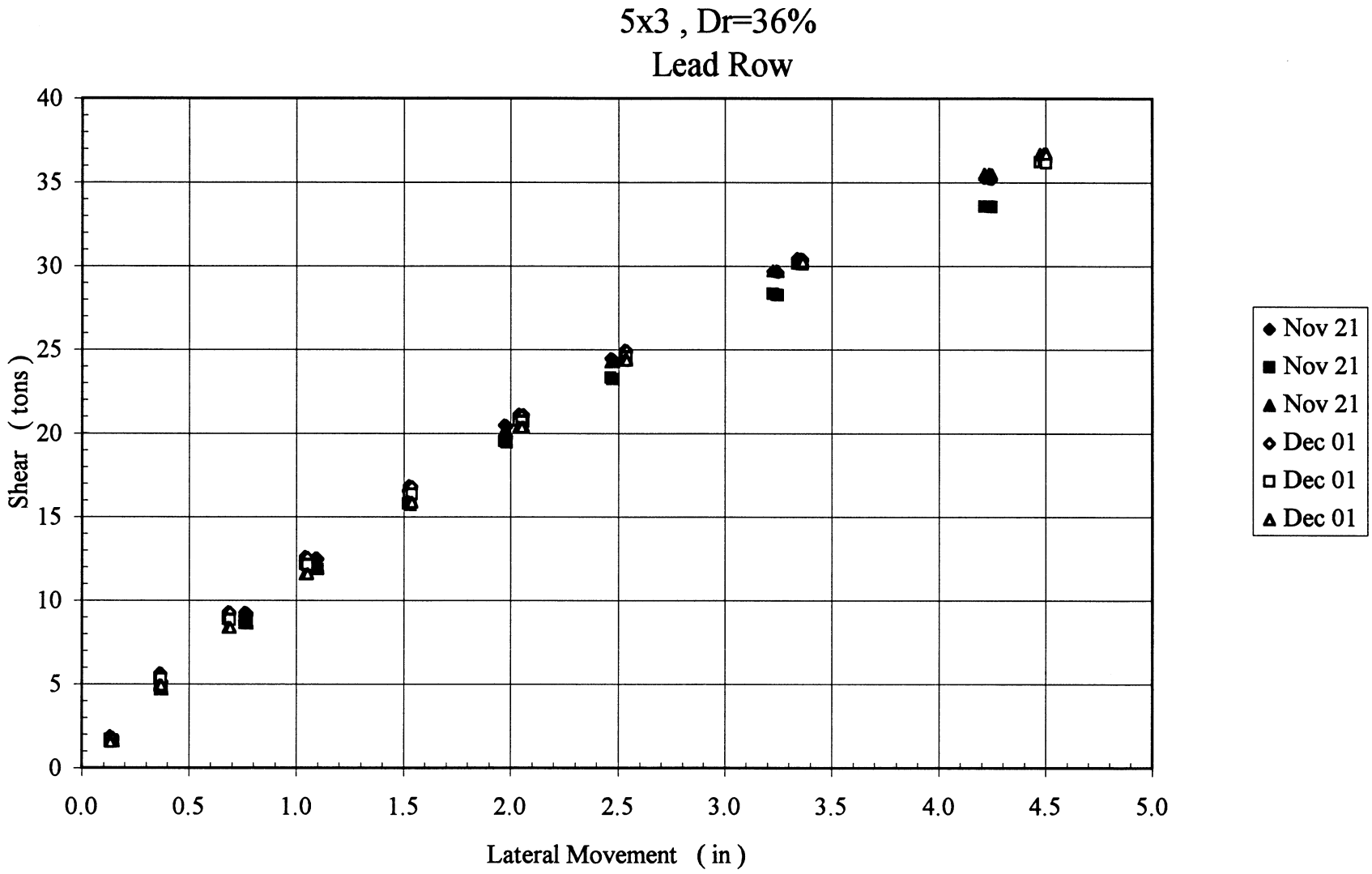

Figure 6-10(b). Results of 5 × 3 Group in Loose Sand, Measured Shear for Each Pile in Lead Row

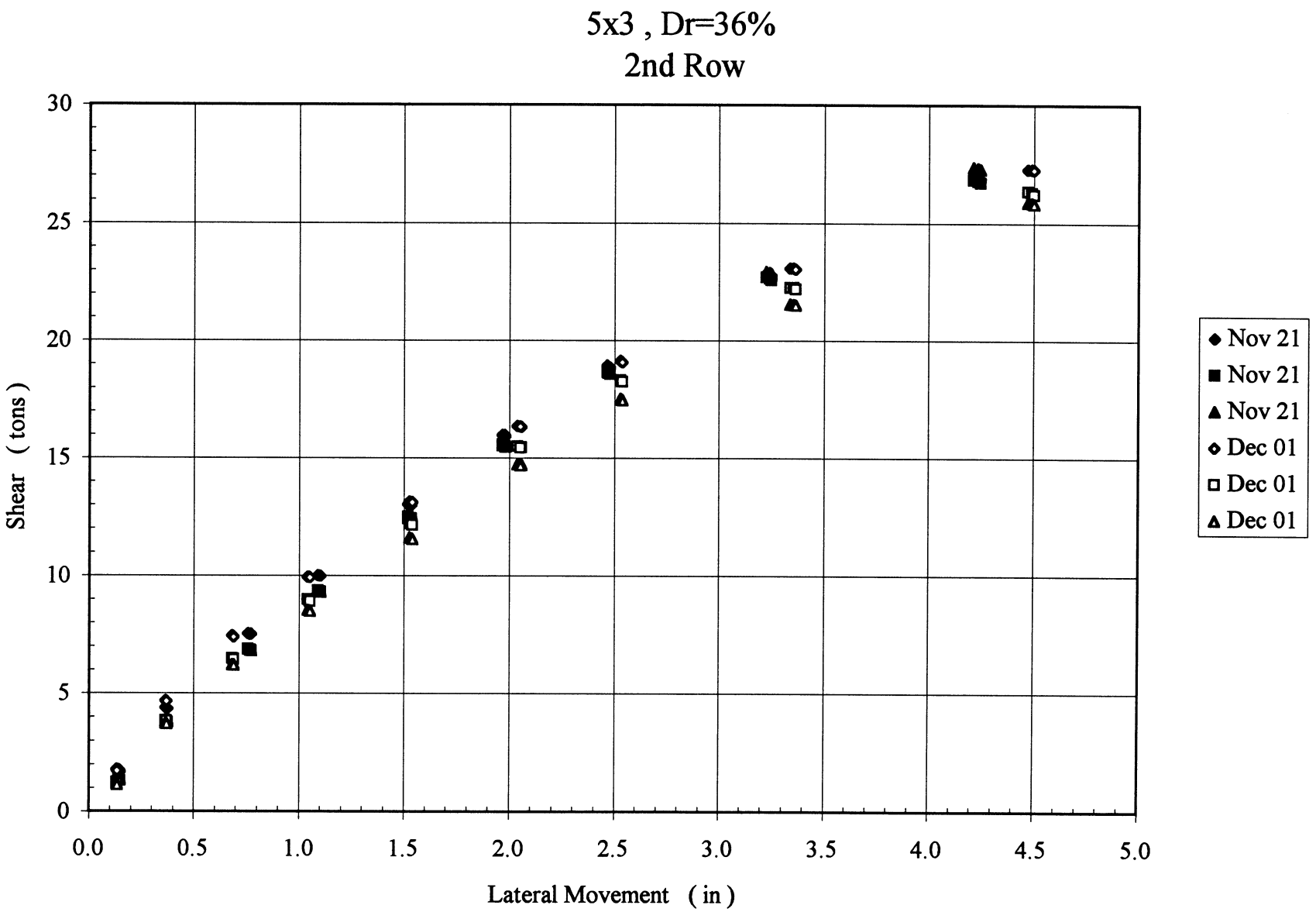

Figure 6-10(c). Results of 5 × 3 Group in Loose Sand, Measured Shear for Each Pile in 2nd Row

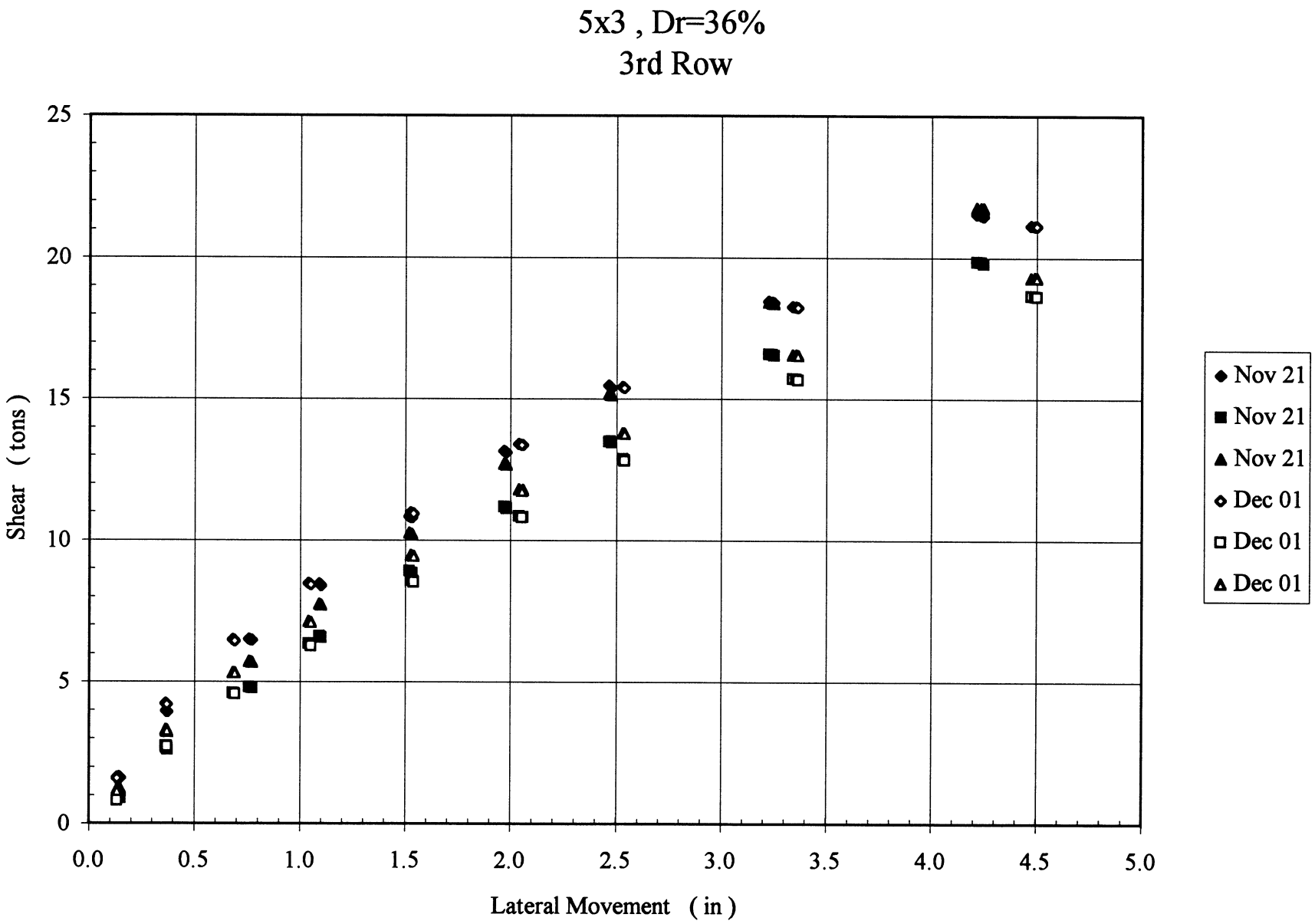

Figure 6-10(d). Results of 5 × 3 Group in Loose Sand, Measured Shear for Each Pile in 3rd Row

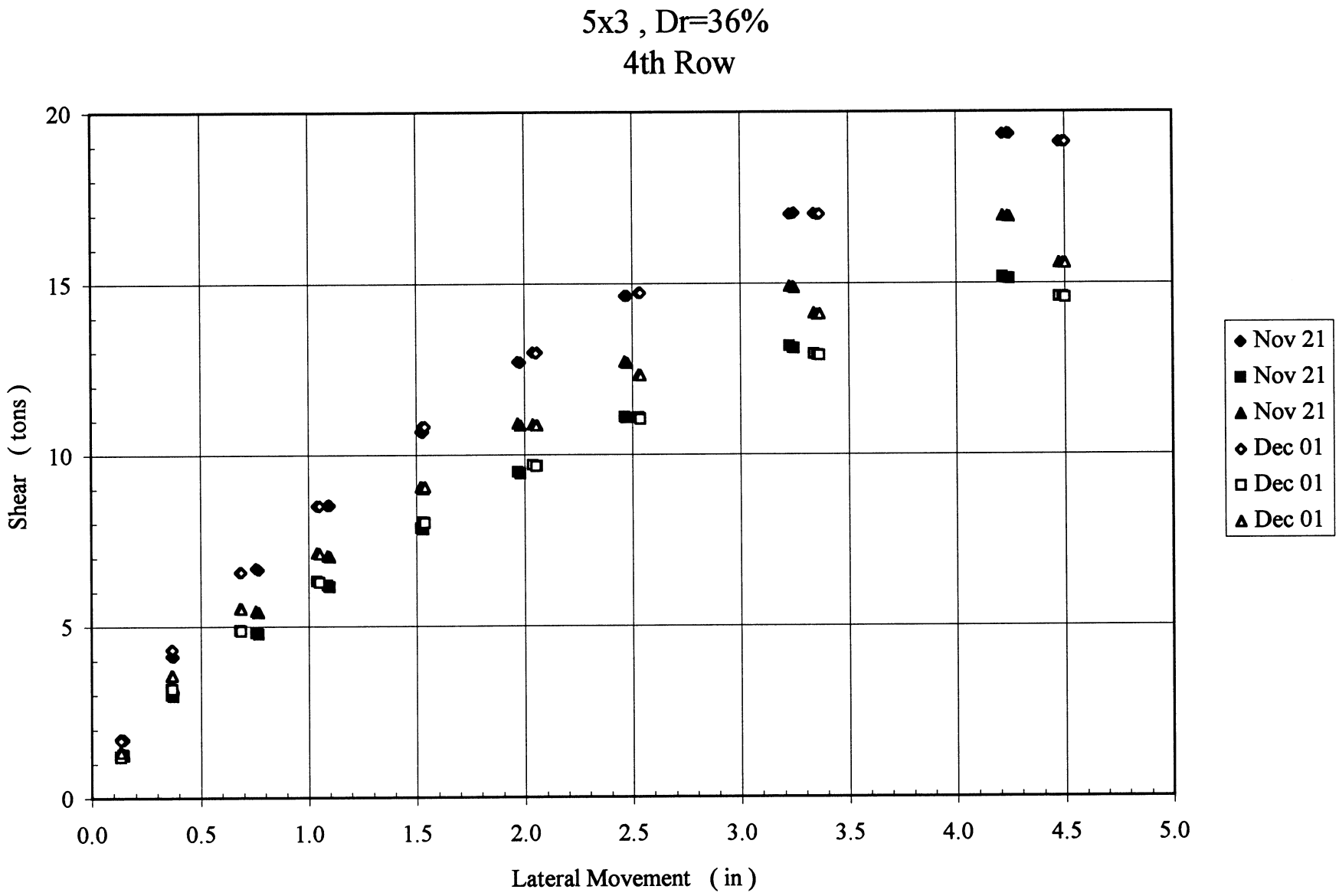

Figure 6-10(e). Results of 5 × 3 Group in Loose Sand, Measured Shear for Each Pile in 4th Row

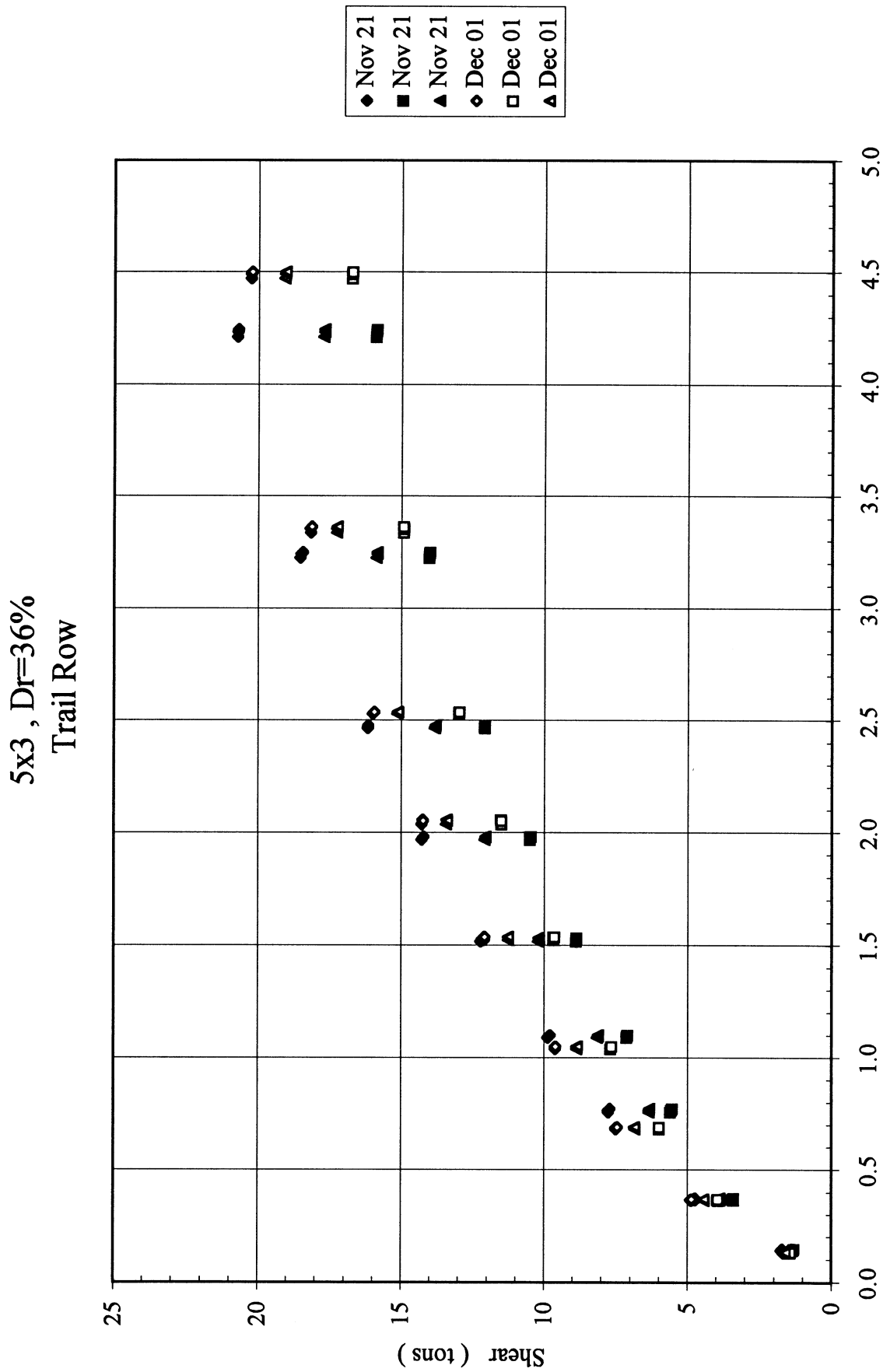

Figure 6-10(f). Results of 5 × 3 Group in Loose Sand, Measured Shear for Each Pile in Trail Row

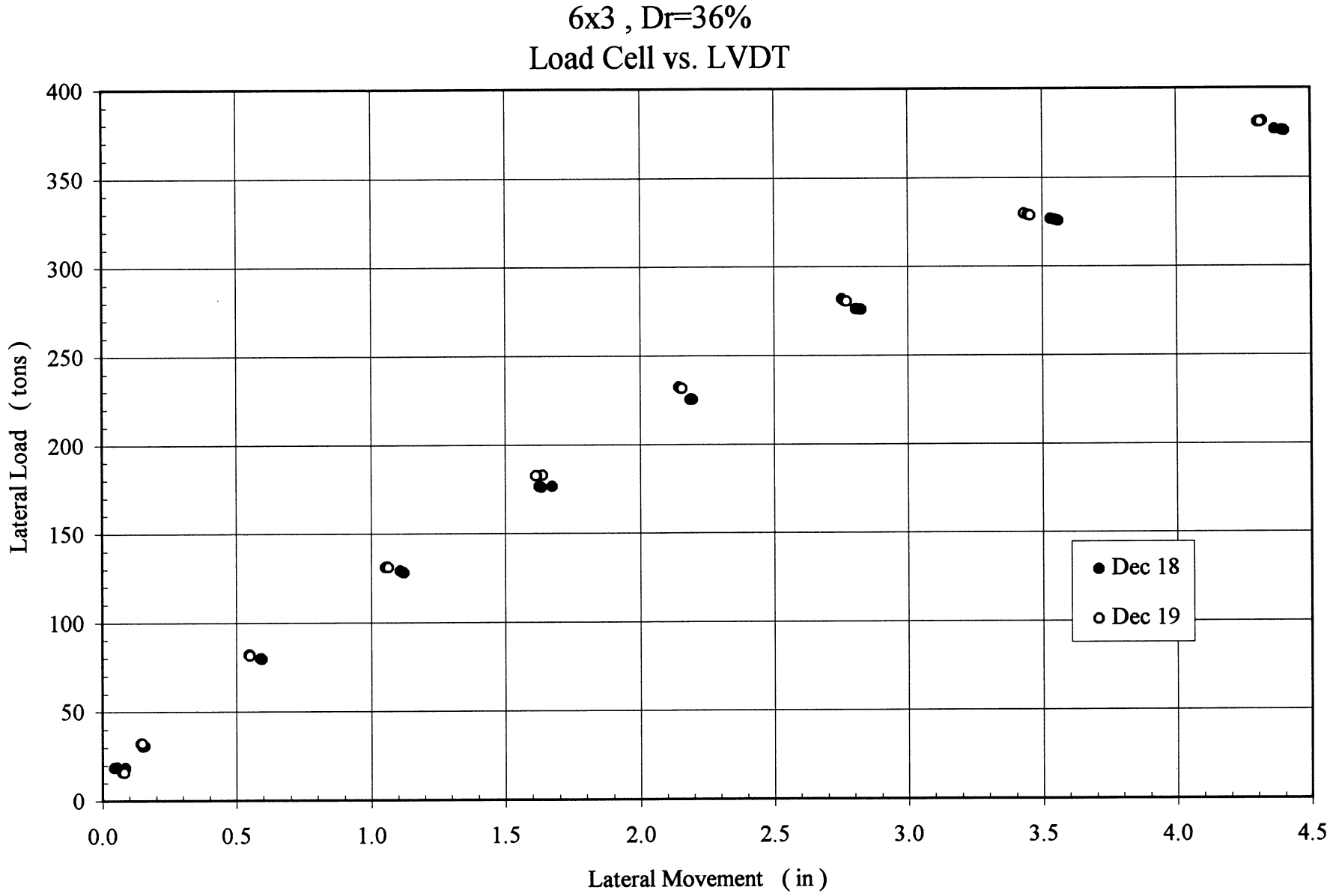

Figure 6-11(a). Results of 6 × 3 Group in Loose Sand, Total Lateral Load vs. Lateral Deflection

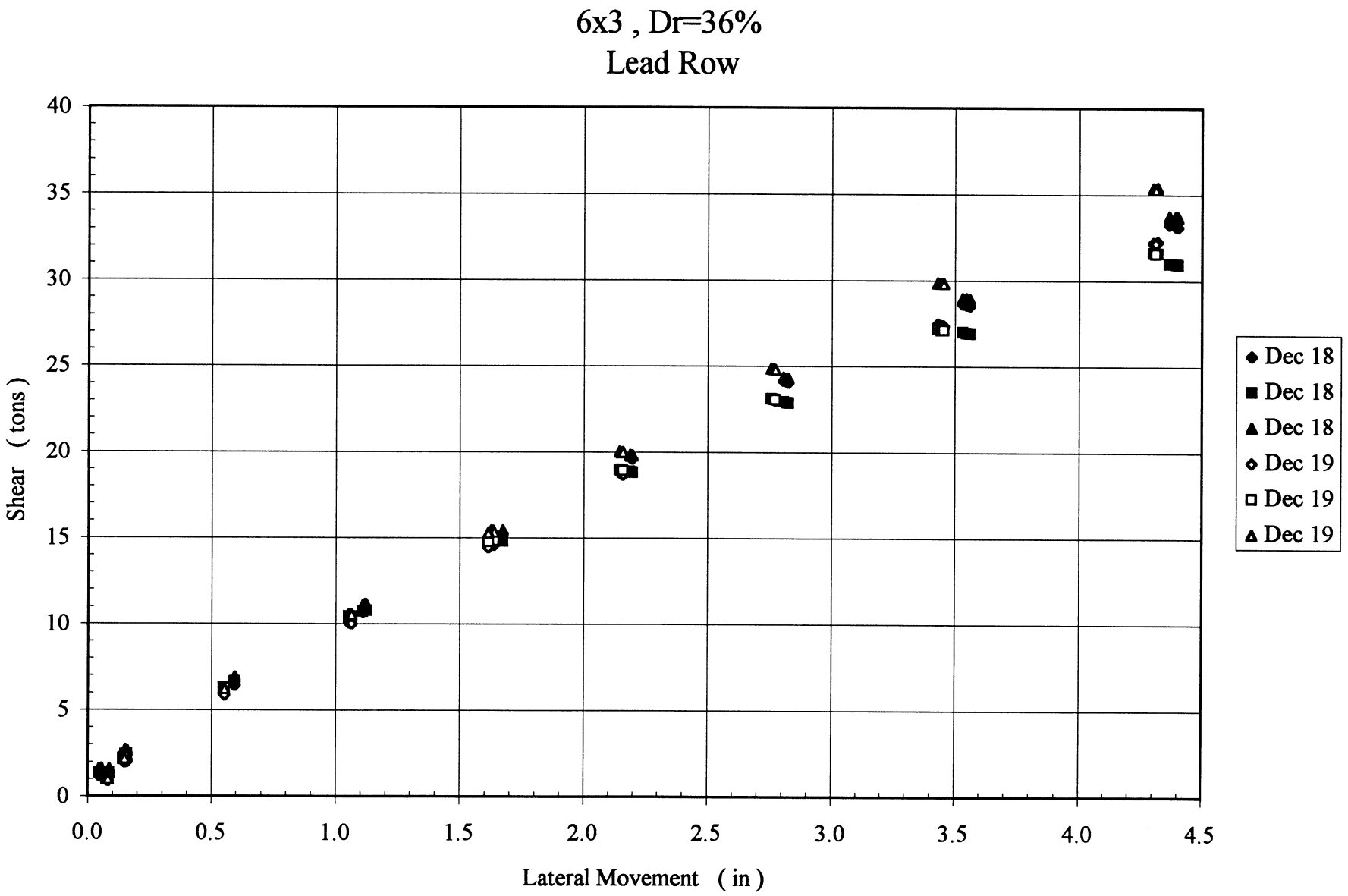

Figure 6-11(b). Results of 6 × 3 Group in Loose Sand, Measured Shear for Each Pile in Lead Row

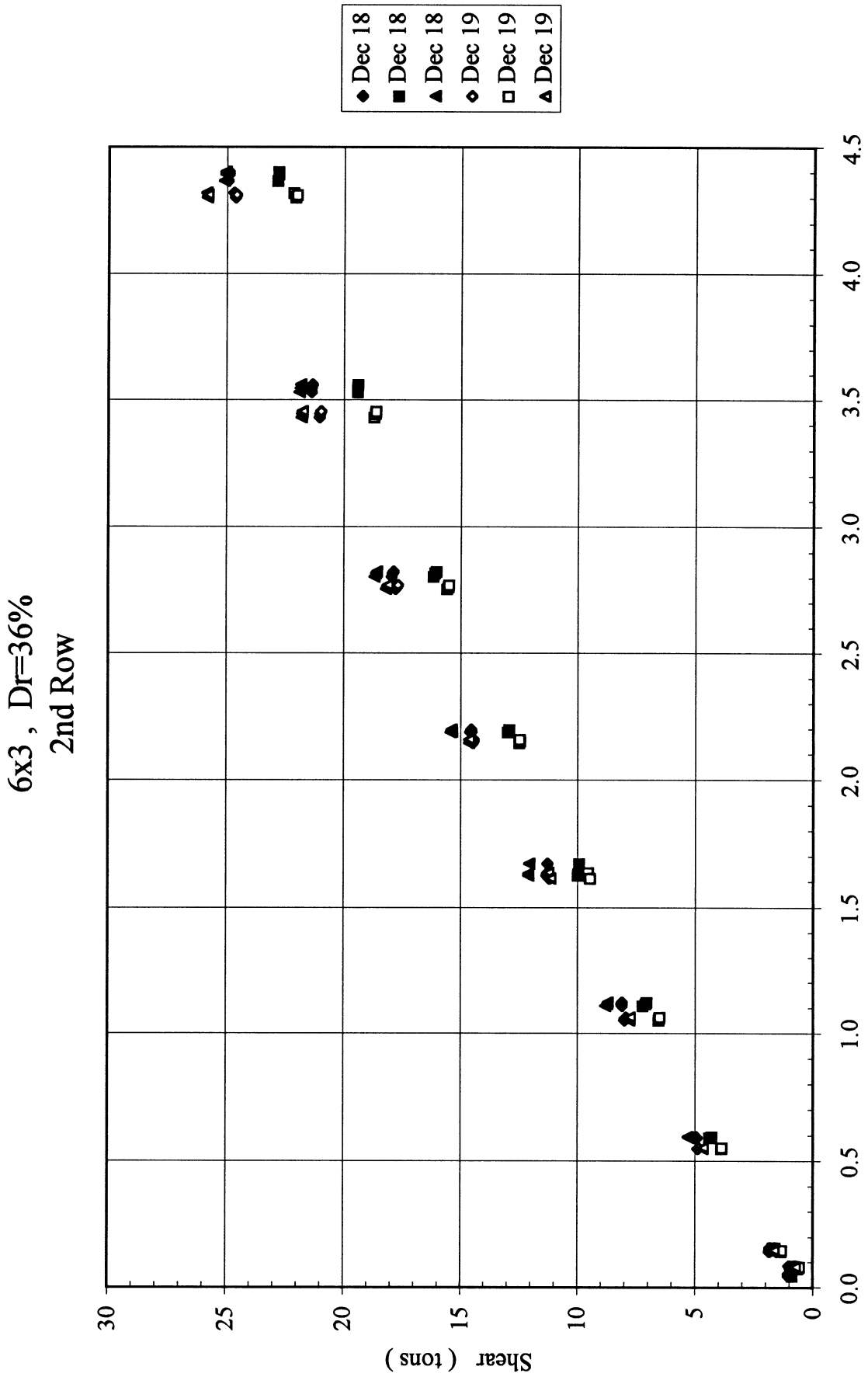

Figure 6-11(c). Results of 6 × 3 Group in Loose Sand, Measured Shear for Each Pile in 2nd Row

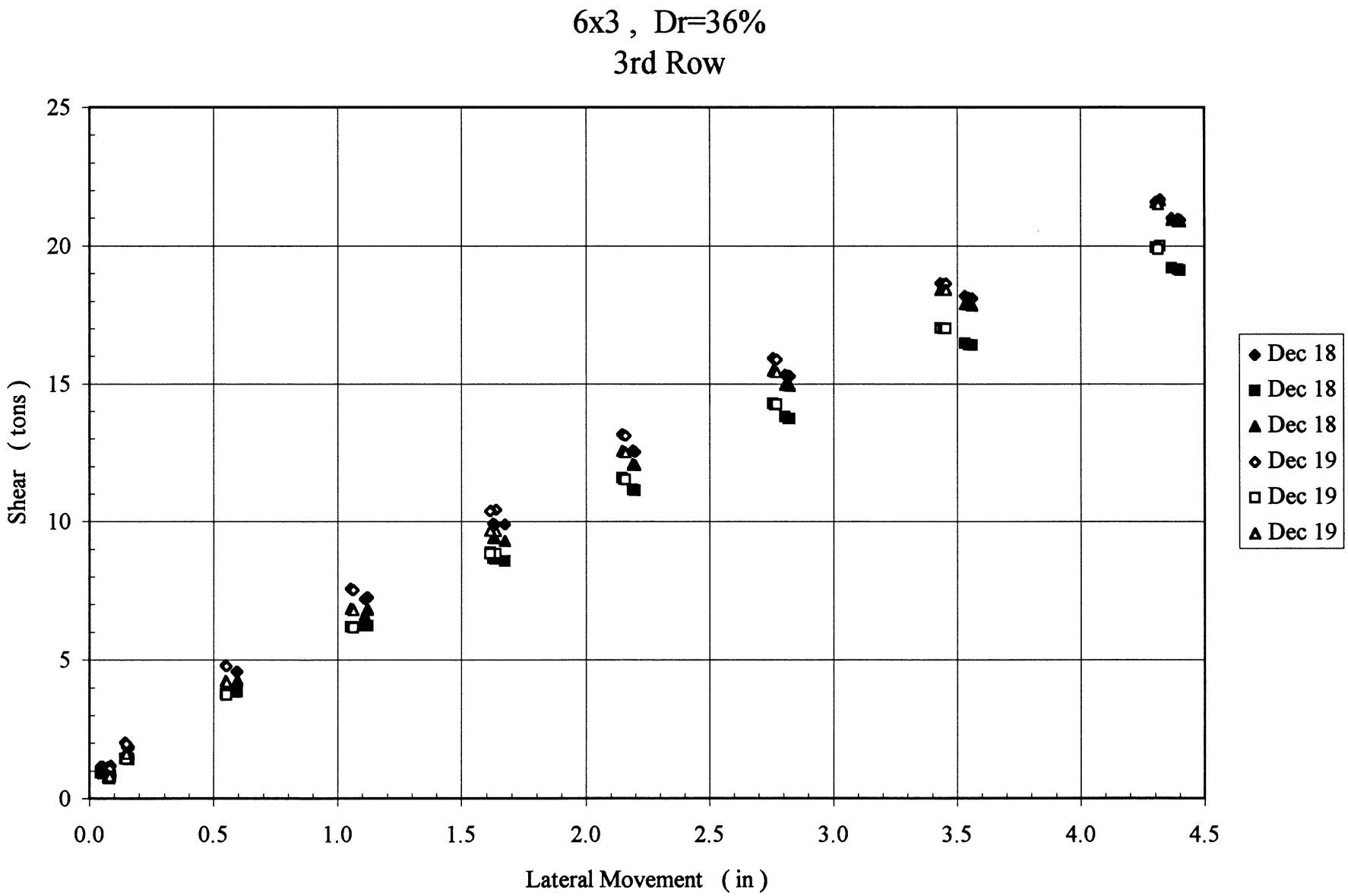

Figure 6-11(d). Results of 6 × 3 Group in Loose Sand, Measured Shear for Each Pile in 3rd Row

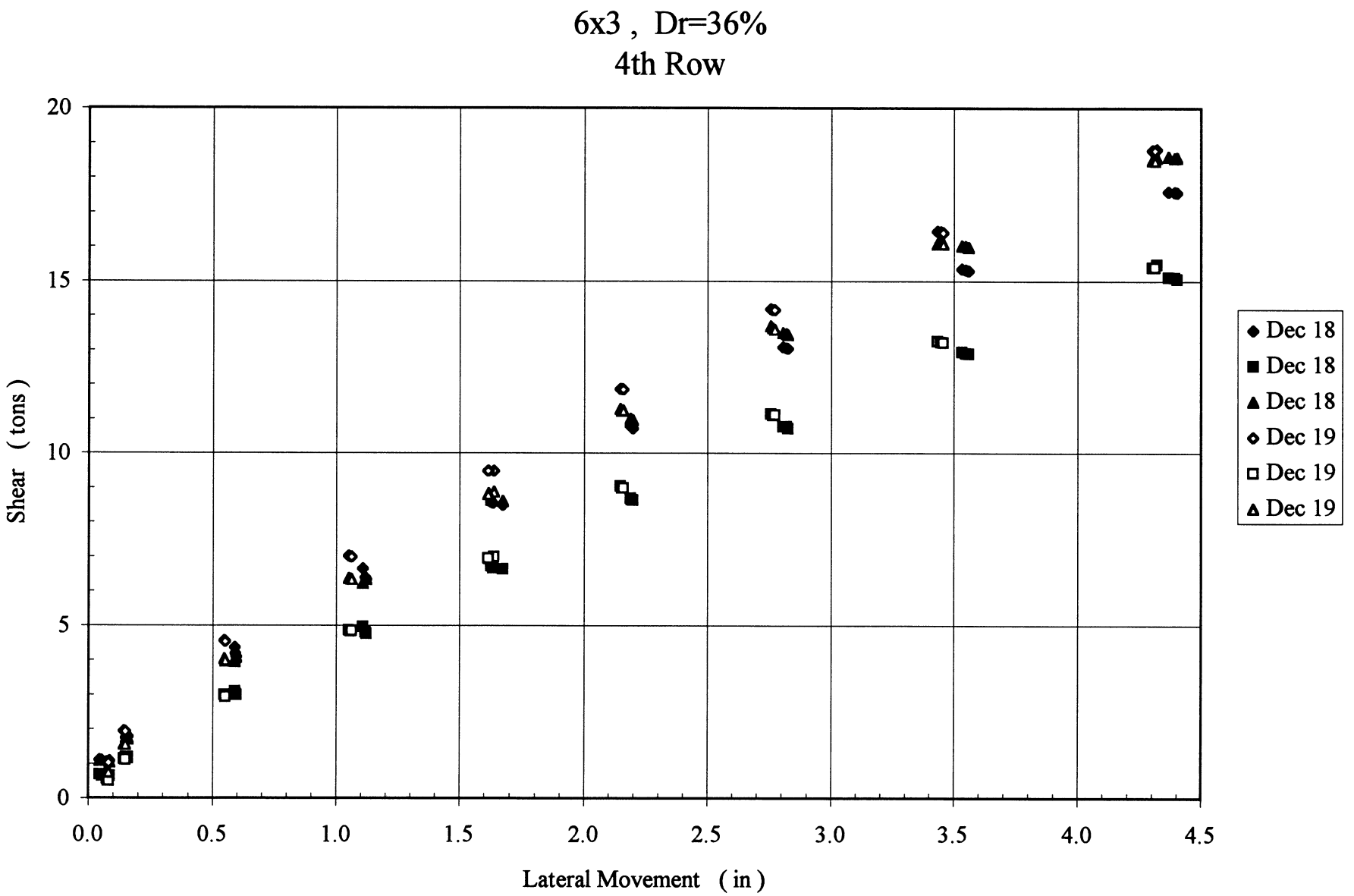

Figure 6-11(e). Results of 6 × 3 Group in Loose Sand, Measured Shear for Each Pile in 4th Row

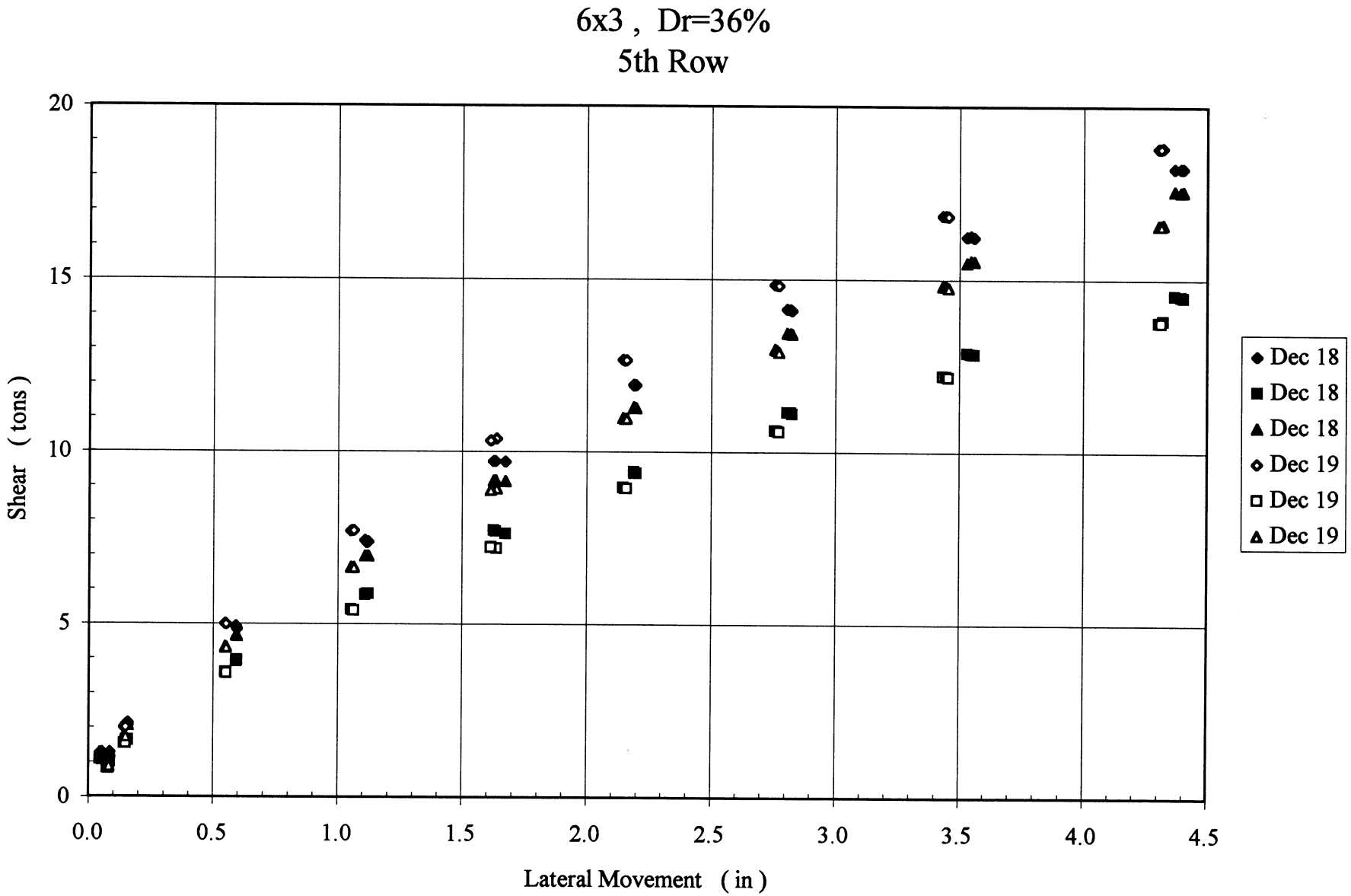

Figure 6-11(f). Results of 6 × 3 Group in Loose Sand, Measured Shear for Each Pile in 5th Row

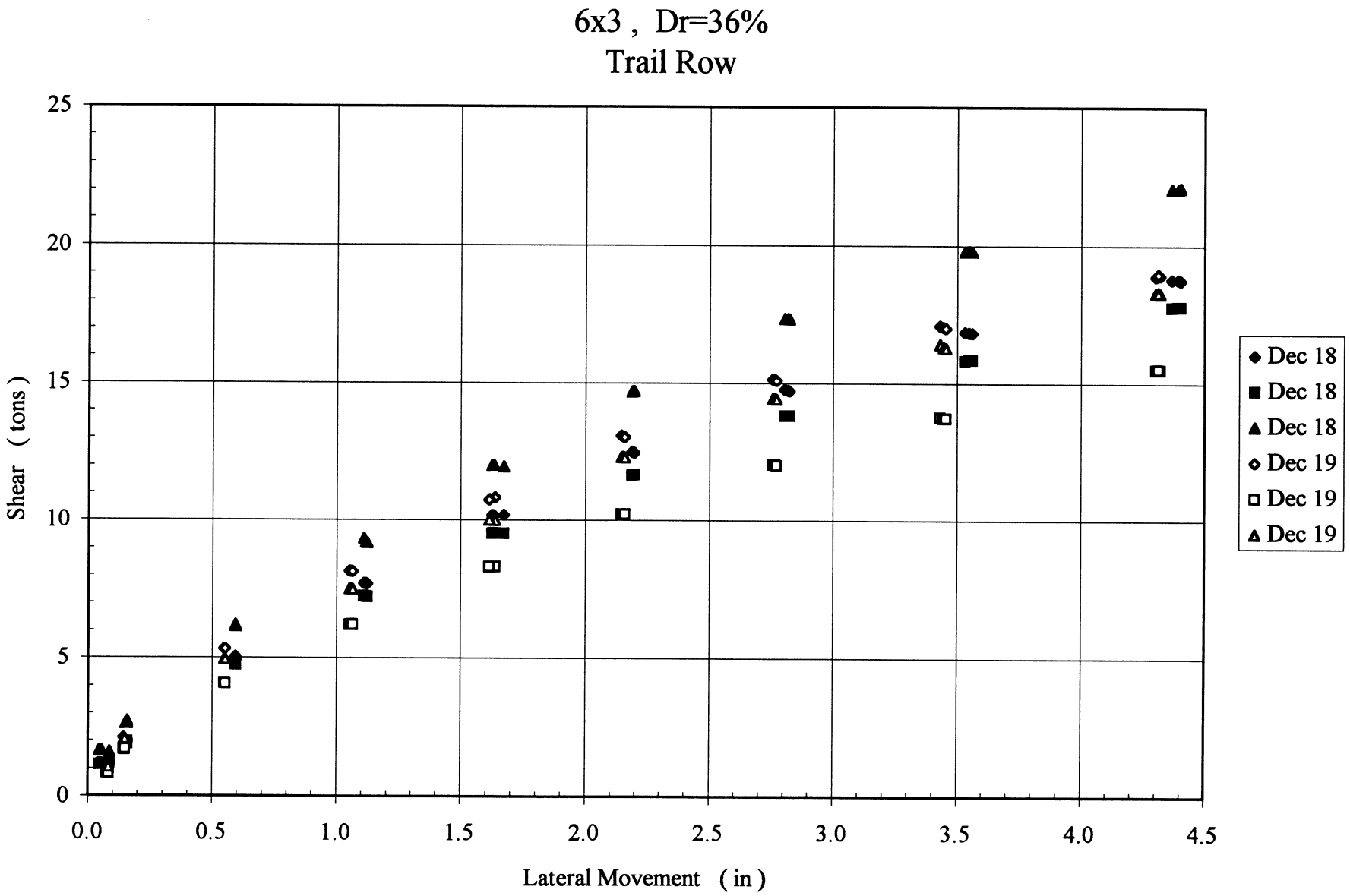

Figure 6-11(g). Results of 6 × 3 Group in Loose Sand, Measured Shear for Each Pile in Trail Row

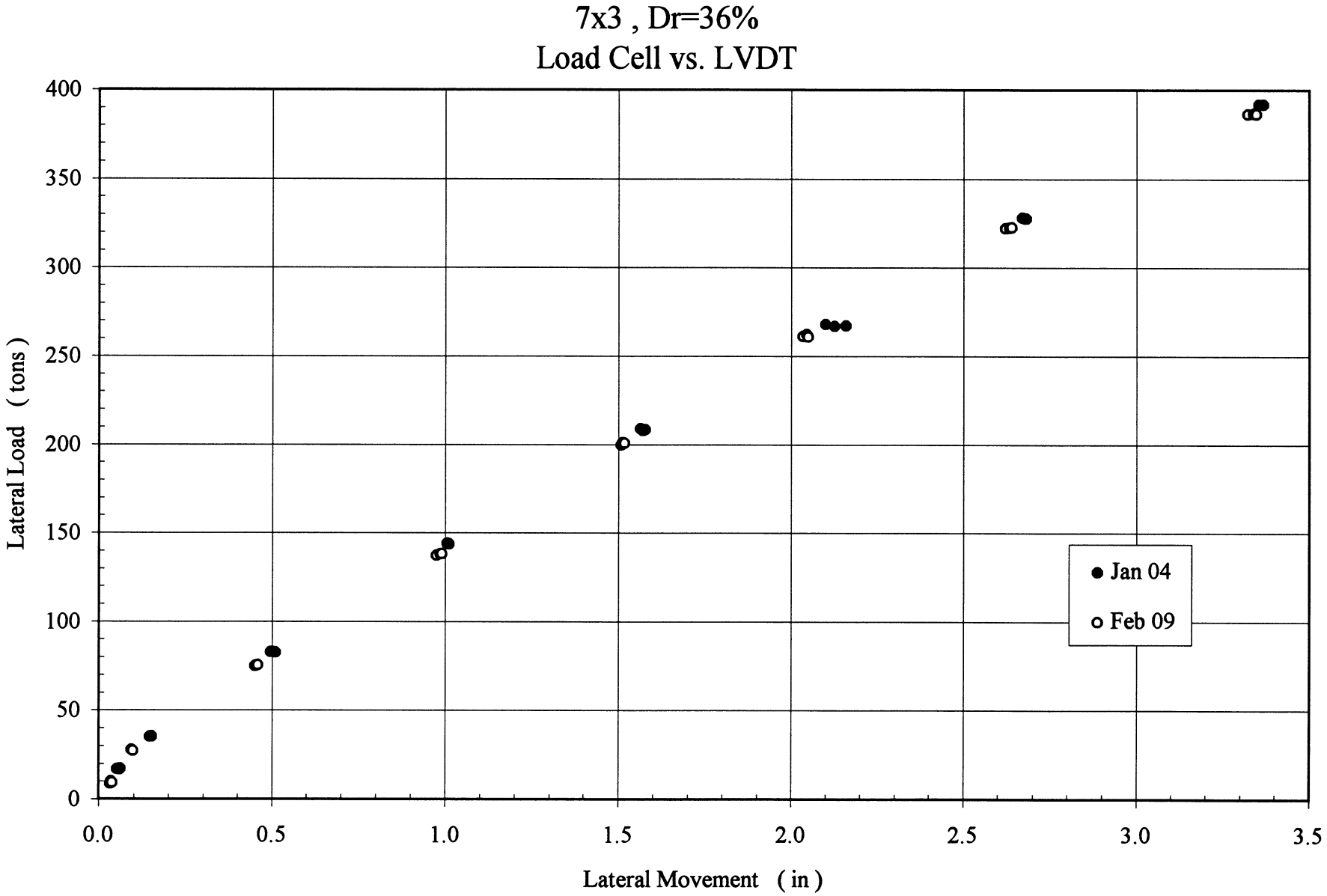

Figure 6-12(a). Results of 7 × 3 Group in Loose Sand, Total Lateral Load vs. Lateral Deflection

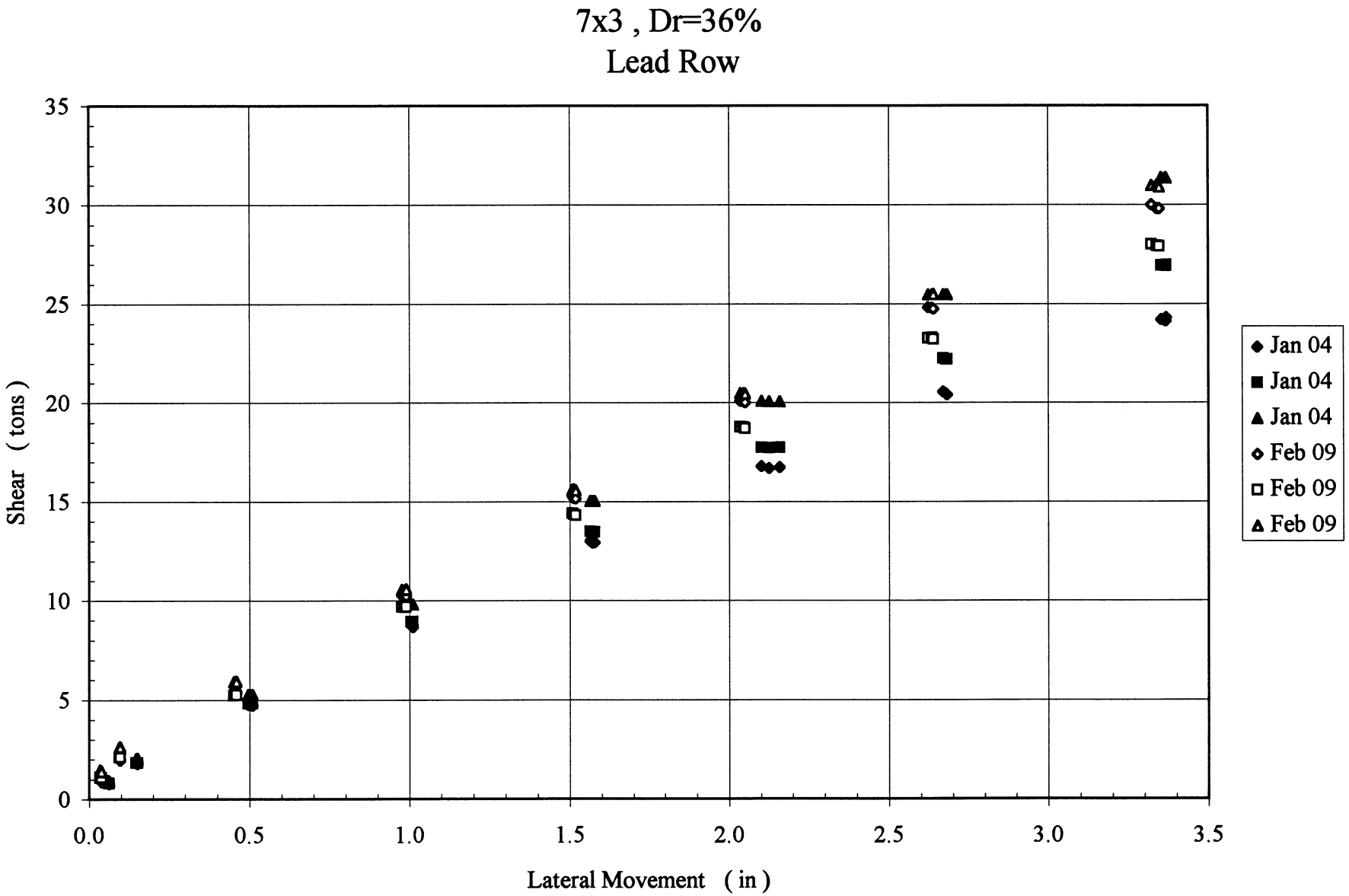

Figure 6-12(b). Results of 7 × 3 Group in Loose Sand, Measured Shear for Each Pile in Lead Row

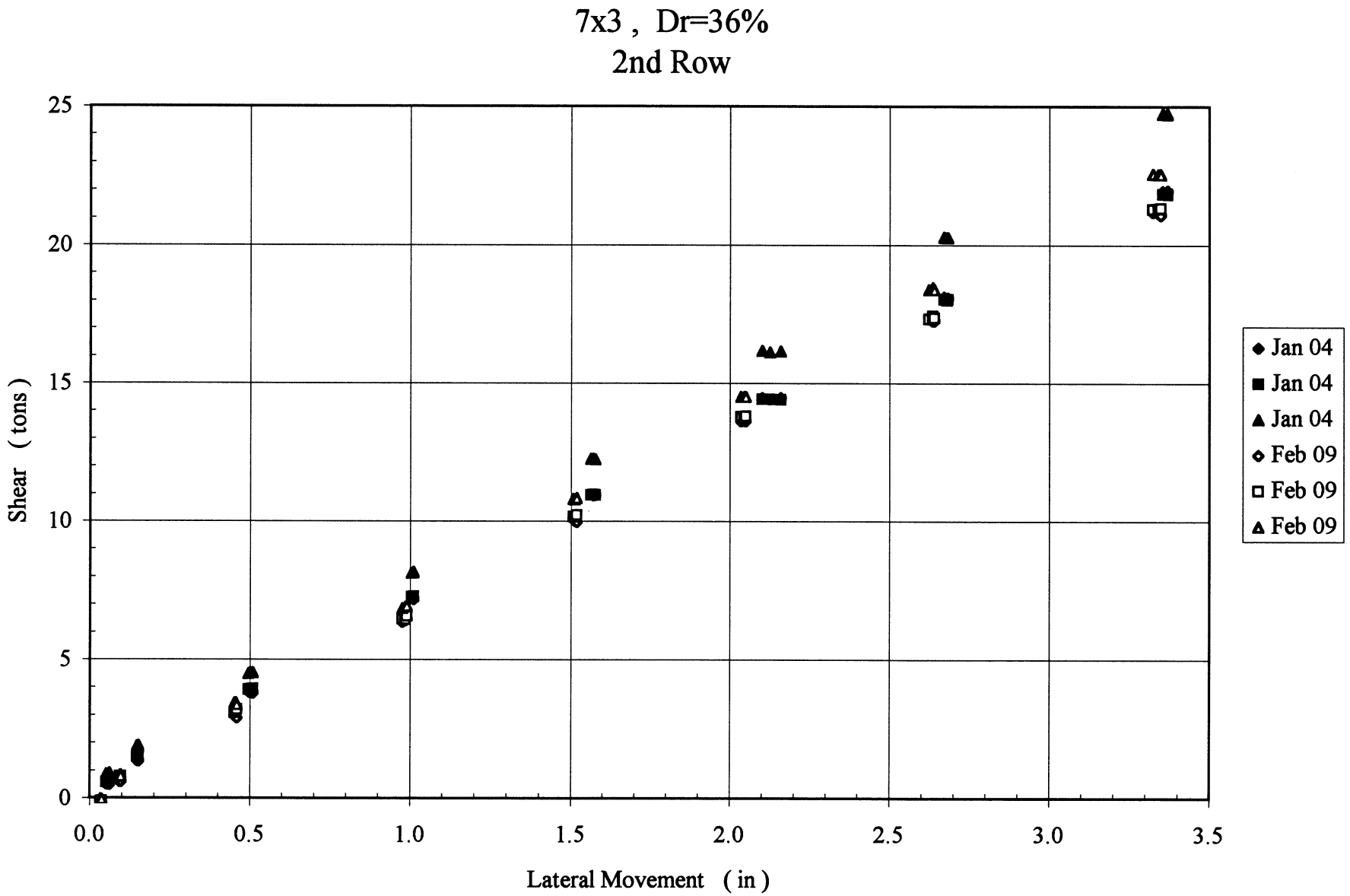

Figure 6-12(c). Results of 7 × 3 Group in Loose Sand, Measured Shear for Each Pile in 2nd Row

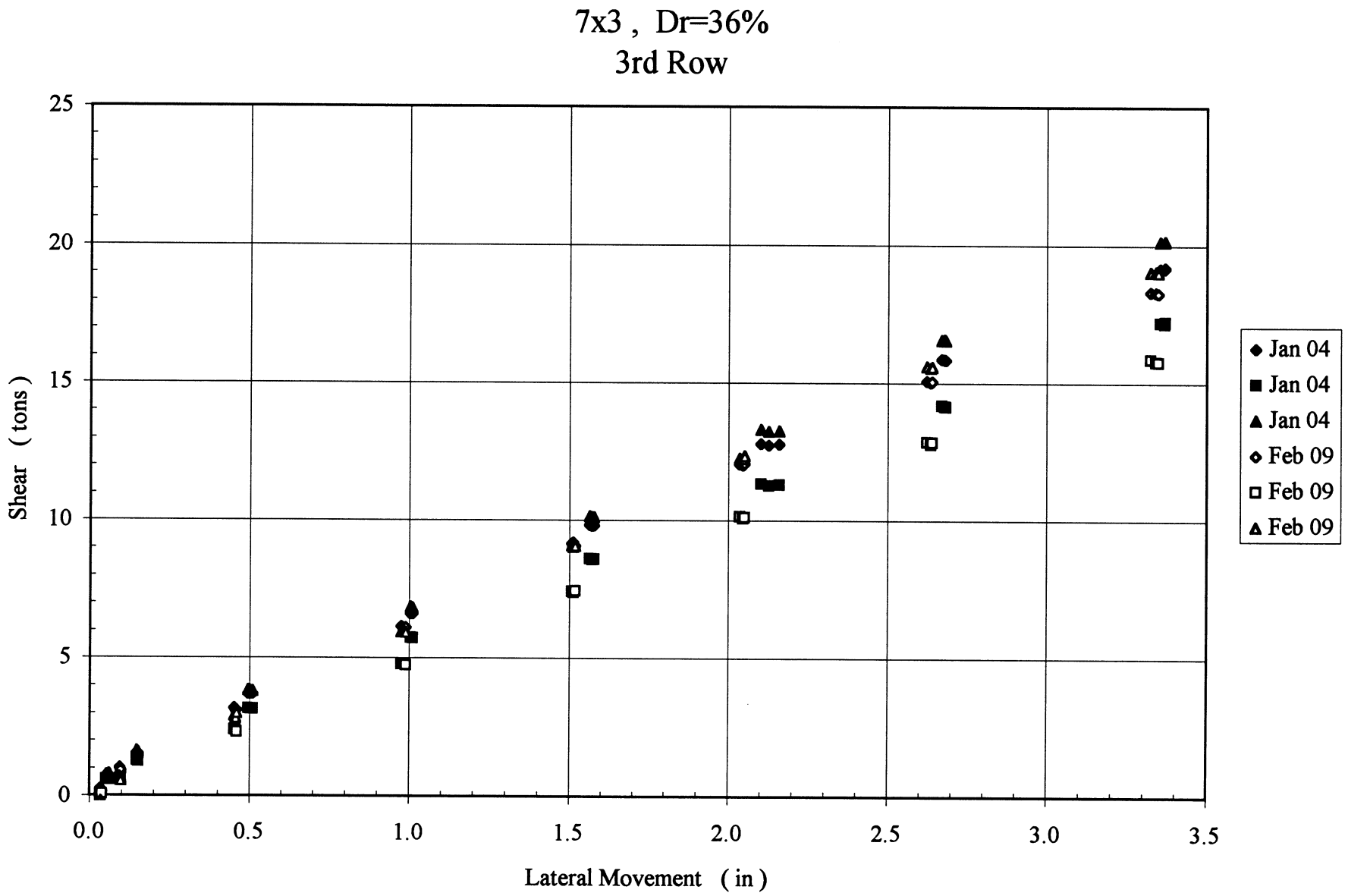

Figure 6-12(d). Results of 7 × 3 Group in Loose Sand, Measured Shear for Each Pile in 3rd Row

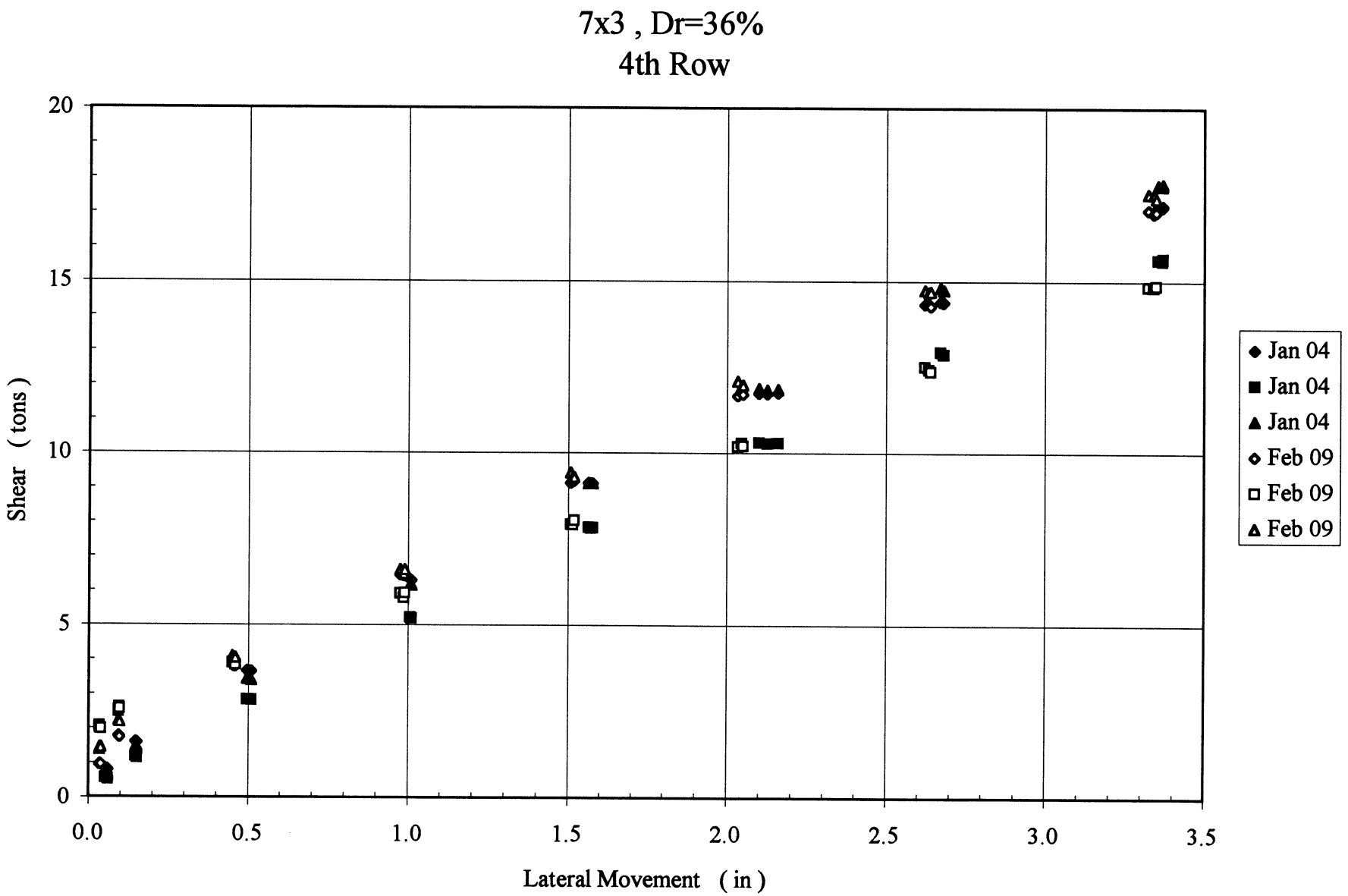

Figure 6-12(e). Results of 7 × 3 Group in Loose Sand, Measured Shear for Each Pile in 4th Row

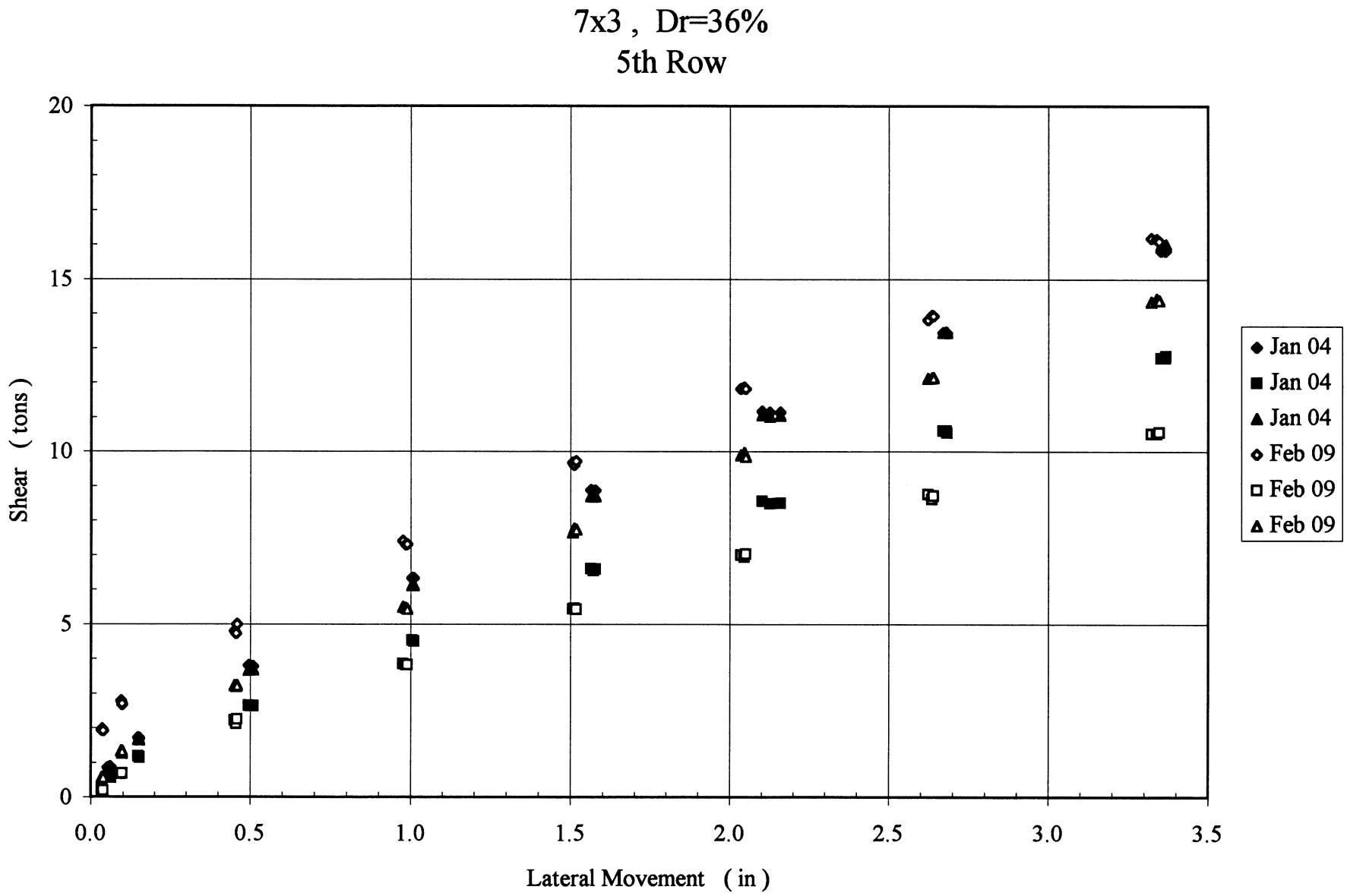

Figure 6-12(f). Results of 7 × 3 Group in Loose Sand, Measured Shear for Each Pile in 5th Row

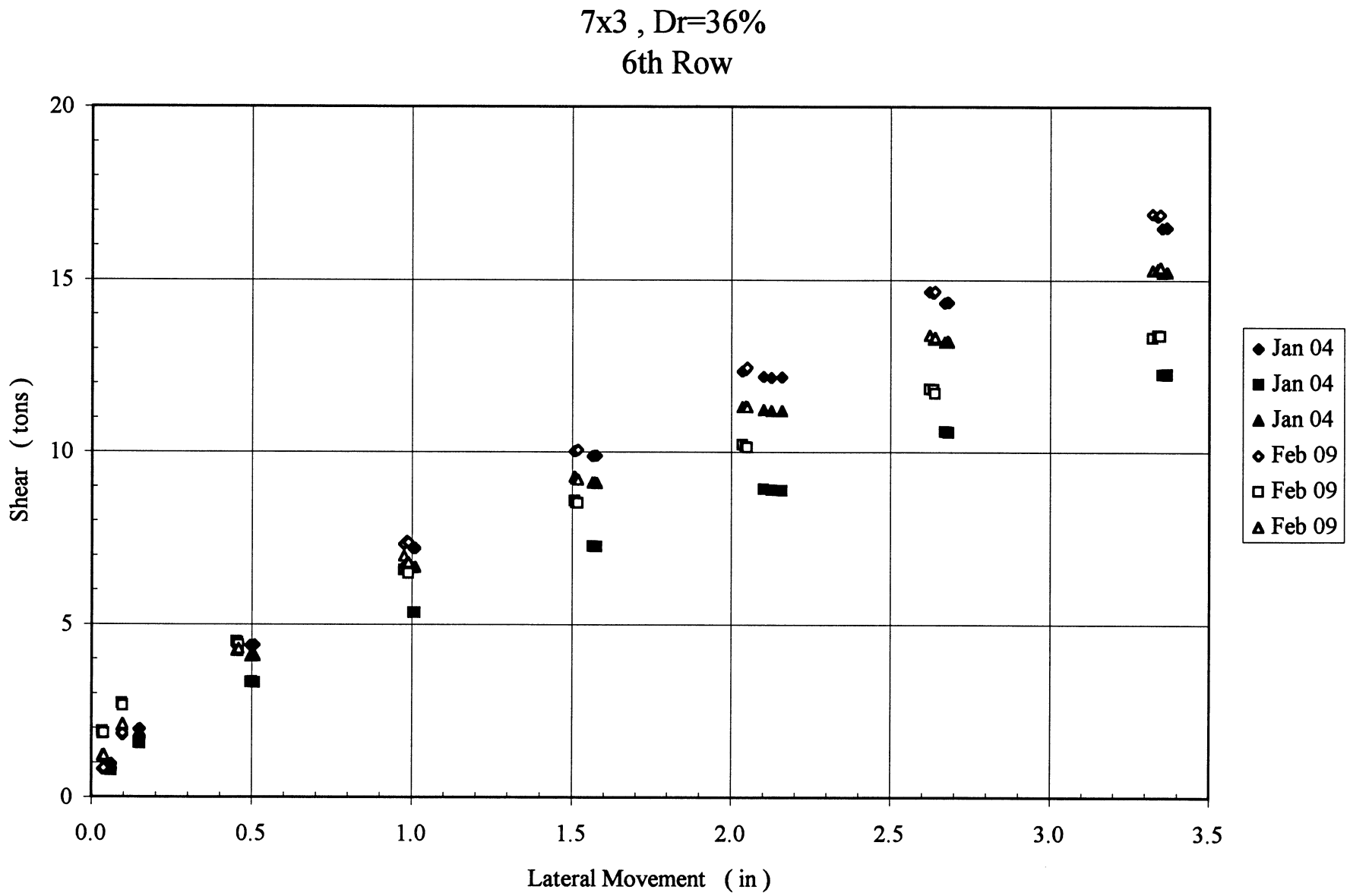

Figure 6-12(g). Results of 7 × 3 Group in Loose Sand, Measured Shear for Each Pile in 6th Row

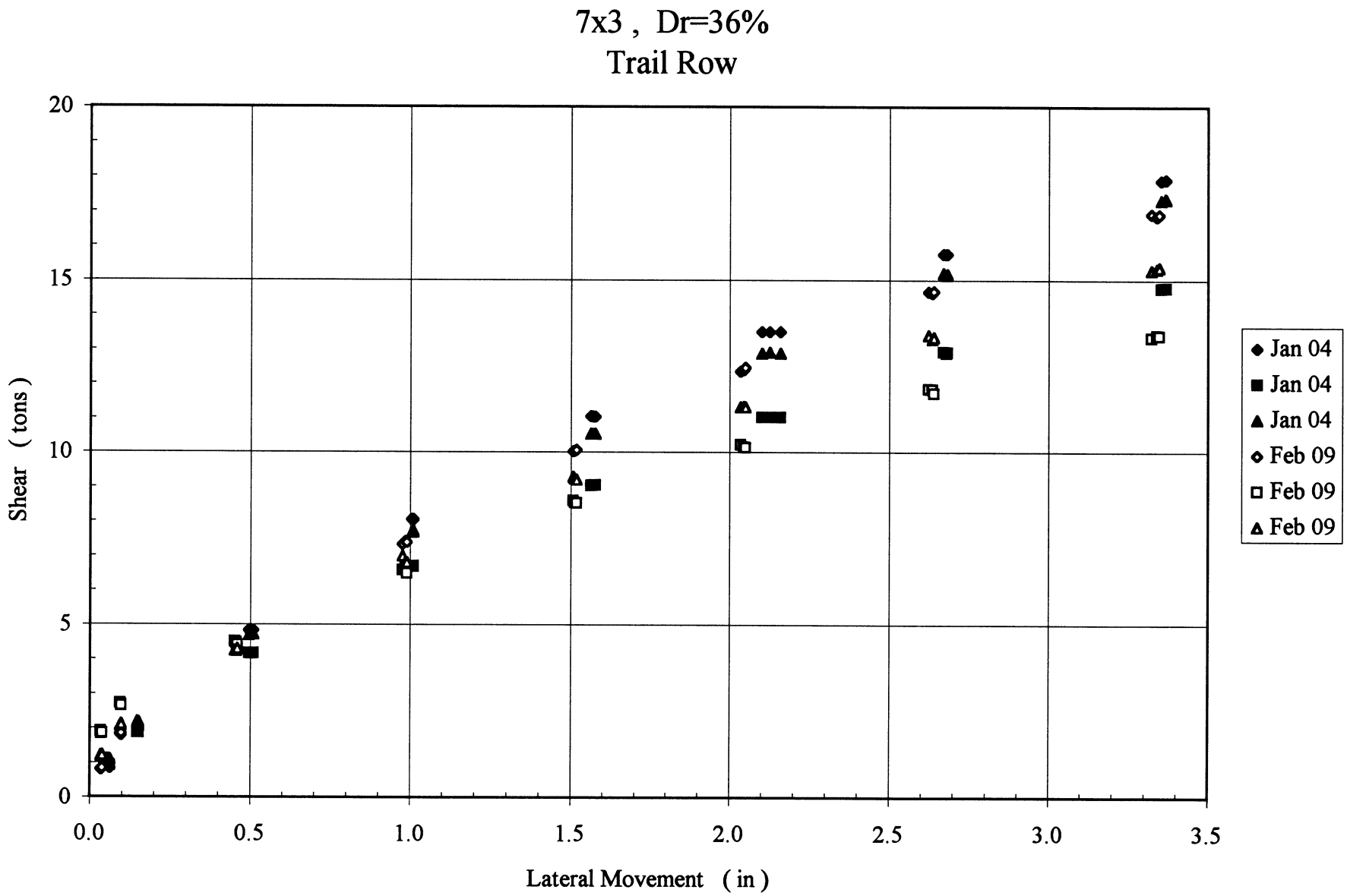

Figure 6-12(h). Results of 7 × 3 Group in Loose Sand, Measured Shear for Each Pile in Trail Row

For instance all the piles had to be driven (with instrumentation) and then laterally loaded; many times during the driving the instrumentation approached the gauge's limits, and upon laterally loading they decreased.

Presented in Table 6-1 is the summary of the individual row contributions for all the groups tested at 3 in. of lateral movement. An important finding presented in this table is that an individual row's lateral resistance is independent of group size (i.e. 4 × 3 or 7 × 3), but is a function of row position (i.e. 2nd, 3rd, etc-see Table 6-1,Average values) and soil density. For instance, using the row's average values, both the loose and medium dense sands group results were predicted (3" of lateral movement, see table), and the maximum error was less than 5% for any group. The concept of an average row value, supports the use of p-y multipliers, since they are usually fixed for a given row, but vary based row position within the group and soil density.

6.2 FLORIDA-PIER's Prediction of Centrifuge Tests

Using the results of Figures 6-2 through Figures 6-12, and FLORIDA-PIER, the group p-y multipliers for each group were back computed. For instance, the 5 × 3 and 6 × 3 group in medium dense sand (Dr=55%) are given in Figures 6-13 (a)&(b) and 6-14 (a)&(b); the 5 × 3 and the 6 × 3 and medium loose sand (Dr=36%) results are presented in Figures 6-15 (a)&(b) and 6-16 (a)&(b). The medium dense (Dr=55%) predictions were performed with multipliers of 0.8, 0.4, 0.3, 0.2, and 0.2, and the medium loose sand (Dr=36%) were accomplished with multipliers of 1., 0.4, 0.3, 0.2, and 0.2, respectively. Since all the groups were found to have similar multipliers (loose sands were higher for lead row - conservative to use lower value) the following values are recommended: 0.8 for lead, 0.4 for 2nd row, 0.3 for 3rd row, and 0.2 for all successive rows.

Table 6-1. Group Test Results

Medium Dense Sand (Dr=55%)						
	3 × 3 rows	4 × 3 rows	5 × 3 rows	6 × 3 rows	7 × 3 rows	Average
Lead row (tons)	27.5	33	33	34	32	32
2nd row (tons)	20	23	25	23	25	23.2
3rd row (tons)	16	17	18	20	20	19
4th row (tons)	--	16	17	16	17	17
5th row (tons)	--	--	16	16	16	16
6th row (tons)	--	--	--	16	16	16
7th row (tons)	--	--	--	--	16	16
Measured(tons)	210	267	327	375	426	
Predicted(tons)	213.6	270.6	321.6	369.6	417.6	
Error (%)	1.7	1.3	1.7	1.4	2.0	
Loose Sand (Dr=36%)						
	3 × 3 rows	4 × 3 rows	5 × 3 rows	6 × 3 rows	7 × 3 rows	Average
Lead row (tons)	27	27	27	25	27	26.6
2nd row (tons)	17	17	21	17	20	18.4
3rd row (tons)	14	15	16	16	16	15.8
4th row (tons)	--	15	14	14	15	14.3
5th row (tons)	--	--	15	13	13	13.0
6th row (tons)	--	--	--	15	13	13
7th row (tons)	--	--	--	--	15	14.8
Measured(tons)	170	220	270	300	360	
Predicted(tons)	179.4	226.8	269.7	311.7	353.7	
Error (%)	5.5	3.1	.1	3.9	1.8	

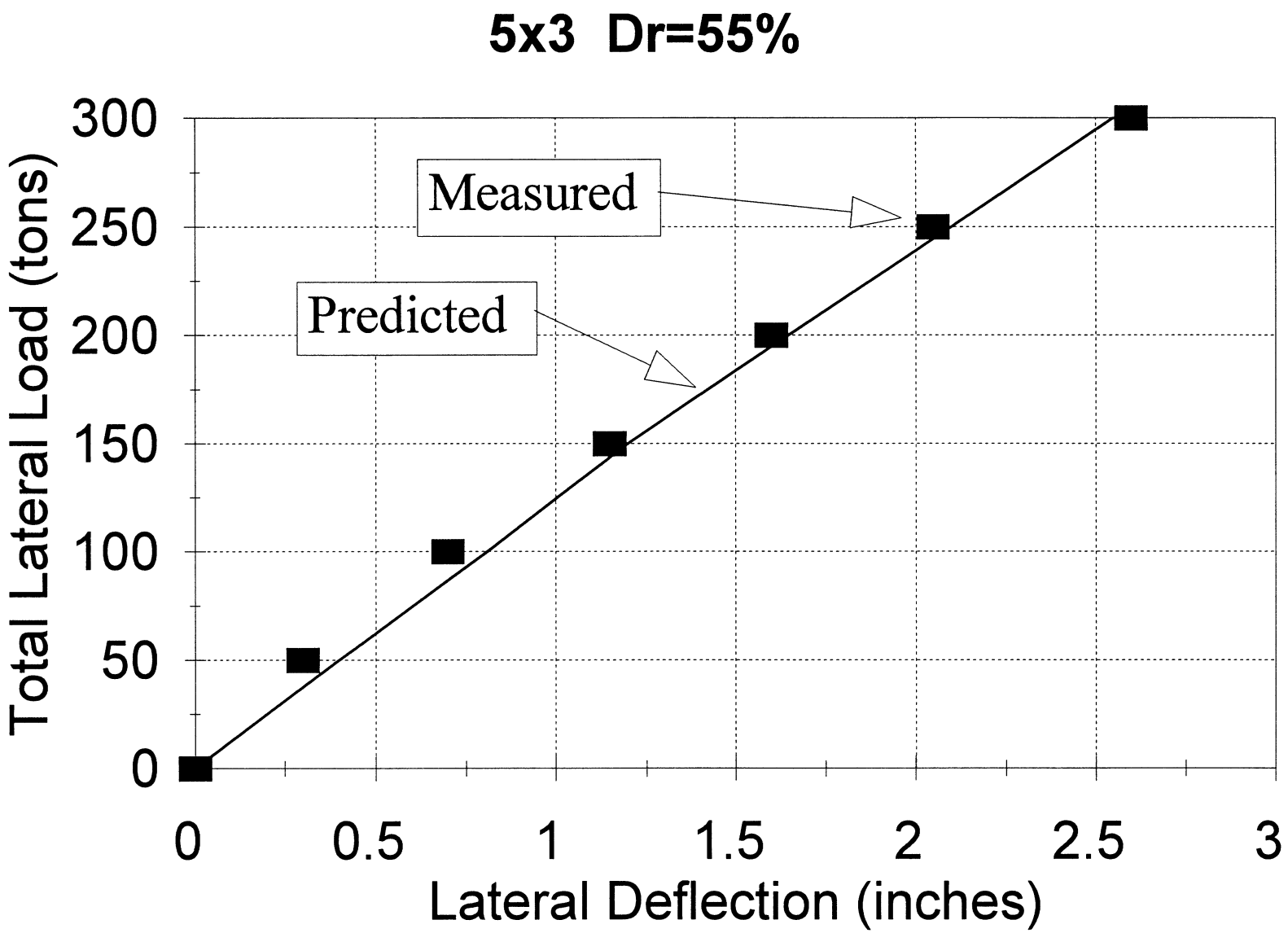

Figure 6-13(a). Measured vs. Predicted 5 × 3 Group, D_r = 55%

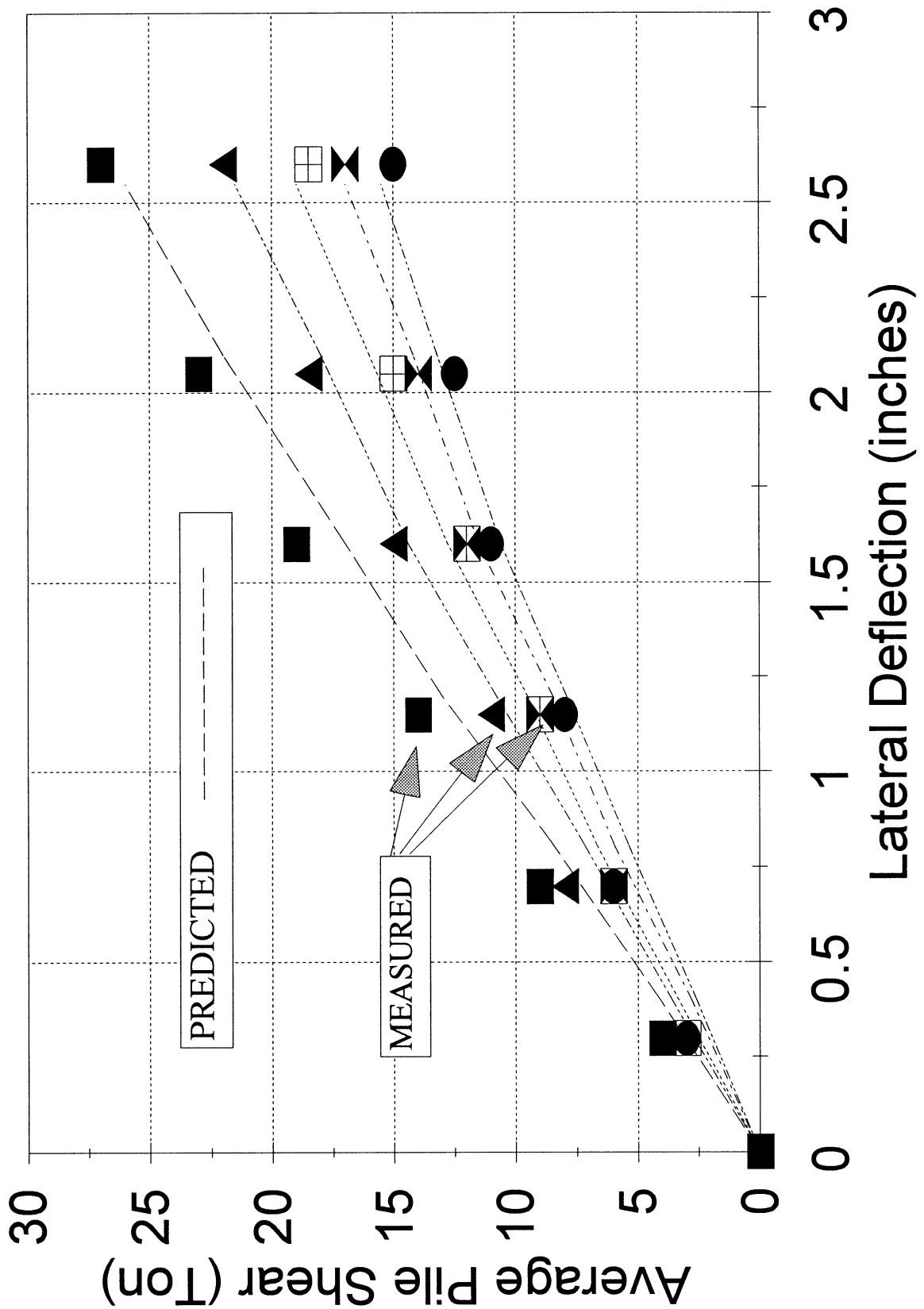

Figure 6-13(b). Measured vs. Predicted 5 × 3 Group, D_r = 55%

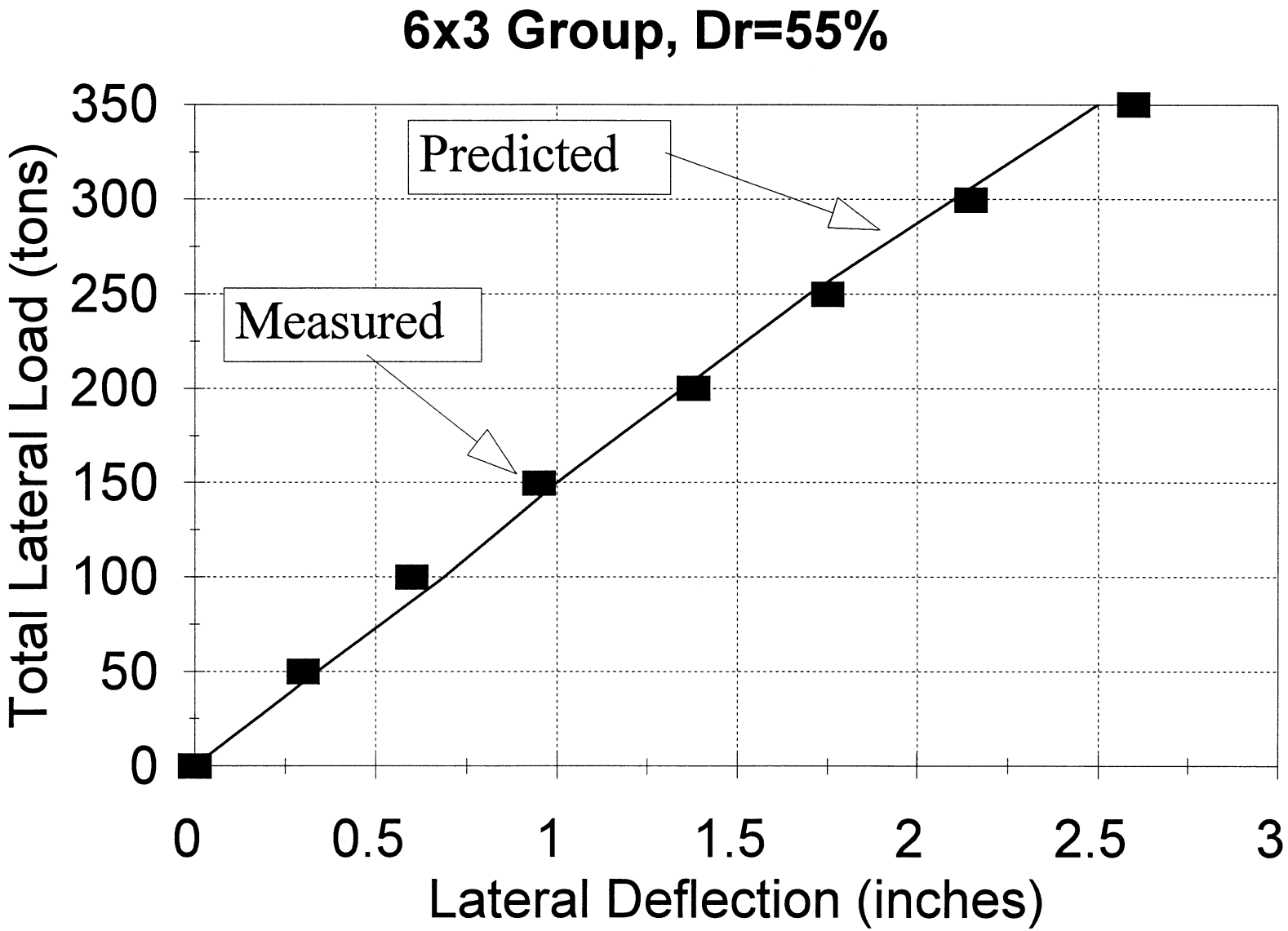

Figure 6-14(a). Measured vs. Predicted 6 × 3 Group, D_r = 55%

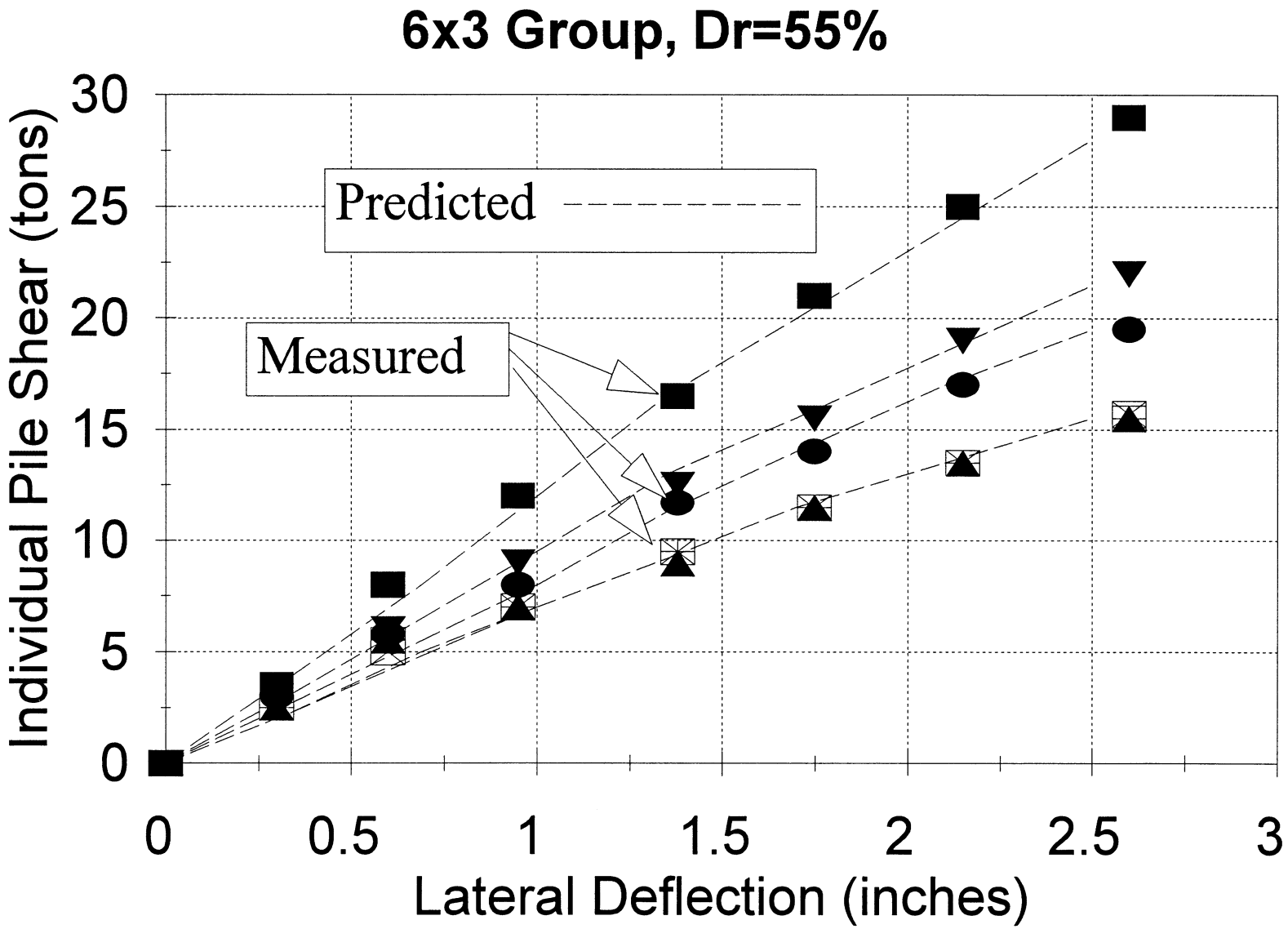

Figure 6-14(b). Measured vs. Predicted 6 × 3 Group, D_r = 55%

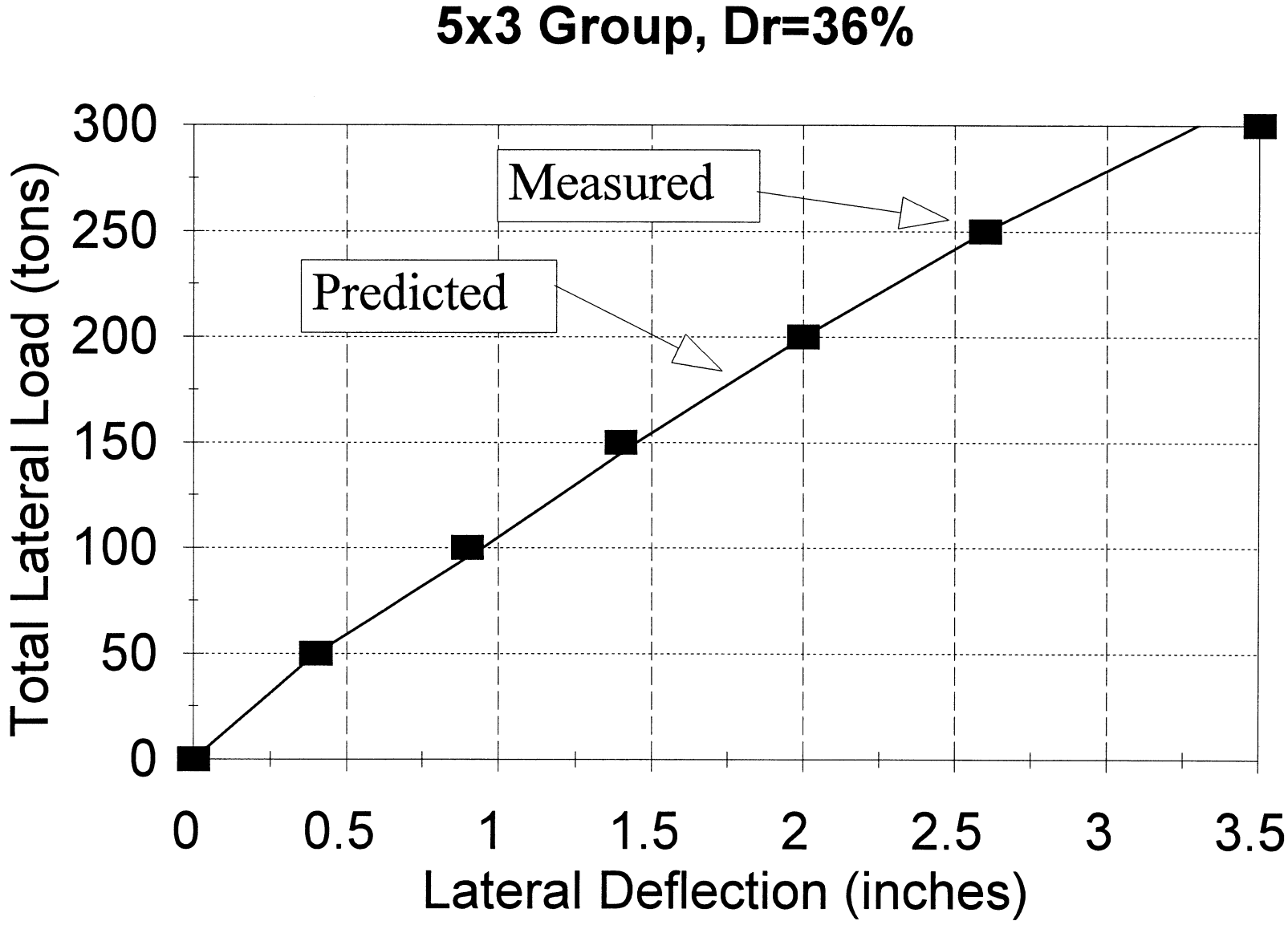

Figure 6-15(a). Measured vs. Predicted 5 × 3 Group, D_r = 36%

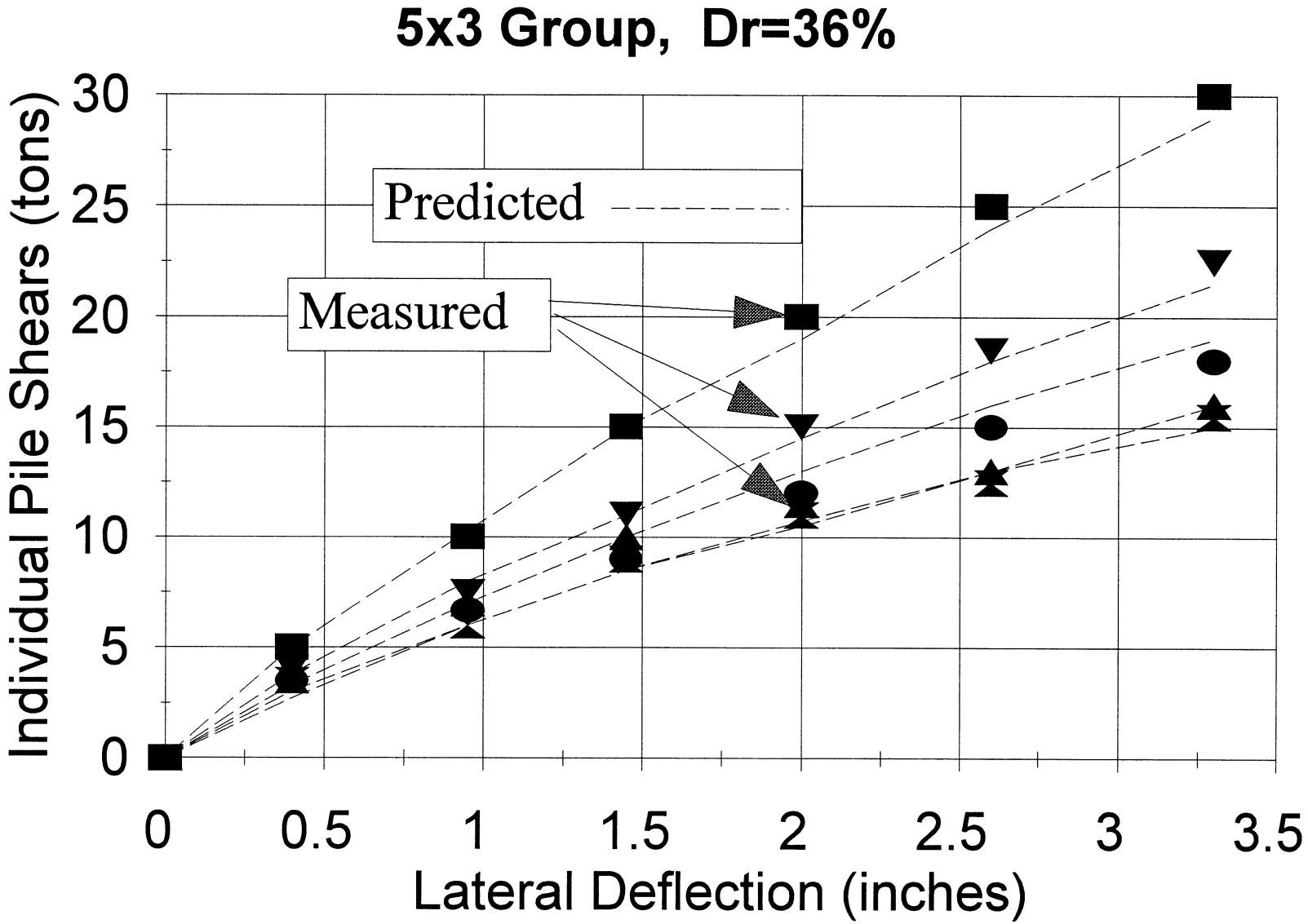

Figure 6-15(b). Measured vs. Predicted 5 × 3 Group, D_r = 36%

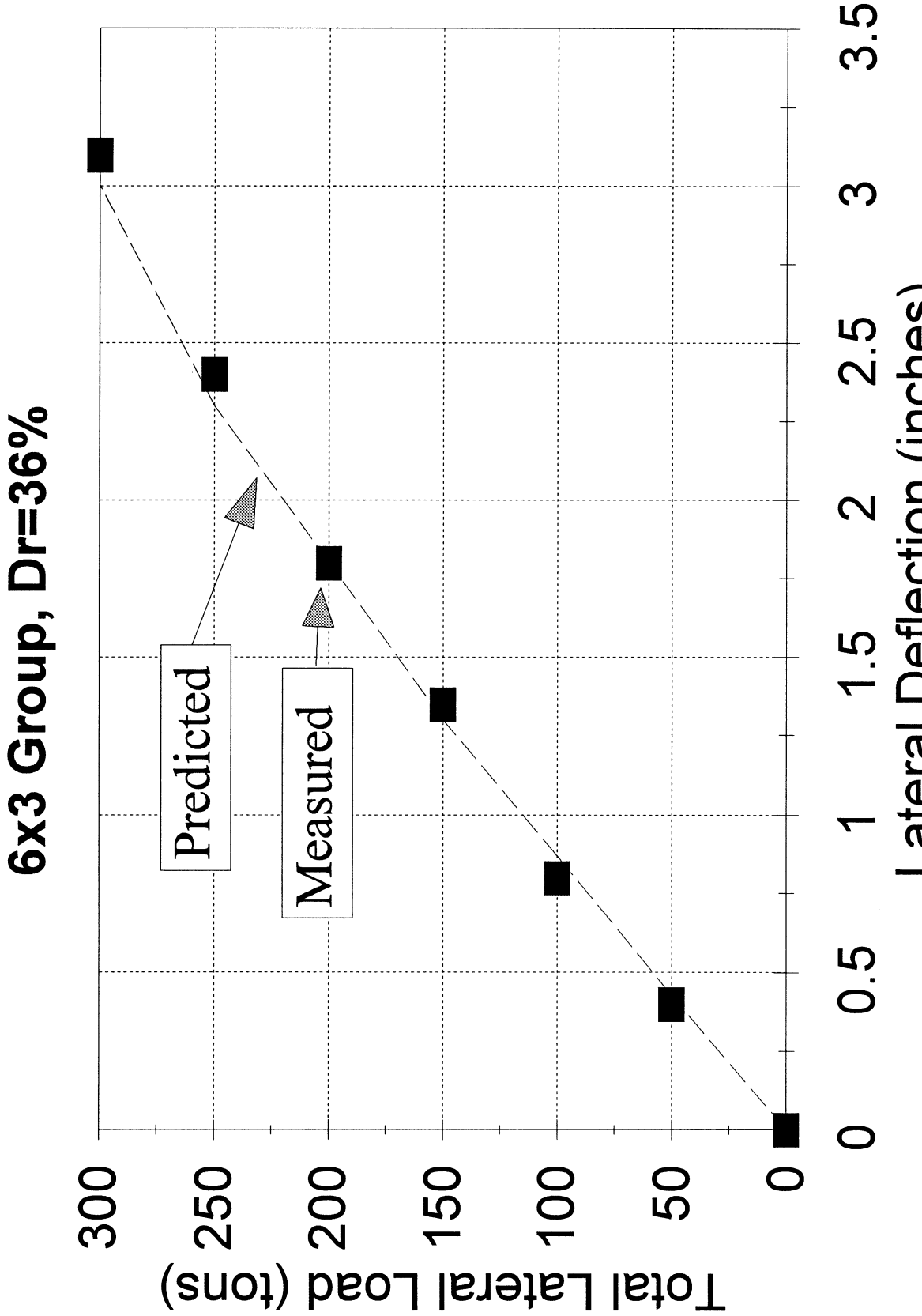

Figure 6-16(a). Measured vs. Predicted 6 × 3 Group, D_r = 36%

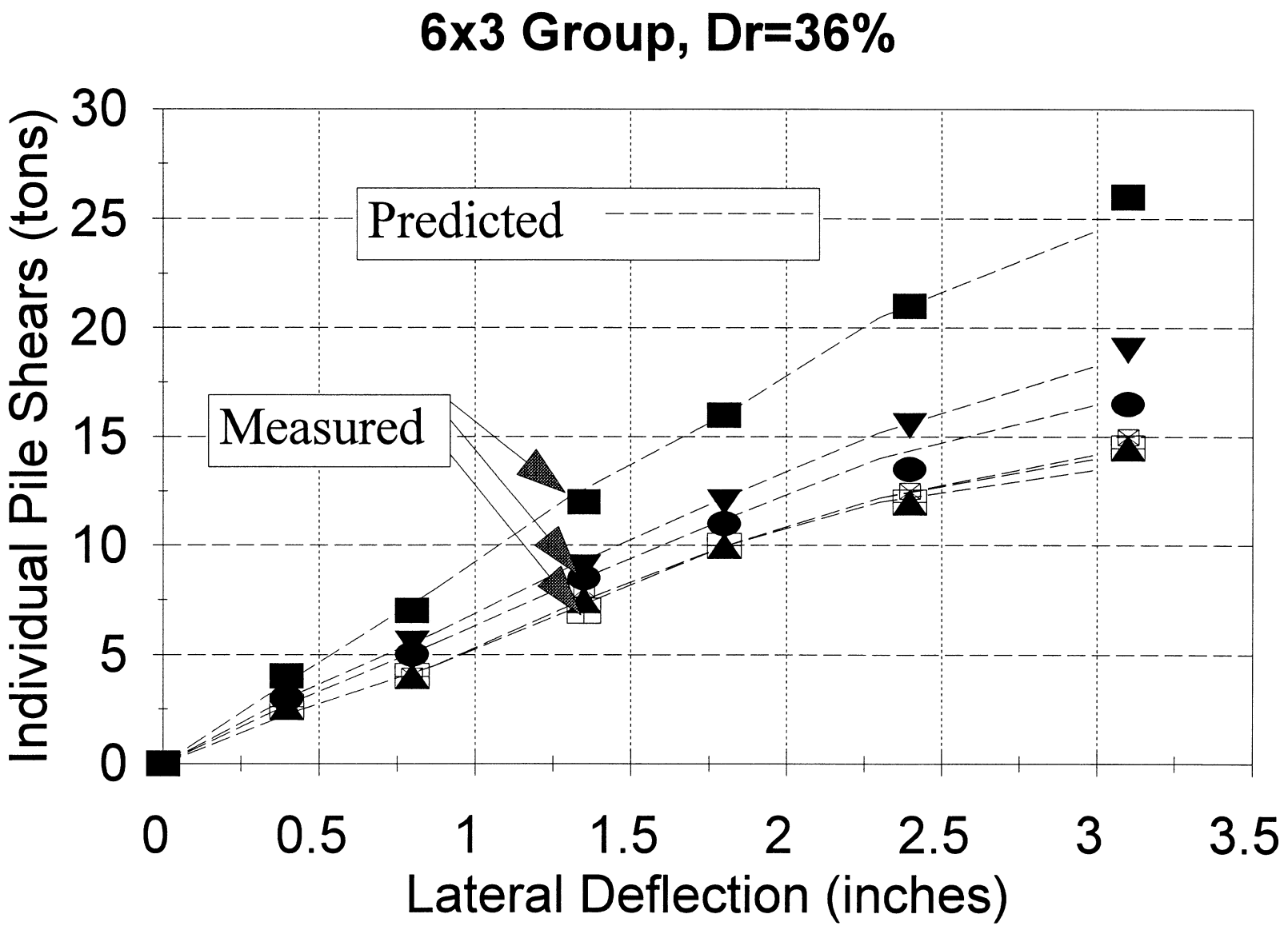

Figure 6-16(b). Measured vs. Predicted 6 × 3 Group, D_r = 36%

LIST OF REFERENCES

Bradley, G.S., Townsend, F.C., Fagundo, F.E., and Davidson, J.L. (1984). "Centrifuge Scaling Laws for Ground Launch Cruise Missile Shelter." ESL-TR-84-07, Air Force Engineering Services Center, Tyndall Air Force Base, Florida, April.

Brown, D.A., Morrison, C., and Reese, L.C. (1988). "Lateral Load Behavior of a Pile Group in Sand." ASCE, Journal of Geotechnical Engineering, Vol. 114, No. 11, pp. 1261-1276.

Clausen, J.B. (1992). "Centrifugal Model Tests on Lateral Loaded Pile Groups in Homogeneous Sand." Master's Thesis, University of Florida, Gainesville, Florida.

Cox, W.R., Reese, L.C., and Grubbs, B.R. (1974). "Field Testing of Laterally Loaded Piles in Sand." 5th Annual Offshore Technology Conference, Houston, Texas, Paper No. 2079.

Feld, T. (1990). "A Centrifugal Study of Axially Loaded Piles and Pile Groups in Homogeneous and Layered Soils." Master's Thesis, University of Florida, Gainesville, Florida.

Gill, J.J. (1988). "Development and Testing of a Device Capable of Placing Model Piles by Driving and Pushing in the Centrifuge." Ph.D. Dissertation, University of Florida, Gainesville, Florida.

Gravgaard, J.H. (1990). "Development of a Device Capable of Driving Model Piles Individually in the Centrifuge." Master's Thesis, University of Florida, Gainesville, Florida.

Kofoed, N. (1989). "A Centrifugal Study of Axially Loaded Model Piles and Pile Groups in Reid-Bedford Sand." Master's Thesis, University of Florida, Gainesville, Florida.

Mcadams, P.F. (1993). "Centrifuge Model Testing on Laterally Loaded Nine Pile Groups at Three Diameter Spacing in Sand." Master's Report, University of Florida, Gainesville, Florida.

McVay, M.C., and Hoit, M. (1994). User's Manual for LPGSTAN. Department of Civil Engineering, University of Florida, Gainesville Florida.

McVay, M.C., Bloomquist, D., Vanderlinde, D., and Clausen, J., (1994). "Centrifuge Modeling of Laterally Loaded Pile Groups in Sands." ASTM Geotechnical Testing Journal, Vol. 17, No. 2, pp. 129-137.

McVay, M.C., Casper, R., and Shang, T. (1995a). "Lateral Response of Three Row Groups in Loose to Dense Sands at 3D and 5D Pile Spacing." accepted by ASCE, Journal of Geotechnical Engineering.

McVay, M.C., Casper, R., and Shang, T. (1995b). "Centrifuge Testing of Fixed Head Laterally Loaded Battered and Plumb Pile Groups in Sand." accepted by ASCE, Journal of Geotechnical Engineering.

Reese, L.C. (1993). Behavior of Piles and Pile Groups Under Lateral Load. Report No. FHWA/RD-85/106, U.S. Department of Transportation, Federal Highway Administration, Office of Research, Development and Technology, Washington, D.C., July.

Reese, L.C., Cox, W.R., and Koop, F.D. (1974), "Analysis of Laterally Loaded Piles in Sand." 5th Annual Offshore Technology Conference, Houston, Texas, Paper No. 2080.

Shang, T. (1994). "Centrifuge Modeling of Laterally Loaded Three Row Battered and Plumb Pile Group in Sand." Master's Thesis, University of Florida, Gainesville, Florida.

Vander Linde, D.L. (1992). "Development of a Computerized Installation and Lateral Load Testing Device for a Pile Group in the Centrifuge." Master's Thesis, University of Florida, Gainesville, Florida.

Wang, S.-T., and Reese, L.C. (1990). COM624P Program User's Manual, Version 1.0. Report No. FHWA-IP-90-005, 247p, U.S. Department of Transportation, Federal Highway Administration, Office of Research, Development and Technology, Washington, D.C.

Wang, S.-T., and Reese, L.C. (1993). COM624P-Laterally Loaded Pile Analysis Program for Microcomputer, Version 2.0. Final Report from FHWA, Washington, D.C., August.